INFORMATION TO USERS

This manuscript has been reproduced from the microfilm master. UMI films the text directly from the original or copy submitted. Thus, some thesis and dissertation copies are in typewriter face, while others may be from any type of computer printer.

The quality of this reproduction is dependent upon the quality of the copy submitted. Broken or indistinct print, colored or poor quality illustrations and photographs, print bleedthrough, substandard margins, and improper alignment can adversely affect reproduction.

In the unlikely event that the author did not send UMI a complete manuscript and there are missing pages, these will be noted. Also, if unauthorized copyright material had to be removed, a note will indicate the deletion.

Oversize materials (e.g., maps, drawings, charts) are reproduced by sectioning the original, beginning at the upper left-hand corner and continuing from left to right in equal sections with small overlaps. Each original is also photographed in one exposure and is included in reduced form at the back of the book.

Photographs included in the original manuscript have been reproduced xerographically in this copy. Higher quality 6" x 9" black and white photographic prints are available for any photographs or illustrations appearing in this copy for an additional charge. Contact UMI directly to order.

UMI

A Bell & Howell Information Company
300 North Zeeb Road, Ann Arbor MI 48106-1346 USA
313/761-4700 800/521-0600

Juxtamembrane Autophosphorylation in the Insulin Receptor Kinase

By

Aaron Darius Cann

A dissertation submitted to the Graduate Faculty in Biomedical Sciences in partial fulfillment of the requirements for the degree of Doctor of Philosophy.

The City University of New York.

1998

This manuscript has been read and accepted by the Graduate Faculty in Biomedical Sciences in satisfaction of the dissertation requirement for the degree of Doctor of Philosophy.

12/19/97

Date

Dr. Terry Ann Krulwich

Executive Officer

12/19/97

Date

Dr. Terry Ann Krulwich

Chair, Examining Committee

Dr. Jonathan M. Backer

Dr. Ronald A. Kohanski

Dr. Robert Krauss

Dr. J. B. Alexander Ross

Examining Committee

The City University of New York

Abstract

Juxtamembrane Autophosphorylation in the Insulin Receptor Kinase

By Aaron Darius Cann

Thesis Advisor: Dr. R. A. Kohanski

The insulin receptor is a $\alpha_2\beta_2$ receptor tyrosine kinase which is activated by autophosphorylation of its kinase-bearing β subunits in response to insulin. The molecular mechanism of β subunit autophosphorylation has long been a matter of dispute, with some groups reporting intramolecular (*cis*) and others intermolecular (*trans*) autophosphorylation. We used site directed mutagenesis of the complete cytoplasmic kinase domain (CKD) in conjunction with the standard criteria of enzyme concentration dependence to study the molecular mechanism of autophosphorylation. The apparent mechanism of autophosphorylation was dependent on the particular residues involved in the reaction. Thus, tyrosines in the juxtamembrane region of the receptor (Y^{965} and Y^{972}) autophosphorylate in *cis*, but tyrosine residues in the activation loop (Y^{1158}, Y^{1162}, and Y^{1162}) and carboxyl terminus ($Y^{1328}$and Y^{1334}) autophosphorylate in *trans*. Under conditions where activation loop autophosphorylation did not occur (but in the presence of an intact activation loop), *cis* autophosphorylation of the juxtamembrane tyrosines was observed to correlate with activation of the CKD. This was measured with a new HPLC-based *in vitro* peptide phosphorylation assay using a peptide derived from insulin receptor substrate-1. Moreover, a mutant enzyme with both Y^{965} and Y^{972} mutated to F

(but not a mutant with the carboxyl terminus tyrosines mutated to F) showed very little peptide phosphorylation activity. Thus, we have observed a novel *cis* activation process in the insulin receptor. This process appears to explain previous conflicts in the insulin receptor literature.

The crystal structure of a truncated CKD lacking the juxtamembrane region (S. R. Hubbard *et al.*, Nature **372** 746; 1994) has been solved, and identifies residues in the unphosphorylated activation loop that stabilize it for *cis* inhibition. We found that disruption of these residues caused an increased rate of juxtamembrane *cis* autophosphorylation, primarily due to a 30-fold drop in K^{MnATP} or K^{MgATP}. This implies that the wild-type unphosphorylated activation loop slows *cis* autophosphorylation by blocking the interaction with ATP. The converse observation has also been found: the truncated CKD, without the juxtamembrane region, autophosphorylates at the activation loop much more readily than the full-length enzyme (L. Wei *et al.*, J. Biol. Chem. **270** 8122; 1995). Taken together, these observations suggest a new model of the basal state of the insulin receptor's kinase. In this model, the unphosphorylated state of the insulin receptor's kinase is inhibited by reciprocal *cis* inhibition by the unphosphorylated juxtamembrane and activation loop regions. Either region can occupy the peptide binding site, but only the activation loop blocks ATP binding. This dual mode of autoinhibition may be required for prevention of *trans* activation in the constitutively tetrameric insulin receptor holomer. If *cis* autoinhibition is relieved by insulin, which remains to be established, then a much smaller conformational change than previously thought may suffice to transmit insulin's activating signal across the cell membrane.

Acknowledgments

I would like to thank my thesis advisor, Dr. R. A. Kohanski, for his continuous advice and support. The advice and encouragement of other faculty members in the Department of Biochemistry at the Mt. Sinai School of Medicine, particularly Dr. T.A. Krulwich and Dr. H.C. Li, have also been invaluable.

Just as the faculty of Mt. Sinai has given me the opportunity to embark on this project, my family has given me the love and support necessary to bring it to fruition. I cannot thank my wife Miriam enough for her patient encouragement and quiet wisdom, without which this work could never have been done.

Table of Contents

List of Figures

List of Tables

Abbreviations Used

AL	Activation loop (residues $DF^{1151}G$-$AP^{1172}E$)
AMP-PNP	Adenylyl imidodiphosphate
BSA	Bovine serum albumin
CaM	Calmodulin
CaMK	Calcium/calmodulin dependent protein kinase
cAMP	Cyclic adenosine 5'-monophosphate
cAPK	Cyclin AMP-dependent protein kinase
cdk	Cyclin-dependent kinase
CIP	Calf intestinal phosphatase
CKD	Cytoplasmic kinase domain (of the human insulin receptor, residues R^{953}-S^{1355})
CT	Carboxyl terminus (K^{1283}-S^{1355})
DTT	Dithiothreitol
EGFR	Epidermal growth factor receptor
HPLC	High performance liquid chromatography
IR	Insulin receptor
IRS-1	Insulin receptor substrate-1
IRS939	Peptide substrate for the CKD (see Table 3-1)
JM	Juxtamembrane region of the IR (residues 953-984)
MAPK	Mitogen-activated protein kinase
MgAc	Magnesium acetate
MnAc	Manganese acetate
NIDDM	Non-insulin dependent diabetes mellitus
NRTK	Nonreceptor tyrosine kinase
PCR	Polymerase chain reaction
PDGFR	Platelet derived growth factor receptor
P-IRS939	Phosphorylated IRS939
PH	Pleckstrin homology (domain)
P-CKD	Phosphorylated CKD
PKA	Protein kinase A, also cAPK.
PKC	Protein kinase C
PTB	Protein tyrosine binding (domain)
RP-HPLC	Reverse-phase HPLC
SDS-PAGE	Sodium dodecyl sulfate-polyacrylamide gel electrophoresis
SH-2	*src* homology-2 domain

TE	Tris-EDTA buffer
TFA	Triflouroacetic acid
TLC	Thin layer chromatography
TNF-α	Tumor necrosis factor-α

Nomenclature for mutant versions of the CKD (ALY2F, JMY2F, etc.) are described in Table 2-2. Amino acids are designated using the single-letter or three-letter amino acid code listed on the following page. Numbering is according to the complete cDNA of the insulin receptor precursor, which includes both α and β subunits. Differential splicing of exon 11, which encodes 12 amino acids in the α subunits, has lead to two numbering schemes for the receptor which differ by twelve amino acids (residues 718-729). In this work, we use the numbering scheme of Ebina *et al.*(1), based on the IR isoform including this exon.

Amino Acid Designations.

Single Letter Code	Three Letter Code	Full Name
A	Ala	Alanine
C	Cys	Cysteine
D	Asp	Aspartic acid
E	Glu	Glutamic acid
F	Phe	Phenylalanine
G	Gly	Glycine
H	His	Histidine
I	Ile	Isoleucine
K	Lys	Lysine
L	Leu	Leucine
M	Met	Methionine
N	Asn	Asparagine
P	Pro	Proline
Q	Gln	Glutamine
R	Arg	Arginine
S	Ser	Serine
T	Thr	Threonine
V	Val	Valine
W	Trp	Tryptophan

pY and pT are used to denote the modified amino acids *O*-phosphotyrosine and *O*-phosphothreonine.

1. Introduction

Since its isolation in 1923 by Banting *et al.* (2), insulin has been found to be a key peptide hormone involved in the normal homeostasis of carbohydrate metabolism. Binding of insulin to its receptor, first purified by P. Cuatrecasas (3), leads to a wide range of short-term metabolic effects necessary for normal homeostasis, as well as longer-term growth promoting effects necessary for normal development. Defects in insulin signaling (which can occur at several levels) lead to human disease, most notably diabetes mellitus. On a molecular level, insulin's actions are mediated *via* the insulin receptor (IR). This receptor transmits its signal across the cell membrane *via* its insulin-dependent protein kinase activity. The IR is an important member of this class of enzyme, which is involved in almost every aspect of cellular signaling. The insulin receptor lies at the crossroads of human health and the scientifically intriguing problem of protein kinase regulation. It is no surprise, then, that the activation of this receptor by insulin has been an active area of research since its purification in 1972. But for every process of *activation*, there must be a corresponding regulation of the *basal* state of the receptor. Put another way: the question of why the IR's kinase is *inactive* in the absence of insulin is critical to an understanding of the barriers that must be overcome to achieve activation. In this dissertation, we will examine a novel component of insulin receptor kinase regulation and its implications for the basal state of the IR.

The Insulin Receptor Contains a Regulated Protein Tyrosine Kinase

The ATP: protein tyrosine phosphotransferase activity of the first known protein tyrosine kinase, $pp60^{v\text{-}src}$, was originally identified using TLC to demonstrate phosphorylation of tyrosyl residues (4,5). Not long thereafter, it was realized that the IR became tyrosine phosphorylated in response to insulin (6-9). Indeed, the receptor itself was the responsible kinase, as demonstrated by photoaffinity labeling the β subunit of the IR with [α-^{32}P] 8-azidoATP (10,11), labeling with oxidized [α-^{32}P]ATP (12), or co-purification (13). The kinase was shown to be activated by autophosphorylation (14). Thus, the first known substrate for the insulin receptor kinase was the insulin receptor itself. As determined by [^{125}I] insulin cross linking studies (15) or biosynthetic labeling with [^{3}H] sugars (16), the physiological IR contains two disulfide- linked 135 kDa α subunits and two 95 kDa β subunits as shown in Figure 1-1. When the cDNA for the receptor was cloned and sequenced (1,17), the receptor was indeed found to contain a protein kinase domain. This domain is common to almost every known protein Ser, Thr, or Tyr kinase (18-20). The catalytic core of the insulin receptor was the first protein tyrosine kinase to be crystallized, revealing the same bilobal three-dimensional structure conserved in other protein kinase structures (21).

This receptor kinase activity appears to be essential for all the metabolic effects of insulin. Patients with normal insulin binding activity can still have disorders of the insulin axis (22), but kinase mutations lead to insulin resistance (23-28). Similarly, transfection of cells with kinase-inactive IR (29,30) or various kinase-impaired mutants (31) confers corresponding insulin sensitivity of glucose transport or other insulin

dependent effects. Although kinase activity is necessary for insulin signal transduction, it is not sufficient: mutations in the juxtamembrane region of the receptor can block phosphorylation of a major substrate, insulin receptor substrate (IRS)-1, and signal transduction despite grossly normal autophosphorylation (32).

The substrate preference of the insulin receptor kinase provides much of the specificity of insulin signaling. The substrate specificity of the IR was originally characterized as similar to other tyrosine kinases known at the time, namely the epidermal growth factor receptor (EGFR) and Src (33,34). However, the substrate specificity of the IR, and other tyrosine kinases, has since been found both unique and essential to their signal transduction (35,36). Using degenerate peptide libraries, one group (37) found an optimal peptide sequence of EEEYMMM for the IR. This and previous studies are consistent with the numerous YMXM motifs phosphorylated in IRS-1 (38), discussed below. A practical demonstration of the importance of the kinase domain's specificity was made when the extracellular portion of the IR was fused to the intracellular tyrosine kinase domain of the UR2 virus transforming protein $p68^{gag\text{-}ros}$. The resulting chimera showed insulin-dependent autophosphorylation and phosphorylation of synthetic substrates but did not signal increased glucose uptake or DNA synthesis (39). As discussed below, IRS-1, a similar protein termed IRS-2, and Shc appear to be the major direct physiological substrates of the IR.

Structure and Biosynthesis of the Insulin Receptor

The gene for the IR, consisting of 22 exons on the short arm of chromosome 19 (1,40), encodes a single 1355 amino acid polypeptide with a membrane insertion

sequence preceding the N-terminus; this signal peptide is cleaved during translocation. The insulin receptor is translated as a 160kDa protein in the endoplasmic reticulum, which is either cotranslationally or very rapidly glycosylated to an apparent 190kDa form (41,42). After further glycosylation, the protein (the IR precursor) is cleaved at a basic cleavage signal at residue 732 to generate mature α and β subunits. The receptor is also acylated (43,44) at least on the intracellular β subunit. The final IR has an $\alpha_2\beta_2$ structure; this is the only physiological form of the mature insulin receptor (45,46). The α subunits are linked by two disulfide bonds, between C^{524} and C^{682} (47-50). α subunits are linked to β subunits by disulfides as well; this involves C^{647} in the α subunit (51) and an unknown Cys in the β subunit. Interestingly, $C^{647}S$ mutants do not autophosphorylate in either the presence or absence of insulin (51). The structure of the IR holomer is shown schematically in Figure 1-1. As will be discussed further below, this tetrameric structure of the IR places unique demands on the regulation of the insulin receptor and its close relatives.

Despite its central location, the transmembrane region of the receptor plays an unclear role in signal transduction. Introduction of an oncogenic point mutation identified in ErbB-2 into this region ($V^{938}A$) showed no effect in the IR (52-54), nor did a series of nested deletions in the transmembrane domain (53). Replacement with PDGFR transmembrane domain or normal ErbB-2 transmembrane domain also had no apparent effect (54). However, replacement of the entire transmembrane sequence with the oncogenic form from ErbB-2 yielded a constitutively activated receptor with persistent stimulation of growth (52), and inversion of the transmembrane domain blocks insulin

signal transduction (55). Other mutations designed to increase the α-helix content of this region were shown to increase internalization of the receptor *via* accelerated lateral transport, but again without alteration of insulin binding or insulin-dependent autophosphorylation.(56). It therefore seems unlikely that specific amino acid side chains in the transmembrane region play distinct roles in signal transduction. Conformational changes involving rotation or translation around this putative α helix are perhaps more likely means of signal transduction.

Autophosphorylation at Multiple Tyrosines Regulates the Kinase and its Interactions

It was eventually recognized that the autophosphorylation of the receptor played a key role in the insulin-dependent activation of the receptor *in vitro* (14,57) and *in vivo* (58) and that autophosphorylation occurred at multiple sites in the β subunit of the receptor (9,59). Phosphopeptide mapping studies traced the insulin-stimulated autophosphorylation to tyrosine residues of the β subunit, including Y^{1158}, Y^{1162}, and Y^{1163} in the activation loop (AL) of the kinase domain, and Y^{1334} and Y^{1328} in the carboxyl terminus (CT) tail (60-65). Later mapping studies also identified Y^{965} and Y^{972}, in the juxtamembrane region as autophosphorylation sites (66,67) although a role for Y^{972} in insulin signal transduction had already been demonstrated by mutagenesis (32). These autophosphorylation sites were difficult to identify because of the hydrophobicity of that portion of the kinase and their small contribution to net insulin-stimulated autophosphorylation.

The AL sites Y^{1158}, Y^{1162}, and Y^{1163}, are regarded as the primary autophosphorylation sites responsible for activation. Phosphorylation of these sites

correlates with receptor activation (62,65,68) and mutation of these sites prevents activation and signal transduction (69-73) and receptor internalization (70,74). Moreover, multiple mutants in these sites show a decreasing activity that correlates with decreasing insulin signal transduction (31). The structural basis for activation by autophosphorylation in the AL has been clarified by crystallography studies on several protein kinases, including the IR, and will be discussed below.

Juxtamembrane tyrosine autophosphorylation, at Y^{965} and Y^{972} (66,67), is a smaller fraction of insulin-stimulated autophosphorylation (although this depends on ATP concentration, with lower ATP concentrations favoring juxtamembrane autophosphorylation over other sites (75)). Nevertheless, these sites are very important for receptors whose signaling involves phosphorylation of IRS -1 or IRS-2. Y^{972}, when phosphorylated, docks with a protein tyrosine binding domain (PTB) of IRS-1 (76,77), IRS-2 (78) or Shc (79,80). Disruption of this residue blocks insulin signal transduction and IRS-1 phosphorylation *in vivo* (32,81-84). The homologous residue in the insulin-like growth factor I receptor (IGF-IR) is also involved in docking IRS-1 and Shc (85). Blockade of the Shc PTB domain results in the specific loss of Shc phosphorylation by the IR (86). The receptor for IL-4 also docks IRS-1 through a very similar sequence TPLVIAGNPAY^{497}RSFSNSL, which is also blocked by mutation of Y^{497} to F (87). Unexpectedly, disruption of the PTB-pY972 interaction *in vitro* has very little effect on IRS-1 phosphorylation *in vitro* (88).

Internalization of the receptor is a molecular process requiring both phosphorylation of the activation loop and elements in the juxtamembrane region of the receptor (89). Roles for the autophosphorylation sites Y^{965} and Y^{972} in internalization

have been proposed. Peptides from these regions exist as β-turn signals in solution (90) and in complex with IRS-1 (76), and large deletions including these regions can have an effect on internalization (91,92). However, conflicting observations have been made regarding the effect of point mutations of these sites or their surroundings on internalization (83,90). Mutation of the dileucine motif $L^{992}L$, to AA, does reduce insulin internalization 5-fold (93), and since the conformation of this motif could be affected by the 12-amino acid mutation 966-977 that originally implicated the juxtamembrane region in internalization, involvement of these residues could constitute the entire contribution of the JM region to internalization.

The role of the carboxyl terminus autophosphorylation sites is less well defined, but they do not appear to play a role in kinase activation or receptor internalization. Phosphorylation of this region has been shown to have a poor correlation with enzyme activation (62,94). Deletion of this region (82,95) or point mutations of the autophosphorylation sites (70) was found to have minimal effects in some studies. Others found the same deletion to block insulin-dependent glucose transport (96) albeit without affecting kinase activity or receptor internalization (97). Antibodies against this region (98) or mutation of these sites (99) inhibit the growth and mitogenic effects of the IR without affecting metabolic or transport effects. Replacement of this region with the homologous sequence from IGF-I blocked insulin-dependent mitogenic effects (100). In contrast to virtually every other mapping study of the IR (done using partially purified IR or IR from cell culture), one group found no evidence of phosphorylation of these sites in IR from intact rat liver (101), leading the authors to propose that phosphorylation of these

sites is an artifact of heterologous IR expression. The role of the CT region remains only partially defined, but what role it does play appears likely to be limited to docking of downstream effectors, as compared to modulating activity of the receptor. The three clusters of autophosphorylation sites in the IR thus play different roles in insulin signal transduction.

Although the IR is normally considered an exclusive tyrosine kinase, it has been reported that the IR possess some intrinsic ability to autophosphorylate on serine residues (102-104). In particular, S^{1287} and S^{1321} have been identified as autophosphorylation sites of both the purified receptor and its cloned cytoplasmic kinase domain (105). Other studies have reported the absence of autophosphorylation (13,106-109) or substrate phosphorylation (33,110,111) on serine residues. Possible sources for this discrepancy include the existence of a tightly associated serine kinase, discussed below, and the reaction conditions employed by Klein and co-workers (105), which employed the artificial stimulatory agent poly-lysine.

Molecular mechanism of IR Autophosphorylation

The literature contains conflicting reports of the molecular mechanism of insulin receptor autophosphorylation. There are three possible molecular mechanisms of autophosphorylation in the IR holomer, which are illustrated in Figure 1-2. The standard method of distinguishing among these reaction methods is a study of the enzyme concentration dependence of autophosphorylation. This technique, introduced by Todhunter & Purich in the study of the cyclic AMP dependent protein kinase (cAPK) (112), has since been used to study many protein kinases, including *trans*

autophosphorylation in the EGFR (113), *trans* activation of Src (114), *cis* activation in cGMP dependent protein kinase (cGPK) (115), or both in the kinase domain of Trk (116), phosphorylase kinase (117), and calcium/calmodulin dependent protein kinase (CaMK)-II (118). Many groups have found that autophosphorylation of the IR is intraholomeric by this method (13,59,119-121). Alternative methods with tetrameric receptors have also been used. IR tetramers with covalently linked insulin are capable of phosphorylating ligand-free tetramers, but this phosphorylation has no apparent effect on the target IR (122). Another study has observed that insulin binding-deficient IR becomes able to bind IRS-1 after exposure to insulin-binding insulin receptors, arguing that *trans* autophosphorylation does have an effect (123). Thus, the preponderance of evidence argues in favor of intraholomeric autophosphorylation in the insulin receptor.

Distinction between the two possible intraholomeric pathways described in Figure 1-2 requires further effort, since none of the above studies could distinguish between intraholomeric *cis* autophosphorylation (within a β subunit) or intraholomeric *trans* autophosphorylation (between two β subunits). Because the two β subunits are covalently linked, their apparent concentration relative to one another is fixed by the structure of the holomer. This concentration, and therefore the rate of autophosphorylation, is independent of the concentration of the holomer in the bulk solution for either *cis* or *trans* intraholomeric autophosphorylation.

A solution to this problem uses the CKD, which has been shown by several criteria to be a good model for the basal state of the native IR (75,124). Studies using CKD rather than tetrameric IR have the advantage that the concentration of CKD can be

varied to distinguish between *cis* and *trans* autophosphorylation, as shown schematically in Figure 1-3. In a *cis*, or intramolecular, autophosphorylation event, there is no interaction between kinase molecules. The rate of formation of phosphorylated CKD (P-CKD) is then expected to depend linearly on the concentration of CKD, so that the ratio P-CKD/CKD (the stoichiometry of autophosphorylation) would be constant with respect to CKD concentration. In contrast, a *trans* molecular mechanism, where one kinase molecule phosphorylates another, requires interaction between kinase molecules, so that formation of P-CKD would be expected to have a second order dependence on total CKD concentration. The stoichiometry of autophosphorylation would then show a linear dependence on CKD concentration. Thus, this technique is able to differentiate between the two simplest mechanism of autophosphorylation. However, studies using this method have presented conflicting observations of CKD autophosphorylation: An exclusively *trans* pathway was observed by Cobb *et al.* (125) and Wei *et al.* (126), but others reported only a *cis* pathway (127,128).

Other techniques have been used to address the problem in the intact tetrameric receptor. Shoelson and co-workers (129) used trypsin-truncated receptors, which consisted of an intact β subunit bound to a fragment of the α subunit (α'β), to identify an activation process as *cis* autophosphorylation. DTT-generated complete αβ halves, however, appeared to proceed *via* a *trans* pathway. Frattali *et al.* (130) also found both *cis* and *trans* autophosphorylation, using $\alpha_2\beta_2$ receptor tetramers with one β-subunit made kinase-minus by mutagenesis. Thus, both *cis* and *trans* autophosphorylations have been

observed in the IR and its CKD. Progress towards the resolution of this apparent conflict will be the subject of Chapter 4.

Ser/ Thr Phosphorylation of the Insulin Receptor

The IR has been observed to be defective in autophosphorylation and substrate phosphorylation in non-insulin dependent diabetes mellitus (NIDDM), a major disorder of the insulin axis that will be discussed further below. Serine phosphorylation of the IR occurs and has been postulated to be responsible for this inhibition. The IR in the basal state is predominantly phosphorylated on serine and threonine (9,45,101,109,131-133). Serine phosphorylation is also insulin stimulated (in intact cells) according to some (9,64,131,132) but not others (45,101,109). Serine phosphorylated receptors autophosphorylate more slowly on tyrosine both *in vivo* and *in vitro* (132,134,135) and do not activate (134) or internalize (136) normally. Impaired IR functioning in both women with polycystic ovary syndrome (137) and streptozocin treated rats (138) has also been attributed to S/T phosphorylation and is corrected by treatment with alkaline phosphatase (138,139). In contrast, dephosphorylation with tyrosine-specific phosphatases deactivates the enzyme (57,58). S^{1090} was identified as an *in vivo* insulin stimulated site (140), and possible serine autophosphorylation may occur as described above, but no clear linkage has been made between any single site of serine or threonine phosphorylation and regulation of the IR.

Possible Regulation of the IR by Other Kinases

Several labs have produced a clearer, but still incomplete picture, of IR modulation by protein kinase C (PKC), a well-known Ser/Thr protein kinase. This enzyme has been observed to directly phosphorylate the IR (141) and its CKD (142) *in vitro*. T^{1348} (143,144) and $S^{1035/7}$ (145) have been identified as PKC phosphorylation sites, both *in vivo* (*via* TPA stimulation) and *in vitro*. Additionally, S^{1327} has been identified as stimulated by phorbol esters *in vivo* (146-148). Phorbol esters inhibit insulin signal transduction (149-151), and this effect is reversed by dephosphorylation of subsequently partially purified receptor (149). Overexpression of protein kinase C led to 3-4 fold stimulation of basal IR phosphorylation, at $S^{1305/6}$, T^{1348} and several other unidentified sites. This blocked insulin-dependent PI-3 kinase activation (152). Thus, PKC has been proposed to be responsible for reduced receptor autophosphorylation and signal transduction despite genetically normal receptor in NIDDM (153).

The above observations suggested an inhibitory role for phosphorylation at T^{1348} or $S^{1305/6}$. While mutagenesis of T^{1348} to neutral or negative residues abolished most insulin-stimulated threonine phosphorylation, this was found to have little effect on insulin-dependent autophosphorylation or tyrosine kinase activity (154,155). Moreover, receptors with a C-terminus truncation lacking T^{1348} were found to be just as susceptible to phorbol ester inhibition as the wild-type receptor (156,157). Other reports describe no difference in S^{1327} or T^{1348} phosphorylation between NIDDM patients and normal controls, and very low stoichiometries of phosphorylation of either site (<6% phosphorylated), while confirming the inhibited tyrosine autophosphorylation of IR derived from NIDDM

patients (158). S^{967-8} in the juxtamembrane region were also identified as insulin- and phorbol ester- stimulated phosphorylation sites (159). However, their mutation to Ala, or removal by deletion, did not alter kinase activation in response to insulin or the inhibitory effects of phorbol esters or glucose on the IR (156,159). While PKC may play a role in inhibiting the IR, direct phosphorylation of the IR may thus not be the causal mechanism (160).

The existence of a closely associated serine kinase was first postulated upon observing the loss of serine kinase activity during progressive purification of the IR (161). Insulin-stimulated cell extracts were able to serine phosphorylate partially purified IR, which itself autophosphorylated only on tyrosine residues (107,162). When copurified with the IR, this kinase phosphorylates the IR on $S^{1305/1306}$ (163,164). This activity can be separated and reconstituted (165) from the IR, and has been purified as a distinct 40kDa protein closely associated with the IR (166), indicating the absence of serine kinase activity in the IR. A second (possibly identical) insulin-receptor associated serine kinase has been identified by another group (167).

The insulin receptor has been described as a substrate for several other protein kinases. cAPK, casein kinase (CK)-1, CK-2, and Src have all been reported to phosphorylate and/or modulate activity of the IR (168-172). However, others have reported that the IR is not an *in vitro* substrate for CK-I, CK-II or cAPK (173,174). No conclusive role for these kinases has been established.

The Insulin Receptor in Health and Disease

Molecular Processes of the Insulin Receptor: Signaling and Cycling

The importance of the insulin receptor's kinase activity points to a role for tyrosine phosphorylation in insulin signal transduction. The first known substrate of the receptor, as discussed on page 2, was the receptor itself. The next major substrate, IRS-1 was first discovered using anti-phosphotyrosine antibodies (175), and the cDNA structure of this protein (176) revealed multiple potential IR phosphorylation sites. IRS-1 docks to the JM region of the IR directly *via* its PTB domain, as discussed above, and is additionally targeted to the membrane compartment by its pleckstrin homology (PH) domain (177).[1] This PH targeting plays a role at least as important as PTB docking, but both are probably required for *in vivo* signaling at physiological quantities of IRS-1 and IR (178,179). Tyrosine-phosphorylated IRS-1 has since been found to serve as a docking protein for many downstream effectors of the insulin signal, including GRB2/Sos (which activates the GTP exchange of $p21^{ras}$) (180,181), PI-3 kinase (182,183), the protein tyrosine phosphatase Syp (184), and others. These proteins bind to specific phosphorylation sites on IRS-1 *via* phosphotyrosine-binding SH2 domains, and this leads to their activation (185,186). Shc is also phosphorylated by the IR, leading to its association with Grb2/Sos. This further links the IR to the growth promoting effects of $p21^{ras}$ and the microtubule associated protein (MAP) kinase pathway (reviewed by Graves *et al.* (187)).

---

[1] See Lemmon *et al.* for a review of PH domains (453)

The IR is unusual among growth factor receptors in relying on a separate protein, IRS-1, to dock most effector molecules. Receptors for other growth factors (such as EGFR and the platelet-derived growth factor receptor (PDGFR)) bind effector molecules directly *via* SH2 domain interactions with autophosphorylation sites on these receptors. Recently, the IR has been found to dock two non-IRS signaling molecules directly: GRB-IR (188) and GRB-IRβ (189). Docking of these molecules is a complex process, involving both SH2 and PH domains binding to both the JM and AL regions. A second intermediate docking protein, Gab-1, plays a similar role to IRS-1 and is also a substrate (190).

The IR- IRS-1 relationship is not an exclusive one. Mice homozygous for IRS-1 deletion showed a minimal phenotype of moderately elevated glucose and reduced birth weight (191,192), but were not overtly diabetic. This was found to be due to alternative signaling through a closely related molecule, IRS-2 (originally termed 4PS), which is also a substrate for the IR and has extensive homology to IRS-1 (193). IRS-2 is the major IRS protein of hematopoetic cells (194), where its phosphorylation can be stimulated by a number of other cytokines including IL-4 (195) and interferons (196,197) using other protein tyrosine kinases, such as Tyk-2, JAK-1 and JAK-3. IRS-2 can also substitute for some of the roles of IRS-1 in NIDDM (198). IRS-1 can also be phosphorylated by the IGF-I receptor (199), which has close sequence homology to the IR and promotes many of the same effects. The IRS-1 signaling system has been extensively reviewed (185,186,200). IRS-3 and IRS-4, two new proteins with significant homology to IRS-1

that are also rapidly tyrosine phosphorylated in response to insulin, were also recently identified (201,202).

Insulin receptor is rapidly moved to an intracellular compartment upon insulin binding. This translocation can be reversed by insulin withdrawal, but prolonged presence of insulin leads to the destruction of the internalized IR and downregulation of IR at the cell surface (203). Thus, the receptor ordinarily has a half-life of about seven hours in 3T3-L1 adipocytes, which decreases to three hours in the continuous presence of insulin (204-206). This internalization of insulin receptor leads to the destruction of bound insulin, but the IR can be returned to the cell surface. Acidification of the endocytic vesicles is required for both insulin degradation and IR recycling (207). This internalization process appears to require structural features of the juxtamembrane region of the kinase, as discussed above.

Disease Processes of the Insulin Axis: Leprechaunism and Rabson-Mendenhall Syndrome

One of the prime motivators for the active study of the insulin receptor has been its possible role in human health and disease. Although diabetes is by far the most common defect in the insulin signaling system, the relationship of IR function to disease has been most clearly delineated in rare genetic (germ-line) disorders of the receptor. Most mildly, Type A insulin resistance is characterized by poor metabolic response to insulin, acanthosis nigricans and hyperandrogenism, which correlate with low (15-50% of normal) tissue insulin binding capacity (208-210). This disorder was found to be hereditary, implicating a genetic defect in the IR (211) which was eventually found in

most patients (212). Type A patients are frequently heterozygotes for the IR gene, and many different mutations in the IR have been found that cause this syndrome.

More severe mutations in the IR gene lead to leprechaunism and Rabson-Mendenhall syndrome, both characterized by acanthosis nigricans, severe insulin resistance, pineal hyperplasia, growth retardation, dental abnormalities and early death (213,214). Like Type A insulin resistance, these diseases were traced to a primary defect in insulin receptors (210,215) and patients are typically double mutants (homozygous or compound heterozygous) in the IR gene (212,216-220). Similar symptoms have been observed in genetically engineered mice (221,222) and fruit flies (223,224) with double mutations in their insulin receptor genes. In contrast, point mutations in the sole insulin receptor family member in *C. elegans* actually *prolong* the lifespan of this organism, secondary to slowed metabolism (225). The poor growth of receptor-deficient patients illustrates insulin's role in development as a key growth hormone in at least mammals.

Disease Processes of the Insulin Axis: Diabetes Mellitus

The best-known disorder of the insulin axis is, of course, diabetes mellitus, which affects 2.5-7.5% of the US population. Insulin-dependent diabetes mellitus (IDDM), or juvenile diabetes, is due to a pancreatic defect in insulin secretion and is not associated with primary abnormalities of the IR. These patients respond normally to, and are dependent on, insulin therapy, acting *via* functional insulin receptors. Antibodies against the IR can also cause insulin resistance (208,226-229). In both cases, the underlying insulin receptors are normal.

Non-insulin dependent diabetes mellitus (NIDDM) is much more common than IDDM (>80% of total diabetes cases), and tends to affect older, obese patients. Although usually genetically normal (212,230,231), insulin receptors in NIDDM patients are nevertheless functionally abnormal. These receptors are defective in insulin-dependent autophosphorylation and phosphorylation of IRS-1 (232-234). Obese (132) or diabetic (235) mice also have retarded receptor autophosphorylation. Several mechanisms have been proposed to explain these observations, including inhibition of the IR's kinase activity by PKC-induced serine phosphorylation (discussed above). More recently, multiple roles for TNF-α in NIDDM pathogenesis have been identified (236). IRS-1, when phosphorylated on serine, may be an inhibitor of the IR (237-239). A structural understanding of this phenomenon awaits further definition and study of the possible interaction between serine phosphorylated IRS-1 and the IR.

The Insulin Receptor and Oncogenesis

Growth factor receptors have often been implicated in cancer, and the IR is no exception. This can occur by two general mechanisms: overexpression of a normal receptor, or alteration of the receptor into a constitutively active form. Upregulation of normal IR has been observed in many patients with breast cancer (240). In breast-cancer derived cell lines, these receptors appear to have normal insulin-dependent kinase activity (241) and insulin-stimulated thymidine uptake into DNA, indicating that insulin may promote cancer growth (241). 3T3 and CHO cells overexpressing IR show a ligand-dependent transformed phenotype (242). Roles for IR have also been proposed in colon cancer (243) and a murine lymphoid T-cell leukemia. The IGF-IR has a much more

prominent role in several human cancers, including Wilm's tumor, osteogenic sarcoma, rhabdomyosarcoma, and many others (reviewed in (244)).

Strangely, no oncogenic mutations of the IR have been reported in humans. Still, the studies of L.H. Wang and coworkers have demonstrated that mutant insulin receptors do have oncogenic potential. v-*ros* (pp68$^{gag\text{-}ros}$) was originally discovered as a viral oncogene in avian sarcoma virus (245), and its cellular homolog c-*ros* appears to be a monomeric transmembrane receptor tyrosine kinase (246,247). The viral form of the enzyme has alterations which leave it constitutively active, while the native protein shows only low levels of tyrosine kinase activity in the absence of its (unknown) ligand (247,248). First, the extracellular domain has been replaced with a viral *gag* sequence. This *gag* sequence is essential for the transforming activity of the gene; altered viruses encoding only the transmembrane and intracellular portions of ros without the *gag* protein are not transforming (249). Second, a three amino acid insert is present in the transmembrane domain of the protein. The membrane insertion is also important to the transforming activity of the oncogene; removal of this insertion causes loss of transformation, IRS-1 phosphorylation and PI3K activation, but not Shc phosphorylation, membrane localization, or tyrosine kinase activity (250).[2] Replacement of the ros sequence in pp68$^{gag\text{-}ros}$ with the IR kinase domain can lead to a transforming retrovirus, with no further mutations in the kinase domain of the IR (251,252). Trypsin treatment of cells also mimics insulin signaling, suggesting that the extracellular α subunits play an inhibitory role (253). How *gag* fusion activates the kinase domains of these constructs is

unknown, but it is unrelated to dimerization potential of the extracellular gag sequence. $pp68^{gag\text{-}ros}$ and its IR cognate are monomers, and alterations of the *gag* domain that prevent dimerization do not change the transforming potential of this protein or $pp68^{gag\text{-}IR}$ (254).

The IR thus plays a role in two broad categories of disease: the metabolic regulation of glucose homeostasis (diabetes) and developmental disorders due to loss of function (leprechaunism and Rabson-Mendenhall syndrome) or overexpression (cancer). These disease processes correspond to dysfunction in the metabolic/transport and growth signaling pathways of the insulin receptor outlined in Figure 1-4.

The Insulin Receptor's Place in the Family of Protein Kinases

The first protein kinase identified, phosphorylase kinase, was found by Krebs & Fischer (255) as an outgrowth of the classic glycogen metabolism studies of Cori & Cori. This enzyme was identified by its ability to activate phosphorylase, and its regulation quickly became an active area of study. Phosphorylase kinase was found to be activated by cAMP (256) *via* a second kinase, the cAMP-dependent protein kinase (cAPK; also called protein kinase A, or PKA) (257,258). Since their discovery, the protein kinase family has expanded to at least several hundred members today (18), involved in information transmission in almost every part of the cell. The study of autophosphorylation in the IR is in a sense a continuation of these early studies of E. H.

---

[2] A third small mutation at the C-terminus of the protein, appeared to play no role in the transforming activity of the protein. (248).

Fischer, E. G. Krebs, B.E. Kemp, D. A. Walsh, and co-workers. In this and the following section, we will review the IR's relation to other protein kinases in terms of structure, function, and regulation. This will provide a framework for designing and understanding the effects of site-directed mutagenesis of the insulin receptor's CKD.

Almost all protein kinases, including the IR, share a conserved catalytic core (1,17,19). On the basis of primary structure within this core, kinases can be divided into four general groupings (18). The first three of these phosphorylate proteins on Ser or Thr (S/T kinases), and the fourth includes the protein tyrosine kinases (PTKs). Among tyrosine kinases, the family of receptor tyrosine kinases (RTKs) is distinguished by the presence of a transmembrane domain and extracellular ligand binding region. RTKs enzymes have been further classified according to the structure of their extracellular domain (259). The insulin receptors' place in the hierarchy of protein kinases is illustrated in Figure 1-5.

The Insulin Receptor Family

As shown in Figure 1-5, the IR is a prototype for subclass IV RTKs (260). In humans, these include the IR, IGF-IR, and insulin receptor related receptor (IRR). More distantly, the insulin-like peptide receptor (ILP-R), mollusk insulin-related peptide receptor (MIP) and DAF-2 have been identified in other species. The $\alpha_2\beta_2$ structure of subclass IV proteins, illustrated for the insulin receptor in Figure 1-1, is unique among the RTKs. Because of this, the activation process of the IR is unique as well.

The insulin receptor shows strong homology between species. For example, insulin from the Atlantic hagfish can stimulate human insulin receptors (261,262). Even

Drosophila has an insulin receptor (263-265) and it also an essential growth factor receptor in this organism (223.224). Avian insulin receptors are also closely homologous to mammalian receptors (266). More distant relatives such as MIP and DAF-2 are as closely related to the IR as they are to the IGF-IR. Most likely, all of the subclass IV RTKs are descended from a common ancestor.

After the insulin receptor itself, the IGF-IR is the best-characterized member of subclass IV. This receptor has also been demonstrated to have tyrosine kinase activity (267.268) and ligand-dependent activating autophosphorylation of its β subunit (269). IGF-IR also uses IRS-1 as a substrate (199). The IRR (270) shows strong homology but binds some other ligand (271).

These receptors are also activated by autophosphorylation at their activation loop, and their juxtamembrane autophosphorylation sites are closely conserved, as shown in Table 1-1. Y^{965} is not as conserved as Y^{972} in invertebrate species

Table 1-1 Conservation of the Juxtamembrane Region in Subclass IV RTKs.

Subclass IV RTKs from various species are shown, grouped by ligand type. The highly conserved tyrosine phosphorylation site Y^{965} and the universally conserved site Y^{972} (numbered according to the IR), are highlighted in **red** and marked with an arrow (↓). The positively charged stop membrane insertion sequence is boxed, and separates the transmembrane domain (underlined) from the intracellular portion of the β subunit. In the case of the IRR and the invertebrate kinases, the ligand is not yet known. All of these receptors also contain tyrosine kinase consensus domain, beginning around human IR residue 993, and the activation loop autophosphorylation motif MTRDXYETDY^{1162}YRKG, where X = V or I. Sequences were aligned using PILEUP (280).

Table 1-1 Conservation of the Juxtamembrane Region in Subclass IV RTKs.

Receptor	Sequence	Ref.
Insulin receptors	↓ ↓	
Human	FSVVIGSIYLFLRKRQPDG.PLGPLYASS NPEY LSASDVFPCSVYVPDEW	(1)
Mouse	FSVVIGSIYLFLRKRQPDG.PMGPLYASS NPEY LSASDVFPSSVYVPDEW	(71)
Rat	FSVVIGSIYLFLRKRQPDG.PMGPLYASS NPEY LSASDVFPSSVYVPDEW	(272)
IGF-I receptors		
Human	VGGLVIMLYVFHRKRNNSRLGNGVLYASV NPEY FSAAD.....VYVPDEW	(273)
Bovine	VGGLVIMLYVFHRKRNSSRLGNGVLYASV NPEY FSAAD.....VYVPDEW	(274)
Frog	LVGIISIVCFVFKKRNSNRLGNGVLYASV NPEY FSAAE.....MYVPDEW	(275)
Rat	VGGLVIMLYVFHRKRNNSRLGNGVLYASV NPEY FSAAD.....VYVPDEW	(276)
IRR receptors		
Human	LIVLAALGFFYGKKRN......RTLYASV NPEY FSASD.....MYVPDEW	(270)
Guinea Pig	LIILAALGFFYSRKRN......GTLYTSV NPEY LSASD.....MYIPDEW	(270)
Invertebrate receptors		
C. elegans DAF-2	MSIAGCIIYYYIQVRYGKKVKALSDFMQL NPEY CVDNK......YNADDW	(225)
D. melanogaster IR	LIVSLFGYVCYLHKRKVPSNDLH.MNTEV NPFY ASMQ.......YIPDDW	(264)
ILP-R	LAVIFGIWYCTKKRFGDKQMPNGVLYASV NPEY MSSDD.....VYVPDEW	(277)
Mollusk MIP-R	VSLIVACVYYKQKIRSDD.....MTVISR NMNY VPSE.....ILYISDEW	(278)
Mosquito IR	FLCSVGFVAFYWYKYKYMSKQIR.MYPEV NPDY AGVQ.......YKVDDW	(279)

Other Receptor Tyrosine Kinases

The other subclasses of RTKs in Figure 1-5 have distinct extracellular domain structures. These RTKs have a single transmembrane domain and, usually, a single polypeptide chain. Some dimerize in response to a conformational change induced by binding of monomeric ligand molecules (subclass I), others dimerize in response to dimeric ligand (subclass III). In each case, ligand-dependent dimerization is responsible for signal transduction *via trans* autophosphorylation, illustrated for Kit in Figure 1-6. Many, but not all, of these other receptors are activated by *trans* autophosphorylation at the activation loop (the EGFR family being a notable exception). Effector docking is primarily *via* SH2 domain interaction with the autophosphorylated kinase domain, rather than primarily *via* IRS-1 as in the IR.

Structure and Function of the Insulin Receptor's Kinase Domain

The cAMP Dependent Protein Kinase as a Reference Point for the Protein Kinase Family

cAPK has long been used as a paradigm for the protein kinase family. The enzyme was the second protein kinase to be identified, but the first to have autophosphorylation sites mapped (281) and the first to be crystallized (282,283). No other protein kinase has been studied as extensively as cAPK. Because of the conservation of the conserved kinase domain, many of the features first deduced in cAPK are applicable to the entire protein kinase family, including the insulin receptor. A

homology table showing a sequence alignment of the kinase domain of the IR with the catalytic subunit of cAPK is shown in Figure 1-7.

The kinetic mechanism of cAPK has been subject to intensive scrutiny. Early studies (284-286) demonstrate several interesting features of the enzyme. The enzyme appears to have a steady state random kinetic mechanism; its maximal catalytic rate (k_{cat}) of 21 s^{-1} is still among the fastest protein kinases known. However, initial binding of peptide substrate leads to a nonproductive E•S complex which can bind ATP but must isomerize to the active form of the enzyme before catalysis can occur. This isomerization step, which can be rate-limiting, causes the peptide substrate inhibition (287) that has been observed by several groups with this enzyme (285,286) (but not the IR). In may be that ATP prebinding directs productive association of peptide substrate (283,287). The product ADP (K_i 10μM) but not phosphorylated peptide (K_d > 1mM) inhibits the enzyme (285), and ADP release appears to be the rate limiting step in catalysis (284,286,287). In tyrosine kinases, phosphoryl transfer is also a rate limiting step (288,289)

Several residues have been found to be key in the catalytic mechanism of cAPK. Mutation of a conserved lysine residue in the ATP binding site (K^{72}) leads to a three orders of magnitude drop in catalytic rate. Mutation of the homologous lysine residue in the IR (K^{1030}) also abolishes kinase activity and signaling (30,290). Although often thought of as preventing ATP binding, mutation of this residue actually impairs catalysis instead (291) by inducing nonproductive ATP binding (292). A nucleotide binding loop with a consensus sequence of GXGXXG is also present in the small lobe of every eukaryotic protein kinase (18-20).

The reaction mechanism appears to proceed by in-line nucleophilic displacement, possibly using D^{166} as a general base catalyst. This residue is positioned correctly for its proposed role in every active protein kinase crystal structure so far (283,293-295) and an Asp at this position is universally conserved in the protein kinase family (18). The equivalent residue in the IR is D^{1132}. Despite its proposed role, mutation of cAPK residue D^{166} to alanine is less inactivating than the mutation of the conserved lysine residue K^{72} (296) and the expected dependence of k_{cat} on pH has not been observed (297). Similar questions have been raised in kinetic studies of the tyrosine kinase Csk (298). Flourotyrosine, which is more easily ionized than tyrosine, shows a similar k_{cat}/K_M ratio to tyrosine-containing gastrin but lower values of both k_{cat} and K_M compared to unmodified gastrin (299). These observations have led these investigators to question whether D^{1132} is actually a catalytic base at all, or whether some other mechanism is involved in phosphoryl transfer.

Like the other protein kinases in Table 1-2, the cAPK's catalytic function is modulated by phosphorylation in the activation loop, at T^{197} (300,301). This residue is homologous to Y^{1162} and/or Y^{1163} in the IR (Figure 1-7). T^{197} is constitutively autophosphorylated *in vivo* and is very resistant to phosphatase treatment *in vitro*, indicating it is inaccessible to phosphatases, extensively stabilized, or both (302). Mutation of this residue to Ala reduces the rate of catalysis up to 500-fold, specifically by reducing the rate of phosphotransfer at the active site (300). Although substitution with Asp (which retains the negative charge) does not change the overall k_{cat} of the enzyme, it does reduce the rate of phosphotransfer 20-fold, which manifests itself as an elevated $K_{M,Peptide}$ (300). This does not reflect reduced peptide binding to the active site. A

negatively charged amino acid can thus partially substitute for phosphothreonine at this position, as it can for the homologous residues S^{218} in Mek1 (303) T^{500} in PKC (304).

Neither Asp nor Glu appears to substitute for phosphotyrosine at Y^{1162} in the IR, however, probably reflecting the much greater length of phosphotyrosine relative to these residues (73).

Table 1-2 Kinases Activated by Phosphorylation in Subdomain VIII.

Kinase	Cat.	Sequence	Ref.
IR	RTK-IV	DFGMTRDIYETDY^{1162}YRKGGKGLLPVRWMAPE	(62)
Lck	NRTK	DFGLARLIEDNEY^{394}TAREGAKFPIKWTAPE	(305)
Src	NRTK	DFGLARLIEDNEY^{416}TARQGAKFPIKWTAPE	(306)
TRK	RTK-I	DFGMSRDIYSTDY^{503}YRVGGHTMIPIRWMPPE	(307)
PDGFR	RTK-III	DFGLARDIMRDSNY^{857}ISKGSTFIPLKWMAPE	(308)
IGF-IR	RTK-IV	DFGMTRDIYETDY^{1135}YRKGGKGLLPVRWMSPE	(310)
CaMK-IV	S/T	DFGLSKIVEHQVLMKTVCGT^{196}PGYCAPE	(311)
cAPK-Cα	S/T	DFGFAKRVKGRT^{197}WTLCGTPEYLAPE	(301)
cdk-2	S/T	DFGLARAFGVPVRTYT^{160}HEVVTLWYRAPE	(312)
ERK-2	S/T	DFGLARVADPDHDHTGFLT^{183}EY^{185}VATRWYRAP E	(313)
PKC-α	S/T	DFGMCKEHMMDGVTTRT^{497}FCGTPDYIAPE	(314)
FGFR-3	RTK	DFGLARDVHNLDY^{583}YKKNGRLPVKWMAPE	(315)

This table shows a partial list of enzymes requiring phosphorylation in subdomain VIII for activation. The categorization of each kinase is also listed, according to Figure 1-5.

The general applicability of the catalytic machinery of cAPK to other kinases is indicated by the universal conservation of its key catalytic residues, as established by

Hunter and co-workers. Recent evidence suggests that a similar mechanism may be even more widely applicable. APH(3')-IIIa, a prokaryotic aminoglycoside kinase involved in antibiotic resistance, shows a very closely homologous three-dimensional structure, despite an almost total lack of primary structure homology (316). The putative catalytic base and the homolog of cAPK residue K^{72}, but not the GxGxxG motif, are still conserved in this structure.

Kinase Regulation Occurs by Multiple Methods

Although all eukaryotic proteins conserve the key catalytic residues mentioned above, and appear to use the same enzymatic mechanism of phosphorylation, their methods of regulation vary widely. As with most proteins, kinase activity is regulated at the level of protein expression. Some kinases, such as cAPK, are involved in "housekeeping" chores and are expressed in nearly every tissue. Others, such as the product of the Drosophila *sevenless* gene, are restricted to a subset of ommatidial precursors in the developing eye (317,318). The IR itself is expressed in virtually every tissue, although at varying levels, with the highest concentrations in liver, fat, and muscle tissue (up to several hundred thousand receptors per cell) (186).[3] IR expression levels also vary in response to insulin levels, chiefly by modulation of degradation of the receptor. Forms of regulation more specific to protein kinases include enzyme quaternary structure, intrasteric regulation, and regulation by phosphorylation. Each of these methods has relevance to the regulation of the insulin receptor by insulin.

---

[3] Note that cell culture systems transfected with IR cDNA frequently express up to several *million* receptors per cell (454), a potential distortion of the IR signaling system that is sometimes overlooked.

Kinase Regulation by Quaternary Structure

Once expressed, the activity of protein kinases can be further modulated by their subunit composition. Unlike other classes of enzymes, such as G proteins (319), no evidence for direct participation by residues outside of the catalytic core has been made. The protein kinase catalytic core is a self contained unit whose intrinsic activity is modulated by, but not intrinsically dependent on, the addition of other subunits. Inhibitory subunits, such as the R subunits of cAPK, can be released by ligand binding, leaving the kinase domains uncomplexed and active (illustrated in Figure 1-8; reviewed in (320)). Addition of a subunit, whose availability can be regulated, can also be required to activate a basally inactive kinase. For example, cyclin addition to cyclin-dependent kinase (cdk)-2 is one of several regulatory mechanisms in this enzyme, and allows the active site of the enzyme to configure itself for catalysis. The insulin receptor itself may be inhibited by the membrane glycoprotein PC-1 (321) or serine-phosphorylated IRS-1 (238), although no structural basis for these interactions has yet been elucidated. However, oligomerization of the intrinsic subunits of RTKs is itself a key regulatory feature in this class of enzyme, as illustrated for Kit in Figure 1-6. Ligand-dependent dimerization of many growth factor receptor tyrosine kinases potentiates further activation and/or signal transduction by autophosphorylation. Subclass IV RTKs such as the IR are the exception to this rule, since they are "pre-dimerized" by disulfide bonds, even in the absence of insulin (Figure 1-1). Thus, regulation by quaternary structure does *not* appear to apply to the IR, which must be activated by other means in response to insulin.

Kinase Regulation by Tertiary Structure

Inhibition of a kinase molecule by an inhibitory conformation of portions of the same molecule is termed intrasteric inhibition (reviewed by Kemp & Pearson (322)). This may occur, for example, by occlusion of the active site by a pseudosubstrate, defined as a protein sequence which conserves the binding sequences of *bona fide* substrates but lacks the actual phosphate acceptor. CaMK- I, II, IV, and V each has a pseudosubstrate in their C-terminus; this region is removed from the active site by binding the calcium/calmodulin complex (whose affinity is regulated by the presence of Ca^{++}). Pseudosubstrates do not have to be comolecular with the active site; they can be part of another regulatory subunit or even free-standing inhibitory peptides (323). Nor does all intrasteric inhibition occur *via* pseudosubstrate mechanisms. As strikingly demonstrated in recent X-ray crystallography studies in the *src* family of nonreceptor tyrosine kinases (NRTKs) (324,325), intrasteric inhibition does not necessarily require occlusion of the active site but can instead involve distortion of catalytic center into an open, inactive form.

Since ligand-dependent dimerization does not occur in the IR, researchers have turned to other means of exploring the conformation of the receptor and ligand-dependent changes. The detailed structure of large membrane proteins is notoriously hard to study. Gross conformation changes in the IR upon insulin binding have been demonstrated by altered α-subunit crosslinking (326), altered proteolysis of cell-surface receptors (327,328), and altered tyrosine fluorescence (329). These methods did not allow detailed

assessment of structure, however. An additional level of refinement has been allowed by the use of anti-peptide antibodies targeted against specific regions of the IR. ATP and insulin, for example, both alter the binding of antibodies to the CT region (330,331) and the AL (332).[4] Thus, insulin- and ATP- dependent conformational changes both occur in the IR.

Kinase Regulation by Phosphorylation ("Primary Structure")

As mentioned on page 5, autophosphorylation plays a dominant role in insulin receptor regulation. Phosphorylation was the first method of protein kinase regulation to be discovered and is perhaps the most general, with potential to alter quaternary, tertiary, and secondary structure. Phosphorylation-induced structural changes can either alter or inhibit protein kinases. Phosphorylation of S^{30} in phosphorylase kinase (333), or $T^{14}Y^{15}$ in cdk-2 (334) directly blocks the ATP-binding sites of these kinases (335,336). Inhibitory phosphorylations can also act by stabilizing inhibitory portions of the kinase. Basal (Ca^{++}/CaM independent) autophosphorylation of CaMK-II at Thr^{306}, in its calmodulin binding domain, blocks subsequent calmodulin binding and calmodulin-dependent relief of autoinhibition (337). The intrasteric inhibition of Src mentioned above is dependent on what is perhaps the best-known inhibitory phosphorylation event, at Y^{527}. Phosphotyrosine at this position allows for the intramolecular interaction with the SH2 domain of Src that locks the enzyme in an inactive conformation. This interaction further prevents the SH2 domain from docking other signaling molecules. In each of

---

[4] Modulation of binding to the JM region also occurs, and will be discussed in the context of a model for IR activation in the Discussion.

these mechanisms, mutation of the phosphate acceptor to Ala (or Phe) is expected to prevent inhibition. $Y^{527}F$ mutants of Src, for example, are activated oncogenic tyrosine kinases (338-340). Deletion of the region containing the inhibitory site distinguishes between the two forms of inhibition: removal of the ATP binding site in phosphorylase kinase would probably render it inactive, while removal of pseudosubstrates relieves inhibition. None of these cases appears to apply to the IR, as no specific site of phosphorylation has been conclusively associated with receptor inhibition.

Stimulatory phosphorylations fall into two general categories: those that promote correct alignment of the catalytic center, and those that eliminate a pseudosubstrate site.[5,6] These correspond to basal state inhibition by distortion or occupation of the active site, respectively, and instances of both methods are known. As will be discussed further later on, pseudosubstrate domains in Type Iβ cGMP dependent protein kinase (cGPK) (115) and the CaMK family (341) are also removed by phosphorylation. Phosphorylation of many protein kinases, including the IR, in subdomain VIII is known to be required for full activity and will be discussed separately below. In either case, one expects that mutation of the phosphate acceptor site (to F or A, as appropriate) will prevent activation. However, *deletion* of the region containing the acceptor will either lock the catalytic center in an inactive state or destroy the pseudosubstrate, resulting in activation or

---

[5] Phosphorylation also frequently creates docking sites for substrates in RTKs, as discussed on page 14, and this is also a necessery component of their signal transduction. This does not activate the kinase activity of the receptor, but rather modulates the availability of substrate.

[6] There are no known cases where enzymatic phosphotyrosine or phosphoserine participates catalytically in eukaryotic protein kinases.

inhibition of the kinase, respectively. Thus mutagenesis can be used to distinguish the method of inhibition in the basal state.

Phosphorylation has several features recommending it as a method of kinase control. First, phosphorylation and phosphorylation-dependent activation can persist after removal of small molecule control elements, such as Ca^{++}. This is thought to be crucial, for example, in the role of CaMK-II in stimulating long-term potentiation in the hippocampus (342). If one kinase molecule of the multimeric complex is dephosphorylated or replaced, its neighbors can quickly rephosphorylate it. Moreover, protein kinases can potentially phosphorylate themselves, reducing the requirement for other enzymes in the signal cascade. If another protein kinase *is* used, such as in the well-known MAP kinase cascade (reviewed in (187)), this allows for amplification of a signal as well.

Protein kinases are often regulated by multiple methods. The cyclin dependent kinase (cdk) family, for example, are regulated by the availability of their cyclin counterparts, which vary with the cell cycle; phosphorylation at their activation loop; and are additionally inhibited by binding of several other proteins (reviewed by Morgan (343)). After calcium binding has released the pseudosubstrate domain in CaMK-II, phosphorylation of this region renders the enzyme calcium-independent; but basal autophosphorylation at the same sites prevents calmodulin binding and activation. In the insulin receptor, only one major regulatory mode has been given a structural basis: activation by autophosphorylation at the AL.

Activating Phosphorylation in the IR: The "Activation Loop"

The best-known mode of regulation of the insulin receptor is autophosphorylation of its activation loop, in subdomain VIII (shown in Figure 1-7). Phosphorylation, or existence of a negative charge, at the homologous position is an activating feature in many protein kinases throughout the protein kinase tree (Table 1-2). This region has been termed the activation loop, defined as extending between the conserved motifs DF^{1151}G and AP^{1178}E (344). In the CKD, trisphosphorylation at Tyr-1158,1162, and -1163 leads to up to 200-fold activation (125,126) and a similar loss of catalytic activity is seen in cAPK upon mutagenesis of the corresponding T^{197} (300).

Structural studies have revealed a conserved basis for activation by phosphorylation of T^{197} and its cognates in Table 1-2. This residue communicates with the catalytic loop of the kinase, in subdomain VI. In kinases regulated by phosphorylation, a conserved Arg (R^{1131} in IR) immediately precedes the catalytic base (345). Interactions between this Arg and pT or pY in the activation loop have been observed between pT^{197} and R^{165} in cAPK (282,283), between pT^{160} and R^{126} in a cyclin/CDK-2 complex (294), and between pY^{394} and R^{363} (*via* a water molecule) in the kinase domain of Lck (293).[7] Similar interactions have been proposed in the IR (21). Furthermore, the IR mutation R^{1131}Q has already been observed in a human patient to cause insulin resistance and diabetes *via* impairment of protein kinase activity (346).

---

[7] This residue need not be a phosphoamino acid for the interaction with the conserved Arg. For example, the catalytic core of phosphorylase kinase has E^{182} at this position, which makes the same interaction with R^{148} (335).

Phosphothreonine-197 and homologs make additional contacts as well. In cAPK, pT^{197} interacts with H^{87} in the small lobe of the kinase, and K^{189} in the activation loop itself. It is conserved in crystal structures of phosphorylated Lck (pY^{394}-R^{387}, (293)), cdk-2/ cyclin A (pT^{160}-R^{150}, (294)). The IR has R^{1155} at this position, which has been proposed to interact with pY^{1162} on these grounds (21). The pT^{197}-H^{87} interaction is thought to promote correct orientation between the ATP-binding small lobe and the catalytic loop bearing large lobe, but is not conserved in kinase structures with phosphorylated activation loops. It is absent in Lck (293) but present in cdk-2/cyclin A complex (pT^{160}-R^{50}). Nevertheless, in cAPK, mutational studies of H^{87} identified this residue as playing a role in peptide binding and conformational stabilization (347) as well as binding of the R subunit (348). The insulin receptor has two Arg residues near the primary structure position of H^{87}, R^{1039} and R^{1041}, which could potentially make a similar interaction in the phosphorylated CKD.

To illustrate these interactions and their modulation by activation loop phosphorylation more closely, we can compare the structures of *cis*-inhibited CKD with phosphorylated cAPK (Figure 1-9). The effect of phosphorylation is more clearly shown, however, by comparing the structures of the cdk-2/cyclin A complex with (294) and without (349) phosphorylation at T^{160} (Figure 1-10). This protein serine/threonine kinase, which has also been crystallized in the apo state without cyclin A (336), is the only protein kinase for which both phosphorylated and unphosphorylated forms have been made publicly available *via* the Brookhaven protein data bank. The position of T^{160} is dramatically shifted by phosphorylation, and the homologs of cAPK residues R^{165} (R^{126}), H^{87} (R^{50}), and K^{189} (R^{150}) are no longer able to interact with the residues. Interestingly,

these three side chains themselves don't show very different positions in the two crystal structures. In the recently reported structure of dually phosphorylated MAPK ERK2 (295) pT183 shows a dense web of hydrogen bonds and ionic contacts similar to pT^{197} in cAPK. pT^{183} is involved in no fewer than 8 such contacts, including R^{68} and R^{65} (*via* a water molecule) in the small lobe, R^{146} in the catalytic loop, and R^{170} in the activation loop; these are the structural homologs of H^{87}, R^{165}, and K^{189} in cAPK, respectively.

Like the insulin receptor, ERK2 requires phosphorylation at additional residues in the activation loop, in this case Y^{185}. pY185 interacts with R^{192} and R^{189} in the large lobe of the kinase, where it forms part of the P+1 recognition pocket. Unlike the AL tyrosines of the IR, this residue in MAP kinases can slowly autophosphorylate by a *cis* mechanism, leading to partial activation of the enzyme (350). This may reflect the unique role of the IR activation loop in autoinhibition of the basal state.

These studies have provided a structural basis for *activation* by phosphorylation at the activation loop. In the absence of phosphorylation, does the enzyme has low activity merely because of the absence of these interactions, or are there additional inhibitory interactions that further inhibit catalysis in the basal state? Structural and kinetic studies of the activation loop by the Hendrickson, Ellis, and Soderling laboratories have provided evidence that the unphosphorylated activation loop blocks catalysis through three additional mechanisms. An autoinhibitory region for this region was proposed when a peptide based on CKD residues 1134-1162 was found to inhibit the IR with an IC_{50} of 100μM (351). In the crystal structure of the CKD, Y^{1162} was found to occupy the peptide-binding site. Secondly, the F^{1151} near the beginning of the activation loop occupies the ATP binding site. Finally, proper lobe rotation in the IR is also prevented by DFG. The

unphosphorylated activation loops of FGFR (352). Src (325). $p38^{MAPK}$ (353). ERK-2 (354). and uncomplexed cdk-2 (336) have all been found to block the peptide binding sites of these kinases. but the inhibition of ATP binding by $DF^{1151}G$ and the lobe-orientation effect of this residue are so far unique to the IR. Motion of the activation loop is required to relieve all of these inhibitory interactions in addition to the activating interactions described above. The autoinhibitory and activating roles of the AL are summarized in Figure 1-11.

The crystal studies of the Hendrickson lab do not tell the whole story of regulation in the CKD. The form of the kinase crystallized in this study omitted both the JM and CT regions. as shown in Figure 1-7. Possible regulation by these regions of the kinase could thus not be elucidated by this structure. Nevertheless, this study was groundbreaking for its characterization of the still-unique form of regulation by the insulin receptor's activation loop, and its first look at the three-dimensional structure of a protein tyrosine kinase. We will make further use of these data in identifying residues that may modulate autoinhibition by the activation loop, as we shall see in Chapter 4.

The main focus of this thesis will be on the mechanism of autophosphorylation in the JM region (Chapter 4) and the resulting activation of the complete CKD (Chapter 5). We will eventually use these results to propose a possible scheme for IR regulation in response to insulin (Chapter 6). First. though, we will discuss the general methods used in this work (Chapter 2) and the development and use of a new assay of the receptor's tyrosine kinase activity (Chapter 3).

Figures for Chapter 1

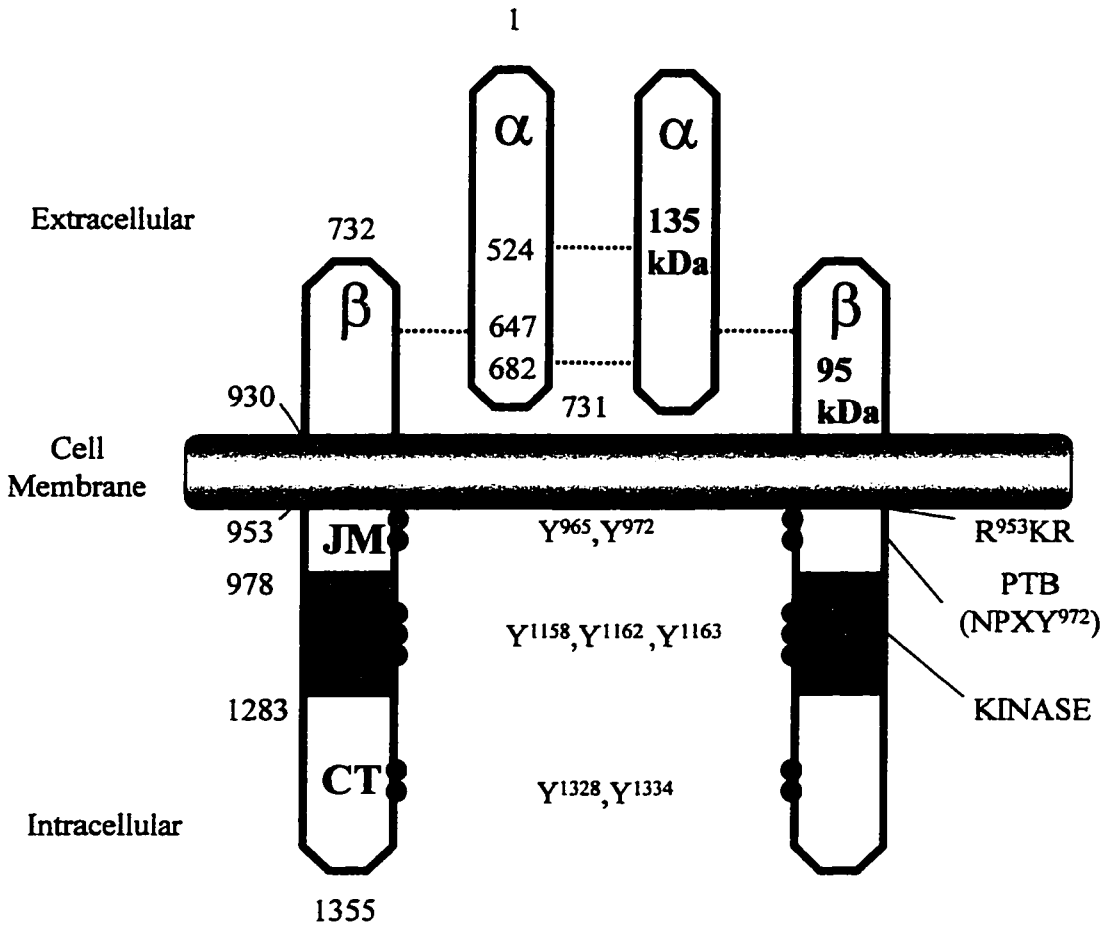

Figure 1-1 Structure of the Insulin Receptor Holomer.

The structure of the $\alpha_2\beta_2$ insulin receptor holomer is shown schematically. Amino acid numbers of domain and subunit boundaries are shown at left. Disulfide bonds (dashed lines), autophosphorylation sites (red circles, identified in center) and the subdomains of the B subunit (JM, juxtamembrane; KD, kinase domain; and CT, carboxyl terminus) are shown. Amino acid numbers of the locations of disulfide bonds and the beginning and end of domains are shown in the left half of the figure; autophosphorylation sites are numbered in the center. At right, the membrane insertion sequence ($R^{953}KR$) and the site of docking of the PTB domain of IRS-1 and Shc are shown. The β-subunit Cys involved in the single disulfide bond to the α subunit is not yet known.

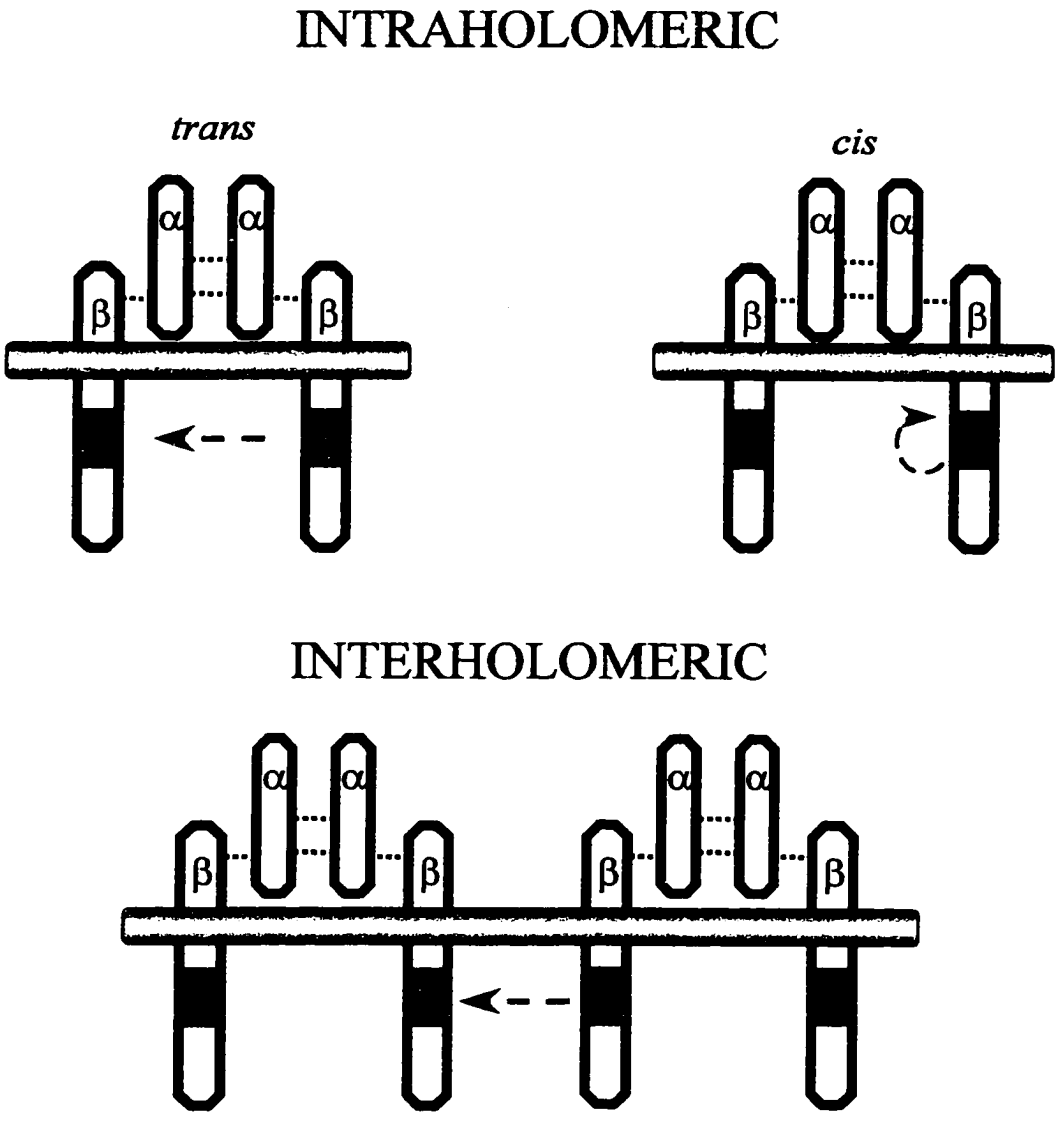

Figure 1-2 Intramolecular vs. Intermolecular Autophosphorylation in the IR.

The three possible routes of autophosphorylation within the holomeric IR are shown. The IR is shown schematically as in Figure 1-1, with the addition of dashed red arrows showing direction of autophosphorylation.

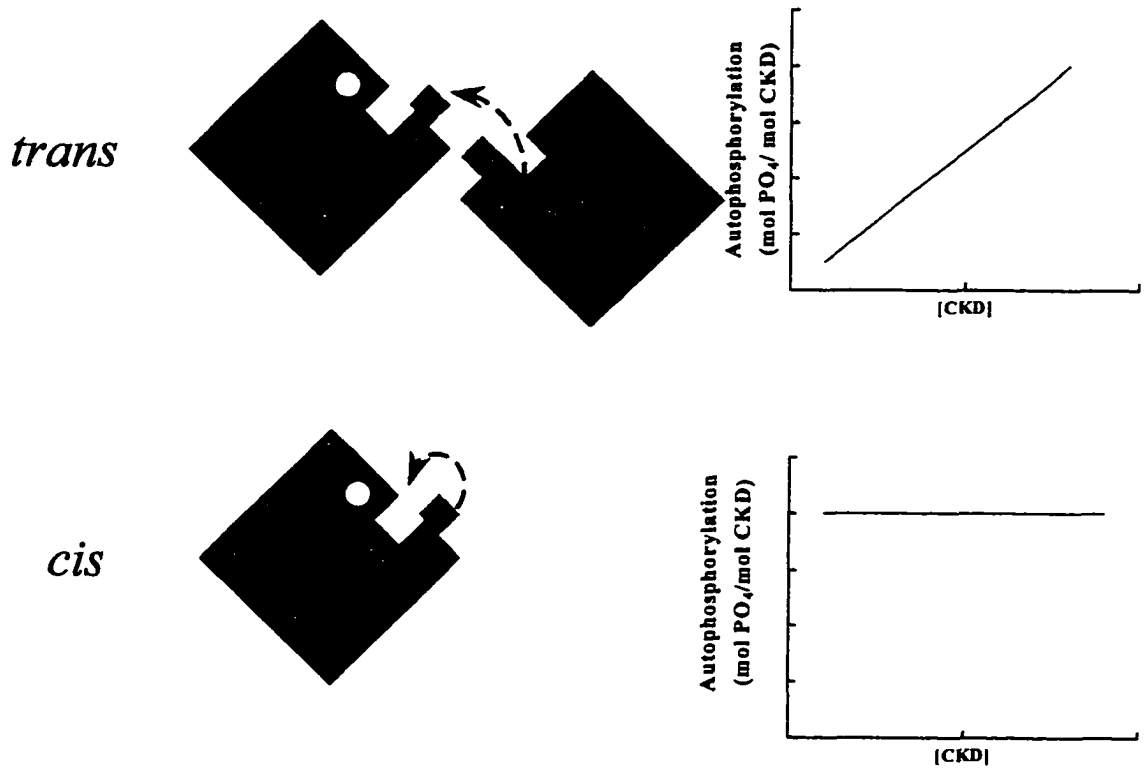

Figure 1-3 *Cis* vs. *Trans* Autophosphorylation in the CKD.

In a *trans* autophosphorylation reaction (*top*), one molecule of CKD phosphorylates another. Autophosphorylation (expressed as mol PO_4/ mol CKD) therefore shows a linear dependence on enzyme concentration (*top right*). In a *cis* autophosphorylation reaction (*bottom*), one kinase molecule phosphorylates itself. Because this reaction does not require interaction between kinase molecules, each molecule of kinase autophosphorylates independent of the presence of other kinase molecules and so the stoichiometry of autophosphorylation is independent of enzyme concentration (*bottom right*). The elements of each CKD molecule are explained in Figure 1-11.

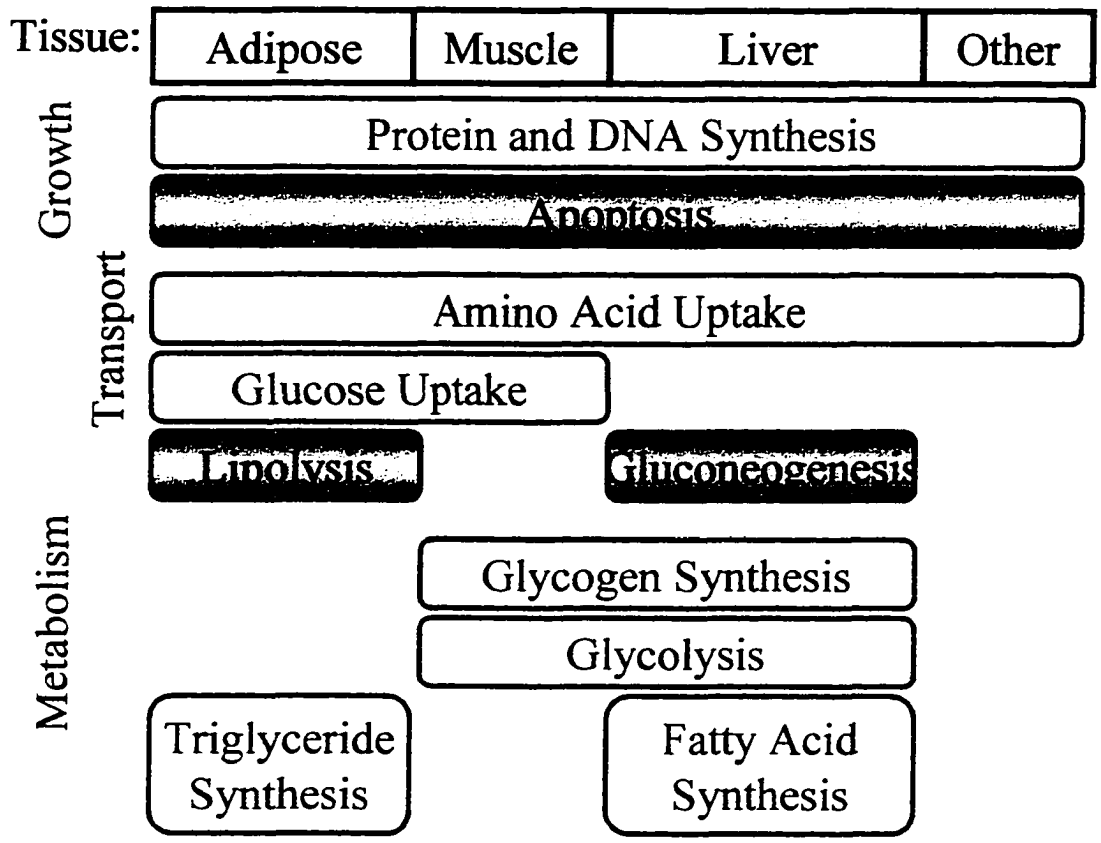

Figure 1-4 Principal Effects of Insulin on Target Tissues.

The chief effects of insulin on its target tissues are shown schematically. All effects described are stimulatory except for those that are shaded; these are inhibitory. The effects of insulin can be loosely grouped into growth-promoting, transport-promoting, and metabolic. Effects are also organized by the tissues they are observed in; the primary insulin-responsive tissues (muscle, fat, and liver) and all other tissues ("other"). The insulin receptor is present and identical in all mammalian tissues measured so far and is responsible for all of these effects. Summarized from (355).

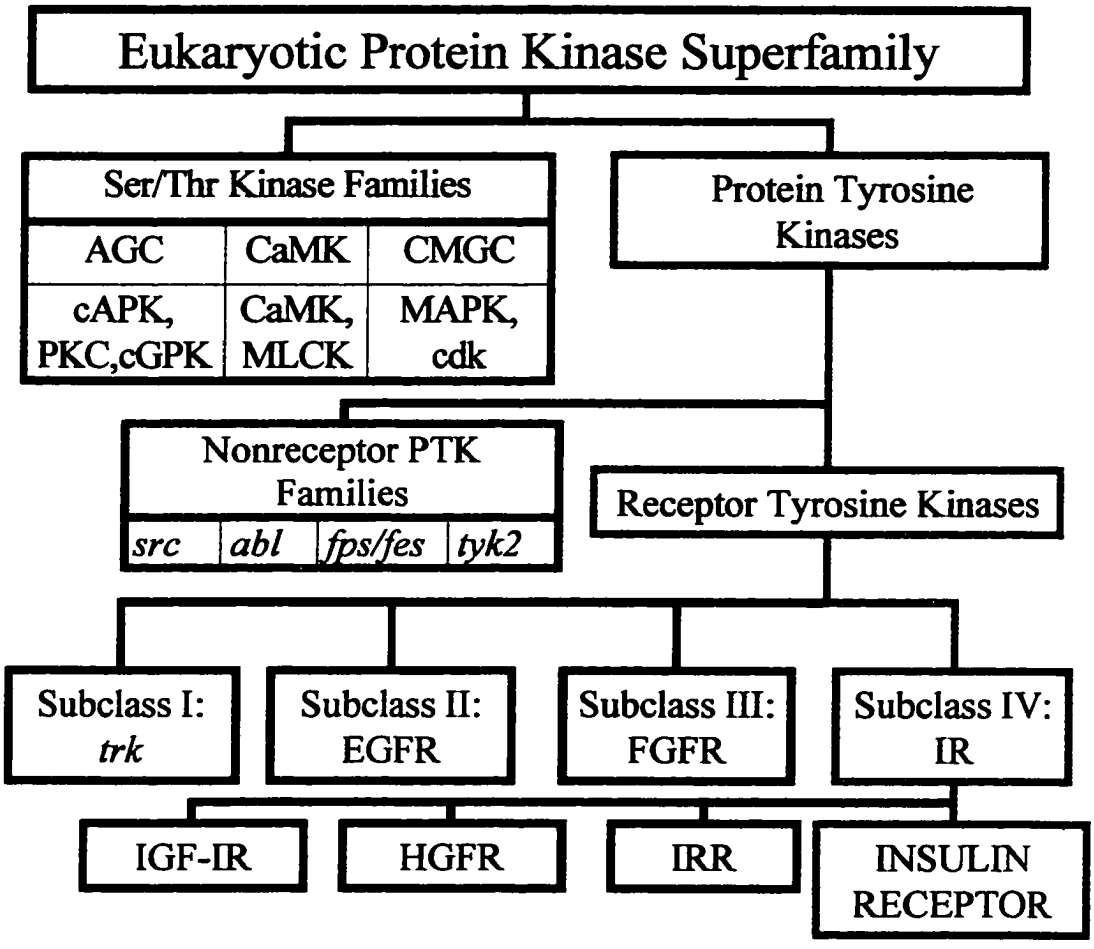

Figure 1-5 Insulin Receptor Phylogeny.

The IR is shown in the context of the eukaryotic protein kinase superfamily. The classifications including the insulin receptor are highlighted in red. The Ser/Thr kinase families are shown classified according to Hanks and co-workers (18,19) on the basis of primary structure within the conserved kinase domain. Nonreceptor tyrosine kinases (NRTKs) are classified as described by Sudol (356), and receptor tyrosine kinases (RTKs) are categorized according to Pulido (260) on the basis of domain structure. Subclass IV RTKs from nonhuman species (such as DAF-2) are not shown here but are listed in Table 1-1.

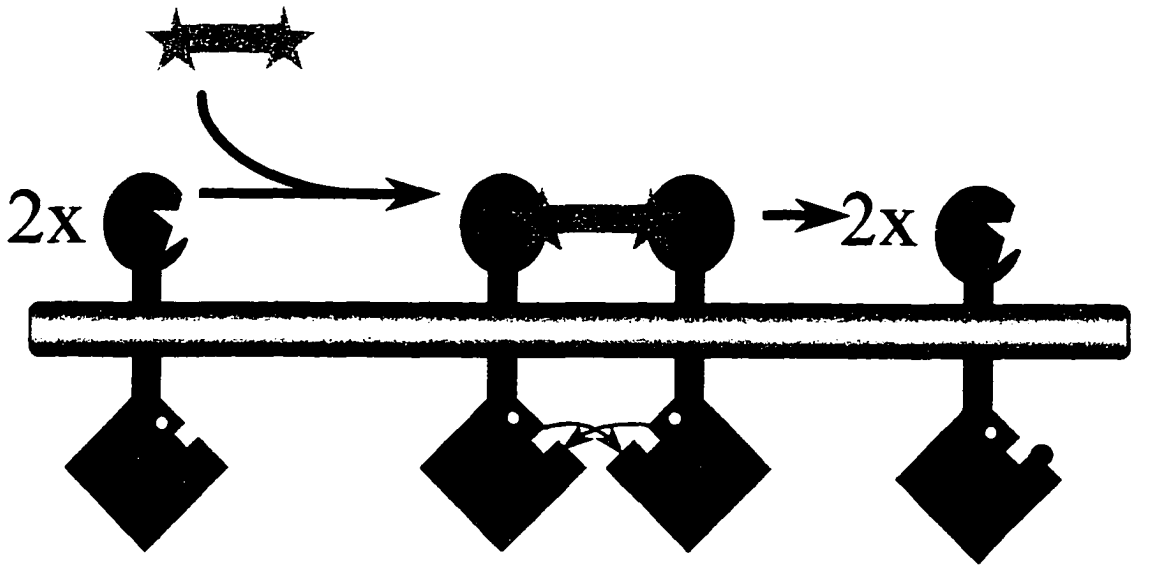

Figure 1-6 Dimerization-Dependent Signaling by Monomeric Receptor Tyrosine Kinases.

The activation of c-Kit is shown. The kinase domain is illustrated as in Figure 1-8. In this figure, it is connected to an extracellular ligand binding domain by a single transmembrane domain. In the absence of stem cell factor (SCF) the receptor is monomeric, unphosphorylated and inactive. SCF is itself dimeric, and is drawn as a double green star. Upon binding SCF, kinase domains are brought into proximity and phosphorylate each other. Note that bivalent ligand alone is not sufficient to cause dimerization; other sequences in the extracellular region are also required. The phosphorylated c-Kit then docks and activates downstream effects, such as PI-3K, *via* SH2 domains. This model is based on the work of Yarden and co-workers (357).

Figure 1-7 Primary Structure of the CKD and Comparison to cAPK.

The primary structure of the CKD, including the entire intracellular β subunit of the IR, is shown in single-letter amino acid code. The primary structure of cAPK is aligned as a reference according to Hanks *et al.* (19). Selected amino acids are highlighted as follows: autophosphorylation sites are shown in red and underlined. The glycine-rich ATP binding loop and conserved lysine involved in ATP orientation are shown in green. The putative catalytic base and adjacent arginine are shown in pink, and the DFG motif involved in autoinhibition of the ATP binding site is shown in blue. These residues and the APE motif marking the end of the activation loop are boxed. IR regions frequently referred to in the text are marked above the IR sequence (JM, AL, CT) and the eleven subdomains of the protein kinase catalytic core, defined according to Hanks & Hunter (18), are shown below the cAPK sequence (**I-XI**). The cAPK sequence shown is from the mouse α catalytic subunit (GCG file: MUSPKCD (358)) and the IR sequence shown is human (GCG file: HUMINSR (1)). The extent of the crystal data for cAPK (PDB entry: 1ATP, (359)) and for the core of the CKD (PDB entry: 1IRK, (21)) are shown by brackets marked with the structure identity (*e.g.* **[1ATP→**).

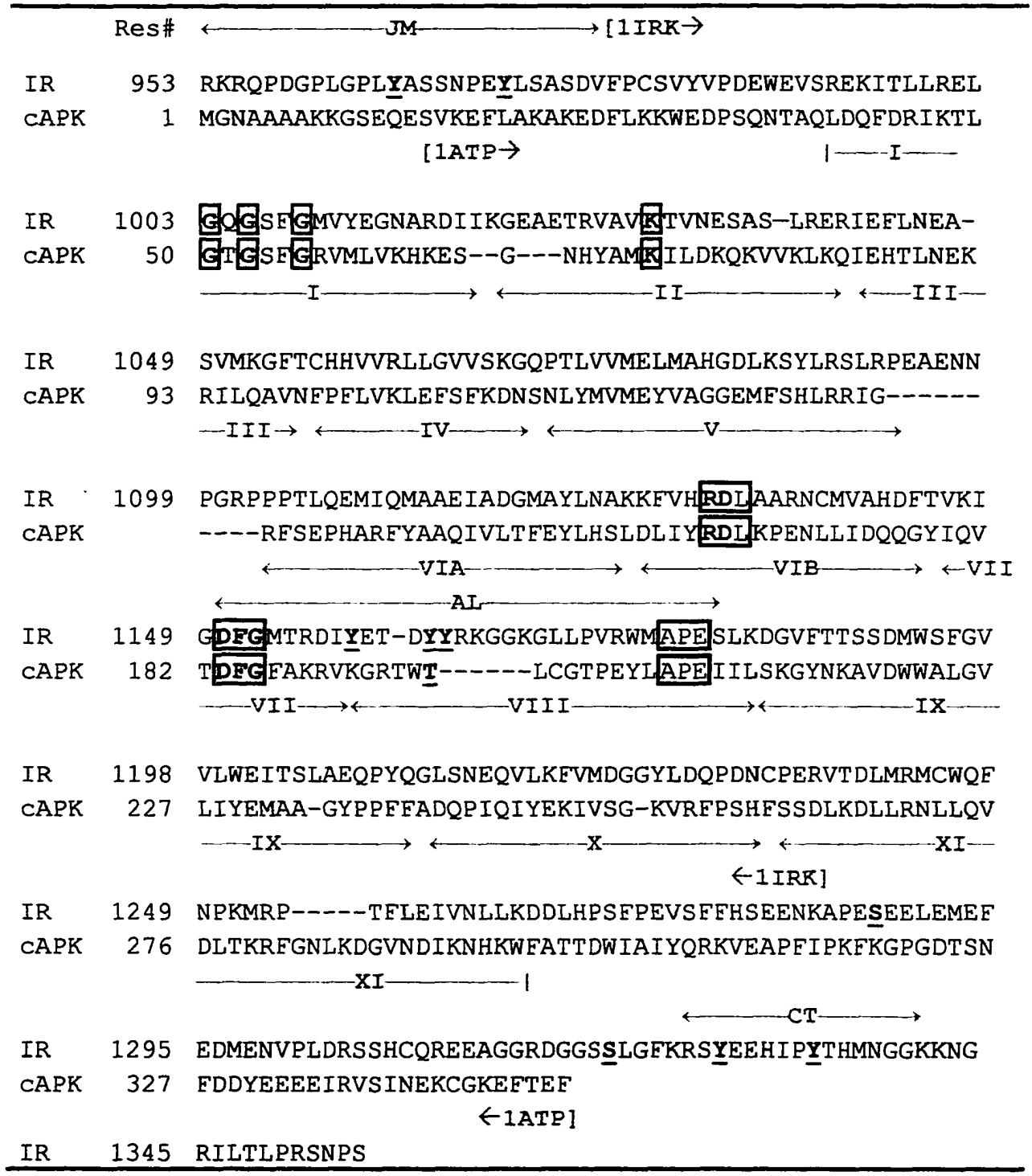

Figure 1-7 Primary Structure of the CKD and Comparison to cAPK.

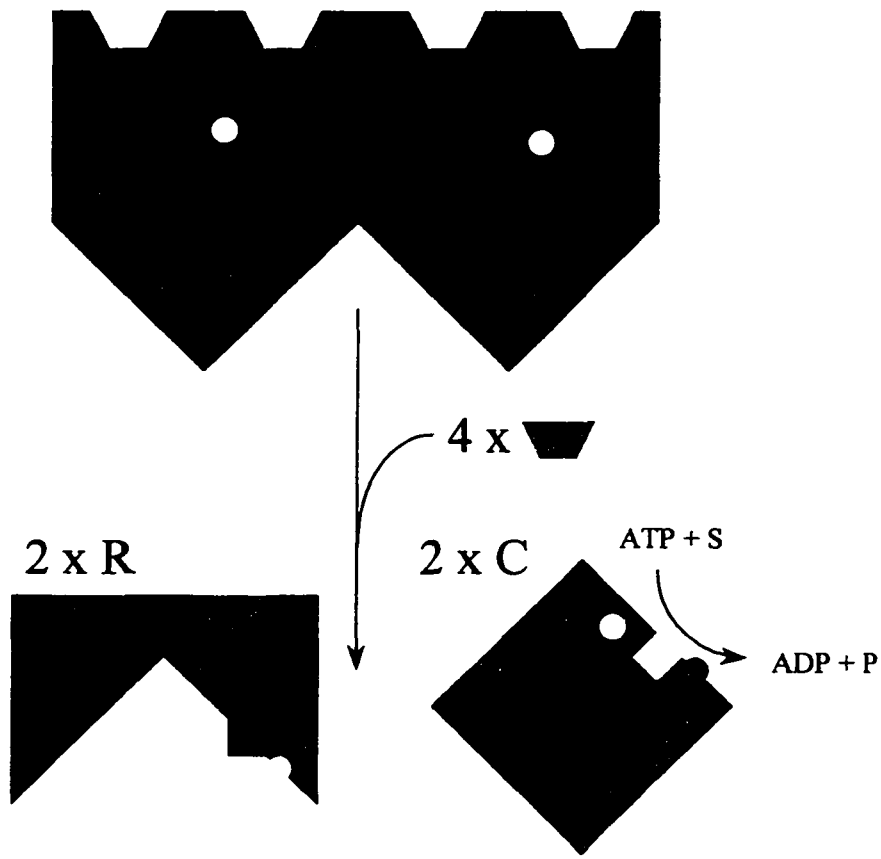

Figure 1-8 Kinase Regulation by Subunit Dissociation: cAPK.

This figure shows an outline of regulation in cAPK. In the absence of cAMP (green trapezoid), the R subunits (dark blue irregular) and catalytic subunits (light blue, drawn similarly to the CKD in Figure 1-11) exist as an R_2C_2 tetramer. The R subunits inhibit the C subunits by binding to the peptide binding site *via* a pseudosubstrate sequence. Binding of cAMP to the regulatory R subunits causes dissociation of the tetramer, leaving free and catalytically active C subunits. Note that T^{197} (solid red circle), the homolog of Y^{1162} in the CKD, is constitutively phosphorylated. T^{197} plays important roles in both active site stabilization and recognition of the R subunit. The ATP binding site (hollow red in the C subunit) is not thought to be directly inhibited.

Figure 1-9 Autoinhibited IRK Compared to Active cAPK.

The diagrams on the following pages show a comparison of the unliganded, autoinhibited catalytic core of the IR kinase core (A) and the ternary complex of cAPK with MgATP and the peptide inhibitor PKI (B). The small lobe is colored in gray, and the large lobe in blue, in both structures. The activation loop is shown in pink. The backbone of the glycine-rich ATP binding motif (IR: G^{1003}-G^{1008}; cAPK: G^{50}-G^{55}) is shown in green, and the putative catalytic base (D^{1132} or D^{165}) is shown in olive. The conserved Phe of the DFG motif (F^{1151} or F^{184}) is shown in yellow in both structures, but occupies very different positions: in the IR kinase it occupies the ATP binding site, whereas in cAPK it occupies a pocket formed by L^{95} and Y^{164}. The corresponding pocket in the CKD, between M^{1051} and H^{1130}, is empty (not shown). This Phe is thus responsible for blockading the adenine binding pocket in IRK. In the cAPK structure, ATP (red) is bound in this pocket. Note also that the unphosphorylated Y^{1162} in IRK is hydrogen bonded to the D^{1132}, occupying the space filled by the phosphate-acceptor analog Ala in PKI (orange, found in cAPK structure only). The activation loop in cAPK adopts a very different conformation from the IR, stabilized by pT^{197} (red) which makes interactions with H^{87} in the small lobe, R^{164} immediately preceding the catalytic base, and K^{192} in the activation loop itself (each shown in green). The homolog of R^{164} in IRK, R^{1131}, is also shown but makes no similar interaction with the unphosphorylated activation loop of IRK. Crystallographic data was taken from the Brookhaven Protein Data Bank, entry 1ATP for the ternary complex of cAPK (359), and entry 1IRK for the inhibited structure of IR (21).

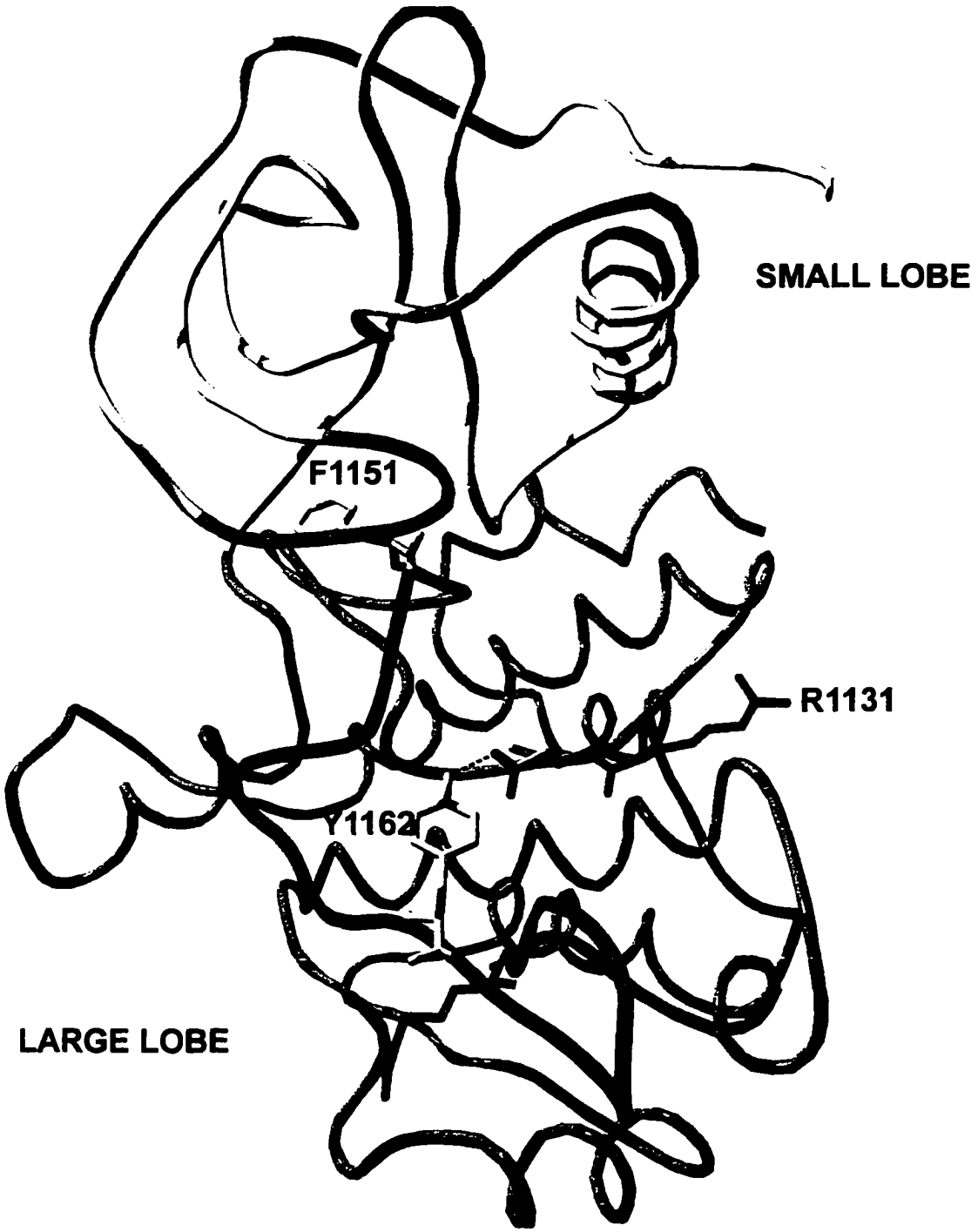

Figure 1-9 Autoinhibited IRK Compared to Active cAPK.

A. Catalytic core of the insulin receptor's kinase domain.

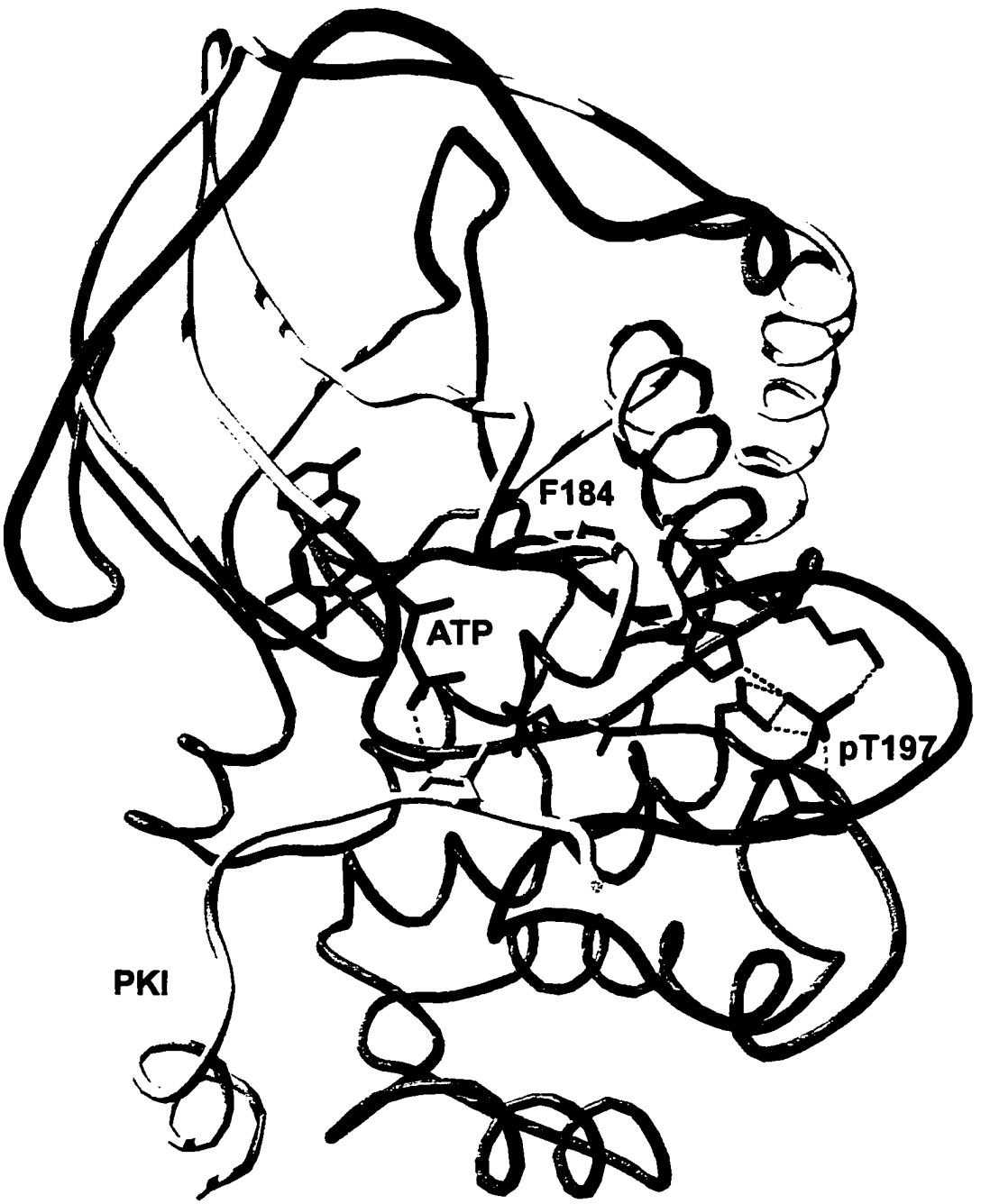

Figure 1-9 Autoinhibited IRK Compared to Active cAPK.

B. Ternary complex of cAPK with peptide inhibitor and MgATP.

Figure 1-10 Modulation of Activation Loop Conformation by Phosphorylation.

The cyclin dependent kinase from yeast, in complex with cyclin A, is the only protein kinase structure for which both unphosphorylated and phosphorylated forms are currently available. These structures are essentially superimposable except around the activation loop. Cyclin A (upper right, in pink) and cdk-2 (lower left, in light blue) are drawn as protein cartoons. The activation loop is drawn similarly in dark blue (unphosphorylated) or red (phosphorylated). Note the very different location of T^{160} (the homolog of Y^{1162} in the IR and T^{197} in cAPK) in the two forms of the activation loop. When phosphorylated (red stick model, center), pT^{160} forms a dense network of hydrogen bonds with positively charged residues. From top to bottom, these residues are R^{50} from the small lobe, R^{1150} from the activation loop itself, and R^{126}, the catalytic-loop homolog of R^{1131} in the IR and R^{164} in cAPK (all drawn as green stick models). There are no direct interactions between pT^{160} and cyclin A, although the cyclin molecule does play a significant role in restructuring the α helix containing R^{50}. In contrast, the unphosphorylated T^{160} is largely exposed to solvent (dark blue ball-and-stick). No other amino acid side chains are shown.

This figure is drawn from crystallographic data from Russo and co-workers, PDB files 1JST (294) for the phospho, and 1FIN (349) for the apo form, of the cdk-2/cyclin A complex.

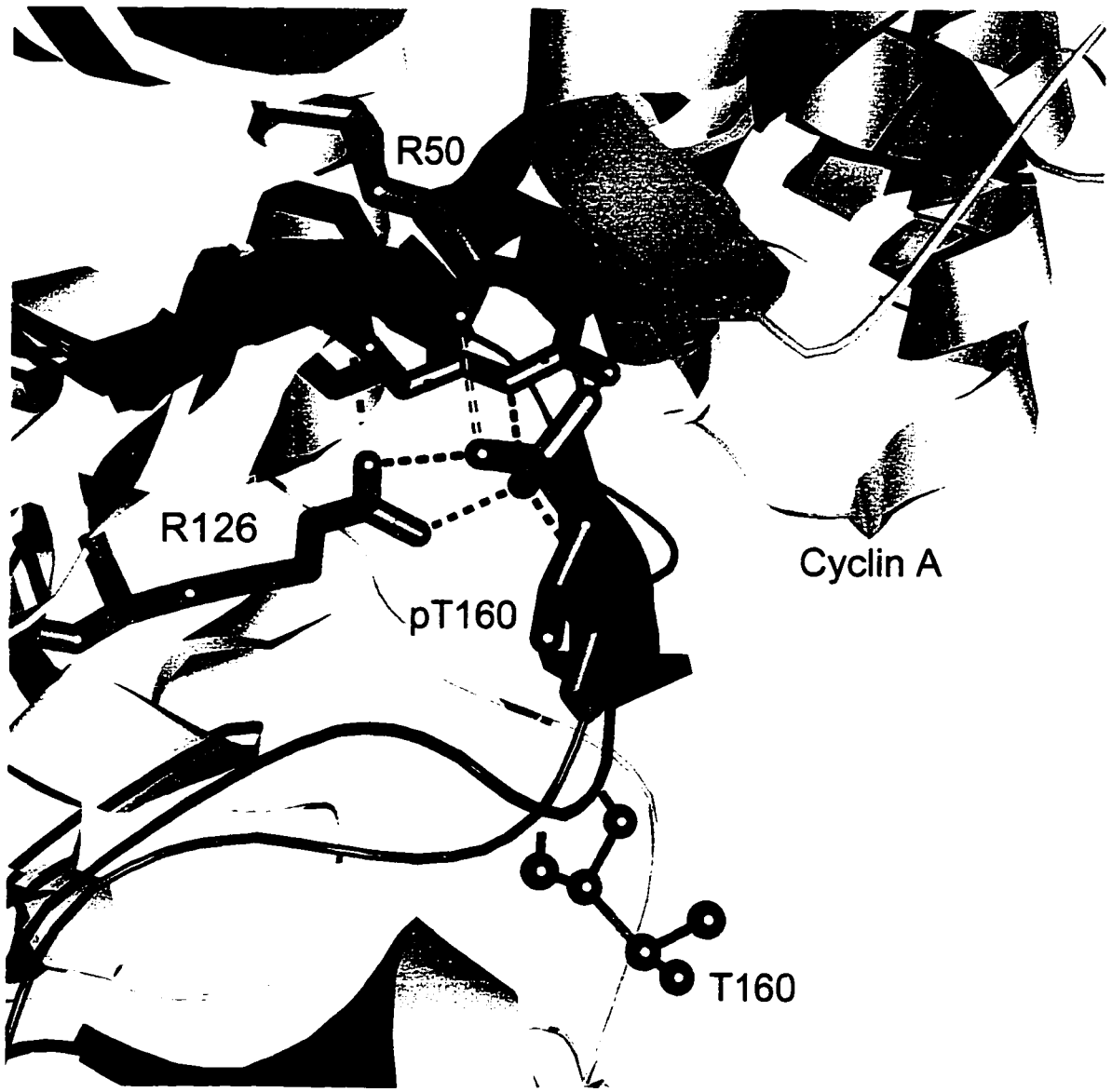

Figure 1-10 Modulation of Activation Loop Conformation by Phosphorylation.

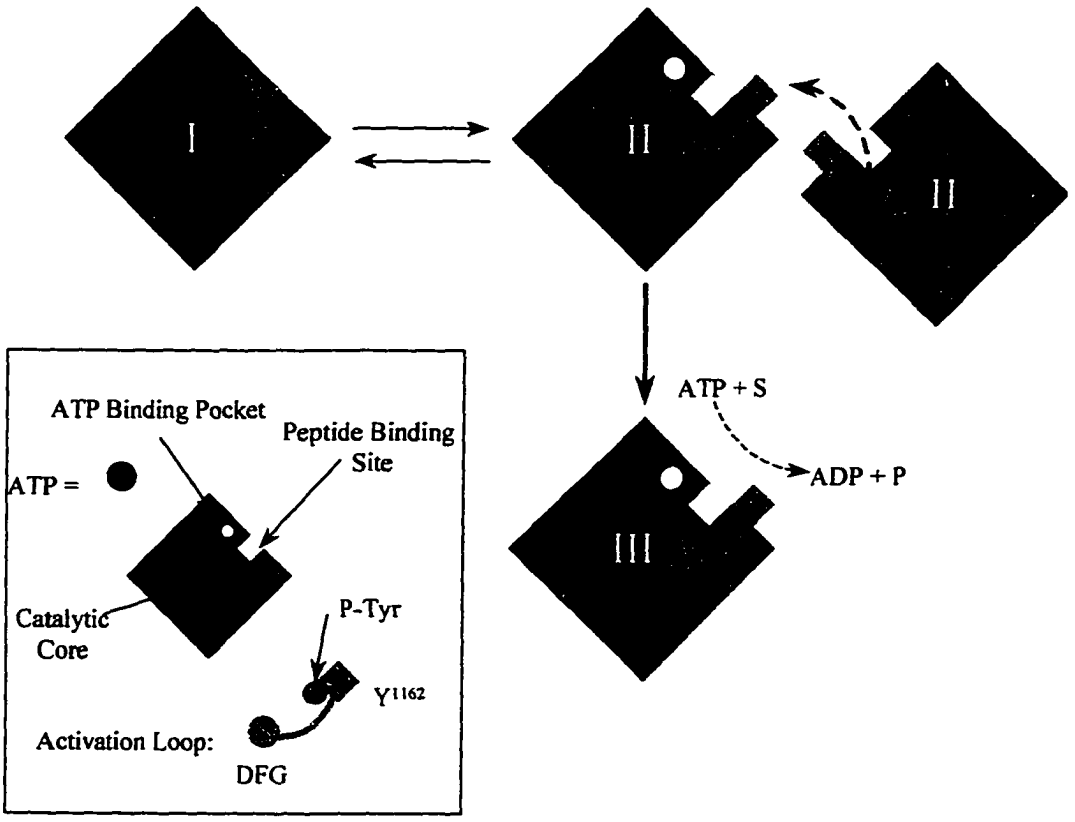

Figure 1-11 Autoinhibition in the Catalytic Core of the CKD.

This is a schematic description of autoactivation and autoinhibition in the truncated catalytic core of the CKD, based on the crystallographic and kinetic studies of the Ellis and Hendrickson (21,126). The CKD is illustrated as a blue diamond, with a circular hole representing the binding site for ATP (pink circles) and a square hole for peptide substrates. The activation loop is shown as an irregular gray dumbbell with end regions capable of occluding both binding sites. In the basal state (I), the activation loop blocks both the ATP and peptide binding sites. In the presence of ATP, however, the activation loop can be autophosphorylated in *trans* (II), leading to the removal of Y^{1162} from the peptide binding site and F^{1151} from the adenine binding pocket. The resulting kinase (III) has free binding sites and shows up to 200-fold activation over the basal state (I). In addition to the loss of autoinhibition shown, the kinase is also thought to be activated by new electrostatic contacts between phosphotyrosine residues in the activation loop and R^{1131}, which is adjacent to the catalytic base, and by a lobe rotation allowed by the repositioning of F^{1151}.

2. Materials and Methods.

Materials.

Insulin-free radioimmunoassay-grade Fraction V bovine serum albumin (BSA, #A-7888), Grade V protamine chloride from salmon, and the disodium salt of ATP from equine muscle (#A-5394), were purchased from Sigma. [γ-^{32}P] ATP was synthesized from $H_3{}^{32}PO_4$ according to the method of Walseth & Johnson (360) and purified (361). Other buffer salts and metals were at least reagent grade.

Agarose was purchased from either Sigma (Low EEO) or Kodak (Molecular Biology Grade). HindIII- or BstEII- digested λ DNA for use as electrophoresis markers were purchased from New England Biolabs or Gibco BRL. All restriction enzymes, polymerases, DNA modification enzymes, and their reaction buffers were purchased from New England Biolabs except for BstXI, which was purchased from Stratagene. dNTP mixtures for polymerase chain reaction (PCR) were purchased from Pharmacia. Wizard Maxiprep kits for large scale plasmid purifications were purchased from Promega. Purification of DNA fragments from agarose gels was done using either the GeneClean II kit or using spin columns (0.45μm Durapore filters, Millipore). Cloning vectors were obtained from the following sources: pBS+, Stratagene; pVL1392 and pVL1393, Invitrogen; pSP72, Promega. The plasmid pTZ19UIR containing the complete IR cDNA was a generous gift of Dr. Whittaker. DNA sequencing was done using the Sequenase 2.0 kit from United States Biochemicals; [α^{35}-S] dATP was from New England Nuclear.

Bacterial growth media were purchased from Gibco BRL. All other materials were at least reagent grade.

Construction and Expression of Mutant Kinases.

Mutant forms of the CKD (residues 953-1355 of the human IR) were constructed by site-directed mutagenesis of plasmids encoding the cDNA for the CKD and expressed in a baculovirus/*Sf9* eukaryotic expression system. A baculovirus encoding the wild-type CKD was a generous gift of the late Dr. Ora Rosen.

General Molecular Biology Methods.

All cloning was done in *E. coli* strain HB101. Agarose gel electrophoresis was done in 1x TAE buffer (362). DNA purification from agarose gels was done using either the GeneClean II kit according to manufacturer's instructions, or using a spin-filter followed by phenol/chloroform extraction and ethanol precipitation. Concentrations of gel-purified DNA fragments were estimated by gel electrophoresis vs. known quantities of HindIII digested λ DNA. Ligations were performed for 3 hours-overnight at 16°C using 12ng/kb of each DNA fragment and 10U T4 DNA ligase in 10μl 1x T4 ligase reaction buffer supplied by the manufacturer. For every ligation reaction, a control ligation reaction, lacking insert DNA, was also done to check for possible vector recircularization. Ligation reaction mixtures were used without further purification to transform competent cells (stored at -80°C), made competent using the calcium chloride method (362). Transformed cells were plated on agar plates containing Luria Broth (LB)

media supplemented with 50μg/ml ampicillin and grown overnight at 37°C. Ligation reactions including the insert cDNA yielded 5- to 50-fold more colonies upon transformation then did their insert-deficient control reactions.

Colonies, 8-36, derived from each ligation reaction were individually inoculated into 2ml LB cultures (50μg/ml ampicillin) and grown with shaking overnight at 37°C. Small-scale plasmid purifications were done by the boiling lysis method (362) and 2μl plasmid DNA (approximately 1-2μg plasmid DNA) from each colony was typically digested with 2-5 U restriction enzyme in a 10μl reaction mixture for 2-4 hours, at the temperature appropriate for each enzyme. The resulting fragments were analyzed by agarose gel electrophoresis and compared with theoretical maps of the plasmid under construction.

The remnants of a single growth culture whose DNA matched the theoretical map was then used to inoculate 400ml of LB supplemented with 100μg/ml ampicillin and grown for 16-24 hours with shaking at 37°C. Large scale purifications were done using the Wizard Maxipreps kits with the following modifications: Bacterial lysis and preparation of the crude nucleic acid pellet were done by the alkaline lysis method (362). Following purification, plasmid DNA was diluted to 1.5 ml and centrifuged for 5 minutes at 15,000x g at room temperature, to pellet resin fines which otherwise could irreversibly bind DNA upon freezing. The supernatant, containing the plasmid DNA, was stored at 4°C for up to two months but was otherwise kept at -20°C for long-term storage. All plasmids described were purified by this large-scale method except where subcloning was done directly from miniprep plasmid DNA, as noted in the text. Every plasmid purified was verified by mapping with at least 8 restriction enzymes selected to give 1-5 different

sized fragments; particular enzymes are noted only when they specifically distinguished between different mutant constructs. Glycerol stocks of bacteria transformed with each plasmid made were prepared by addition of sterile glycerol to 30% (v/v), and stored at -70°C or -150°C.

Preparative-scale restriction enzyme digestions were done at manufacturers' recommended temperature in 100µl volumes using various amounts of purified plasmid; enzymes were generally not heat-inactivated after digestion (unless a subsequent buffer could cause undesired side reactions). Digests using BstXI and TaqI were carried out at elevated temperatures as recommended by the manufacturer. Calf intestinal phosphatase (CIP) treatment, when used, was generally carried out as follows: 10U CIP, 5µl 10x CIP buffer (10x: 0.5M Tris-HCl, pH 9.0, 10mM $MgCl_2$, 1mM $ZnCl_2$, 10mM spermidine), and 5-50µg plasmid DNA in a final volume of 50µl was incubated at 37°C for 30 minutes. Another 10U CIP was then added and incubation continued for another 30 minutes. DNA was then either gel-purified or the following inactivation procedure used: Addition of 1µl 0.5M EDTA, pH 8, then heat inactivation at 68°C for 10 minutes, followed by phenol/chloroform extraction, ethanol precipitation, and resuspension in 20-40µl TE.

Polymerase chain reaction (PCR) was done using Vent polymerase. 100µl PCR reaction mixtures contained 1 pmol DNA template, 100 pmol each primer, 1x reaction buffer, 16µl 1.25mM dNTP mix, and 5 U Vent polymerase; reactions were overlaid with mineral oil to prevent evaporation. Thermal cycling was done on a Perkin-Elmer thermal cycler with three steps per cycle: 1 minute denaturing step (92°C) ; 2 minute annealing

step (36-50°C depending on primers' melting temperatures); and an extension step of 1 minute /kb (72°C). A 10 second equilibration step was inserted before each reaction step to insure the machine reached the desired temperature before beginning each incubation. All reactions were carried out for 30 cycles.

PCR products were separated from template plasmid DNA by agarose gel purification. Second-round PCR reactions, which did not include wild-type template, were only gel purified if more than one PCR product was detected by electrophoresis. Otherwise, second-round PCR products were ethanol precipitated, resuspended in 40µl TE, and digested directly. The resulting fragment was ligated into the recipient plasmid and 4-12 minipreps prepared and phenol-chloroform extracted. All DNA derived from PCR reactions was sequenced to verify mutations and the fidelity of the PCR reaction.

Sequencing was done using the manual dideoxy chain termination method of Sanger (363), using [α-^{35}S] dATP , according to kit manufacturer's instructions (Sequenase 2.0). 20µg purified plasmid DNA or 20µl (approximately 20µg) miniprep DNA was used as template, and 10ng of each of the outer mutagenesis primers was used as primer for the sequencing reaction. Nongradient 0.5mm 5.2% T (5%C) denaturing polyacrylamide gels were prepared as described by Maniatis, Fritsch, and Sambrook (362) and run in 1x Tris-Borate-EDTA buffer. Gels were dried for 1-2 hours at 70°C and subject to autoradiography for 1-4 days to visualize bands, which were loaded, from left to right, in the order G-A-T-C. This allowed for reading the complementary sequence by inverting the autoradiograph.

Subcloning Vectors p72CKD, pBSm3, and p72M5F.

Mutant construction was facilitated by use of the subcloning vectors p72-CKD, pBSm3, and p72m5F, which were constructed by R.A. Kohanski. p72-CKD contained the 1.7kb BglI/BamHI fragment from the human IR cDNA (supplied in pTZ19U-IR by J. Whittaker) ligated to pSP72 digested with KpnI/BamHI and two annealed oligonucleotides, KCKD1 and KCKD2 (Table 2-1). The resulting construct, p72CKD, possessed a Kozak consensus sequence (CGCCACC) immediately upstream from an ATG methionine initiation codon and the in-frame nucleotide sequence encoding the residues R^{953}-S^{1355} of the human IR. A restriction map of p72CKD and constructs derived from it is shown in Figure 2-2.

Table 2-1 Oligonucleotide Sequences for Plasmid Construction.

Name	Plasmid	U/L*	Sequence (5'→3')
KCKD2	p72CKD	L	CATGGCGGTGGTACTCTTTCTCCGTCGGT
KCKD1	p72CKD	U	CGCCACCATGAGAAAGAGGCAGCCAGAT
HBB2	pUC19GSCKD	L	TGGCTGCCTCTTTCTGGATCCA
HBB1	pUC19GSCKD	U	AGCTTGGATCCAGAAAGAGGCAGCCAGAT
PBSKHL	pXCKD	L	AGCTTGATATCGGATCCTCTAGACTAGTAGATCTGGTACCAAGCTTG
S1D3L	pXCKD	L	GTGATGGCAGGTGAAGCCCTTCATGACGCTAG
PBSKHU	pXCKD	U	AATTCAAGCTTGGTACCAGATCTACTAGTCTAGAGGATCCGATATCA
S1D3U	pXCKD	U	CTAGCGTCATGAAGGGCTTCACCTGCCATCACGTG

*

U designates an upper strand, and L a lower strand, oligonucleotide.

pBSm3 was designed to facilitate mutagenesis of the 3' region of the IR cDNA. Annealed oligonucleotides PHBS1 and PHBS2 (containing the 3' BstXI site from the hIR cDNA) were inserted into the cloning vector pBS+ on BstXI and XbaI sites to yield pBSm. The 1.38kb BglI/PstI fragment from pTZ19UIR was ligated with PstI/HindIII-treated pUC19 and the annealed HindIII/BglI adapter oligonucleotides HBB1 and HBB2, yielding pUC19gsCKD. pBSm was treated with BstXI and EcoRI, and ligated with the 1.04kb BstXI/EcoRI fragment from pUC19gsCKD to yield pBSm3. This vector had a unique StuI site and lacked the 5' end of the cDNA, upstream of the internal BstXI site.

pBSm was also digested with BstXI and HindIII and ligated with the BstXI/HindIII insert from pBSH3-FMAKD to yield pBSm5F. The HindIII/EcoRI fragment from this was inserted into HindIII/EcoRI digested pSP72 to yield p72M5F, which was used as the host for the silent StuI->NheI site conversion involved in the construction of pXCKD, described below.

Construction of the Cytoplasmic Kinase Domain Cassette Vector pXCKD.

This vector was designed to allow convenient interchange of CKD mutations and transfer of the CKD into a variety of shuttle or expression vectors, including the baculovirus expression vectors pVL1393 and pVL1392. To facilitate cloning on StuI sites, the 5' StuI site was converted to a unique NheI site, making the 3' StuI site unique as well. There was no change in the encoded amino acid sequence. p72M5F•SN, containing the silent conversion of the 5' StuI site to an NheI site, was prepared as follows: p72M5F was linearized with DraIII, and then further digested with

StuI. (StuI cleavage of DraIII cut p72M5F does not remove enough DNA to be detectable by agarose gel electrophoresis). The DraIII/StuI digested plasmid was ligated to the pre-annealed oligonucleotides S1D3L and S1D3U (Table 2-1) encoding the same amino acids as the wild type sequence but including the StuI -->NheI conversion. Minipreps were tested for both the loss of the StuI site and gain of the NheI site, and the incorporation of the oligonucleotides verified by sequencing.

The plasmid pBS+ was digested with EcoRI and HindIII. The resulting 3.2kb fragment, which lacked most of the MCS, was ligated to the pre-annealed oligonucleotides PBSKHU and PBSKHL (Table 2-1) yielding the 3.2kb plasmid pBX. Minipreps were tested by both the loss of the PstI site from the MCS and the gain of a SpeI site introduced by the oligonucleotides. The 1.8kb XbaI/KpnI fragment from p72CKD, including the cDNA for the CKD, was ligated to the 3.2kb XbaI/KpnI fragment of pBX. Minipreps were screened for linearization with XhoI, indicating the presence of the insert, which contains an XhoI restriction site. The resulting 4.8 kb plasmid was named pBXCKD. pBXCKD was digested with XhoI and BstXI. The resulting 4.6 kb product was gel purified and was discernibly smaller than XhoI-only cut pBXCKD run in an adjacent lane (240 bp difference) indicating that the BstXI digestion was complete. A cDNA fragment containing the StuI->NheI modification, the XhoI/BstXI fragment (237bp) from p72M5F•SN, was ligated into XhoI/BstXI digested pBXCKD, prepared above. Minipreps were screened by NheI cleavage. The resulting construct was pXCKD. A diagram of this plasmid and its derivatives is shown in Figure 2-1.

Overview of Mutagenesis.

The mutants discussed were made using the overlap-extension PCR process (364), using the primers and templates listed in Table 2-2. The overlap-extension process requires two outside primers and two inside primers; either or both of the latter two may be mutagenic. The sequences of oligonucleotides used are given in Table 2-3. Restriction enzyme sites near the ends of the PCR product are used to splice the product into a host vector, generally either p72CKD or pXCKD. From there, the cDNA was generally transferred directly to pVL1393 for baculovirus construction, as described below.

Table 2-2 List of Mutants, Mutations, and Mutagenesis Primers.

The names, specific mutations, locations within the cDNA, and mutagenesis reagents for each mutant CKD construct are listed here. Each mutant also had a methionine at its 5' end. The primers described were used for mutagenesis by the overlap-extension PCR process as described (364); their sequences are given in Table 2-3. Amino acid numbers are according to the complete human IR sequence; nucleotide numbers begin with the initiator methionine of the cDNA for the CKD (residues 953-1355). All PCR products were verified by DNA sequencing.

* cDNAs including these mutations were a generous gift of Dr. L.-H. Wang, and so no PCR mutagenesis was performed. Mutation sites were verified by DNA sequencing.

Table 2-2 List of Mutants, Mutations, and Mutagenesis Primers.

Mutant	Description	Template	5' Upper	5' Lower	3' Upper	3' Lower
ALCTY4F	$Y^{1162,1163,1328,1334}F$	**	**			
ALY2F	$Y^{1162,1163}F$	*	*			
CTY2F	$Y^{1328,1334}F$	p72CKD	U3922	YF1328	YF1334	L4431
D1132N	$D^{1132}N$	pBSm3	PBSRP	32LS	D32N	L3786
D1161A	$D^{1161}A$	pBSm3	PBSRP	1161LS	D1161A	L3786
JMALY4F	$Y^{965,972,\ 1162,1163}F$	**	**			
JMCTY4F	$Y^{965,972,1328,1334}F$	**	**			
JMY2F	$Y^{965,972}F$	p72CKD	SP72X	Y965F	Y972F	P3125L
K1030A	$K^{1030}A$	*	*			
R1136Q	$R^{1136}Q$	pBSm3	PBSRP	LS1136	R1136Q	L3786
Y1158F	$Y^{1158}F$	*	*			
Y1158W	$Y^{1158}W$	pBSm3	PBSRP	Y58W2	Y1158W	L3786
ΔGATE	Deletion 1162...1166	pBSm3	PBSRP	DCNTRL	U3615	L3786
ΔGATE2	Deletion 1161...1165	pBSm3	PBSRP	DGATE2	U3615	L3786
ΔK1283	Truncation after K^{1283}	pTZ19uIR	IR3698	K1283		

Table 2-3 Oligonucleotide Sequences for CKD Mutants.

Name	Mutant	U/L	Sequence (5'→3')
DCNTRL	ΔGATE	L	GAGCAGACCCTTGCC▼ATCCGTTTCATAGATGTCTCTGG
U3615	ΔGATE	U	GGCAAGGGTCTGCTCCC
	ΔGATE2		
DGATE2	ΔGATE2	L	GGAGCAGACCCTTGCC▼ACCCGTTTCATAGATGTCTCTGG
K1283	ΔK1283	L	GCTGCTCGGATCCTCTAGA▼CTACTTGTTCTCCTCGCTGTGG
IR3698	ΔK1283	U	CTTTGGCGTGGTCCTTTGGG
L4431	CTY2F	L	GTTGCCCCAAAGGAGCAGC
YF1328	CTY2F	L	AAGGGATGTGTTCCTCGAAGCTCCGCTTGAAACC
U3922	CTY2F	U	CCAGCTTTCCAGAGGTGTCG
YF1334	CTY2F	U	CGAGGAACACATCCCTTTCACACACATGAACG
L3786	D1132N	L	CCAGATACCCTCCATCC
	D1161A		
	ΔGATE		
	ΔGATE2		
32LS	D1132N	L	CTGCCAGGTTCCGATGC
D32N	D1132N	U	CATCGGAACCTGGCAGC
PBSRP	D1132N	U	GAAACACCTATGACCATG
	D1161A		
	R1136Q		
	ΔGATE		
	ΔGATE2		
1161LS	D1161A	L	CCGGTAGTACGCCGTTTCA
D1161A	D1161A	U	TGAAACGGCGTACTACCGG
P3125L	JMY2F	L	CCATGCCGAAGGATCCCTGC
Y965F	JMY2F	L	CTCAGGGTTTGAAGAAGCGAAAAGCGGTC
SP72X	JMY2F	U	GACTCACTATAGGGAGACCG
Y972F	JMY2F	U	CGCTTCTTCAAACCCTGAGTTCTCAGTGC
Y58W2	Y1158W	L	CGTTTCCCAGATGTCTCTGGTC
Y1158W	Y1158W	U	GACCAGAGACATCTGGGAAACGGATTACTACCG

Mutagenized bases are underlined. ▼ marks the site of deletions.

Construction of Plasmids Containing Activation Loop Mutants: ΔGATE, ΔGATE2, Y1158W, and D1161A.

ΔGATE, Y1158W, and ΔGATE2 were made using the outer primers PBSRP and L3786, using pBSm3 as the template. BstXI and StuI sites were used to digest PCR products and p72CKD (ΔGATE and Y1158W) or pXCKD (ΔGATE2). For p72CKD, this required a partial StuI digest, because of the presence of the two original StuI sites (Figure 2-2). Screening minipreps of candidate p72ΔGATE with StuI allowed distinction between recircularized double-StuI cleaved p72CKD (no StuI insert) and native p72CKD (493 bp fragment) and the desired p72ΔGATE (478 bp). Minipreps for pXΔGATE2 were screened with HindIII for a 1.7 kb insert. EcoRI and PstI cleavage sites were used to move the CKD cDNAs from p72ΔGATE, p72Y1158W, and pXΔGATE2 into pVL1393, where minipreps were screened with either XhoI for a 2.2kb insert (p93ΔGATE2) or with KpnI for a 1.9kb insert (p93ΔGATE). An overview of p93 constructs is shown in Figure 2-3.

Purified and BstXI/StuI digested PCR products containing the D1161A mutation were obtained from Q.X. The insert was ligated into BstXI/StuI digested pXCKD, minipreps were screened for a 1.7kb HindIII fragment, and the mutation site was verified by DNA sequencing. pXD1161A was digested with PstI and EcoRI, and the resulting 1.4kb insert ligated into EcoRI/PstI digested pVL1393. Minipreps were screened for the presence of a 2.2kb XhoI fragment. p93D1161A was purified from a large scale culture and the mutation again verified by sequencing.

Construction of Plasmids Containing the Autophosphorylation Site Mutants: JMY2F, ALY2F, and CTY2F.

PCR for the JMY2F mutant was done using p72CKD, not pXCKD, as the template. The PCR product was digested with XhoI and EcoRI, and the 145bp fragment remaining was ligated to similarly digested pXCKD. Minipreps were verified by DNA sequencing. The 1.6kb EcoRI/PstI insert from pXJMY2F was inserted into similarly digested pVL1393, yielding p93JMY2F. Minipreps were screened for a 2.2kb XhoI fragment. Neither pXJMY2F nor p93JMY2F yield the 1.4kb HindIII fragment found in most other pX and p93 constructs, since the 5' portion of the MCS is derived from p72 (the PCR template, which lacks a 5' HindIII site) rather than pXCKD (which has a HindIII site 5' to the cDNA encoding the cDNA). A similarly derived TaqI site is also found in the 5' MCS of JMY2F constructs. These features were used for plasmid verification.

For the CTY2F mutant, the 510bp PCR product was trimmed and ligated into pXCKD using AvaI and SpeI sites; minipreps were screened for a 1.7kb HindIII fragment. Since pXCKD contained two AvaI sites (Figure 2-1), this required purification of the 0.9 and 3.6 kb fragments from and AvaI/SpeI digest of pXCKD; the 0.4 kb fragment was discarded. The trimmed PCR product (0.4 kb) was then ligated to both the 0.9 and 3.6 kb fragments in a three part ligation, yielding pXCTY2F. Minipreps were screened for a 1.7 kb HindIII fragment. The 1.6kb EcoRI/PstI insert from this plasmid was then inserted into pVL1393, digested on the same sites, to yield p93CTY2F. The mutation induced an additional TaqI cleavage site at the mutation site, which was used to verify the presence or absence of the CTY2F mutation during these and subsequent steps.

A pUIRT19- based plasmid containing the ALY2F mutation was a generous gift of L.-H. Wang. This plasmid was digested with StuI and BstXI to excise the insert containing the mutation sites, and were ligated into p72CKD using the same sites. Minipreps were selected by DNA sequencing. PstI and EcoRI were used to excise the entire cDNA p72ALY2F, which was inserted into pVL1393 on the same sites. Minipreps were verified by the presence of a 1.4kb BstXI fragment generated by the BstXI restriction site in the CKD cDNA and the BstXI site native to pVL1393.

Inserts derived from ALY2F, Y1158W, and ΔGATE mutant, could be distinguished from most other mutations described here by their retention of the native 5' StuI restriction site in the cDNA of the hIR CKD (illustrated in Figure 2-2). The 3' StuI restriction site was not altered in any mutant. These mutants were unique in their yielding an 0.5kb fragment upon StuI digestion. Alternatively, only these constructs lacked the NheI site introduced in pX based vectors. Practically, NheI was found to yield only partial digestion of pX based inserts. Convincing demonstrations of the NheI restriction site required complete linearization with PstI; codigestion with NheI then yielded a 1.4 kb fragment if the NheI site was present.

Expression and Purification of Kinases.

Baculovirus with CKD cDNA in place of the polyhedrin gene were constructed using the BaculoGold kit (Pharmingen) according to manufacturer's instructions. Wild-type and mutant CKD were purified from infected *Sf9* cells by the method of Villalba *et al.* (128) with modifications. Anion-exchange chromatography was performed with a 1 x 10cm diethylaminoethane (DEAE) 8HR column (Waters). The ammonium sulfate fractionation and the phenyl-Sepharose column were omitted. Size exclusion chromatography was done using a

Superdex 75 16/60 or 26/60 column (Pharmacia) Purification was assayed by monitoring A_{280} and Coomassie Brilliant Blue staining of SDS-PAGE separated proteins. 2-5µl of each 1.5 ml fraction was run in each lane of a 10%T.2%C minigel (Mini-Protean II, Hoeffer) and transferred to polyvinyldiflouride (PVDF) membranes. CKD eluted at 8.5% Buffer B from the DEAE column and as a symmetrical single peak from the size-exclusion column at approximately 50kDa. CKD could also be detected by Western blot with polyclonal anti-CKD antibody, autoradiography (following autophosphorylation with [γ-^{32}P] MnATP), or by IRS939 phosphorylation assay, described below. Enzyme concentrations were calculated from the absorbance at 280 nm, using an extinction coefficient of 40200 M^{-1} cm^{-1} (365). Every mutant kinase was verified at least once by each of these methods. Enzyme prepared by this method was typically at least 90% pure (as estimated by Coomassie blue staining), the major contaminant being a ~45 kDa proteolysis product of the CKD.

Other Mutants and Expression Systems.

The pairwise double-cluster mutants JMALY4F, ALCTY4F, and JMCTY4F were built by fragment swapping of plasmids bearing JMY2F, CTY2F, and ALY2F mutations. Baculoviruses encoding $R^{1136}Q$, $D^{1132}N$, and a C-terminus truncation mutant ΔK^{1283} were also constructed. These constructs may facilitate future enzymatic studies of the CKD.

Attempts were made to express the CKD as a glutathione S-transferase fusion protein in several strains of *E. coli*. Although some immunoreactive full-length fusion protein was expressed, the majority of immunoreactive material was degraded and insoluble, and no autophosphorylation activity could be detected. This led to the use of the *Sf9* expression system described above.

Enzymatic Assays

Autophosphorylation Reactions

Unless otherwise noted, autophosphorylation reactions in Chapter 4 were for one minute in 50mM HEPES, pH 7.0, containing 5mM fresh manganese acetate (MnAc), 0.01% bovine serum albumin (BSA), w/v, 1mM dithiothreitol (DTT), and [γ^{32}P] ATP at concentrations as specified in the figure legends. Reactions (20-60µl) were quenched by addition of 0.5 volumes 3x Laemmli sample buffer (initial concentrations: 6% sodium dodecyl sulfate (SDS), w/v, 60mM ethylenediaminetetraacetic acid (EDTA), 20% glycerol, 50mM DTT, in 63.5 mM Tris-HCl, pH 6.8) and analyzed by sodium dodecyl sulfate- polyacrylamide gel electrophoresis (SDS-PAGE) as described by Kohanski & Schenker (124) using 10%T, 2%C slab gels. A similar protocol for measuring autophosphorylation was used Chapter 5, except that most experiments in that section used the same reaction conditions as in the peptide phosphorylation reactions (described below).

Peptide Substrate Phosphorylation Reactions.

IRS939, a peptide substrate based on the phosphorylation site Y^{939} of IRS-1, was used as substrate. All enzyme assay components except for manganese acetate (MnAc) and the enzyme itself were individually adjusted to pH 7.0 with either sodium hydroxide or acetic acid, filtered through 0.45µM or smaller filters, and stored in small aliquots at -80°C. MnAc solutions were made fresh and used immediately. Peptide and nucleotide concentrations were verified spectrophotometrically at 280nm and 259nm, respectively,

except for IRS939F, which was measured by weight (extinction coefficients for peptides are given in Chapter 3.) All kinase reactions were carried out at room temperature in 50mM Tris-acetate, pH 7.0. Unless noted otherwise, 50mM magnesium acetate (MgAc) and 0.1% BSA were also present in reaction mixtures. Reactions were quenched by addition of 0.1-0.5 volumes 5% H_3PO_4 (v/v). Reaction times, enzyme and substrate concentrations, and any preincubation of the enzyme were as described in the text and figure legends. Results from analyses with more that 20% phosphorylation of IRS939 were excluded because of excess substrate consumption. [γ^{32}P] ATP was used only in experiments explicitly intended for autophosphorylation measurements.

Reaction volumes were chosen such that 1-10 nmol of peptide were injected per analysis. This permitted assays at 10μM peptide, with a 100 μl injection volume, or up to 0.5 mM peptide with an injection volume of 20μl. Reactions using higher peptide concentrations required dilution after quenching to fall within the desired range for sample injection and product analysis.

HPLC Analysis.

IRS939 phosphorylation was assayed by HPLC using a Hewlett-Packard 1090 Liquid Chromatograph equipped with an automated injector. The column was a small-bore C8 column, 2x100mm, with MOS Hypersil-2 3μm packing (Keystone Scientific #103-32-2). Detection was done using a Linear Instruments 206 PhD continuous flow spectrophotometer and Linear Instruments UVIS 206 PC computer software for simultaneous monitoring of multiple wavelengths. Quantification of peak heights at 220nm was done with a Hewlett-Packard 3396A integrator.

A gradient system was used with the following solvents: A, 0.12% TFA (w/v), 1% methanol (v/v) and 2% acetonitrile (v/v) in water. B, 0.1% TFA (w/v), 1% methanol (v/v) and 2% water (v/v) in acetonitrile. Solvents were filtered through 0.45μM filters before use. Unless noted otherwise, elutions were performed at a flow rate of 0.25 ml/min using Gradient I: 0-5 min, 2-10% B; 5-16.5 min, 10-22% B; 16.5-16.6 min, 22-2% B, followed by 5.5 minute equilibration at 2% B. The column was washed periodically, as described under Results, using Gradient II: 0-5 min, 2-10% B; 5-16.5 min, 10-22% B; 16.5-30 min, 22-70% B; 30-31 min, 70-2% B; followed by 7 minutes equilibration at 2% B. Further details of this assay method are given in Chapter 3.

Two-Dimensional Phosphopeptide Mapping.

Autophosphorylated ^{32}P-labeled CKD was isolated for proteolytic digestion as described in (124). Proteolysis was done for 16-24hr using 1μg Endoproteinase Lys-C (Wako) in 0.5ml of 50mM ammonium bicarbonate, with a second addition of protease at 12-18hr. Gel fragments were recovered by centrifugation and the supernatant was lyophilized in a Savant Speed-Vac. Samples were resuspended in water and relyophilized 6-7 times. Two-dimensional phosphopeptide mapping for determination of autophosphorylation sites was performed according to Boyle *et al.* (309) with modifications as follows: Samples were reconstituted in 5-15μl 20% acetic acid and a portion (typically 1-5μl) spotted onto 20cm x 20 cm Kodak cellulose TLC plates (#1366061). Electrophoresis at 16°C in 20% acetic acid, 5% n-butanol was for 1 hour at 1000V, with a 19cm separation between electrodes. Under these conditions, the phosphopeptides are all cationic. Under these conditions, the phosphopeptides are all cationic. Ascending chromatography was done in butanol: pyridine : acetic acid : water

(15:10:3:12. v/v). Radiolabelled phosphopeptides were visualized by autoradiography using Kodak XAR X-ray film.

Figures for Chapter 2

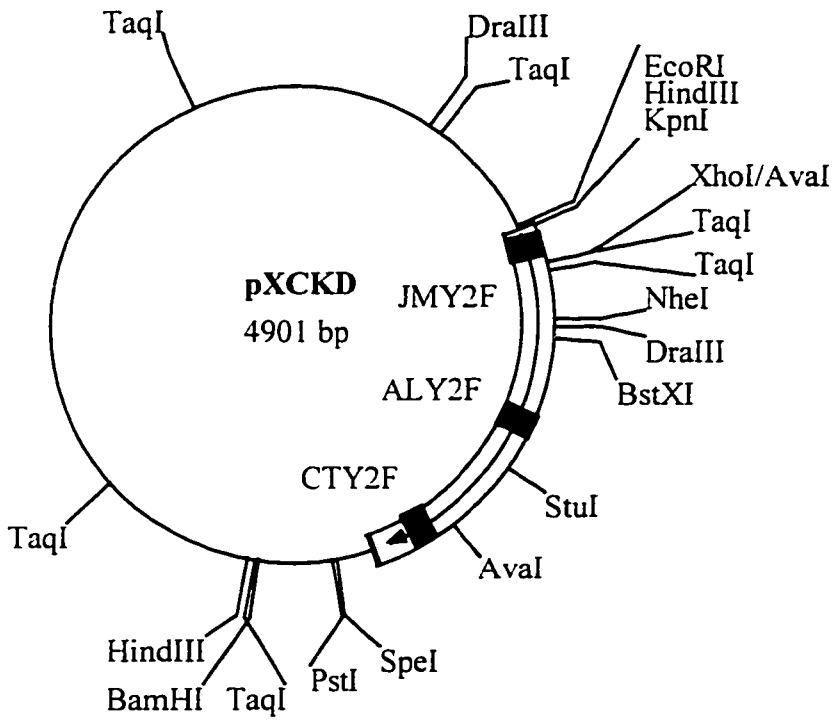

Figure 2-1 Diagram of pXCKD based constructs.

The cDNA of the hIR CKD is shown (boxed arrow) along with the modification sites of the JMY2F, ALY2F, and CTY2F tyrosine mutants (black squares). Restriction sites shown are common to all pXCKD-based constructs except as follows: An additional TaqI site is present at the CTY2F mutation site in pXCTY2F and derivatives; and the HindIII site 5' to the cDNA is replaced with an additional TaqI site in pXJMY2F and derivatives.

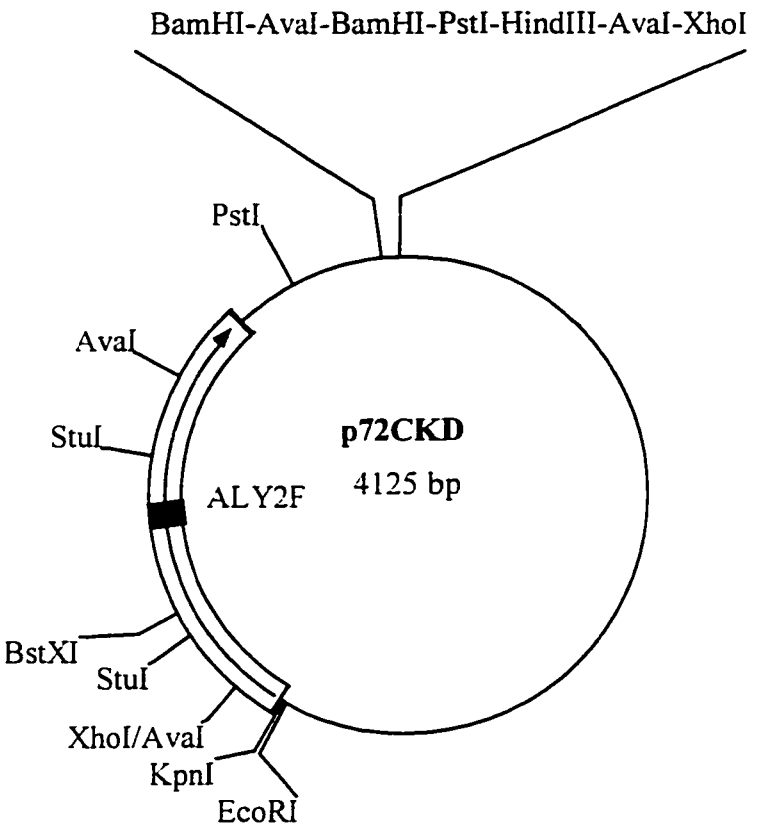

Figure 2-2 Diagram of p72CKD based constructs.

The cDNA of the hIR CKD (boxed arrow) in the context of p72, along with the modification site of the ALY2F mutant (black square).

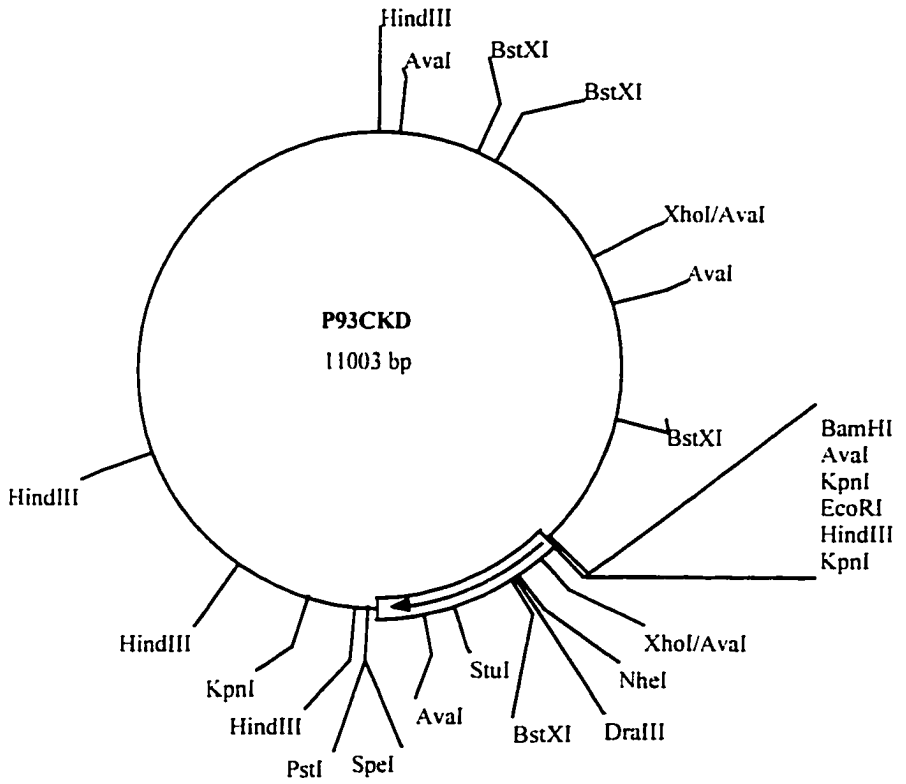

Figure 2-3 Diagram of pVL1393-based constructs.

The cDNA of the hIR is shown (boxed arrow) inserted to the vector pVL1393. Restriction sites shown are common to all mutant constructs except as follows: In constructs based on p72CKD (Y1158W, ΔGATE, ALY2F) the NheI site is silently replaced with a StuI site, and the HindIII site just 5' to the insert is missing. In the JMY2F construct the NheI site is retained but the HindIII site lost. All 33 TaqI sites, and mutation sites within the cDNA, are omitted for clarity.

3. Development of an HPLC-Based Peptide Phosphorylation Assay.[8]

Synthetic peptide reagents have several advantages over other commonly used tyrosine kinase substrates such as 4:1 poly Glu-Tyr copolymer (366), reviewed in (367), histones (5), and reduced and thio-carboxamidomethlyated lysozyme and its proteolytic fragments (124,368). Peptides are readily synthesized in any desired sequence and are commercially available at high purity, and have thus been used widely in the characterization of protein tyrosine kinases since their introduction to the field (369). To facilitate the kinetic study of the CKD, we developed a peptide-based assay for the IR kinase.

Assay of protein kinases began with indirect assays of the earliest studied protein kinase, phosphorylase kinase, which phosphorylates serine and threonine residues (255). Direct observation of phosphorylation was first done using [γ-^{32}P] ATP to radiolabel the protein substrate, followed by trichloroacetic acid precipitation (255). Since then, isotope-based quantitation of polypeptide product has become the dominant form of assay of protein kinases. Refinements have included use of filter paper binding (258,370,371), TLC (369,372), (SDS-PAGE, as in (124)), polyethyleneimine-cellulose chromatography (373), HPLC (374,375), or ferric-chelate paper (376) to recover ^{32}P-labeled

---

[8] This work has been reported (455).

phosphoproteins or phosphopeptides.[9] ^{32}P use is hazardous and inconvenient because of the need to replenish stocks frequently and the increasing difficulties of radioactive waste disposal. Use of [γ-^{32}P] ATP in protein kinase assays, although common, is therefore becoming problematic.

The most popular kinase assay is probably the phosphocellulose filter binding assay (reviewed in (377)). In addition to the use of [γ-^{32}P] ATP, the method requires peptide substrates with at least two positively charged residues. This requirement was advantageous in early studies of protein kinase A, whose preferred substrates include at least basic residues (378). Tyrosine kinases, however, have consensus sequences with few basic residues, and a predominance of acidic residues instead (37). Most physiologically derived peptide substrates of the IR, for example, have therefore been used with added basic residues to facilitate this assay (38,379,380). These additional residues may alter the kinetic properties of the substrates *via* altered charge or length, or even modulate the activity of the enzyme itself. The homopolymers poly-Lys and poly-Arg are already known to dramatically stimulate the insulin receptor kinase (381) and it is possible that similar effects could stem from high concentrations of polybasic peptides. Thus, modifications of peptide substrates specifically for isolation of the product could alter or mask important properties of these substrates.

Nonradioactive assays, which could avoid such complications, have been described. Nuclear magnetic resonance techniques can be used to follow phosphopeptide production directly, but requires high peptide concentrations because of low sensitivity

---

[9] The method of Toomik *et al.* (376) employs tritiated peptides instead of [γ-^{32}P] ATP. Many of the same

(382). Mass spectrometry (383) and capillary zone electrophoresis (384) show promise as kinase assays, but are not yet widely deployed. Techniques for quantifying ADP or P_i have been applied to the assay of protein kinases (114,385,386). However, these products may not be formed stoichiometrically with phosphopeptide in all cases, because of the variable levels of intrinsic ATPase activity common to most protein kinases (387,388) including the insulin receptor (389). Nonradioactive "tags" have also been added to peptides for recovery or detection in kinase assays: Biotinylated peptides can be selectively recovered (390) or quantified (391) by their tight binding to avidin. Detection of fluorescently labeled phosphopeptides has been done by a commercially available ferric chelate system (Spinzyme, Pierce Chemical Co.) or by electrophoretic mobility shift using peptides fluorescently labeled before (392) or after (393) the kinase reaction. When added before the kinase reaction, these nonradioactive labels may also affect the properties of the substrate.

In the present study, we have developed a nonradioactive assay for protein tyrosine kinase activity. Phosphorylation of peptides lowers their retention times from an RP-HPLC column, allowing for the separation and spectrophotometric quantitation of both apopeptide substrate and phosphopeptide product. This assay is suitable for the kinetic characterization of tyrosine kinases.

---

disadvantages apply.

HPLC Separation of Reaction Components and Products

The peptide substrate IRS939 (Table 3-1) is based on the sequence of the known IRS-1 phosphorylation site Y^{939}. When incubated with MnATP and CKD, IRS939 (peak 1) was converted into a second peak (Peak 2, Figure 3-1). The identity of Peak 2 as phosphorylated IRS939 (P-IRS939) was established in several ways: (1) when [γ-^{32}P] ATP was included in the reaction mixture, P-IRS939 (but not IRS939) was radioactive. (2) Direct sequencing by automated Edman degradation showed the selective absence of the ninth amino acid in P-IRS939, eluted at 11.8 minutes, whereas Tyr was the ninth amino acid sequenced in IRS939, eluted at 14.3 minutes. (3) The A_{220}/A_{280} ratio of P-IRS939 was 8 times higher than that of unmodified IRS939 (Table 3-1), as expected (394). (4) P-IRS939 was formed only upon incubation of IRS939 with CKD in the presence of ATP and Mg^{2+} or Mn^{2+}. Prequenching of the complete reaction mixture, or omission of enzyme or ATP, abolished formation of P-IRS939.

No HPLC peak was attributable to the enzyme itself, which in any event was usually present in subpicomolar quantities. The assay therefore gave no information about enzyme autophosphorylation.

Table 3-1 Physical Properties of Peptide Substrates and Inhibitors.

Peptide	Sequence	Retention Time (min)	ε_{220} ($M^{-1} \cdot cm^{-1}$)	ε_{280} ($M^{-1} \cdot cm^{-1}$)
IRS939	REETGSEE**Y**MNMDLG	14.3	15100	1280
P-IRS939	REETGSEE**pY**MNMDLG	11.8	15100	160
IRS939F	REETGSEE**F**MNMDLG	17.1	15100	<30

This table shows the primary sequence and physical properties of the substrate, product, and inhibitor forms of IRS939. The sole tyrosine, phosphotyrosine, or phenyalanine residue is shown in **red**. All sequences were verified by automated Edman sequencing, including the absence of tyrosine in P-IRS939. Peptide synthesis and sequencing were done by the Protein Core facility of the Mt. Sinai School of Medicine. Retention times were measured using Gradient I or II. ε_{280} for IRS939 was calculated using the PEPTIDESORT computer program (280), and ε_{220} calculated using the A_{220}/A_{280} ratio measured from elution profiles. ε_{220} for P-IRS939 and IRS939F were assumed equal to that of IRS939, and their ε_{280} values calculated using their measured A_{220}/A_{280} rations. Since IRS939F had no detectable absorption at 280nm, its ε_{280} is stated as an upper bound.

Use of Carrier BSA

When we began analyzing the recovery of stable reaction products, we observed that net peptide recovery was incomplete at low concentrations of peptide and ATP. Therefore, we added carrier BSA to the reaction mixtures, since this was known to have no effect on CKD autophosphorylation (124). Titration of BSA led to 0.05% as the minimum saturating concentration for both complete peptide recovery and optimal kinase activity (Figure 3-2). To provide a margin of safety, we routinely used 0.1% BSA as a carrier in out kinase reactions. This necessitated periodic washing of the column to prevent BSA buildup, as discussed below.

To further assess the assay method, we followed the formation of P-IRS939 and the net recovery of peptide over time (Figure 3-3). Recovery of IRS939, measured as the sum of apo-IRS939 and P-IRS939 recovered, was independent of the extent of reaction. This indicated that accurate quantitation of apo- and phosphopeptide, using integrated peak areas at 220nm, was not affected by phosphorylation. Moreover, IRS939 could be completely converted to P-IRS939, suggesting a homogenous pool of phosphate acceptor.

Compatibility of the Assay with Reaction Components

IRS939F, which was identical to IRS939 except for the replacement of the tyrosine residue with phenylalanine (Table 3-1), was used to demonstrate the compatibility of this assay system with peptide inhibitors (Figure 3-4). Substitution of the less-polar Phe for Tyr typically increases the retention of peptides on RP-HPLC

columns. IRS939F was found to elute after IRS939 (Figure 3-4 and Table 3-1) and thus did not interfere with quantitation of IRS939 and P-IRS939. The inhibitory nonhydrolyzable analog of ATP, adenylyl imidodiphosphate (AMP-PNP) was also used as an inhibitor of peptide phosphorylation in the insulin receptor kinase (Figure 3-4). Since AMP-PNP coeluted with ATP, it did not interfere with quantitation of peptide species. Therefore, inhibitor studies, important for kinetic analyses, may be done with this assay.

Tyrosine kinases have been studied using either magnesium or manganese as the required divalent cation (for example, (395)). However, DTT is a common preservative in enzyme reactions and purifications, keeping cytoplasmic proteins in a reduced state. We found during the development of this assay that the combination of manganese and DTT led to instability of the quenched reaction mixture. Reactions done with DTT present could be analyzed immediately, but upon standing in DTT-containing acidified reaction mixture, IRS939 was converted to a series of new peaks (Figure 3-5). These peaks were *not* P-IRS939 because they occurred even when CKD or ATP were excluded from the reaction mixture. Moreover, P-IRS939 was itself converted to a similar mixture of peaks under the same conditions. The modification(s) responsible for the new peaks was not determined, but these artifacts did not occur if manganese or DTT were omitted from the reaction mixture. However, these peaks were never observed in experiments using magnesium as the divalent cation, even with 1mM DTT present in the reaction mixture. Therefore, experiments were typically done using MgAc as the metal cofactor.

Chromatography Details

BSA was not eluted from the HPLC column by Gradient I. We found that multiple analysis using BSA-containing reaction mixture led to progressively delayed elution of ATP and the earlier elution of peptides (Figure 3-6). This eventually led to a loss of separation of peptides from ATP, which made quantitation of peptides inaccurate, especially at low peptide concentrations or with little conversion of apo- to phosphopeptide. This effect was prevented by periodically eluting the BSA from the column by performing an assay using Gradient II instead of Gradient I. Gradient II is identical to Gradient I before 16.5 minutes, so peptide elution is unaffected; but since Gradient II is longer, it reduces the number of samples that can be analyzed per day.

700μg of injected BSA was the largest amount that did not interfere with phosphopeptide quantitation under the conditions shown in Figure 3-6. As a precaution, we generally washed the column after 300μg net BSA has been injected. Assays at elevated ATP concentrations required more frequent washing, since the interfering ATP peak is broader. In an experiment identical to that in Figure 3-6, but with 10mM ATP instead of 0.5mM, 300μg BSA (five runs) was sufficient to interfere with analysis. If more than 500nmol ATP are injected per analysis, it is best to perform all analyses with Gradient II. The frequency of wash cycles can be reduced by injecting smaller volumes, which decreases both the BSA bound in each run and the amount of "interfering" ATP.

There was a small (<0.5% peak area) run-to-run carryover of peptides. This is normally below the margin of error of measurement. However, a blank gradient needed

to be run between injections producing large peptide peaks and injections producing much smaller peaks.

The choice of gradient is a major factor in the time required for assay. The principle gradients described here (Gradient I and II) were chosen for general applicability to a wide range of ATP and peptide concentrations assayed in the presence of carrier BSA. For some applications, this is not necessary, and a shorter gradient can be used. For example, the gradient used in Figure 3-4 eluted both IRS939 and P-IRS939 in under ten minutes without compromising the accuracy or net peptide recovery. We were not successful in establishing an isocratic elution system; these were found to yield broad peaks and poor resolution of ATP from phosphopeptide.

Limits of This Assay

Our IRS939 preparation included a small (0.3% total peptide) contaminant which coeluted with P-IRS939. Because of this, each experiment included a prequenched control which was subtracted from the measured P-IRS939 peak area. The lower limit of detection was the higher of either 0.5 % conversion to P-IRS939 or 10 pmol P-IRS939. Reproducibility of integrated peak areas, based on repetitively injected samples from a single quenched reaction mixture, was typically ± 5% phosphopeptide peak area for P-IRS939 peaks representing 2% conversion of IRS939.

Discussion

The present assay technique has several advantages over most other protein kinase assays. Since nucleotides are well separated from peptide substrates and products (Figure 3-1), the ATP concentration can be as high as necessary to achieve saturation of the enzyme. We have successfully measured reaction rates from 50μM - 15mM ATP. This is an advantage over methods using [γ-^{32}P] ATP, whose sensitivity actually *falls* as total ATP concentration increases due to the decreasing specific radioactivity of [γ-^{32}P] ATP. The range of ATP usable in this assay is limited only by the lower detection limit for phosphopeptide, discussed below.

The range of usable peptide concentrations is also broad. Since the chromatography technique used is retentive, injection volumes can be raised to increase sensitivity at low peptide concentrations. Figure 3-6 demonstrates analysis with a 2.4% conversion of 20μM IRS-939, using 75μl injections; we have performed assays successfully at peptide concentrations as low as 10μM, using an injection volume of 200μl. Purity of the peptide substrate can also be a limiting factor in the sensitivity of phosphopeptide detection. In our preparation of IRS939, for example, a very small (0.3%) impurity was found to co-elute with P-IRS939, and was subtracted from every experiment during quantitation. This nevertheless prevented accurate quantitation of P-IRS939 peaks much below 0.5% the area of the apopeptide. Reaction mixtures can be diluted prior to analysis, so there is no upper bound on assayable peptide concentration other than solubility. We have assayed IRS939 phosphorylation at concentrations up to 1mM.

The ability to isolate peptides of varying sequences by reverse phase HPLC has already been established. Phosphorylation decreases the retention time of peptides from RP-HPLC columns because of the increased hydrophilicity of the phosphate group compared to the hydroxyl group (Table 3-1 and Figure 3-1). This has been observed for a range of phosphorylated peptides (396) and for tryptic phosphopeptides derived from the CKD itself (67). A basic substrate of a serine kinase has been assayed using this principle (397). Reduction in peptide retention by phosphorylation appears to be a general phenomenon allowing the separation of apo- and phosphopeptide by reversed-phase HPLC under acidic conditions .[10]

Inhibition studies are essential for distinguishing between closely related kinetic mechanisms by initial velocity studies (398). Construction of peptide inhibitors of protein kinases is commonly done by synthesizing a pseudosubstrate: replacing the phosphate acceptor hydroxyl group of a known substrate with a hydrogen atom (323). We tested our assay for compatibility with one such inhibitor, IRS939F, where the phosphate-accepting tyrosine residue in the substrate IRS939 was replaced with a phenylalanine residue. IRS939F was in fact an inhibitor of IRS939 phosphorylation (Figure 3-4). IRS939F eluted after apo-IRS939 and thus did not interfere with quantitation of either IRS939 or P-IRS939. This was expected, since the phenylalanine residue in IRS939F was more hydrophobic than the tyrosine in IRS939. This compatibility of IRS939F with our assay system is probably a general feature of the Tyr-to-Phe class of pseudosubstrate peptide inhibitors.

---

[10] Ferry *et al.* (375) observed both increasing and decreasing retention of various peptides upon

AMP-PNP, a nonhydrolyzable inhibitory analog ATP, coelutes with ATP and did not interfere with quantitation of peptide species (Figure 3-4). The present assay is therefore generally compatible for studies with both peptide and nucleotide inhibitors.

During the development of this assay, we detected and corrected an apparent problem with peptide recovery (Figure 3-2). The nature of this loss was not determined, but was probably binding of peptide to the plastic walls of the reaction tubes or the glass walls of the HPLC vials. The assay has a built-in control for such losses: total peptide recovery is quantifiable with every assay Most other assays, including the phosphocellulose filter binding assay, lack this control and may consequently underreport enzyme activity (399).

There are several possible extensions to this assay. This technique could be used to study other protein kinases or phosphatases. Studies of reverse reactions of these enzymes is also possible. Moreover, for some kinetic paradigms, it is useful to monitor the phosphorylation of multiple substrates in the same reaction mixture. This should be possible if a gradient can be established where the substrates and products are resolved from each other. If necessary, slight modification of peptides can produce large changes in elution times. For example, a peptide equivalent to IRS939 except for the absence of the carboxy-terminal glycine residue eluted at 16.1 minutes instead of 14.3 minutes (using Gradient I).

In summary, the method described here is applicable to a broad range of substrate concentrations and compatible with common types of kinase inhibitors. Peptides do not

---

phosphorylation, but their chromatography was carried out at pH 7.4.

require special modifications to facilitate detection or the separation of products from substrates. Radioisotopes are not needed for detection, and the net recovery of apo- plus phosphopeptide can be monitored as an internal control for the reactions. Finally, it is compatible with inhibitor studies for the kinetic analysis of protein kinases. These properties suggest that reverse phase HPLC may prove generally useful in the study of protein tyrosine kinases, their peptide substrates, and inhibitors, and possibly other enzymes that metabolize phosphopeptides as well.

Figures for Chapter 3

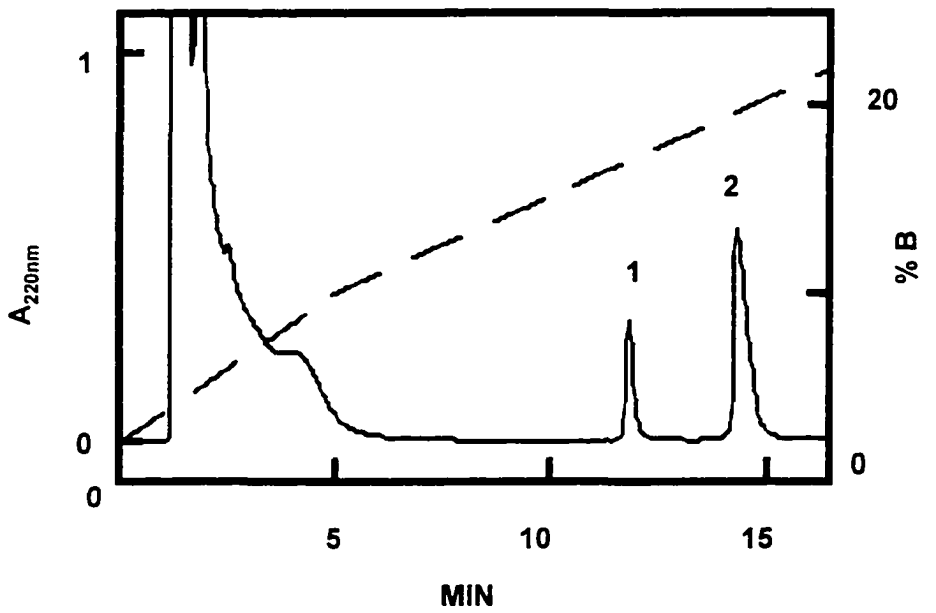

Figure 3-1 Separation of IRS939 from P-IRS939.

A typical chromatogram of an IRS939 phosphorylation reaction mixture is shown. 112μM IRS939 was phosphorylated using 360nM CKD in 50 mM MgAc, 50mM Tris acetate, and 1mM ATP for 4 min before acidification of 0.2 volumes 5% H_3PO_4. A 50 μl aliquot was injected onto a 2 x 100 mm MOS-Hypersil-2 column and eluted using the gradient shown. P-IRS939 (peak 1) is readily resolved from IRS939 (peak 2); peaks were identified as described in the text.

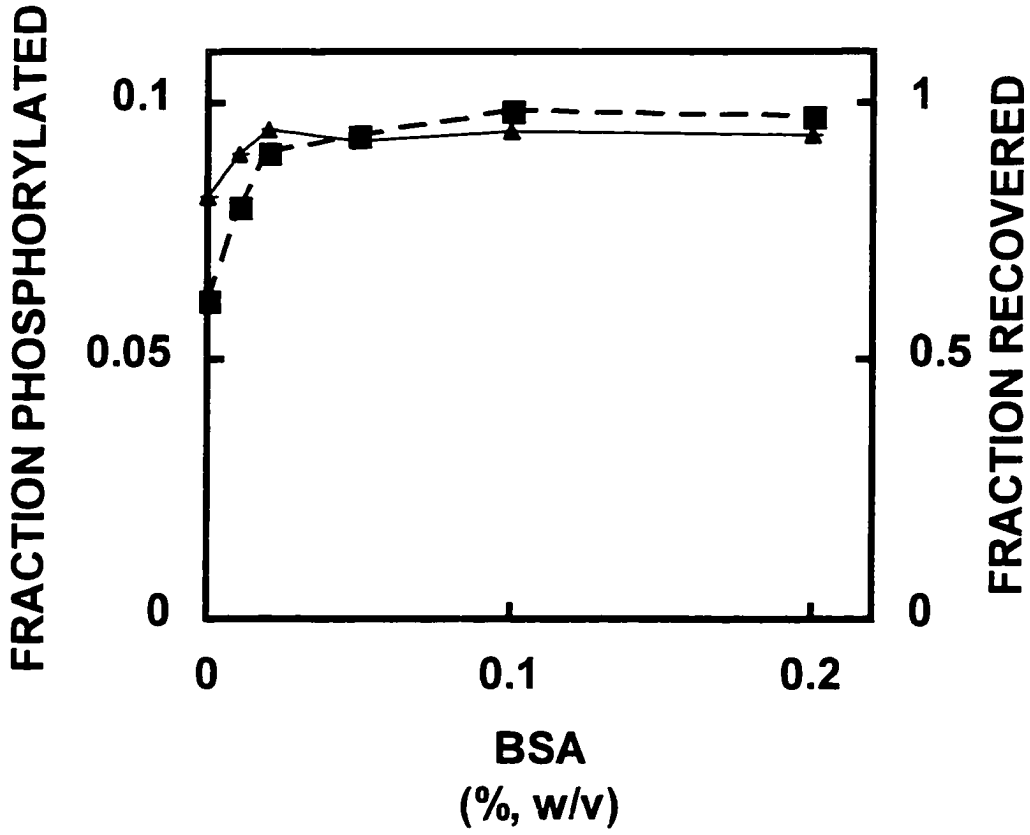

Figure 3-2 Effect of BSA on Peptide Recovery and Phosphorylation.

The BSA concentration was varied in a series of 80µl reaction mixtures containing 50µM IRS939, 100nM CKD, and 1mM ATP. Reactions were quenched after five minutes with 8µl of 5% phosphoric acid and 30µl were analyzed by HPLC using the following gradient: 0-2.5 minutes, 2-12% B; 2.5-16.5 minutes, 12-25% B. P-IRS939 recovered, expressed as a fraction of total IRS939 injected (■), and the net recovery of apo- and phosphopeptide (i.e., the sum of recovered P-IRS939 and recovered IRS939, expressed similarly: ▲) are shown as a function of BSA concentration. These values were determined from duplicate reaction mixtures by integration of the appropriate peaks on HPLC chromatograms. Error bars are ±1 standard deviation.

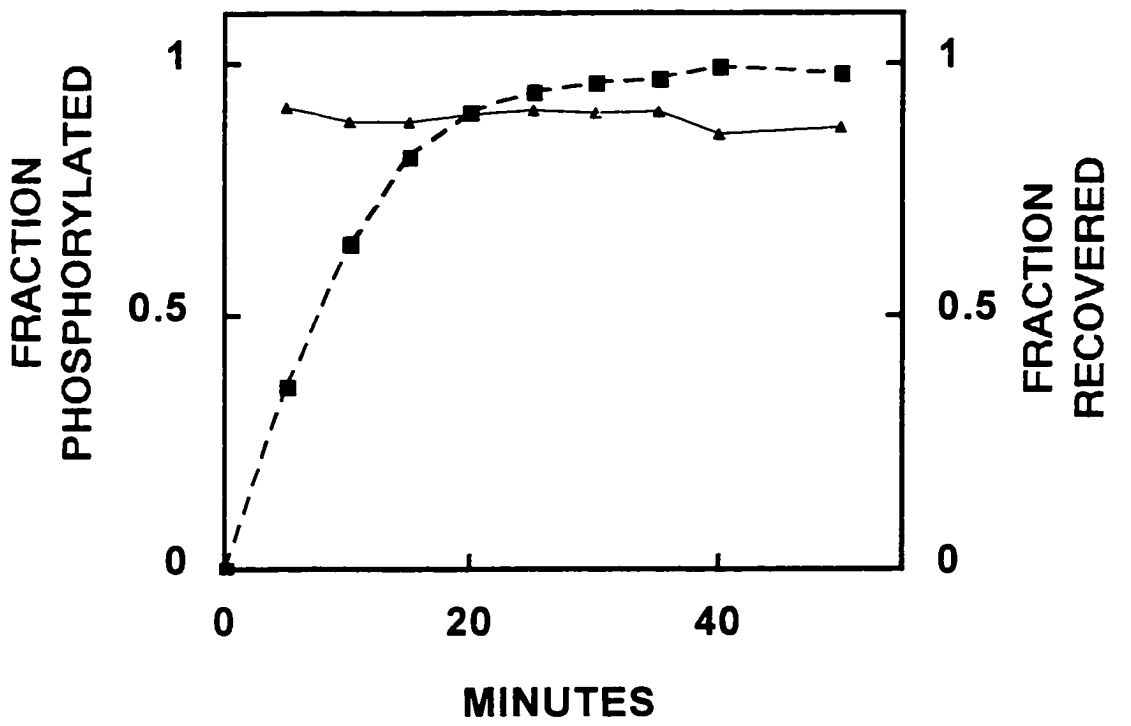

Figure 3-3 Time Course of IRS939 Phosphorylation by CKD.

500nM CKD was activated by pre-autophosphorylation with 500μM ATP in the presence of 30μg/ml protamine chloride. After 20 minutes, the enzyme was diluted to 7.2nM in a reaction mixture containing 500μM ATP and 50μM IRS939. 100μl aliquots were withdrawn at the indicated times and quenched by addition of 20μl 5% H_3PO_4, and 90μl were then analyzed by HPLC using Gradient I. IRS939 phosphorylation (■) and net recovery of apo- plus phosphopeptides (▲) as a function of reaction time, are expressed as in Figure 3-2, except without error bars since only single determinations were made.

Figure 3-4 Inhibition of IRS939 Phosphorylation by Peptide or Nucleotide Inhibitors.

Reaction mixtures, of 20µl each, containing 290µM IRS939 in the presence of 0.5mM ATP were incubated for ten minutes (A), or phosphorylated for ten minutes in the presence of 80nM protamine-stimulated CKD, prepared as in Figure 3-3 (B), or 80nM protamine-stimulated CKD plus 1.5mM IRS939F (C). Reactions were quenched and diluted by addition of 180µl reaction buffer containing 0.22% phosphoric acid, and 80µl aliquots were analyzed by HPLC. IRS939 phosphorylation was inhibited by AMP-PNP (D-F). 40µl of 2mM AMP-PNP in water was acidified by adding 10µl of 5% phosphoric acid and 20µl were analyzed by HPLC (D). 112µl IRS939 was phosphorylated for 1.5 minutes with 200µM ATP and 36nM protamine-stimulated CKD without (E) or with (F) 2mM AMP-PNP, and quenched and analyzed similarly. In this experiment the flow-rate was increased to 0.3 ml/min and the elution gradients were are shown (- - - -). P-IRS939, IRS939, and IRS939F, when present, eluted at 7.8, 9.6, and 11.5 minutes, respectively.

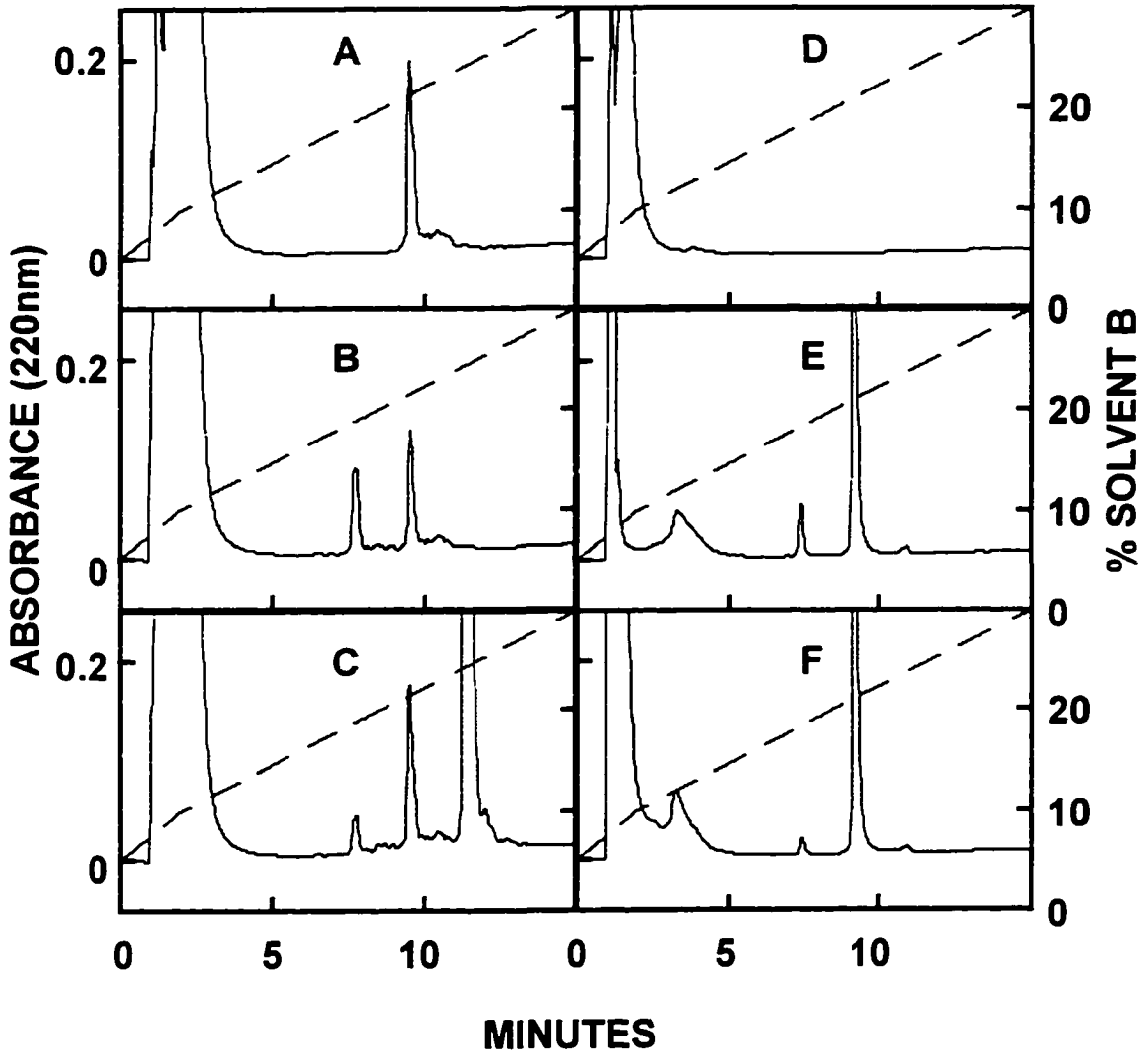

Figure 3-4 Inhibition of IRS939 Phosphorylation by Peptide or Nucleotide Inhibitors.

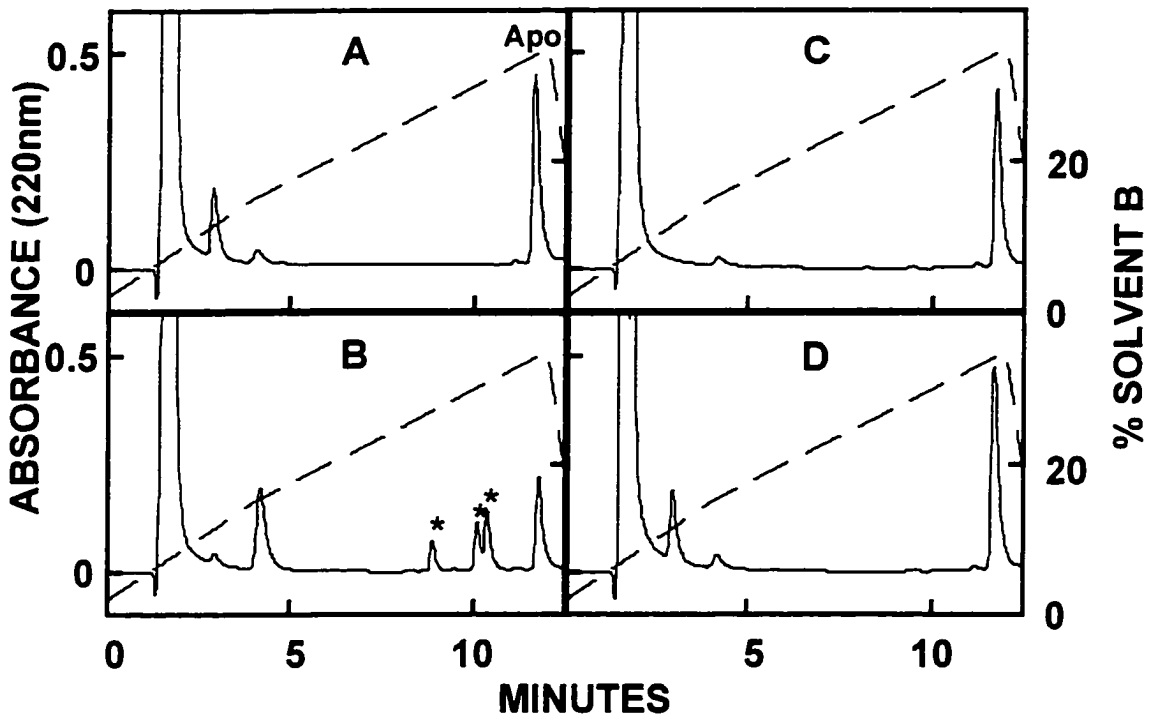

Figure 3-5 Stability of the Apopeptide in Quenched Reaction Mixtures.

Because routine automated assay of hundreds of samples would necessarily involve a delay between sample preparation and assay of later samples, we investigated the stability of reactants in quenched reaction mixtures. Mixtures of 100 µl each containing 100µM IRS939, 1 mM ATP, 5mM MnAc, and 1mM DTT, but no MgAc, BSA, or CKD, were acidified with 10µl of 5% H_3PO_4 *before* the addition of CKD to a final concentration of 200nM. 25µl aliquots were analyzed either immediately (A) or after standing for 18 hours at room temperature in a sealed glass HPLC vial (B). Reaction mixtures omitting DTT (C) or MnAc (D) were also analyzed after standing for 18 hours. Unmodified IRS939 eluted at 11.7 minutes using the gradient shown (- - - -). Unmodified P-IRS939, not present in this experiment, eluted at 10.0 minutes using this gradient.

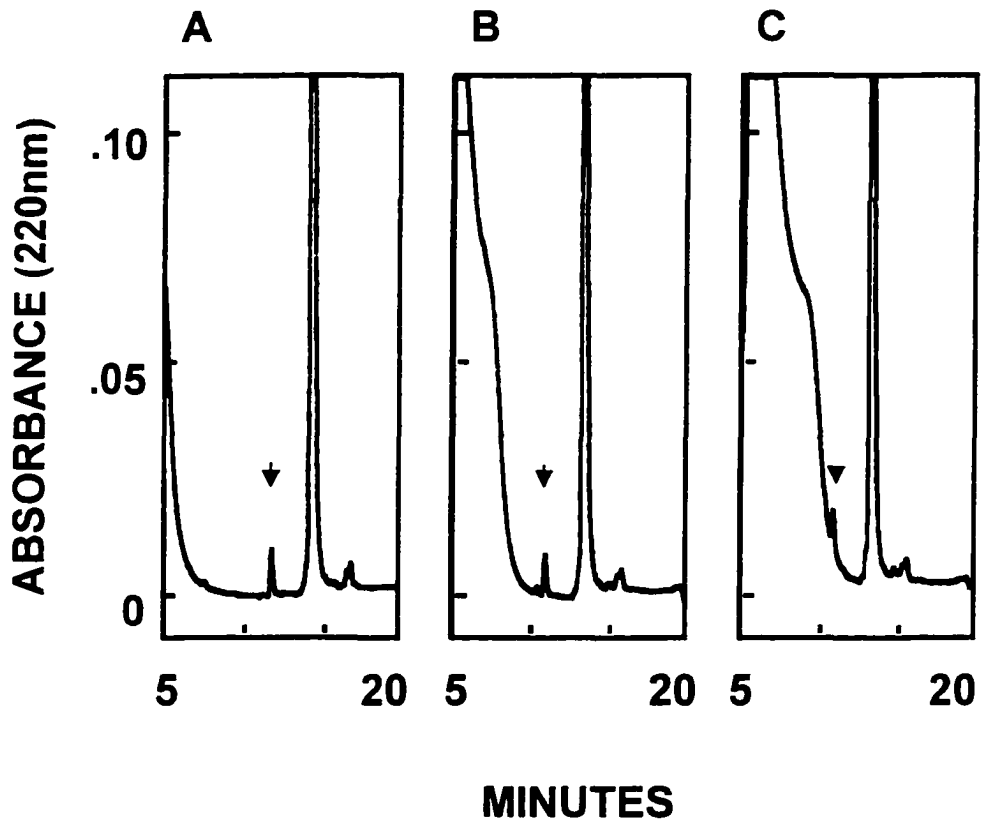

Figure 3-6 Cumulative Effect of Multiple Injection on Phosphopeptide Elution and Detection.

To determine how frequently the HPLC column needed to be regenerated, we investigated the effect of sequential analyses on recovery and quantitation of reactants and products. 20μM IRS939 was phosphorylated by 50nM CKD in the presence of 1mM ATP and quenched after four minutes by addition of 0.2 volumes 5% phosphoric acid. Repeated injections of 75μl aliquots of the quenched reaction mixture were made sequentially. Elutions were done using Gradient I, without intervening wash cycles, so that BSA accumulated on the column. Chromatograms from the 1st (A), 12th (B) and 16th (C) injections are shown. The trailing edge of the large peak at the left- hand side of each chromatogram is ATP. The elution times of P-IRS939 (▼) were 11.8, 11.1, and 10.9 minutes, and the elution times of IRS939 were 14.3, 13.6, and 13.4 minutes, in panels A, B, and C, respectively. The phosphopeptide peak shown represents 2.2% phosphorylation of the peptide, or 42 pmol P-IRS939.

4. *Cis* Autophosphorylation of Juxtamembrane Tyrosines.[11]

In this chapter, we examine the hypothesis that clusters of the multiple autophosphorylation sites in Figure 1-1 proceed *via* different molecular mechanisms. The JM autophosphorylation sites proceeded *via* a kinetic pathway that is distinct from that of the other sites, as a function of both ATP dependence and reaction rate (67). It seemed plausible, therefore, that these sites could proceed *via* a distinct molecular mechanism as well. We use the technique of Todhunter & Purich (illustrated in Figure 1-3), in conjunction with site-directed mutagenesis, to resolve the site-specific contributions of both *cis* and *trans* autophosphorylation in the CKD.

Kinetics of Juxtamembrane Autophosphorylation

In order to most clearly demonstrate the mechanism of the JM sites, we utilized reaction conditions where these sites were the dominant component of autophosphorylation. A previous kinetic study (75) had revealed that the JM sites are favored relative to other sites by low ATP concentration. We therefore used 10μM ATP in our initial studies. We chose a reaction time of one minute as the minimum experimentally reproducible reaction time, so that net autophosphorylation would most nearly reflect the rate of initial autophosphorylation rather than an endpoint

---

[11] These results have been reported (456).

stoichiometry. To maintain the constraint ATP>>CKD for pseudo-first order reactions while maximizing radioisotope incorporation, we used 1.4μM CKD.

We verified that these conditions yielded juxtamembrane autophosphorylation by using [γ-^{32}P] ATP to radiolabel CKD under the above reaction conditions, followed by two-dimensional TLC analysis of radiolabeled peptides generated by Endo-Lys C protease digestion (Figure 4-1). The same procedure was applied to mutant CKD molecules lacking pairs of major autophosphorylation sites $Y^{965,972}F$ (JMY2F), $Y^{1162,1163}F$ (ALY2F), and $Y^{1324,1334}F$ (CTY2F). We found that juxtamembrane autophosphorylation was the dominant (>90%) component of autophosphorylation in the wild-type, ALY2F and CTY2F CKDs. The ALY2F construct showed more carboxyl terminus autophosphorylation than the WT or CTY2F CKDs.

Map assignments were made using two techniques. First, we monitored the loss of each spot in the appropriate mutant using reaction conditions (1.4 μM CKD, 20 minute reaction time, 500μM [γ-^{32}P] MnATP) where all spots were populated in the wild-type kinase (Figure 4-1, panel E). For example, the J spot is absent in the map of the JMY2F-CKD under these conditions (D). Engl *et al.* (400) also found a very similar tryptic peptide from the JM region at this location, using a similar mapping technique, but another group did not (401). We therefore further verified the identity of the JM peptide by reverse phase HPLC exactly as described in (67,75). The tryptic peptide derived from the JM spot eluted at the position previously determined for the principal juxtamembrane tryptic peptide. Moreover, an apparently identical tryptic peptide was observed, by both

two-dimensional TLC and HPLC, in both the ALY2F and ΔGATE constructs (Table 2-2), confirming that this site could not have been at the activation loop.

Independence of JM Autophosphorylation on CKD Concentration

Once we had determined that our reaction conditions permitted chiefly JM autophosphorylation, we investigated the molecular mechanism of autophosphorylation by measuring the concentration dependence of autophosphorylation.

In the plot shown in Figure 4-2 the stoichiometry of autophosphorylation for each versions of the CKD is shown as a function of CKD concentration. Autophosphorylation of the WT- and CTY2F-CKD is qualitatively independent of enzyme concentration, and quantitatively showed a first-order (WT, 1.04±.02 ; CTY2F, 1.05±.03) dependence on enzyme concentration over the ranges tested. The WT and CTY2F-CKDs therefore meet the above criteria for a *cis* autophosphorylation reaction, which occurs at the JM autophosphorylation sites.

Deviation from *cis* autophosphorylation was found to correlate with a shift towards phosphorylation at other sites. The ALY2F mutant autophosphorylates by a *cis* reaction below 150nM (apparent reaction order, 1.03±0.02) but shows a detectable contribution of *trans* autophosphorylation above 290nM (reaction order 1.13 ± 0.04). This mutant also shows a larger component of CT autophosphorylation compared to the WT-CKD, as measured at 1.4 μM enzyme in Figure 4-1. Autophosphorylation of the JMY2F-CKD is highly enzyme concentration dependent (an apparent slope of 1.5 ±0.05) and very slow (about 10% that of the WT construct even at 1.1 μM enzyme, Figure 4-2), consistent with the absence of the dominant *cis* JM autophosphorylation pathway. Thus,

in these four versions of the CKD. then, deviation from pure *cis* autophosphorylation (Figure 4-2) and deviation from pure juxtamembrane autophosphorylation (Figure 4-1) both follow the order JMY2F>>ALY2F>CTY2F=WT.

Dependence of Juxtamembrane Autophosphorylation on ATP Concentration

The average stoichiometries of autophosphorylation in Figure 4-2 were 0.23±0.02, 0.04±0.01, and 0.04±0.01 for the ALY2F, WT, and CTY2F enzymes, respectively. These three reactions all involved the same JM autophosphorylation sites (Figure 4-1). Thus, removal of two potential (but unused) autophosphorylation sites in the ALY2F construct caused a 6-fold increase in the rate of *cis* autophosphorylation at the JM sites. To investigate the kinetic basis for this observation, we varied the only accessible parameter of the reaction, ATP concentration (Figure 4-3).

The WT and CTY2F enzymes showed similar second-order rate constants for *cis* JM autophosphorylation (k_{JM}/K^{MnATP} of 3200 and 4900 min^{-1} M^{-1}, respectively; Table 4-1). We use k_{JM} to denote the apparent catalytic constant for juxtamembrane autophosphorylation, and K^{MnATP} to denote the half-saturation point with the substrate MnATP (this value does not apply when using Mg^{++} as cofactor). The ALY2F construct showed a much more efficient JM autophosphorylation reaction (k_{JM}/K^{MnATP} of 121000 min^{-1} M^{-1}) due primarily to a 24-fold drop in K^{MnATP}. Using the constants in Table 4-1, we calculated autophosphorylation stoichiometries at 10μM MnATP of 0.03, 0.04, and 0.30 mol PO_4/mol CKD, which compares well to the observed averages of 0.04, 0.04, and 0.23 for the WT, CTY2F, and ALY2F kinases respectively. Thus, the increased

autophosphorylation of the ALY2F at 10μM MnATP appears to be a function of its lowered K^{MnATP}.

Table 4-1 ATP Dependence of Juxtamembrane Autophosphorylation.

Enzyme	K^{MnATP} (μM)	k_{JM} (mol mol^{-1} min^{-1}	k_{JM}/K^{MnATP} (x10^{-3} min^{-1}M^{-1})	$\Delta\Delta G$ kcal/mol)
WT	75 ±3	0.24 ±0.02	3.2	N/A
CTY2F	120 ±16	0.59 ±0.06	4.9	-0.25
ALY2F	3.2 ±0.3	0.39 ±0.10	121	-2.2

The data from the Eadie-Scatchard plots in Figure 4-3 were analyzed by linear regression to extract an apparent first-order rate constant for JM autophosphorylation (k_{JM} from the *x*-axis intercept) and the apparent dissociation constant for ATP binding (K^{MnATP}, the negative reciprocal of the slope). $\Delta\Delta G$ was calculated from the formula $\Delta\Delta G = -RT\,ln\left[\frac{(k_{JM}/K^{MnATP})_{mut}}{(k_{JM}/K^{MnATP})_{WT}}\right]$. Errors shown are ±1 standard deviation.

Kinetics of AL and CT Autophosphorylation.

It is generally accepted that the kinase domains of RTKs autophosphorylate in *trans*, and this has been supported by crystallographic data (21,352). Here, we have reported *cis* autophosphorylation in the unique juxtamembrane subdomain of the IR-CKD, which was not present in those crystallographic studies. To provide a positive control for our study, we set out to verify the occurrence of *trans* autophosphorylation at

AL and CT sites in the WT-CKD. To accomplish this, we employed the activating polycation protamine chloride (125,381) and 500μM MnATP, a concentration known to enhance autophosphorylation of these sites (75). Under these reaction conditions, autophosphorylation occurred chiefly at the AL and CT sites, with a predominance of bis- and tris-phosphorylated activation loop phosphopeptides (Figure 4-4). These reaction conditions were thus suited for studying the molecular mechanism of the fast phase of autophosphorylation. We used the same concentration-dependence technique used above (Figure 4-2, illustrated in Figure 1-3) to study the molecular mechanism of autophosphorylation (Figure 4-5). Autophosphorylation was very rapid and showed an apparent reaction order of 1.8, with a maximum incorporation at one minute reaction time of 3.2 +/- 0.5 mol PO_4/ mol kinase (out of a possible 7). No further enhancement of rate was observed above 200nM CKD, suggesting that either the enzyme-enzyme interaction was saturated, the enzyme had reached its V_{max} for autophosphorylation, or near-endpoint conditions were being observed at this point. This showed that the CKD employed here *is* capable of intermolecular autophosphorylation, and the *cis* autophosphorylation in WT, ALY2F, and CTY2F-CKD detected in Figure 4-2 results from the intrinsic molecular mechanism and not from any technical difficulty or systematic error obscuring *trans* reactions.

Interaction with ATP

The activation-loop autoinhibited form of CKD is partially stabilized by a hydrogen bond between the catalytic base and Y^{1162} (21). During this study, we also observed enhanced initial autophosphorylation in the ALY2F construct (Figure 4-2),

which we ascribed to a reduced K^{MnATP} for autophosphorylation (Figure 4-3 and Table 4-1). Elevated basal activity in activation loop Tyr-> Phe mutants has been previously observed (70,73) but not addressed kinetically. The most likely structural explanation for this reduced K^{MnATP} is then not the prevention of formation of pY^{1162} (which does not occur in any case, Figure 4-1), but loss of the hydrogen bond between *tyrosine*-1162 and D^{1132}. Removal of this constraint in the ALY2F construct would be expected to make it easier to remove the activation loop from its autoinhibitory conformation. This would facilitate ATP access for autophosphorylation at remaining autophosphorylation sites, explaining the reduced K^{MnATP} observed for this reaction.

To further explore the connection between activation loop mutations and the ATP dependence of *cis* autophosphorylation, we measured the ATP dependence of autophosphorylation for mutants in the activation loop. A view of key residues involved in stabilizing the activation loop is shown in Figure 4-6. D^{1161} makes four ionic interactions in a solvent-shielded environment, evidently playing an important role in loop stabilization. We constructed a $D^{1161}A$ mutant to examine the effect of disrupting these interactions. Additionally, we constructed mutants with deletions of a large portion of the activation loop (ΔGATE and ΔGATE2). A $Y^{1158}W$ mutant was originally intended to facilitate tryptophan fluorescence studies of gate conformation, but is also useful to examine alteration of this residue (in comparison to the ALY2F mutants). ATP data for autophosphorylation of these mutants is shown in Figure 4-7 and Table 4-2. Interestingly, the D1161A, ΔGATE and ΔGATE2 enzymes all have approximately the same kinetic parameters as each other and ALY2F, a 30-fold drop in K^{MnATP} for JM

autophosphorylation. This suggests that the activation loop is a bistable construct, as will be discussed further in Chapter 6.

Table 4-2 ATP Dependence of JM Autophosphorylation in AL Mutants.

Enzyme	K^{MnATP} (μM)	k_{JM} (mol mol^{-1} min^{-1}	k_{JM}/K^{MnATP} (x10^{-3} min^{-1}M^{-1})	$\Delta\Delta G$ kcal/mol)
D1161A	3.9	0.31	79	-1.9
ΔGATE2	4.0	0.17	42	-1.6
Y1158W	79	0.21	2.6	+0.13

The data from the Eadie-Scatchard plots in Figure 4-7 were analyzed and described as in Table 4-1.

We also measured the JMY2F mutant's dependence on ATP by the same protocol used in Figure 4-3 (Figure 4-8). JMY2F showed a ninefold increase in K^{MnATP} (to 640μM) and a twofold drop in k_{JM} for autophosphorylation, measured at 200nM kinase. Since the overall rate of JMY2F autophosphorylation is concentration-dependent (Figure 4-2), one or both of these parameters (probably k_{JM}) must be enzyme-concentration dependent as well. These parameters must apply to autophosphorylation of the activation loop and/or carboxyl terminus residues. It has already been observed that these sites proceed *via* a different kinetic phase with an elevated K^{MnATP} for autophosphorylation relative to juxtamembrane autophosphorylation (75). The altered K^{MnATP} observed in this experiment for the JMY2F construct may then reflect the properties of the sites

undergoing autophosphorylation rather than a change in the enzyme's interaction with ATP, as we will discuss further in Chapter 6.

The Two Phases of Autophosphorylation Have Distinct Molecular Mechanisms

Earlier work on the kinetics of the CKD and tetrameric IR identified two reaction phases, a high-affinity slow phase occurring at the juxtamembrane autophosphorylation sites and a low-affinity fast phase at the activation loop and carboxyl terminus sites (75). To determine whether each reaction phase progressed in *cis* or *trans*, we studied the enzyme concentration dependence of autophosphorylation of the wild-type CKD and several site-specific mutants under conditions where they autophosphorylated principally by the slow phase (Figure 4-1 through Figure 4-3) or fast phase (Figure 4-4 and Figure 4-5). The first-order dependency observed in the wild-type CKD reacting by the slow phase (Figure 4-2) is a hallmark of *cis* reaction. Under the same reaction conditions, deviation from first-order dependence on enzyme concentration among the mutants correlated with the appearance of autophosphorylation at non-juxtamembrane sites (Figure 4-1). Stimulated autophosphorylation in the wild-type CKD, which occurred at sites characteristic of the fast phase of autophosphorylation (Figure 4-4), also occurred by a *trans* mechanism (Figure 4-5). These results provide compelling evidence that both *cis* and *trans* pathways exist in the CKD, and that the *cis* pathway specifically applies to the juxtamembrane autophosphorylation sites.

Figures for Chapter 4

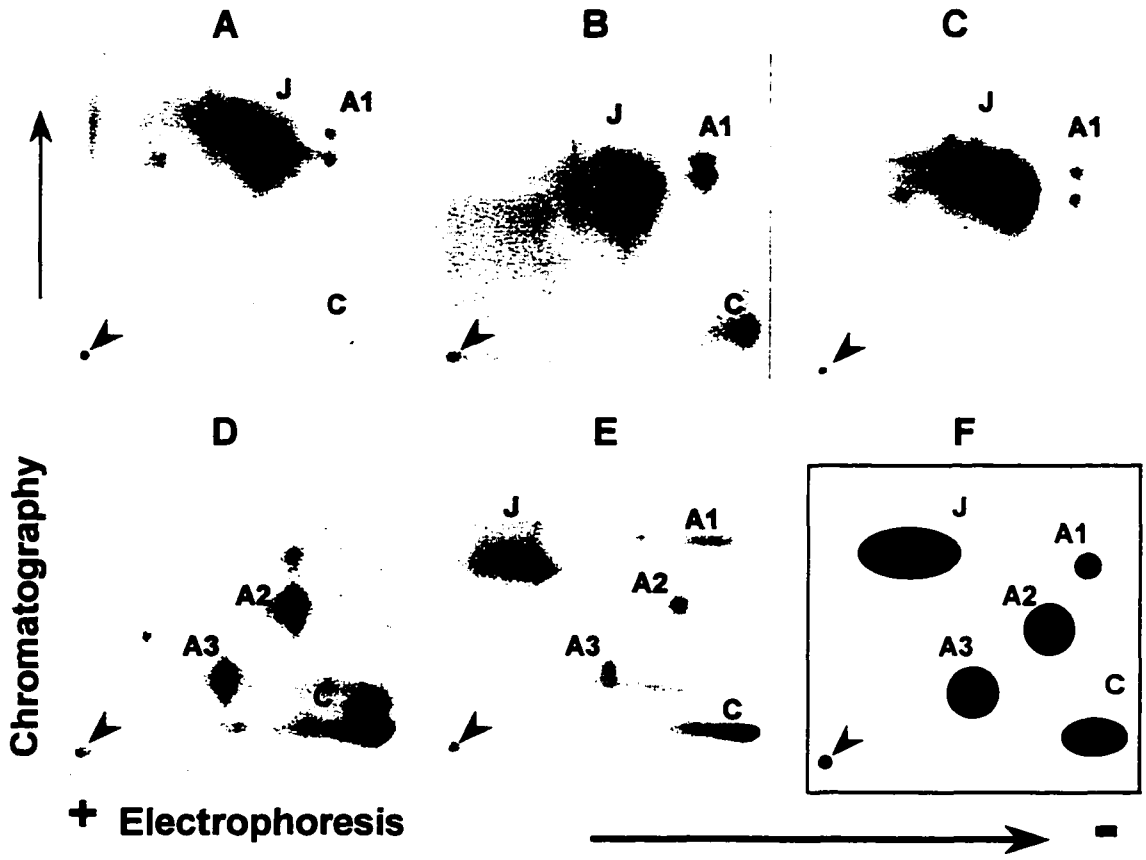

Figure 4-1 Site distribution of initial autophosphorylation.

These autoradiograms show two-dimensional [^{32}P]-phosphopeptide maps generated by endoproteinase Lys-C digestion of autophosphorylated CKD molecules. WT (A), ALY2F (B), or CTY2F (C) -CKD were autophosphorylated for 1 minute using 10μM [γ-^{32}P] ATP at 1.4μM enzyme concentration. Twenty-minute reactions at 500μM [γ-^{32}P] ATP and 1.4μM CKD were also done for JMY2F (D) and WT-CKD (E). [^{32}P]-phosphopeptides were resolved by electrophoresis in the first dimension and ascending TLC in the second, as described in Materials and Methods. *Arrowheads* denote the point of sample application. Spot assignments (F) were made as described in the text: J, juxtamembrane; A1, A2, and A3, activation loop, mono-, bis-, and tris- phosphorylated; C, carboxyl terminus autophosphorylation sites. Autoradiogram exposure times were adjusted to give approximately equal saturation of the film for the J spot.

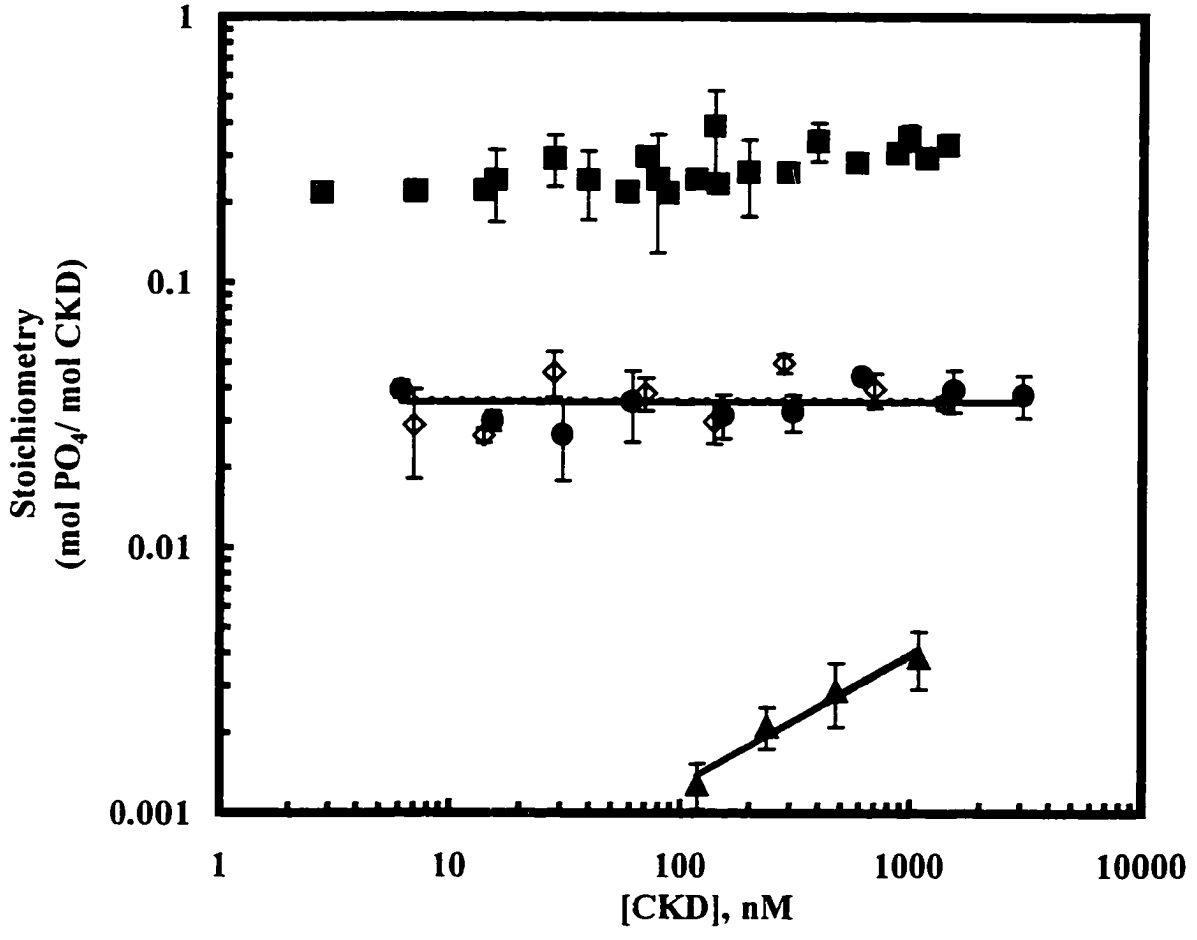

Figure 4-2 Concentration Dependence of Autophosphorylation.

Various concentrations of WT (●), ALY2F (■), JMY2F (▲), and CTY2F (◇) were incubated with 10μM ATP for 1 minute and assayed for autophosphorylation by SDS-PAGE as described in Materials and Methods, except for the use of 0.1% BSA as carrier. Data points, collected in quadruplicate, are shown ± 1 standard deviation. Results are expressed as moles phosphate incorporated per mol kinase. Specific activities of [γ-^{32}P] ATP ranged from 10000 to 27000 cpm/ pmol, measured at the time of data collection.

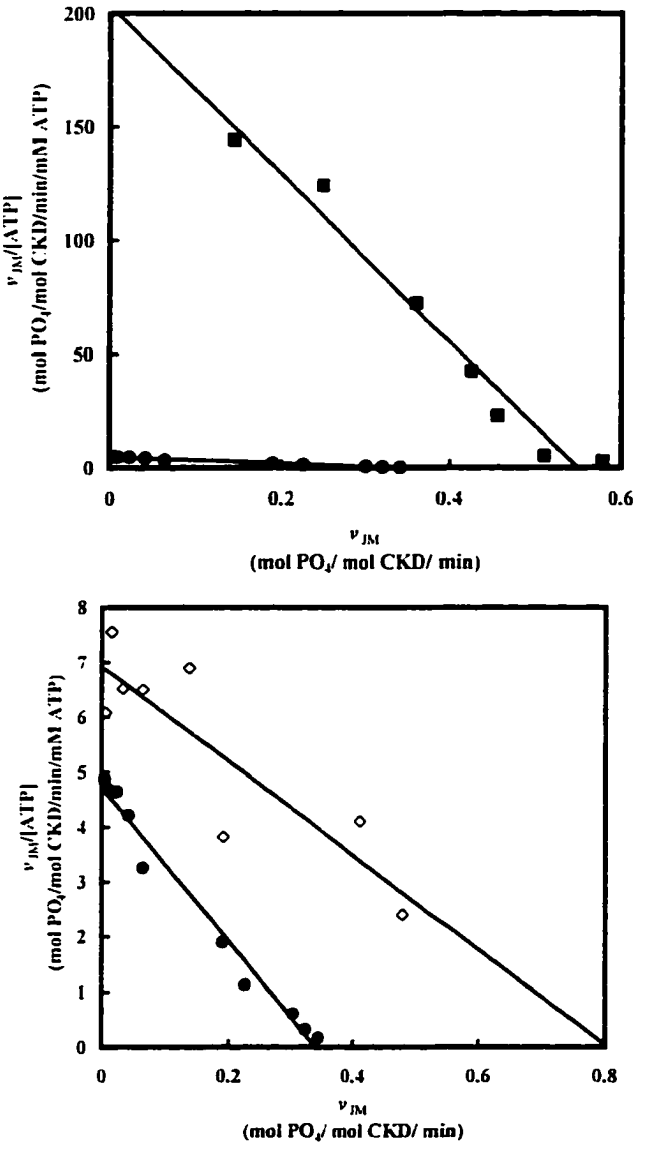

Figure 4-3 Dependence of JM Autophosphorylation on MnATP.

100nM WT (●), 120nM ALY2F (■), or 120 nM CTY2F (◇) were incubated with various concentrations of [γ-^{32}P] ATP for one minute and the reaction products measured as in Figure 4-2; data points are the average of two determinations. The data are shown as an Eadie-Scatchard plot. A fixed number of cpm [γ-^{32}P] ATP was used for each reaction series as follows: WT, 3.4 x 10^6 cpm per 40µl reaction; ALY2F and CTY2F, 3.6 x 10^6 cpm per 60µl reaction. The right panel is rescaled to allow visibility of the ALY2F dataset.

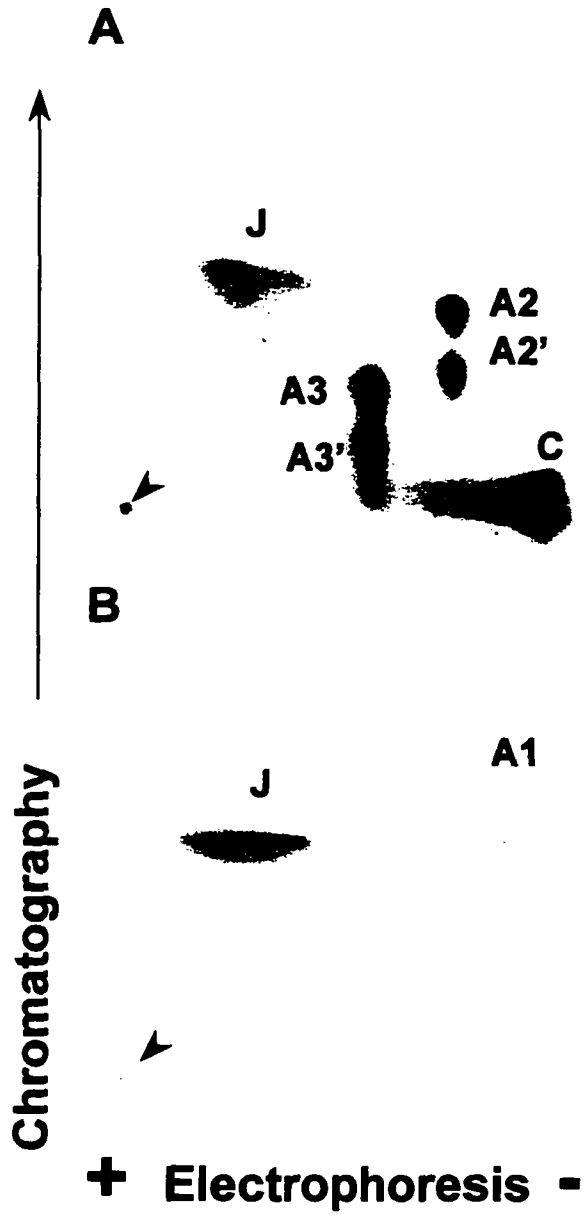

Figure 4-4 Site distribution of initial stimulated autophosphorylation.

These autoradiograms show two-dimensional [^{32}P]-phosphopeptide maps from WT-CKD autophosphorylated for 1 minute with 500μM [γ-^{32}P] ATP, at 0.7 μM enzyme concentration, with (A) or without (B) 30μg/ml protamine chloride. Mapping techniques and site assignments are as in Figure 4-1.

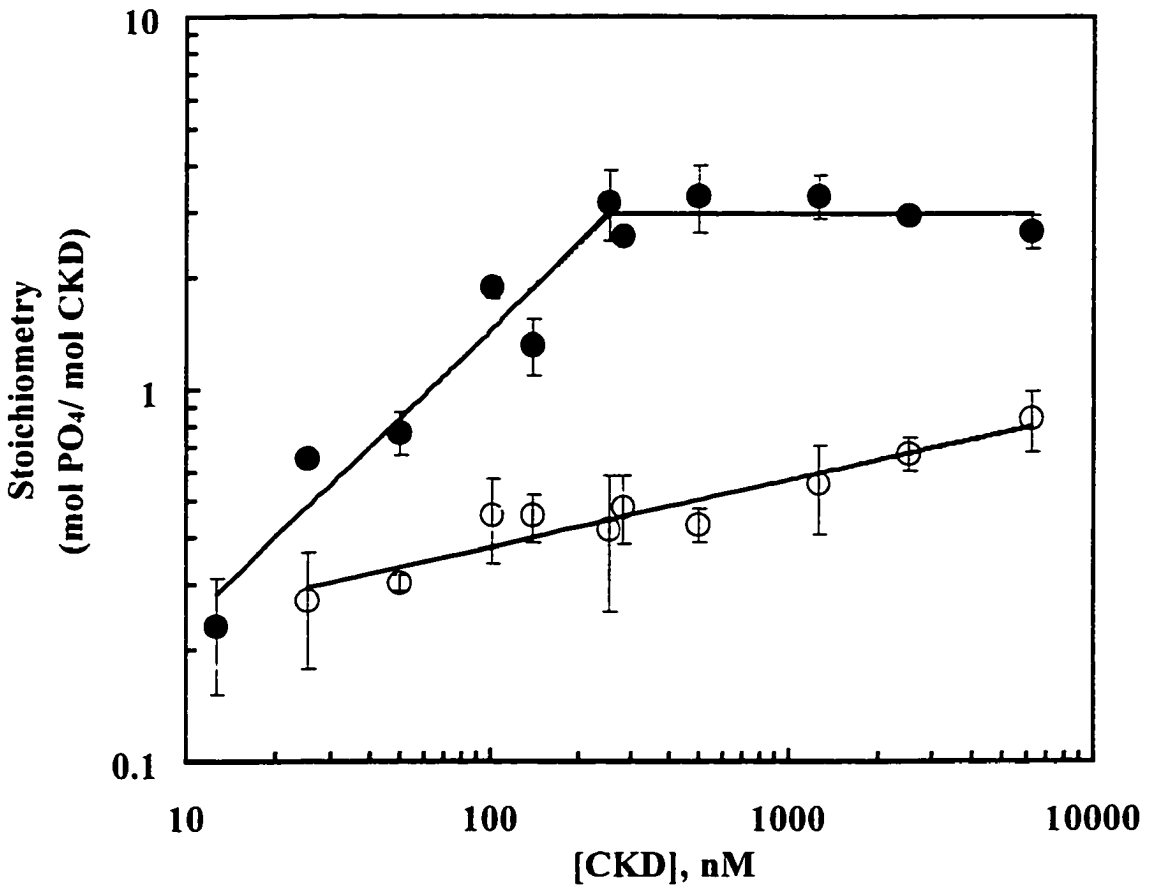

Figure 4-5 Enzyme Concentration Dependence of AL and CT Autophosphorylation.

To determine the molecular mechanism of CKD autophosphorylation at AL and CT sites, WT-CKD was autophosphorylated under conditions that favored these domains. The indicated concentration of WT-CKD was autophosphorylated with 500μM MnATP with (●) or without (○) 30μg/ml protamine chloride, using 0.1% BSA as carrier in either case. Data were measured in at least triplicate and expressed as in Figure 4-2. Specific activities of [γ-^{32}P] ATP ranged from 320 to 3200 cpm/ pmol, measured at the time of data collection.

Figure 4-6 Residues Stabilizing the Activation Loop in IRK.

This figure shows the interactions between the variable portion of the activation loop and the rest of the kinase molecule in IRK. The three potential autophosphorylation sites in the activation loop (Y^{1158}, Y^{1162}, and Y^{1163}) are shown from left to right as bright red stick models. As before, Y^{1162} can be seen hydrogen bonded (dotted lines) to the catalytic base D^{1132} (olive). The rest of the activation loop is drawn in bright pink stick models, except for E^{1159}-D^{1161}. E^{1159} and T^{1160} are omitted for clarity; these residues are pointing towards the viewer, into solvent. Note in particular that D^{1161}, shown in yellow, makes numerous contacts with residues from the large lobe and is a key site of stabilization for the activation loop. Residues not in the activation loop are drawn as green stick models (for those residues making H-bonds with the activation loop) or blue spheres (all others).

This figure was arranged with SwissPDB-View (402) and rendered with POV-RAY (403).

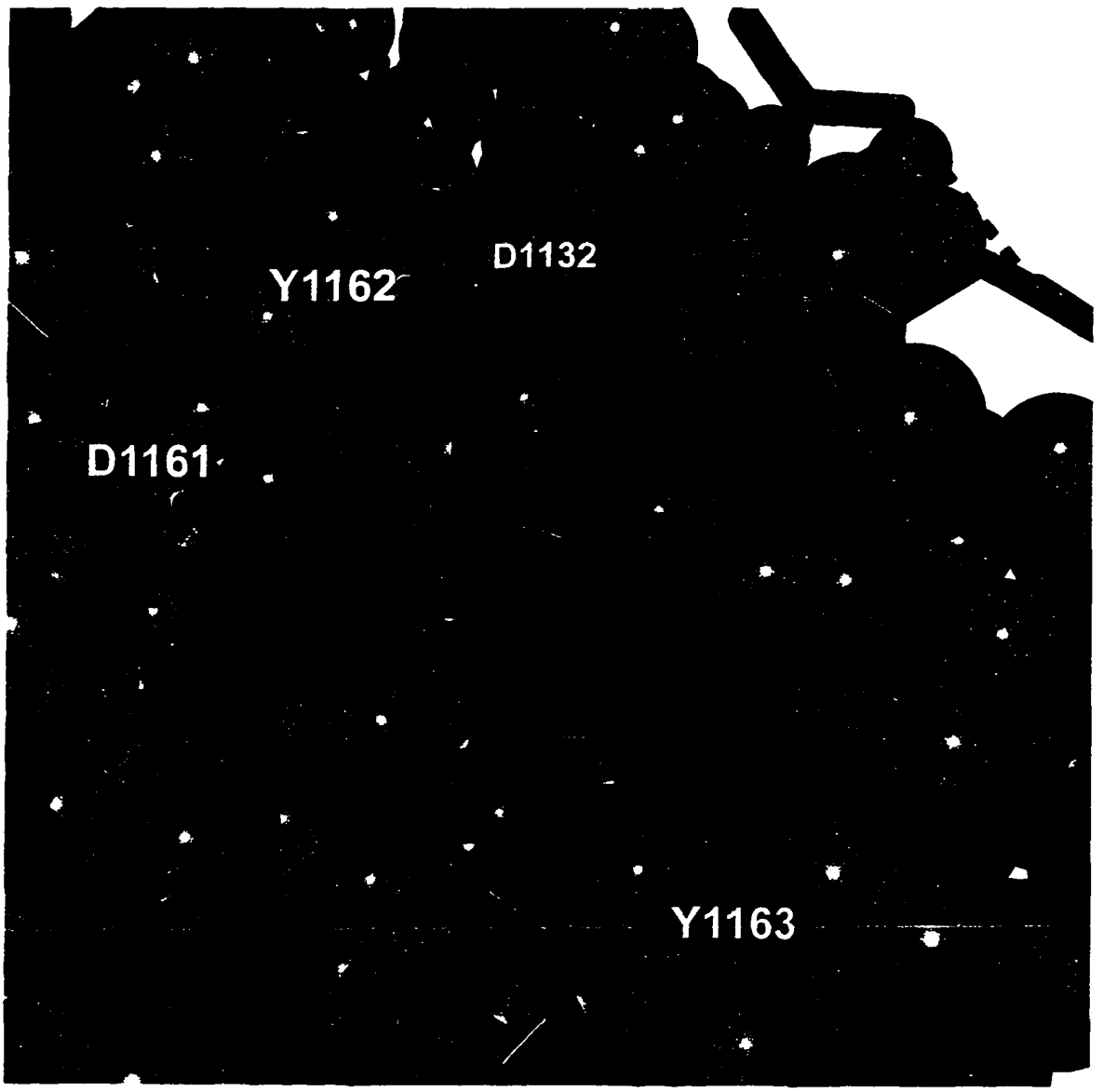

Figure 4-6 Residues Stabilizing the Activation Loop in IRK.

Figure 4-7 ATP Dependence of Autophosphorylation in AL Mutants.

Autophosphorylation of activation loop mutants was measured and shown as in Figure 4-3. Autophosphorylation data is shown for the Y1158W (◆), WT (●), ALY2F (X), D1161A (■), and ΔGATE2 (··) enzymes. Data for the ALY2F and WT kinases are redrawn from Figure 4-3. The lower panel is rescaled for better visibility.

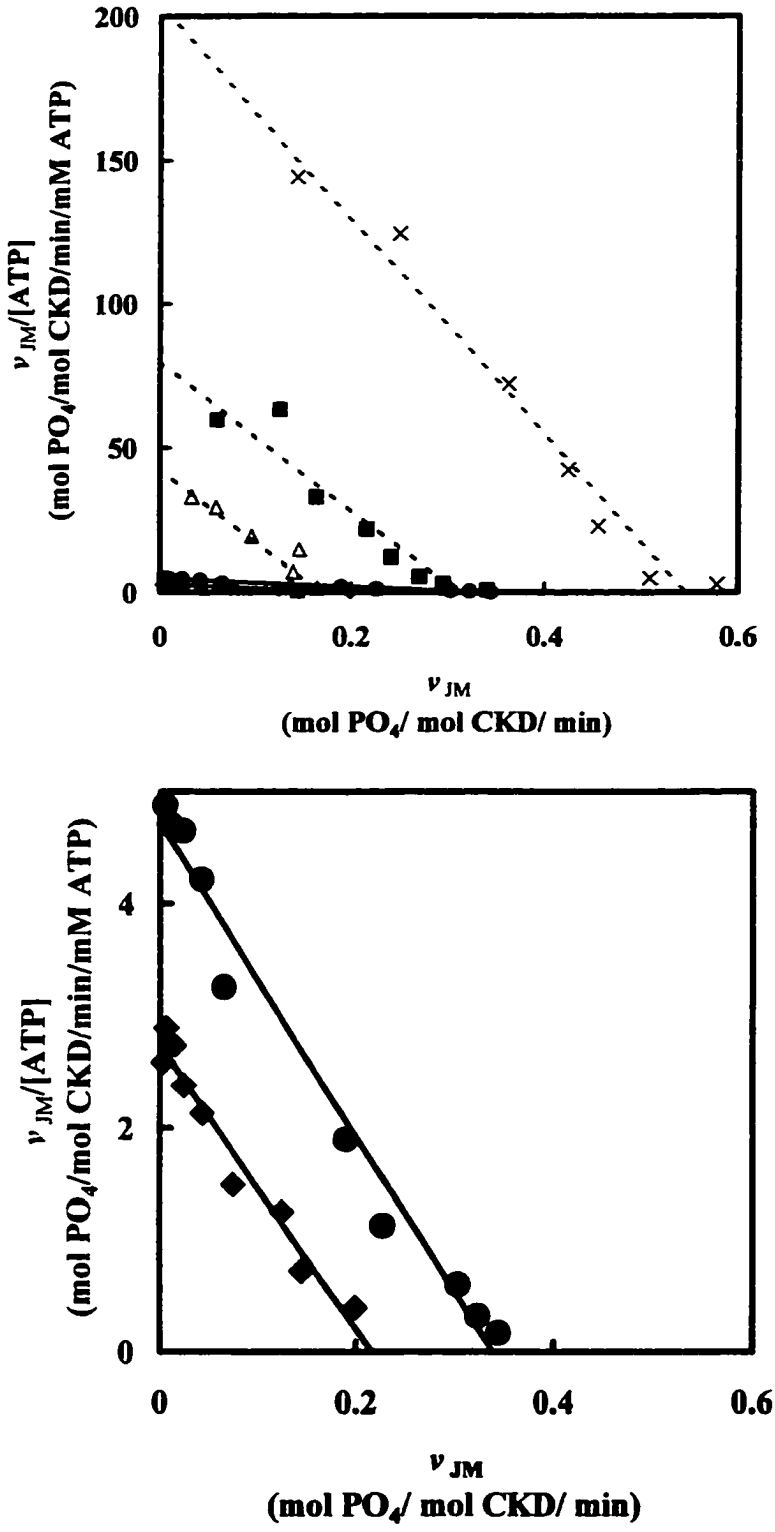

Figure 4-7 ATP Dependence of Autophosphorylation in AL Mutants.

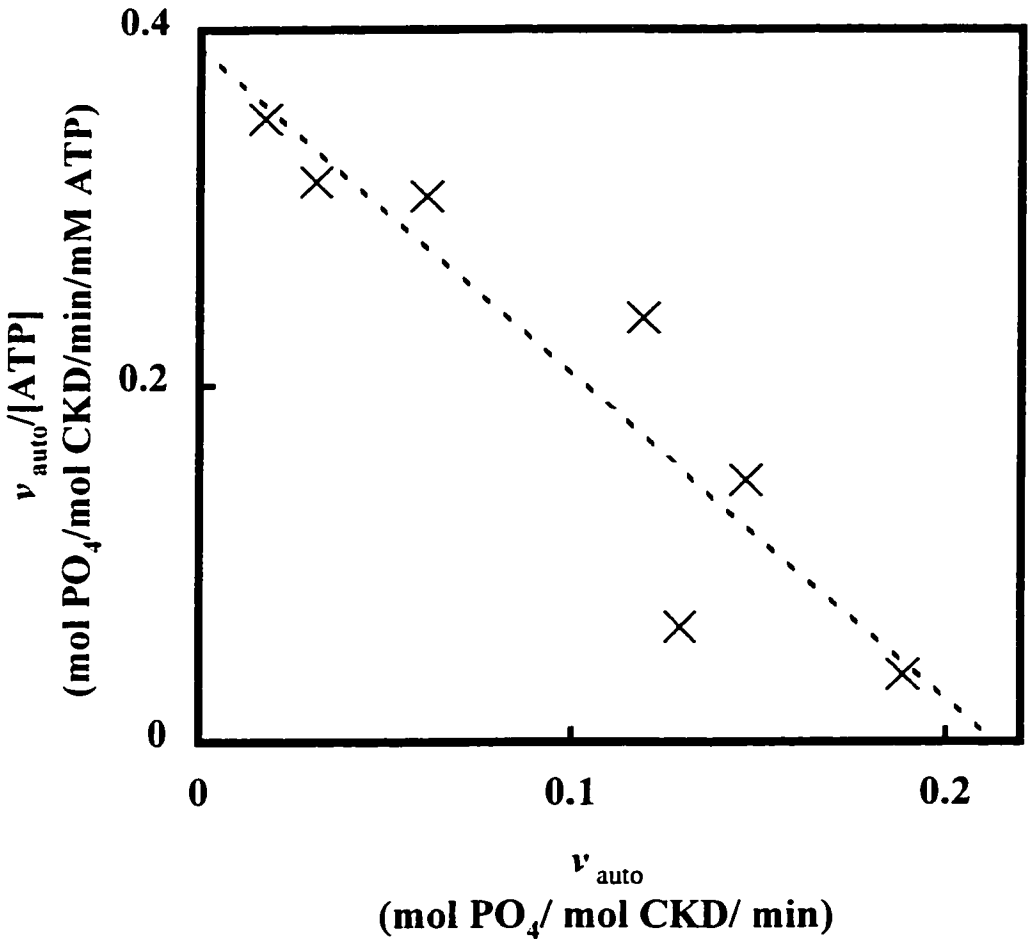

Figure 4-8 ATP Dependence of JMY2F Autophosphorylation.

The ATP dependence of autophosphorylation in the JMY2F construct was measured and displayed as in Figure 4-3. v_{auto} is used instead of v_{JM} because JM autophosphorylation does not occur in this construct.

5. Activating Effects of Juxtamembrane Autophosphorylation[12]

Lag Phase in IRS939 Phosphorylation.

To characterize the basal state of the CKD, we studied the phosphorylation of IRS939 in the presence and absence of activating agents. When assayed in the presence of 50 mM MgAc and 0.5 mM ATP, we found a lag phase in the phosphorylation of IRS939 (Figure 5-1). Naive enzyme (reaction begun by addition of enzyme, without preincubation) did not show a strictly initial linear reaction progress (R^2 = 0.98 when measured over 0-50 min, and note the upward curvature) but did eventually reach a steady state at a final velocity of 29 min^{-1} (measured over 25-50 min, R^2 = 0.997). This reaction showed a lag phase, measured as a time intercept, of 7.6 ± 1.0 minutes; this observation was statistically significant when compared to the null hypothesis (no lag phase; p=.006). When the enzyme was preincubated with MgATP and protamine chloride, the subsequent reaction was linear (R^2 = 0.996), showed no significant lag phase (time intercept, 0.8 ± 0.55 minutes; p = 0.21), and was much faster (260 min^{-1}). Enzyme preincubated with MgATP alone showed a small lag phase of questionable significance (1.0 ± 0.46 minutes, p = 0.06) and was also linear (R^2 = 0.998); the rate, however, was nearly unchanged from enzyme assayed without preincubation (37 min^{-1}). Other preincubation experiments showed that preincubation with 50 mM MgAc, 50μM IRS939,

---

[12] Preliminary portions of this work were presented at the Tenth Symposium of the Protein Society

2mM AMP-PNP (a nonhydrolyzable ATP analog), or buffer alone did not affect the course of the subsequent IRS939 phosphorylation reaction (Figure 5-2). Thus, the lag phase was abolished by preincubation with only those conditions that would be expected to support autophosphorylation: it required both divalent cation and hydrolyzable ATP, and was not due to a peptide-induced conformational change.

These observations suggested that the lag phase might be due to progressive autophosphorylation of the enzyme during the substrate phosphorylation reaction. As discussed on page 3, autophosphorylation at the activation loop is known to activate the enzyme. However, several other explanations were possible. The enzyme could be activated by ADP formed during the preincubation period (activation by P-IRS939 was unlikely, since the lag phase was abolished by preincubation with MgATP alone). The observation that AMP-PNP did not abolish the lag phase argued against a nucleotide-dependent conformation change being the initial activating event, but did not rule this out; AMP-PNP is not always a kinetic model for ATP (285). To further characterize the lag phase and its possible linkage to enzyme autophosphorylation, we studied the time course of IRS939 phosphorylation under different reactant concentrations.

Surprisingly, the phosphorylation of IRS939, expressed as moles phosphorylated IRS939 (P-IRS939) per mole of enzyme, was independent of enzyme concentration (Figure 5-3). This conflicted with the standard model of activation by *trans* autophosphorylation at the activation loop shown in Figure 1-11. If progressive autophosphorylation were the cause of the acceleration observed during the steady state,

---

(457).

than higher enzyme concentrations would be expected to autophosphorylate more rapidly (by the law of mass action) and hence show shortened lag phases. This suggested that if autophosphorylation was the activating event, either the activation loop was not involved or it could autophosphorylate in *cis*. The observations in Chapter 4, that autophosphorylation at Y^{972} and Y^{972} could occur in *cis*, made these sites tempting candidates for the activation process.

The independence of IRS939 phosphorylation with respect to enzyme concentration also allowed us to vary the enzyme concentration. This was needed to keep IRS939 conversion above the sensitivity limit of our assay (0.5% phosphorylation) and below 20% phosphorylation, to prevent effects due to excess consumption of substrate.

To further evaluate the dependence of the lag phase on reactants, and determine steady-state kinetic parameters for IRS939 phosphorylation, reactions were studied at various ATP and IRS939 concentrations. Although the steady-state *rate* of IRS939 phosphorylation was dependent on IRS939 concentration, the time required to reach that rate was not. Both the reaction rate and the duration of the lag were strongly dependent on ATP concentration, however, with elevated ATP both increasing the reaction rate and shortening the lag phase (Figure 5-5). These results appear consistent with the results described in Figure 5-1. Neither IRS939 preincubation nor the concentration of IRS939 (at least over the range 10-200μM) in the assay affects the duration of the lag phase. Preincubation with MgATP, however, abolishes the lag phase; similarly, when reactions are done without preincubation, the lag phase is attenuated at higher ATP concentrations. As expected, the reaction rate with respect to each substrate appeared saturable.

Closer inspection of the dependency of the lag phase (L, with units of minutes) on [ATP] shows an apparent hyperbolic dependence. A replot of this relationship showing L vs. 1/[ATP] (lower right panel of Figure 5-5) suggests a minimum lag time (L_{min}) of 1 minute; half-minimal lag is observed at 2.5 mM ATP ($K^{ATP,lag}$). The saturability of the lag phase demonstrates that the activation process involves an enzyme-catalyzed step and is not, for example, caused by a breakdown product or contaminant in the ATP modulating the activity of the enzyme. Kinetic parameters extracted from Figure 5-4 and Figure 5-5 are summarized in Table 5-1.

Table 5-1 Kinetic Parameters of IRS939 Phosphorylation.

Varied Substrate	Parameter	Value
IRS939[a]	$K_{M,IRS939}$	44 ± 15 μM
	$V_{M,app}$	38 ± 7 min^{-1}
MgATP[b]	$K_{M,MgATP}$	510 ± 200 μM
	$V_{M,app}$	82 min^{-1}
	$K^{ATP,lag}$	2.5 mM
	L_{min}	0.98 ± 0.45 min

Values were determined from linear regression analysis of the data in Figure 5-4 and Figure 5-5 ; line fits are illustrated in these figures. *a*, IRS939 varied at fixed 0.2 mM MgATP. *b*, MgATP varied at fixed 100μM IRS939.

Correlation between Enzyme Autophosphorylation and the Lag Phase

Direct demonstration of a linkage between autophosphorylation and the lag phase required measurement of enzyme autophosphorylation. Measurement of enzyme autophosphorylation at the nanomolar enzyme concentrations used in Figure 5-1 through Figure 5-5 is difficult. To circumvent this, we took advantage of the independence of reaction rate with respect to enzyme concentration (Figure 5-3). Instead of using a single continuous reaction mixture containing enzyme, ATP, and IRS939, as was done earlier, we used a two-step procedure. The enzyme was incubated with MgATP alone and aliquots periodically removed diluted into reaction mixture containing both MgATP and IRS939. These secondary assays were conducted for very short times (3 minutes) and used much higher enzyme concentrations (50-140 nM) to produce a measurable amount of product during this brief time. This technique had two advantages over the simpler continuous method. First, because enzyme concentration in the primary reaction mixture was high (700 nM), enzyme autophosphorylation was readily measurable by use of radiolabeled ATP. Secondly, progressive peptide consumption was not a problem in the assay, since each secondary assay began with a fresh stock of IRS939 and ATP.

The use of this technique allowed us to simultaneously measure enzyme autophosphorylation and reaction rate (Figure 5-6, top), which were shown to correlate as a function of time. Removal of ATP by dialysis did not restore the lag phase to prephosphorylated enzyme (Figure 5-6, bottom). This argued for the causal role of autophosphorylation in activation, as compared to a coincidental role (such as both being due to an ATP-dependent conformational change). Reaction rates measured by this

protocol were very similar to those obtained by the earlier method, despite the much higher enzyme concentration during autophosphorylation (a final rate of 19 min^{-1} in Figure 5-6 *vs.* 21 min^{-1} measured under the same concentrations of MgATP and IRS939 in Figure 5-4). This suggested that the final states of the enzyme were the same, i.e., no new activation process was induced by the higher enzyme concentration used during autophosphorylation. The duration of the lag phases was also similar (this will be addressed further below), indicating that the existing activation process did not proceed faster at the higher enzyme concentration. This extended the independence of L with respect to [E], originally established in Figure 5-3, up to 700nM. Moreover, the lag phase was observed during autophosphorylation in the absence of IRS939; every data point in Figure 5-6 was exposed to IRS939 for the same 3 minutes. This verified that the lag phase was not due to continuous exposure to IRS939 or P-IRS939, as was suspected from the earlier results.

We also studied the ATP dependence of initial autophosphorylation (Figure 5-7) to determine whether they were linked as a function of ATP concentration. The observed K^{MgATP} in this process was approximately 2.6+/-0.2 mM, very similar to the 2.5mM $K^{ATP,lag}$ observed previously for the lag phase (Table 5-1). A maximum rate of 0.6 min^{-1} was observed.

Mathematical Model of Activation by Autophosphorylation

In Figure 5-5, the duration of the lag phase appeared to show saturation with ATP:

$$L = L_{min}\left(1+\frac{K^{ATP.Lag}}{[ATP]}\right)$$ **Equation 5-1**

where L is the observed lag phase, and L_{min} and $K^{ATP.Lag}$ are experimentally derived constants representing the minimum lag time and the ATP concentration at which the lag is at twice its minimum duration, respectively (Table 5-1). We will relate these constants to a kinetic model of IRS939 phosphorylation or CKD activation. Building such a model will allow us to rewrite Equation 5-1 in terms of kinetic parameters of the activation process, and to generate an equation that should describe progress curves such as those in Figure 5-5. If activation due to autophosphorylation is the process underlying the lag phase, the rate of autophosphorylation should determine the rate of enzyme activation during the lag phase. Although similar to the formal treatment of enzyme hysteresis (404), hysteresis does not apply to our case because of the involvement of a covalent modification to the enzyme (phosphorylation).

The simplest scheme for *cis* autophosphorylation that allows for saturation by ATP is

$$\mathbf{E + ATP \Leftrightarrow E \bullet ATP \xrightarrow{k_{JM}} EP + ADP}$$ **Scheme 5-1**

where E is unphosphorylated enzyme, EP is phosphorylated enzyme, and E•ATP is the binary complex with ATP. We use k_{JM} here as in Chapter 4, and use K^{ATP} because the treatment below can be applied to both MnATP and MgATP (although the correct value

must be selected for actual calculations). To generate a mathematical model describing the autophosphorylation process, we make the following assumptions:

1) The enzyme exists in only two kinetically relevant forms, whose concentrations are [E] (apo) and [EP] (phospho). They are related by $[E]_T = [E] + [EP]$, where $[E]_T$ is the total enzyme concentration. This is justified, despite the presence of multiple autophosphorylation sites, by the observation that autophosphorylation under the reaction conditions of Figure 5-6 occurred almost exclusively at juxtamembrane sites (see page 129).
2) The total enzyme concentration $[E]_T$ is much less than the total ATP concentration $[ATP]_T$, so that the free ATP concentration [ATP] is approximately constant ($[ATP] \cong [ATP]_T$). This is justified by the pseudo-first order reaction conditions used, where ATP was typically two to four orders of magnitude in excess of enzyme.
3) The reverse reaction does not occur or occurs slowly (the equilibrium lies to the right).
4) The process is not affected by the presence of IRS939, whether phosphorylated or not. This is justified by the observations that L is independent of [IRS939] (Figure 5-4), that CKD activation occurs even in the absence of IRS939 (Figure 5-6), and preincubation with IRS939 had no effect on subsequent reaction of the CKD (Figure 5-2).

5) ATP binding to the enzyme is near equilibrium. This holds even for cAPK, whose maximal rate of catalysis (21 s^{-1}) is much higher than rates of autophosphorylation in the CKD (maximum, approximately 0.1 s^{-1}).

The rate of new formation of phosphoenzyme should then be proportional to [E] and the saturation of the enzyme with ATP:

$$\frac{d[EP]}{dt} = -\frac{d[E]}{dt} = k_{JM}[E]\left(\frac{[ATP]}{[ATP] + K^{ATP}}\right) \qquad \textbf{Equation 5-2}$$

Integration over time using the starting conditions [EP] = 0, [E]=$[E]_T$ then gives [E] (and hence [EP]) as a function of time:

$$[EP] = [E]_T\left(1 - e^{-t\left(\frac{k_{JM}[ATP]}{[ATP]+K^{ATP}}\right)}\right) \qquad \textbf{Equation 5-3}$$

so that the fraction of phosphorylated enzyme F (dimensionless) is given by the simple exponential decay

$$F = \frac{[EP]}{[E]_T} = 1 - e^{-t\left(\frac{k_{JM}[ATP]}{[ATP]+K^{ATP}}\right)} \qquad \textbf{Equation 5-4}$$

Proposing that EP is an activated form of E, and that E is essentially inactive except for autophosphorylation, means that the two forms of the enzyme have different constants for catalysis. If E has a catalytic constant for IRS939 phosphorylation of k_E and

EP has a different rate constant k_{EP}, and the Michaelis constants are the same[13], than the overall rate constant for substrate phosphorylation by a mixed pool of kinase molecules is

$$k_{cat} = (1-F)\ k_E + (F)\ k_{EP}$$ **Equation 5-5**

But if $(1-F)\ k_E << F\ k_{EP}$, we can approximate that over the population of enzyme E_T,

$$k_{cat} \approx (F)\ k_{EP}$$ **Equation 5-6**

If the Michaelis constants are different, Equation 5-5 takes on a more complex form requiring information about substrate concentrations. However, if we are either near the Michaelis constants for EP *or* these constants are similar or *lower* than those for E, than the approximation in Equation 5-6 still holds, because the rate of phosphorylation by E will still be less than that by EP given the other assumptions described below. No study has described an increase in K_M values upon phosphorylation or activation of the IR (indeed, this would constitute *deactivation*.)

This approximation is justified by several factors. First, we principally study the enzyme under conditions where $F>0.1$, because data before this is technically difficult to acquire anyway with the wild-type enzyme. Since autophosphorylation begins as soon as we add ATP, we cannot measure IRS939 phosphorylation in the absence of *cis* autophosphorylation without mutagenesis. Second, a kinetic model for E that cannot convert to EP, the JMY2F mutant, (F=0) showed almost no IRS939 phosphorylation

---

[13] Phosphorylation has been observed to activate the enzyme solely by changes in k_{cat} without change in the Michaelis constant (33,111,408,417). It is not clear, however, which autophosphorylation sites this activation was caused by (JM, AL or both).

activity near the K_M values of EP (see below). This suggests that E has very little catalytic activity. Third, we were able to adequately describe our data without a k_E different from 0, and extensions of the model with $k_E > 0.05\ k_{EP}$ no longer fit the data.

The velocity equation for a two-substrate enzyme with rapid equilibrium random order kinetic mechanism, such as the insulin receptor kinase (111), is (398):

$$v' = \frac{v}{[E]_T} = k_{cat}\left(\frac{[ATP]}{[ATP] + K_{M.ATP}}\right)\left(\frac{[IRS939]}{[IRS939] + K_{M.IRS939}}\right) \qquad \textbf{Equation 5-7}$$

Here, v is the absolute rate of IRS939 phosphorylation and has units of $M^{-1}\ min^{-1}$. v', the turnover rate per molecule of enzyme, is shown for easy comparison with the figures and has units of min^{-1}. The assumptions used in deriving Equation 5-7 require that $[IRS939] \cong [IRS939]_T$ and $[ATP] \cong [ATP]_T$, that is, that we restrict ourselves to initial velocity conditions *with respect to substrates* (but not necessarily with respect to autophosphorylation).

Substituting Equation 5-4 and Equation 5-6 into Equation 5-7 we obtain

$$v' = k_{EP}\left[1 - e^{-t\left(\frac{k_{IM}[ATP]}{[ATP] + K^{ATP}}\right)}\right]\left(\frac{[ATP]}{[ATP] + K_{M.ATP}}\right)\left(\frac{[IRS939]}{[IRS939] + K_{M.IRS939}}\right) \qquad \textbf{Equation 5-8}$$

Inspection of Equation 5-8 shows that as t increases, v' asymptotically approaches a final steady state value, which we will term v'_{ss}.

$$v'_{ss} = \lim_{t \to \infty} v' = k_{EP}\left(\frac{[ATP]}{[ATP] + K_{M.ATP}}\right)\left(\frac{[IRS939]}{[IRS939] + K_{M.IRS939}}\right)$$

Equation 5-9

This steady-state rate is just what we would have obtained from Equation 5-7 with k_{cat} set to k_{EP}. To relate these parameters to L, the observed time intercept in a plot of P-IRS939/$[E]_T$ *vs.* time (such as Figure 5-1 through Figure 5-5) we must first integrate Equation 5-8 with respect to time. We obtain

$$T = \int_0 v' dt = k_{EP}\left(\frac{[ATP]}{[ATP]+K_{M.ATP}}\right)\left(\frac{[IRS939]}{[IRS939]+K_{M.IRS939}}\right)\left[t+\frac{1-e^{-t\left(\frac{k_{JM}[ATP]}{[ATP]+K^{ATP}}\right)}}{\left(\frac{k_{JM}[ATP]}{[ATP]+K^{ATP}}\right)}\right]$$

Equation 5-10

where $T = [P\text{-}IRS939]/E_T$, i.e. cumulative turnovers per enzyme molecule. For large t (after the lag phase) we can see that T approaches the limiting line T_{lim}

$$T_{lim} = \lim_{t\to\infty} T = k_{EP}\left(\frac{[ATP]}{[ATP]+K_{M.ATP}}\right)\left(\frac{[IRS939]}{[IRS939]+K_{M.IRS939}}\right)\left[t+\left(\frac{k_{JM}[ATP]}{[ATP]+K^{ATP}}\right)^{-1}\right]$$

$$= v_{ss}\left[t+\left(\frac{k_{JM}[ATP]}{[ATP]+K^{ATP}}\right)^{-1}\right]$$

Equation 5-11

The lag phase L is then the time point where this limiting line intersects the time axis (we used this method to obtain values of L in Figure 5-4 and Figure 5-5, for

example). We obtain an expression for L by solving for t in Equation 5-11, constraining $T_{lim} = 0$.

$$L = \left(\frac{k_{JM}[ATP]}{[ATP] + K^{ATP}} \right)^{-1} \qquad \textbf{Equation 5-12}$$

This equation allows us to predict the lag phase of substrate phosphorylation in terms of kinetic parameters for autophosphorylation. Most immediately,

$$L_{min} = \lim_{[ATP] \to \infty} \left(\frac{k_{JM}[ATP]}{[ATP] + K^{ATP}} \right)^{-1} = \frac{1}{k_{JM}} \qquad \textbf{Equation 5-13}$$

And, using Equation 5-1,

$$K^{ATP,Lag} = K^{ATP} \qquad \textbf{Equation 5-14}$$

So far, the mathematical model appears to correlate with our experimental results. The equality predicted by Equation 5-14 is observed in Figure 5-7 and Table 5-1. Equally important is what is *absent* from these equations: the independence of T on $[E]_T$ mirrors the results in Figure 5-3 and is a direct result of the use of the *cis* autophosphorylation mechanism in Scheme 5-1 to generate Equation 5-2.[14] Likewise, we have not found any basis for the inclusion of an IRS939 term in L, in keeping with the results in Figure 5-4.

To test whether progress curves such as those shown in Figure 5-4 and Figure 5-5 are actually described by Equation 5-10, we gathered data over a range of different ATP

(100-15000μM) and IRS939 concentrations (10-500μM) (Figure 5-10). Using the lag parameters from Table 5-1 and refining the steady-state parameters by global error minimization (Table 5-2), we found a good fit between progress curves calculated using Equation 5-10 and the results in Figure 5-10. Thus, *cis* autophosphorylation as an activating progress was able to predict the observed progress curves.

Table 5-2 Kinetic parameters of IRS939 phosphorylation from global fit.

Parameter	Value
$K_{M,IRS939}$	44 μM
$K_{M,MgATP}$	410 μM
V_M	106 min^{-1}

These parameters were obtained by minimizing the error function $E = \Sigma(T - T_{obs})/T^2$ against the dataset in Figure 5-10, using Equation 5-10 and the lag parameters in Table 5-1 to calculate T.

Site Assignment of Enzyme Autophosphorylation

Two-dimensional phosphopeptide mapping showed that autophosphorylation under the reaction conditions of Figure 5-6 occurred at the juxtamembrane autophosphorylation sites Figure 5-8. To confirm the causal role of autophosphorylation at these sites in activation of the enzyme, we measured IRS939 phosphorylation by the

[14] A *trans* mechanism would have resulted in a dependency of L on $[E]_T$, in contrast to these results, as mentioned on page 118.

$Y^{965,972}F$ construct (JMY2F) and studied its phosphorylation of IRS939. Substrate phosphorylation was greatly reduced (Figure 5-9). This indicates that juxtamembrane autophosphorylation is a nonessential activator of IRS939 phosphorylation by the CKD. Mutation of the carboxyl terminus sites had little effect, and there was still a lag phase, confirming that phosphorylation of these sites was not the activating autophosphorylation event.

Choice of Enzyme

These findings were made possible by the establishment of reaction conditions allowing for almost exclusive phosphorylation of the JM region. The absence of autophosphorylation at other sites in the kinase was a requirement for clear interpretation of our results, to allow for clear assignment of which sites are required for the activation process. Selective JM autophosphorylation was allowed by the CKD construct and reaction conditions employed. The version of the CKD employed in this study, originally constructed in the laboratory of the late O.R. Rosen, (128), includes the entire intracellular portion of the β subunit of the IR (residues 953-1355) and shows substantial autophosphorylation in its juxtamembrane region (128), like the complete IR (67,75). This CKD shows similar kinetics of autophosphorylation as well (67,75).[15] The similarity of this CKD to tetrameric IR, and our success in using it to identify *cis* autophosphorylation in the JM region, suggested our use of this construct as a starting point in characterizing the kinetic effects of this autophosphorylation.

---

[15] Another version of the insulin receptor's kinase domain, including residues 959-1355, shows very little JM autophosphorylation (Table 6-1) and would not have been suitable for this study.

Choice of Reaction Conditions

Although the ability to autophosphorylate at the JM sites is intrinsic to the CKD (67,128), the actual choice of the JM sites as the near-exclusive sites of autophosphorylation were dictated by the reaction conditions employed. In Chapter 4, we attained this by using very short reaction times and low ATP concentrations (Figure 4-1). While suitable for characterizing *cis* autophosphorylation, these restrictions would not allow production of sufficient P-IRS939 for reliable assay. Fortunately, we found that the use of MgATP instead of MnATP abrogated AL phosphorylation even at one hour reaction time, and CT autophosphorylation was only slight (Figure 5-8). This result was not an artifact of the mapping technique used, as we were able to demonstrate activation loop autophosphorylation using this technique and appropriately autophosphorylated CKD (Figure 4-1 and Figure 5-8). The absence of protamine, a polycation stimulatory agent of the CKD and IR (125,381,405), was also required for the absence of activation loop autophosphorylation using MgATP as substrate, as protamine appeared to specifically stimulate *trans* autophosphorylation (Figure 4-5) of the AL and CT sites using either Mn^{++} (Figure 4-4) or Mg^{++} (Figure 5-8). In keeping with the trend that both protamine and Mn^{++} preferentially stimulate AL/CT autophosphorylation, protamine has been observed to alter the metal requirements of the enzyme, bringing Mg^{++} on par with Mn^{++}(405). By appropriate choice of reaction conditions, we were able to study the role of juxtamembrane autophosphorylation in IRS939 phosphorylation in the absence of potentially confounding autophosphorylation at other sites.

The reason why Mg^{++} should not support AL autophosphorylation may involve conformational differences in the enzyme. Starting with the first biochemical characterizations of the IR kinase (406) and continuing with the CKD (125) autophosphorylation has been observed to be grossly weaker in the presence of saturating Mg^{++} than saturating Mn^{++} (405,407). The K^{MgATP} for juxtamembrane autophosphorylation (2.5 mM, Figure 5-7) is much higher than observed values of K^{MnATP} (75 μM, Figure 4-3 and Table 4-1; 60-180μM, (75)). A similar finding has also been made for overall autophosphorylation of the receptor (408) MgATP and MnATP bind CKD with similar affinity (407), so the observed differences in autophosphorylation are not due solely to different affinities for metal-ATP. Kinetic studies of substrate phosphorylation have indicated the existence of a regulatory metal-binding site, in addition to the metal-ATP binding site, which is more stimulated by Mn^{++} than Mg^{++} (395,409,410). None of this explains *why* one metal should alter the apparent substrate specificity of autophosphorylation; an answer to this question will require more detailed structural studies of the enzyme bound to the two forms. First steps towards this have already begun: Mn^{++}, but not Mg^{++}, has been shown to produce an activating conformation change in the CKD (407). An alteration of substrate preferences in response to protamine has been noted in the IR (411), and choice of divalent cation has altered the substrate specificity of phosphorylase kinase with regards to both diffusible substrates (412) and selection of autophosphorylation sites(413). Although our understanding of the differential effects of Mn^{++} and Mg^{++} are as yet incomplete, we were

nevertheless able to exploit our observations to study the kinetic effects of JM autophosphorylation.[16]

---

[16] Since the physiological metal is likely to be Mg^{++} rather than Mn^{++}, which is present at only micromolar concentrations *in vivo*, one could describe Mn^{++}-supported enhanced AL and CT autophosphorylation as "artificial" in a sense. This alone does not alter the usefulness of Mn^{++} as an effective cosubstrate for *in vitro* studies. Indeed, most studies with the insulin receptor have used Mn^{++} or mixed Mn^{++}/Mg^{++}, because these allow the maximum signal of autophosphorylation. Our finding that metals have a differential effect on the site distribution of autophosphorylation points out that such choices may have unintended consequences and should be related to *in vivo* situations only with care.

Figures for Chapter 5

Figure 5-1 Preincubation with MgATP Abolishes the Lag Phase in IRS939 phosphorylation.

The phosphorylation of IRS939 by the CKD was monitored over time after various pretreatments of the enzyme. 1μM CKD was either not preincubated (▲) or preincubated for 20 minutes with 0.5 mM MgATP without (■) or with (◆) 30μg/ml protamine before dilution into reaction cocktail containing 50μM IRS939 and 0.5mM MgATP. Aliquots were removed and quenched at the indicated times and assayed for P-IRS939 by RP-HPLC as described in Chapter 3. Data is expressed as cumulative turnovers per enzyme molecule, with units of mol P-IRS939/mol CKD. The lower panel is rescaled for better visibility of the lag phase and omits the protamine stimulated series. Final enzyme concentrations were 5.6 nM (▲), 10 nM (■), or 1 nM (◆).

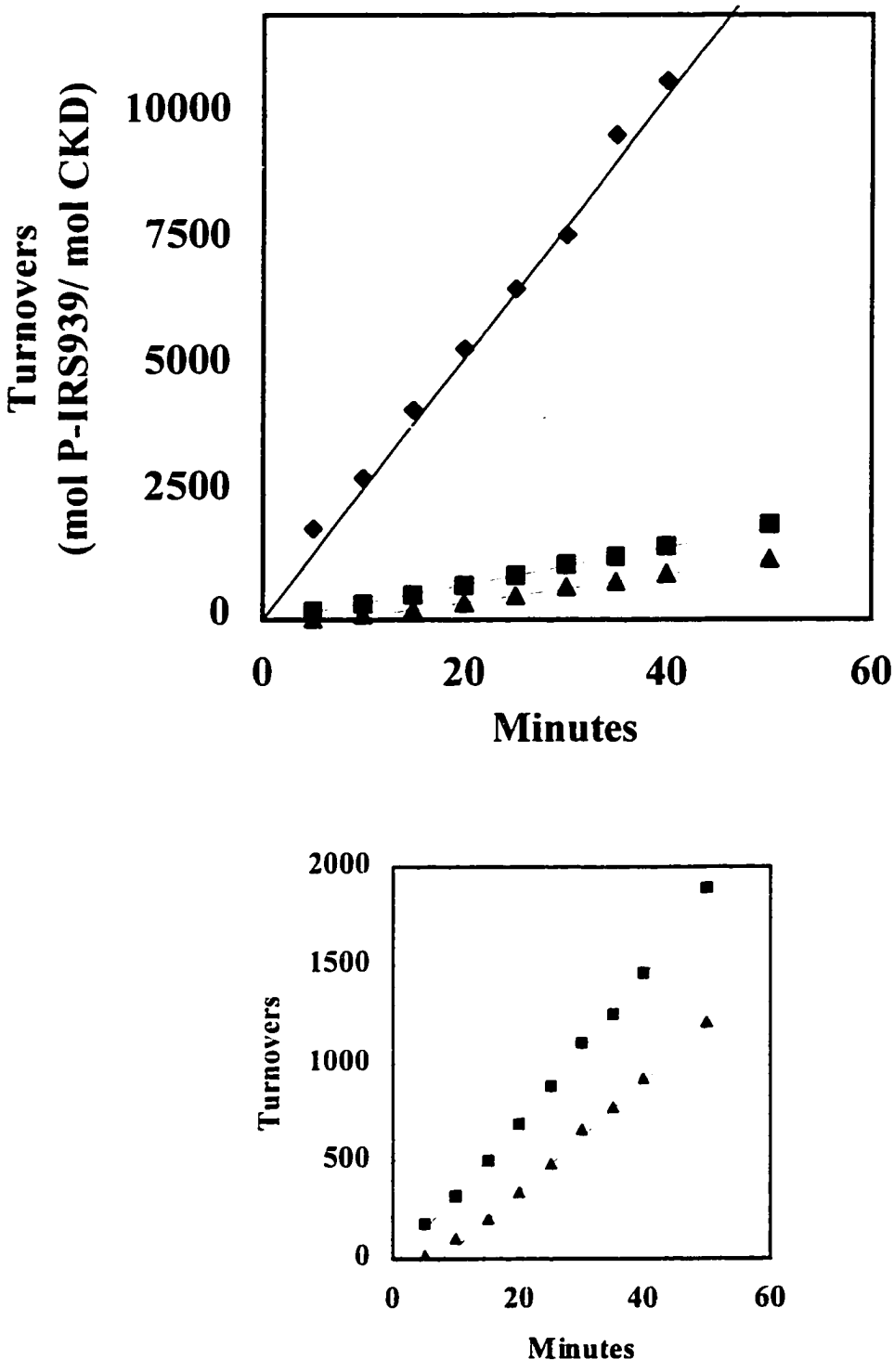

Figure 5-1 Preincubation with MgATP Abolishes the Lag Phase in IRS939 phosphorylation.

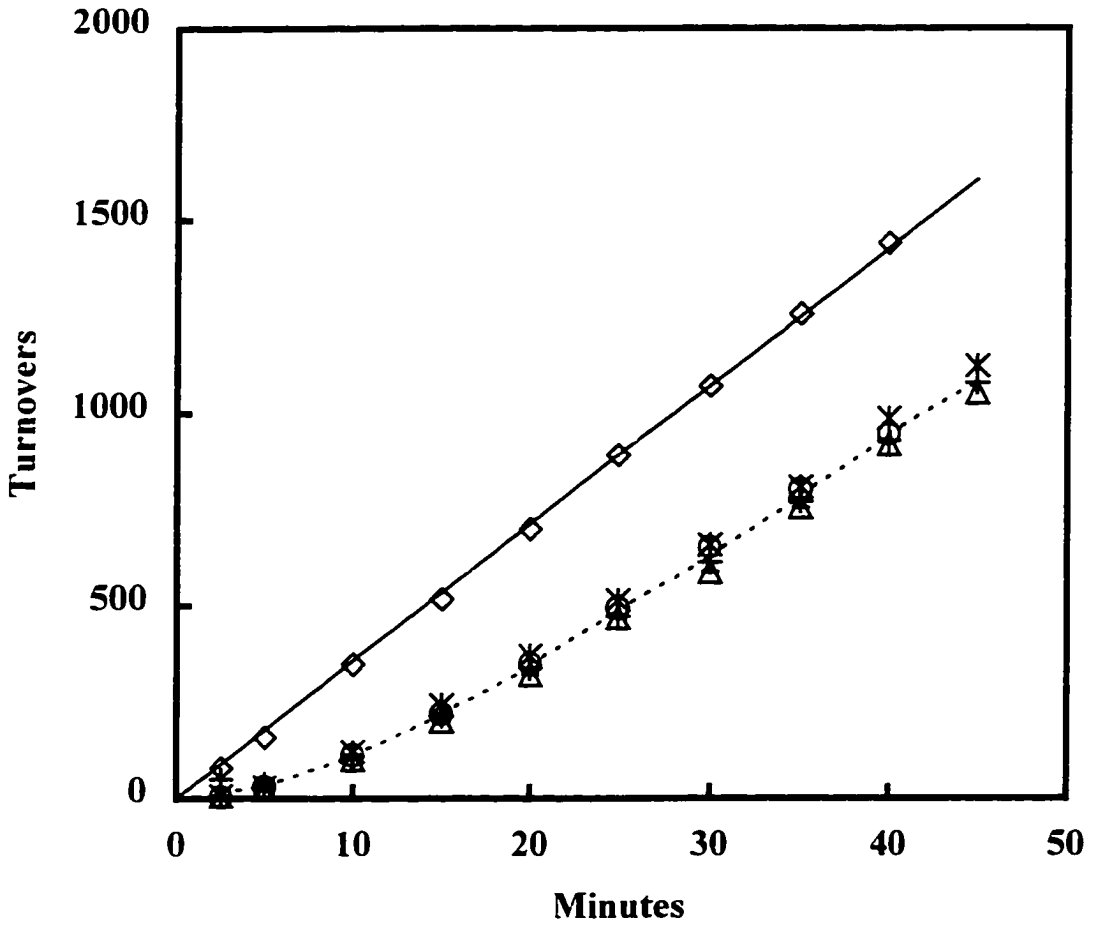

Figure 5-2 CKD Preincubation with IRS939, Mg^{++} alone, or ATP Analog Does Not Affect Subsequent IRS939 Phosphorylation.

The phosphorylation of IRS939 by the CKD was monitored over time after various pretreatments of the CKD. 0.7 μM CKD was preincubated for 25 minutes with 2mM AMP-PNP with 50mM MgAc (□), 50μM IRS939 (✱), 0.5mM ATP with 50mM MgAc (△), 50mM MgAc alone (+) or buffer alone (○) before 1:100 dilution into reaction cocktail containing 50μM IRS939 and 0.5mM MgATP.

Figure 5-3 Enzyme concentration dependence of IRS939 phosphorylation.

Top. To determine whether the rate of IRS939 phosphorylation was a function of CKD concentration, phosphorylation of IRS939 was measured using 1.4-28 nM CKD. 100μM IRS939 was phosphorylated using 200μM MgATP, using 28 (◆), 14 (■), 7 (▲), 2.8 (X), or 1.4 (*) nM CKD without preincubation. IRS939 phosphorylation was measured over time and expressed as in Figure 5-1 , that is, cumulative moles P-IRS939/ mol enzyme. A dashed line is shown through the average of the points. The results shown are representative of three experiments. *Bottom.* A residuals plot is shown with residuals grouped by time and plotted against the enzyme concentration. 5 (■), 30 (▲), 60 ( ), 90 (*), or 120 (●) minutes. A linear fit of the residuals showed no apparent trend with increasing enzyme concentration (p=0.14).

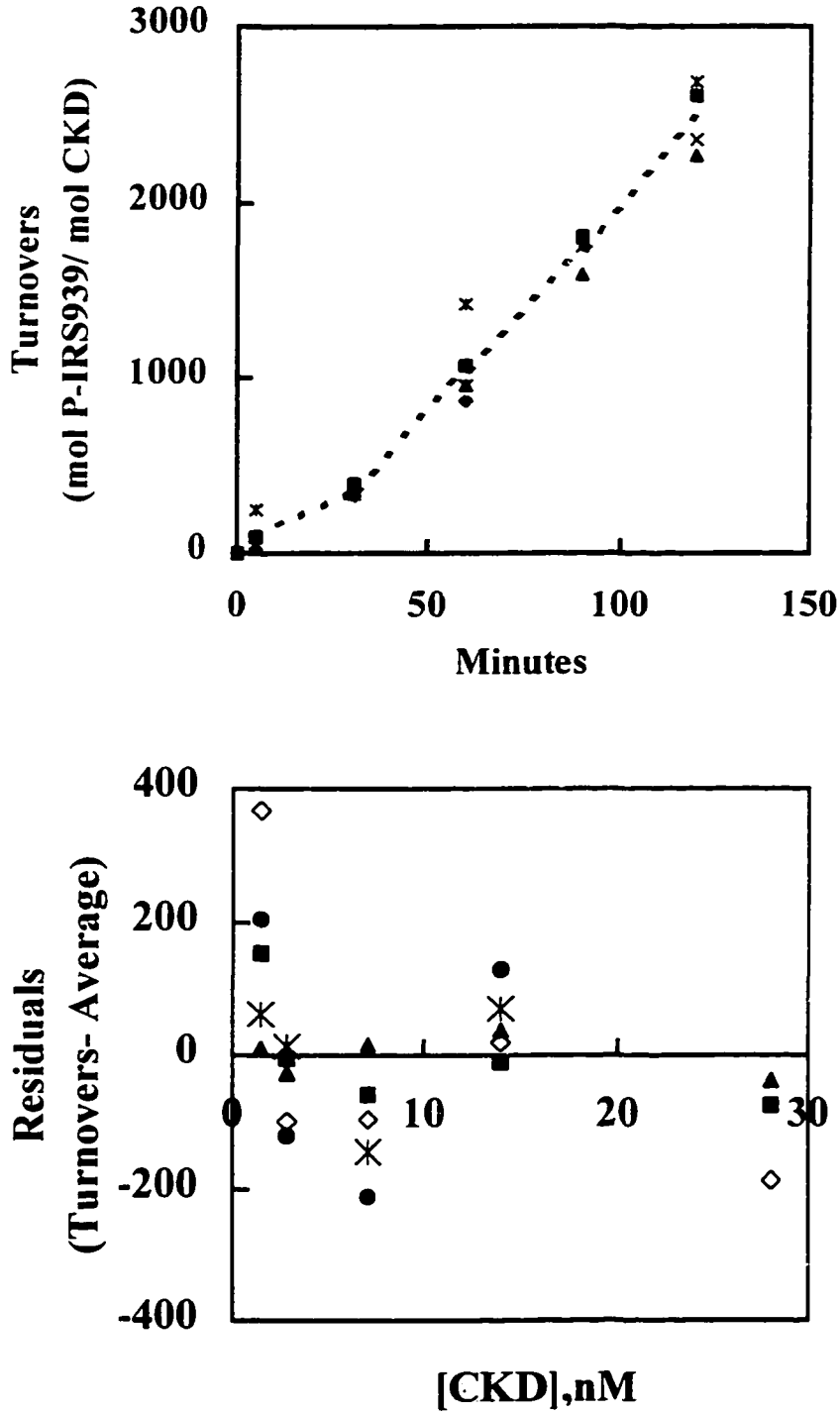

Figure 5-3 Enzyme concentration dependence of IRS939 phosphorylation.

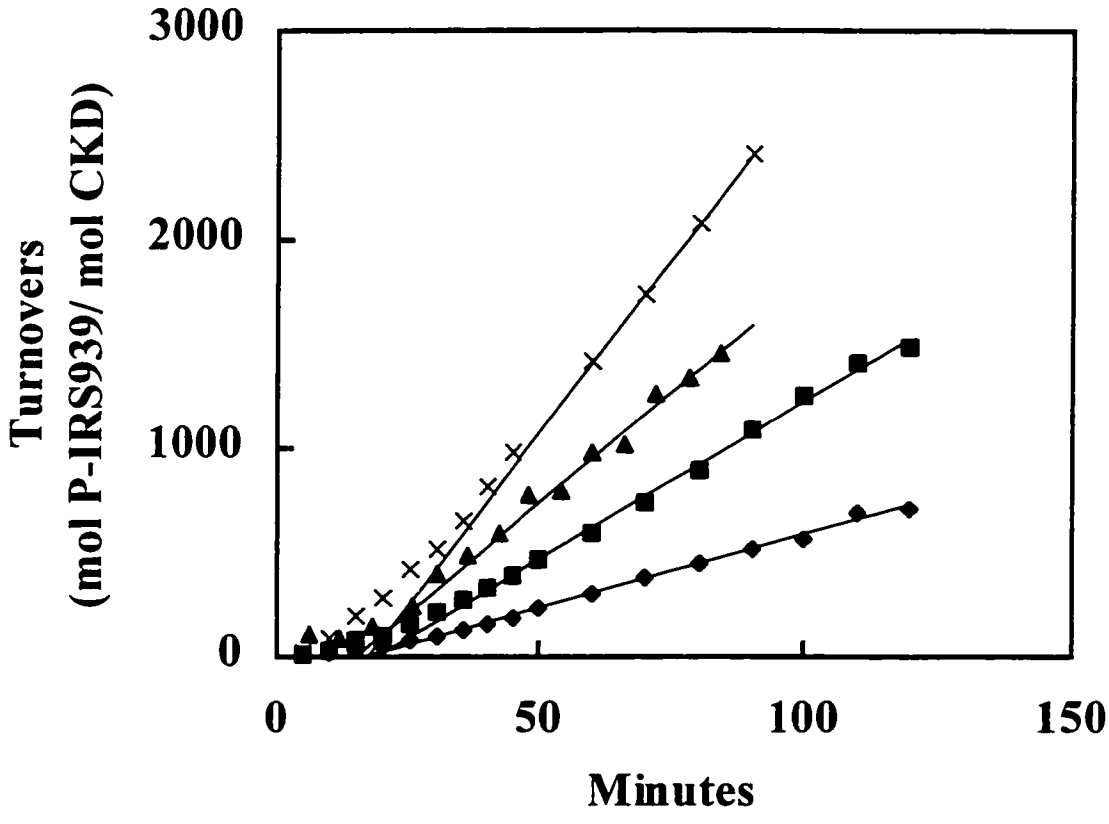

Figure 5-4 Dependence of lag on IRS939 concentration.

(*This page*) 10 (◆), 25 (■), 100 (▲), or 200 (X) μM IRS939 was incubated with 200μM MgATP and 2-10nM CKD. IRS939 phosphorylation was measured over time and expressed as in Figure 5-1. The replot of steady-state velocities v'_{ss} (*Next page, top*) shows a Eadie-Scatchard plot of v'_{ss}/[IRS939] *vs.* v'_{ss}. Time intercepts (L) in minutes, were measured by linear regression through the terminal datapoints from each time series in panel A (fits are shown as lines) and are shown plotted against peptide concentration (*Next page, bottom*). The slope of this line (.003 min/μM) was not significantly different from 0 (p=0.79).

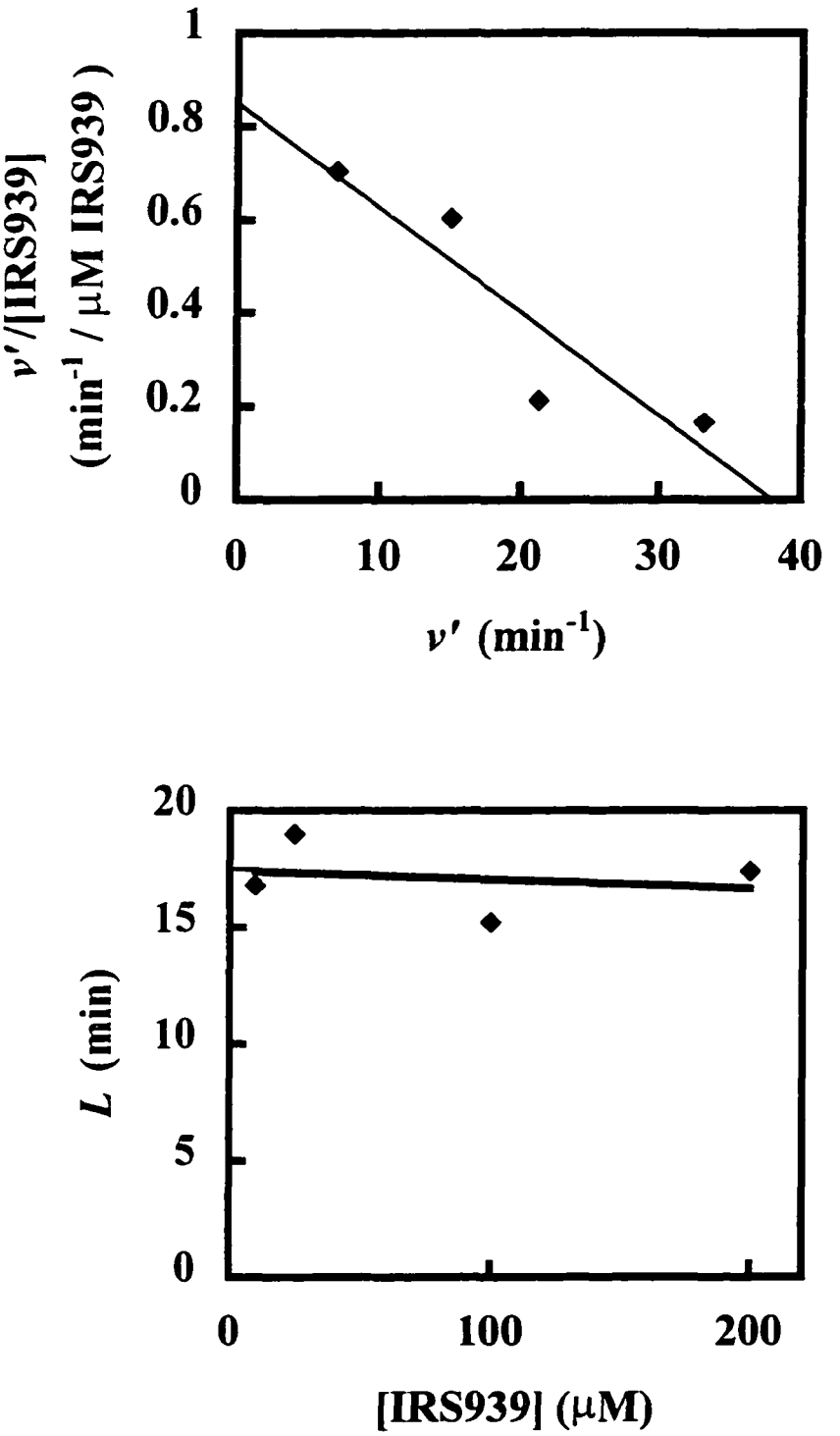

Figure 5-4 Dependence of lag on IRS939 concentration

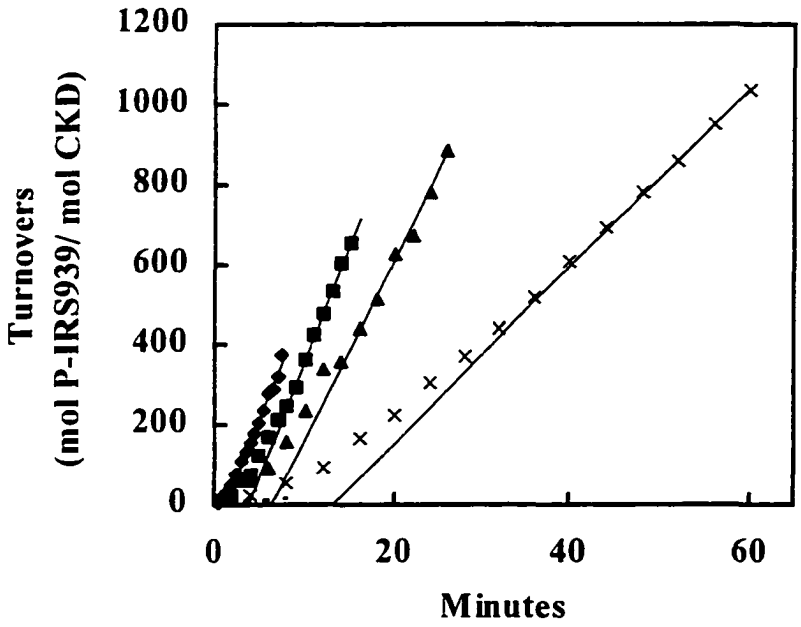

Figure 5-5 Dependence of Lag on ATP Concentration.

(*This page*) 2500 (◆), 1000 (■), 500 (▲), or 200 (X) μM MgATP were incubated with fixed 100μM IRS939 and 20nM CKD IRS939 phosphorylation was measured over time and expressed as in Figure 5-1. (*Next page, top*) A Lineweaver-Burke plot was used for determination of steady-state kinetic parameters is shown. (*Next page, bottom*) Time intercepts, L, were measured by linear regression through the terminal datapoints from each time series (fits are shown as lines (A)) and are shown are against MgATP concentration.

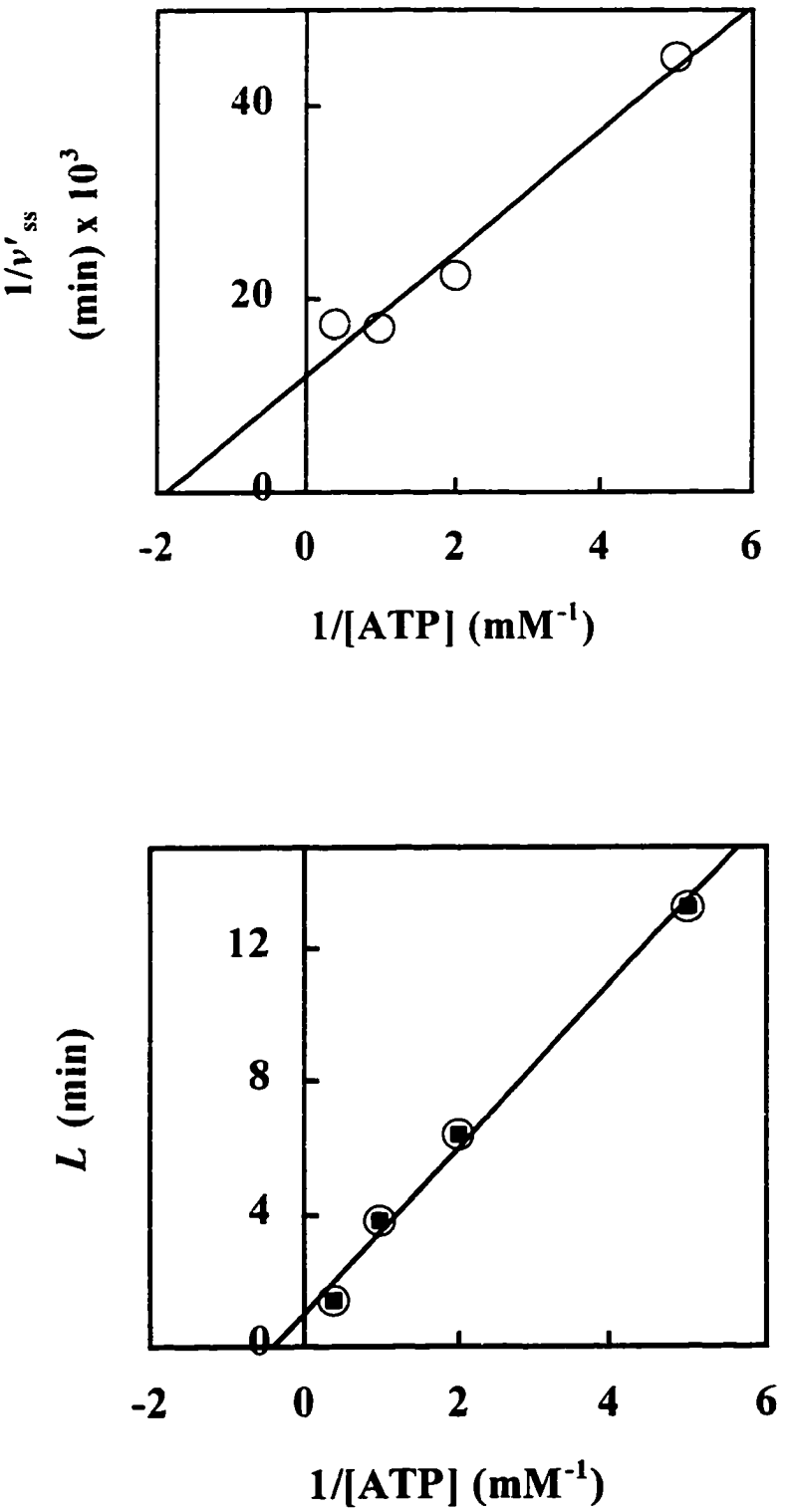

Figure 5-5 Dependence of Lag on ATP Concentration.

Figure 5-6 Correspondence between reaction rate and autophosphorylation.

Top. 700nM CKD was preincubated with either 0.2mM MgATP, in a reaction volume of 200µl, or 0.2mM [γ-^{32}P] ATP at a specific activity of 5900 cpm/ pmol in a reaction volume of 500µl. 20µl aliquots were periodically removed from the radiolabeled pool, quenched by addition of 10µl 3x Laemmli buffer, and analyzed for phosphate incorporation by SDS-PAGE ( ). 10µl aliquots of the nonradioactive pool were removed and added to 40µl reaction mixture containing IRS939 and MgATP for final assay concentrations of 140nM CKD, 100µM IRS939, and 0.2mM ATP. These assays were quenched after three minutes by addition of 10µl 5% phosphoric acid and IRS939 phosphorylation determined as in Figure 5-1. The *rate* of IRS939 phosphorylation during sequential three minute assays is shown (◆) at the midpoint of each 3-minute assay. All reactions and analysis were done in duplicate and the averages shown.

Bottom. After one hour, the remainders (260µl each) of the radiolabeled reaction mixtures were quenched by addition of 60µl 0.5M EDTA and then pooled. The pooled reaction mixtures (total volume, 640µl) were dialyzed for 4 hours at 4°C vs. 400ml 50mM Tris acetate, pH 7.0 (at room temperature), 0.1%BSA, 1mM EDTA, and 1mM DTT, then overnight vs. 800ml fresh buffer, and finally dialyzed for 4 hours against 500ml of the same buffer except without DTT and EDTA. As measured by ^{32}P counting, dialysis was at least 98% complete with respect to ATP. Enzyme autophosphorylation and IRS939 phosphorylation activity were then monitored as above, except that enzyme concentrations were 180nM and 35nM for the enzyme incubations with MgATP and IRS939/MgATP, respectively, and 40µl aliquots (instead of 20µl) were used to monitor enzyme autophosphorylation.

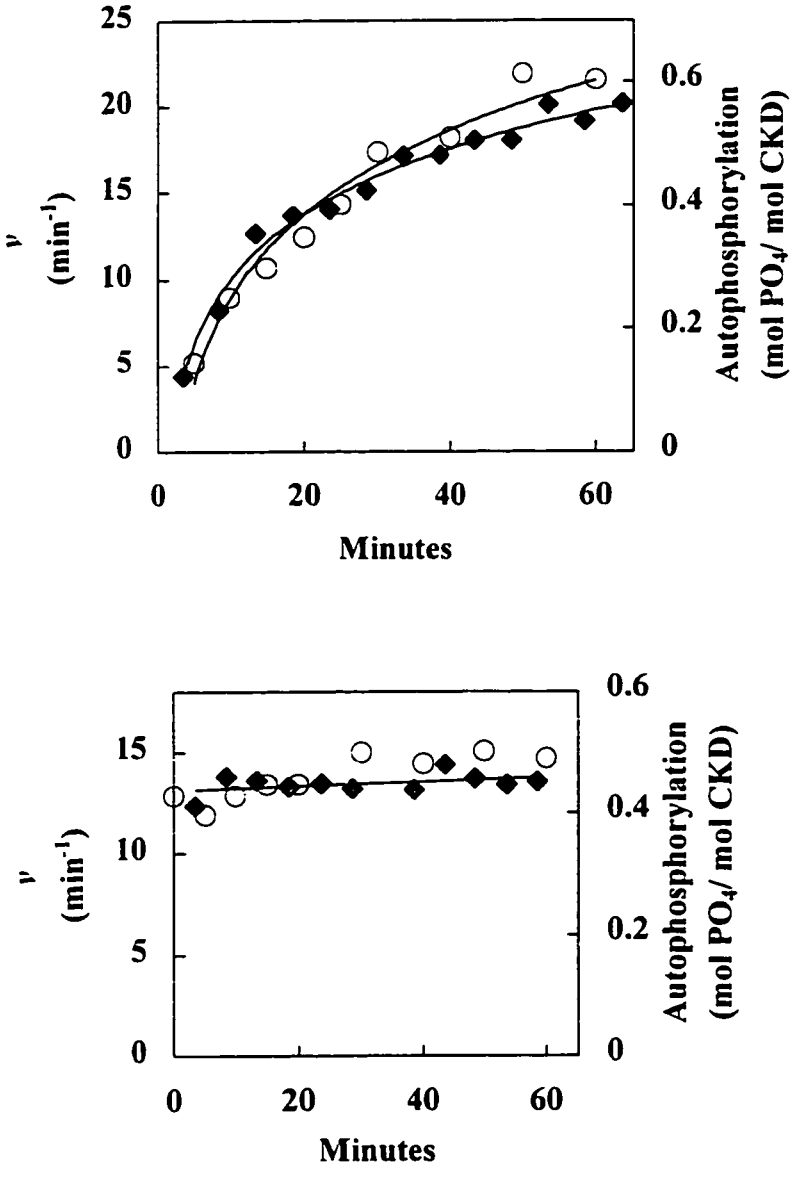

Figure 5-6 Correspondence between reaction rate and autophosphorylation.

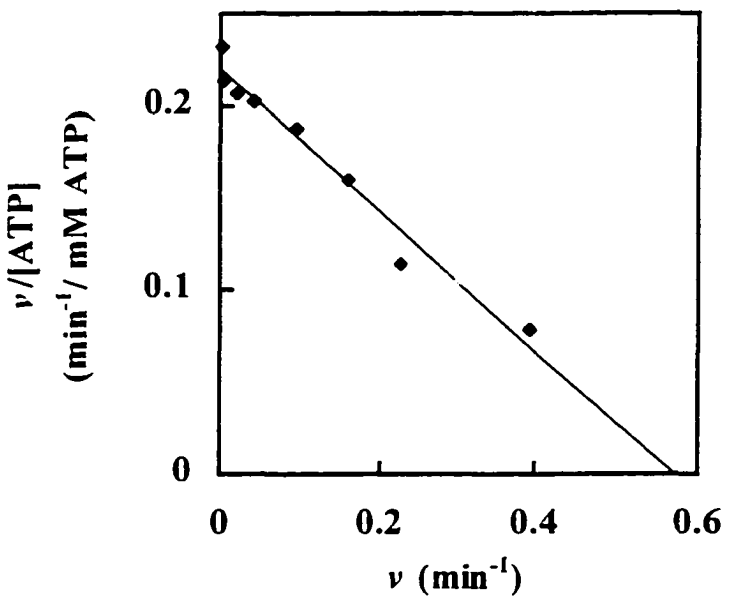

Figure 5-7 Dependence of JM autophosphorylation on MgATP.

280nM CKD was autophosphorylated in 40µl reactions with 10-5000µM [γ-^{32}P] MgATP (constant 5.6 x 10^6 cpm/ reaction) and quenched after one minute with 20µl 3x Laemmli buffer. Autophosphorylation was analyzed by SDS-PAGE. Points shown are the average of duplicate determinations.

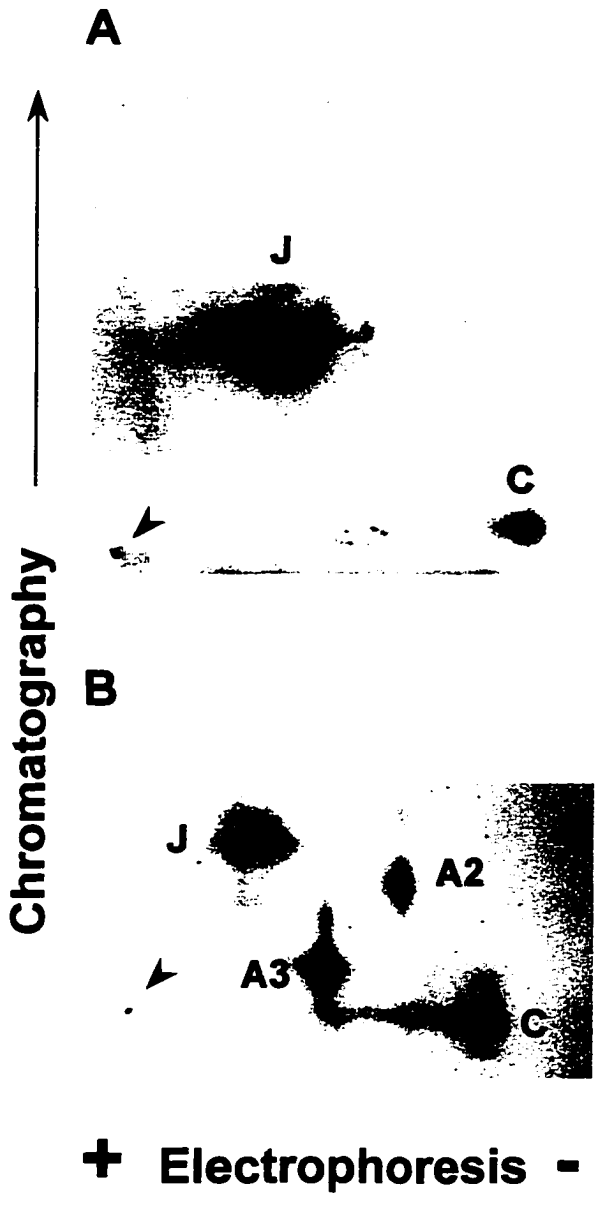

Figure 5-8 Two-Dimensional Phosphopeptide Mapping.

Autophosphorylation sites were mapped using the same methods and assignments as Figure 4-1 (A) Autophosphorylation under the conditions of Figure 5-6. (B) With 30μg/ml protamine.

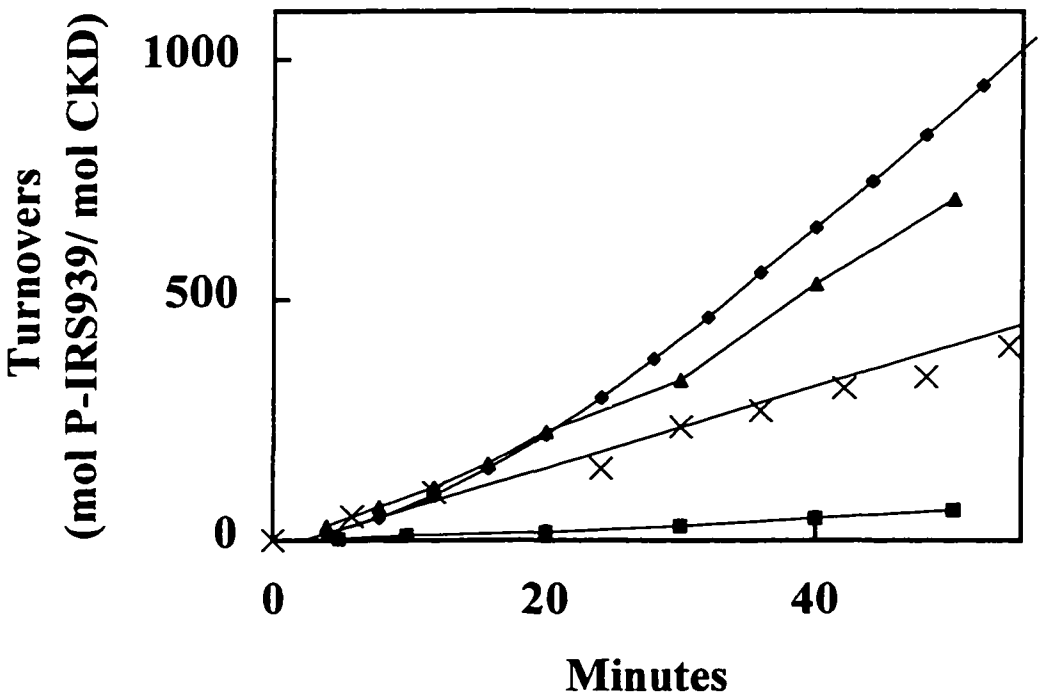

Figure 5-9 Effect of Tyr->Phe Mutations on IRS939 Phosphorylation.

Wild-type CKD (◆), JMY2F (■), CTY2F (▲) or ALY2F (X) were used to phosphorylate 100μM IRS939 with 200μM MgATP. IRS939 phosphorylation over time was measured and expressed as in Figure 5-1.

Figure 5-10 Fit of Mathematical Model for IRS939 Phosphorylation.

IRS939 phosphorylation data were collected at 10 (A), 25 (B), 50 (C), 100 (D), 200 (E), or 500 (F) μM IRS939 and 50 (▲), 100 (◆), 200 (–), 500 (● or +), 1000 (*), 2500 (■), 5000 (-), 10000 (· -) or 15000 ( ) μM MgATP. Results are expressed as in Figure 5-1. CKD concentration varied from 3.5 –140 nM CKD, as allowed by the independence of T on [CKD] established in Figure 5-3. To confirm this, two series were collected at two different [CKD] concentrations: 500μM ATP in panels C (5.6 and 35 nM CKD) and F (35 and 140 nM CKD). All curves shown were drawn using Equation 5-10 and the constants in Table 5-1 and Table 5-2.

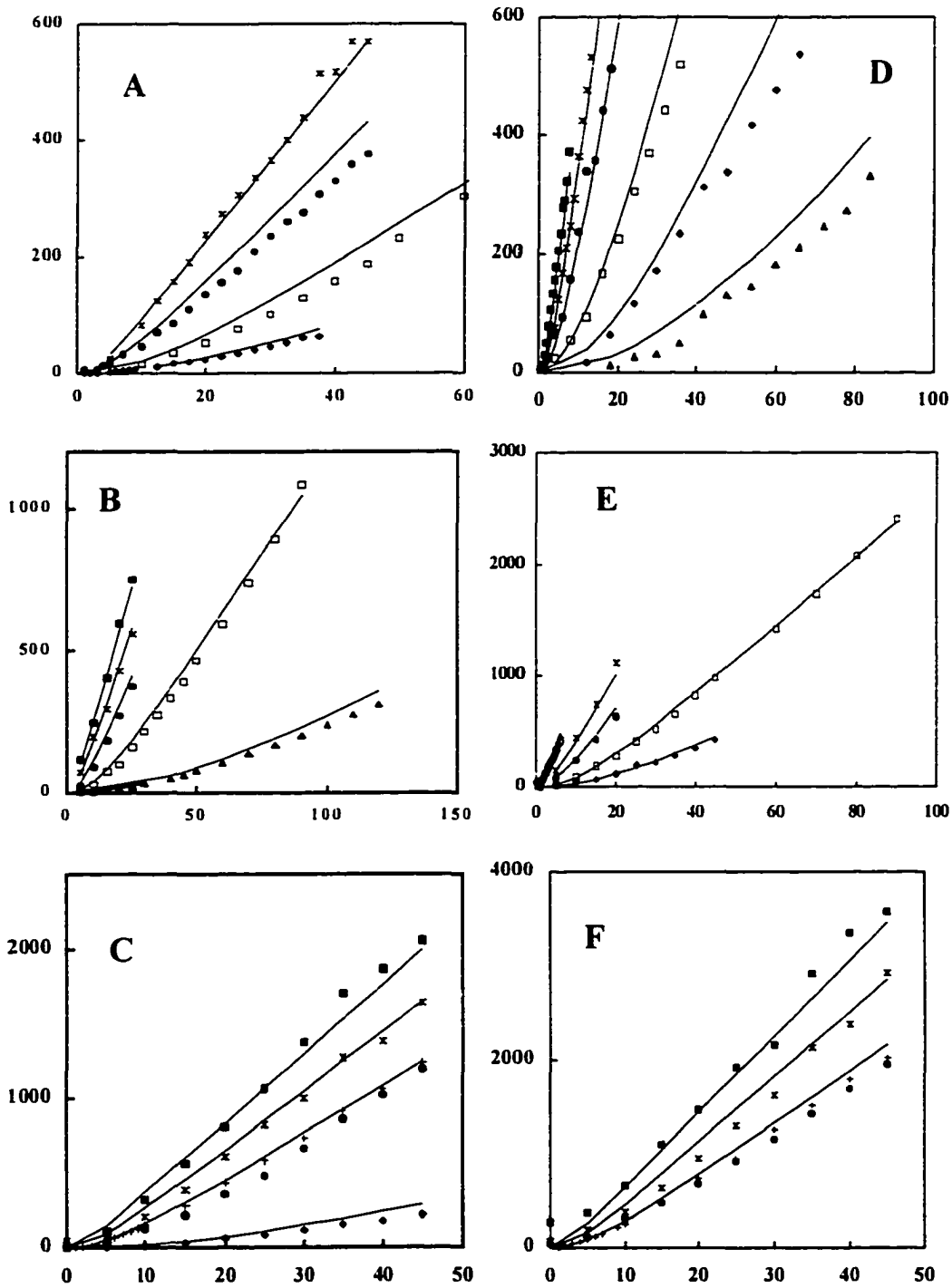

Figure 5-10 Fit of Mathematical Model for IRS939 Phosphorylation.

6. Discussion.

Cis Autophosphorylation in the Insulin Receptor's Kinase

The use of the complete CKD as a model for studying IR autophosphorylation patterns was based on previous work, in which the CKD was shown to be a good model for the basal state of the tetrameric IR (75,124). In this study, we took advantage of the monomeric nature of the CKD to apply the concentration-dependence technique of Todhunter & Purich (112) to the problem of the molecular mechanism of autophosphorylation. We have shown that while the complete CKD can autophosphorylation by both *cis* (Figure 4-2) and *trans* (Figure 4-5) pathways, it is the JM region that participates in the *cis* reaction (Figure 4-1). Thus, the answer to our question of the molecular mechanism of autophosphorylation appears to be that *both* the *cis* and *trans* pathways illustrated in Figure 1-3 exist. A unified picture of CKD autophosphorylation incorporating these findings is shown in Figure 6-1. While the present results do not *rule out* the possibility of JM autophosphorylation in *trans* , this event seems unlikely, since insulin (which stimulates dimerization of αβ half receptors, as described below) causes a *decrease* in the fraction of autophosphorylation occurring at the JM sites (75). As we shall discuss, our findings reconcile discordant results in the literature and contribute to an understanding of the basal state of the insulin receptor's kinase.

Previous Kinetic Studies of Autophosphorylation in the CKD

Several other groups have studied the molecular mechanism of autophosphorylation of the CKD, and two of them have reported exclusive *trans* autophosphorylation of the enzyme (summarized in Table 6-1). At first glance, this appears to contradict our present findings of the existence of *cis* autophosphorylation. However, JM autophosphorylation was at most a minor component of the autophosphorylation reactions studied by these two groups. The CKD employed by Wei *et al.* (126) was a truncated form which lacked the juxtamembrane region of the enzyme entirely, so no *cis* autophosphorylation process at these sites could have been observed. Although the JM sites are present in the CKD used by Cobb *et al.* (125), they were a very minor component of autophosphorylation (401). Thus, the lack of *cis* autophosphorylation in both studies reflects the lack of JM involvement in the autophosphorylation reaction.

Autophosphorylation in the construct of Cobb and co-workers is similar to autophosphorylation of our JMY2F construct, as a function of enzyme concentration dependence, overall rate and site distribution. However, Cobb's version of the CKD *does* possess intact JM autophosphorylation sites. This lack of JM autophosphorylation may be explained if one notes that the versions of the CKD employed were not identical to the CKD used in studies observing a *cis* JM pathway (Table 6-1). The version of the CKD employed by Cobb *et al.* was slightly truncated at its very N-terminus, and lacked the sequence $R^{953}KRQPD^{958}$. This sequence is present in both the complete IR and in all CKD molecules employed in this study. The comparison in Table 6-1 appears to suggest

a role for this positively charged cluster in acting as a binding determinant for *cis* autophosphorylation of the nearby Y^{965} and Y^{972}.

Whatever the reason for the low amounts of JM autophosphorylation observed by these groups, their findings of *trans* autophosphorylation in autophosphorylation reactions involving AL and/or CT sites are in agreement with our own findings (Figure 4-4 and Figure 4-5) and the scheme in Figure 6-1. Similarly, groups that reported *cis* autophosphorylation reported that a large fraction of their autophosphorylation occurred near the N-terminus of the CKD (Table 6-1).

Table 6-1 Concentration-Dependence Studies of CKD Autophosphorylation.

Enzyme	Autophosphorylation Kinetics					Distribution			Source
	RO	Mol PO_4 mol CKD	[CKD] µM	[ATP] µM	Cond.*	JM	AL	CT	
R^{963}- S^{1355}	1	0.03	0.006-3	10	Mn	>90			This work
R^{963}- S^{1355}	2	0.13-3	0.012-6	500	Mn,P	5	65	30	This work
R^{963}- S^{1355}	1	0.08	0.3-3	100	Mn	40			(128)
G^{959}- S^{1355}	2	3?	0.02-1	60	Mg,P	<10			(125,401)
V^{978}- K^{1283}	2	0.9	0.2-9	1000	Mg	--	100	--	(126)

This table summarizes the studies on the molecular mechanism of autophosphorylation in the CKD. The apparent reaction order (RO), with respect to CKD concentration, is shown, along with the ranges of CKD concentration used and the ATP concentration employed.

* Mn and Mg indicate the metal cofactor used; P indicates the presence of protamine chloride.

Studies using Holomeric $\alpha_2\beta_2$ IR or $\alpha\beta$ Halves.

If the JM sites autophosphorylate in *cis*, one might expect that dissociation of $\alpha_2\beta_2$ IR into $\alpha\beta$-halves would shift an autophosphorylation reaction towards these sites. Insulin-binding, kinase active $\alpha\beta$-halves can be produced by brief treatment of insulin receptors with reducing agents under alkaline conditions (414) or by mutagenesis of the cysteine residues involved in intrachain disulfide bonds (48). Insulin-independent autophosphorylation in DTT-generated $\alpha\beta$ halves occurs at a similar rate to that in $\alpha_2\beta_2$ IR (129,414,415), and this autophosphorylation occurs in *cis* within an $\alpha\beta$ half (129). Direct verification of JM involvement in this reaction has not been reported, chiefly because the autophosphorylation sites involved in $\alpha\beta$ autophosphorylation have not been described[17]. However, the low insulin-responsiveness of *cis* autophosphorylation in these studies showed that *cis* autophosphorylation was less dependent on insulin then *trans* autophosphorylation. $\alpha\beta$-halves show strong responsiveness to insulin only under conditions where they reverted to a covalent $\alpha_2\beta_2$ or noncovalently associated $(\alpha\beta)\bullet(\alpha\beta)$ structure (129,414,416-419) and this autophosphorylation was concentration-dependent (129,417). $\alpha\beta$-halves of IGF-I receptors also show strong ligand responsiveness under reassociating conditions (420). Apparent autophosphorylation of a DTT-generated $\alpha\beta$ half receptor was stimulated 2-3 fold by addition of a 5-fold excess of $\alpha\beta^{(K1030A)}$ receptor,

---

[17] Millimolar DTT itself has been shown to preferentially enhance tyrosine phosphorylation at the JM sites in native receptor preparations (400), but it is not clear that the reducing conditions used in this study resulted in nonassociating $\alpha\beta$ halves (419).

and much of the autophosphorylation was revealed to be on the inactive $\alpha\beta^{(K1030A)}$, requiring a *trans* pathway (421). The *cis*- autophosphorylation of the active $\alpha\beta^{WT}$ was stimulated only 3-fold by insulin, but *trans* autophosphorylation of the inactive $\alpha\beta^{(K1030A)}$ by its active $\alpha\beta^{WT}$ partner was stimulated 20-fold (130). This insulin dependence mirrors that of the JM sites in the purified IR: up to 2-fold for the JM sites, but up to 20-fold for AL and CT sites (75). These reports are therefore consistent with both *cis* autophosphorylation of the weakly insulin dependent JM sites and *trans* autophosphorylation of the strongly insulin-dependent AL and CT sites.

One group has argued for an all *cis* mechanism of insulin regulation (48). Using analytical ultracentrifugation, this group observed dimerization of otherwise $\alpha\beta$ form $C^{524,628}S$ receptor[18] with an association constant of 20μM. $\alpha_2\beta_2$ WT and $\alpha\beta$ $C^{524,628}S$ receptors both showed the same 2-3 fold stimulation of autophosphorylation and exogenous substrate phosphorylation, as well as enzyme concentration-independent autophosphorylation in the presence and absence of insulin. On the basis of these parities between the WT and $C^{524,628}S$ receptors, this group reported that insulin-dependent activation is all *cis*, and dimerization of $\alpha\beta$ halves is not necessary for insulin-stimulated kinase autophosphorylation or kinase activation. Interpreted in the light of the present findings, however, their results can be reconciled with the many groups that have observed activation in *trans*. Like our results in Chapter 4, their results were probably limited to observation of *cis* (JM) autophosphorylation by their use of a low 5μM ATP

---

[18] Mutation of these two cysteine residues was the minimum change necessary to produce $\alpha\beta$ halves (48,50), and this was the observation that identified these residues as those involved in the disulfide bonds linking the two halves of the receptor (Figure 1-1).

concentration in their activation studies. The all *cis* mechanism proposed—while it explains the data observed—is probably not applicable to the more general case of reaction conditions allowing *trans* autophosphorylation, such as physiological ATP concentrations. Similarly, the 2-3 fold stimulation of autophosphorylation by insulin observed in these studies is characteristic of the JM sites *in vitro* (75). The absence of *trans* pathways in this study reflects the reaction conditions employed rather than an intrinsic absence of these pathways from the IR.

Activation by Juxtamembrane Phosphorylation.

The findings of *cis* autophosphorylation in the JM region of the CKD (Chapter 4) are complemented by the observation that this autophosphorylation activates the enzyme (Chapter 5). We observed that activation of the CKD paralleled autophosphorylation as a function of time (Figure 5-6) and ATP concentration (Figure 5-5 and Figure 5-7) under conditions where this reaction was limited to JM sites (Figure 5-8). A mathematical model of *cis* autophosphorylation was able to account for the observed progress curves of IRS939 phosphorylation over a wide range of substrate and enzyme concentrations (Figure 5-10 and Equation 5-10). Finally, our findings were confirmed by the observation that the JMY2F construct showed very little IRS939 phosphorylation activity (Figure 5-9). These findings were made possible by the establishment of an experimental system that allowed almost exclusive JM autophosphorylation together with phosphorylation of IRS939.

Autoinhibition by the JM Region.

What is the means by which JM autophosphorylation activates the CKD? The juxtamembrane region of the kinase is certainly not required for catalysis or maximal activity of the enzyme, since a truncated catalytic core lacking this region (126) is at least as active as either version of CKD including this region (125,128). Moreover, the activation observed in Chapter 5 was *partial*; at least 10-fold further stimulation could be attained by autophosphorylation under conditions that promote activation loop autophosphorylation (Figure 5-1). The findings of *cis* autophosphorylation require that Y^{965} and/or Y^{972} must be able to access the active site of its own β-subunit. It is thus likely that, when so bound, they can block peptide substrate binding, especially since they are present at very high effective concentration relative to any diffusible substrate. Phosphorylation of the JM sites in response to insulin could then release them from the active site and make them available to recruit IRS-1 and other substrates *via* PTB domains, as proposed (76,77,79). Activation through autophosphorylation of the JM region would still be partial because of a persistent lack of the hydrogen-bond network thought to be promoted by pY^{1162}, as discussed in the Introduction. We will elaborate further on this possible mechanism after comparison to other protein kinases in the next section.

The juxtamembrane region of the kinase has been described as playing a role in ATP binding, which could also potentially be evoked in a proposed regulatory role for this area. The ATP binding loop G^{1003}-G^{1008} illustrated in Figure 1-9 is nearby in the amino acid sequence, and a deletion mutant Δ966-977 had an elevated K^{MnATP} for insulin-

stimulated autophosphorylation (210 μM *vs.* 27 μM) (81). In this study, a point mutant $Y^{972}F$ showed a normal K^{MnATP} of 35μM, and all three kinases showed about the same k_{auto}. In light of more recent evidence, however, the proposed role of the juxtamembrane region in ATP binding seems unlikely for three reasons. First, this region is outside the conserved catalytic core necessary for catalysis in protein kinases in general (19) or the IR in specific (126). Secondly, the three-dimensional structure of the IR (like that of other protein kinases including either only a catalytic core or N-terminal additions) appears to contain a complete ATP binding site. There is no evident place for a contribution from the JM region. Nevertheless, the crystal structure of the IR contained neither ATP nor a JM region, and inhibitory interactions between the ATP binding site and regions outside the catalytic core have been observed for at least CaMK-I (422). Finally, the truncated form of the CKD studied by Wei *et al.* (lacking the JM region) showed the same $K_{M.ATP}$ for peptide substrate phosphorylation as the 48kDa form of the enzyme (126). Thus, the proposed explanation for alterations in K^{MnATP} in JM mutants, while it explained the observations made at the time, has become unlikely in the results of subsequent evidence.

Our results suggest an alternative explanation for the results of Backer *et al.* The deletion Δ966-977 removes Y^{972} and radically alters the environment of Y^{965}, resulting in the loss of juxtamembrane autophosphorylation (66). In Figure 4-8, we observed that mutation of *both* these sites resulted in a similar large increase in K^{MnATP} for overall autophosphorylation. In both the CKD and the insulin-stimulated tetrameric IR, autophosphorylation sites change drastically as the ATP concentration is raised, with

lower ATP concentrations involving predominantly JM autophosphorylation (75). Removal of both these sites would be therefore be expected to greatly reduce kinase autophosphorylation at low concentrations of ATP. Thus, the altered composite K^{MnATP} in the Δ966-977 construct may simply reflect an alteration in the autophosphorylation sites involved in the reaction, rather than a structural role for the JM region in modulation ATP binding. This highlights one of the difficulties in studying autophosphorylation, especially *cis* autophosphorylation, in protein kinases: the enzyme *is* the substrate, and "substrate-level" effects can be difficult to distinguish from "enzyme-level" effects.

There are several other protein kinases whose activity has been found to be regulated by *cis* autophosphorylation, and one striking example whose activity *isn't* modulated by *cis* autophosphorylation. Examination of the circumstances and mechanisms of these regulatory events will help shed further light on the potential mechanism of activation by *cis* phosphorylation in the IR.

Regulation of Other Kinases by *Cis* Autophosphorylation.

The type Iβ cGMP-dependent protein kinase (115) is a homodimeric S/T protein kinase with regulatory and catalytic sequences both contained in each 78kDa polypeptide chain. The N terminus 100 residues contain the dimerization and cGMP binding domains. cGMP-dependent autophosphorylation occurs in *cis* at S^{63} and S^{79}, even in monomeric forms of the enzyme (115). Autophosphorylation at this latter residue activates this enzyme, through relief of a nearby pseudosubstrate sequence (Table 6-2). R^{75} in this nearby consensus sequence is required for autoinhibition (423). Thus, the enzyme is activated by *cis* autophosphorylation at a site close to an autoinhibitory site,

but the autophosphorylation site is not the site that directly occupies the active site in the inhibited state.

Table 6-2 Autoinhibitory Sequences Modulated by *Cis* Autophosphorylation.

Enzyme	Family	Amino Acid Sequence	Ref.
IR	RTK-IV	RKRQPDGPLGPL**Y**^{965}ASSNPE**Y**^{972}LSASDVFPC	Ch. 4-5
CaMK-II*	CaMK	HRQE**T**^{286}VDCLKKFNARRKLKGAILT**T**^{306}MLAT	(118,424, 425)
CaMK-IV	CaMK	MLKVTVPSCP**S**^{12}**S**^{13}PCSSVTSSTENL	(426-428)
cGPK-Iβ	AGC	QKQ**S**^{63}ASTLQGEPRTKRQAISAEP	(115,423)
A similar situation *not* relieved by phosphorylation:			
PKC-βII	AGC	PPSEGEE**S**^{16}**T**^{17}VRFARKGALRQ	(429)

The primary structure of known or suspected autoinhibitory domains modulated by *cis* autophosphorylation is given for several protein kinases from diverse parts of the protein kinase family. Residues thought to be binding determinants for peptide pseudosubstrates, or *bona fide* autophosphorylation sites, are underlined; the phosphate acceptor cognates themselves, when known, are boxed. Autophosphorylation sites are in **boldfaced red** and are numbered.

* T^{286} in CaMK-II is a *trans* autophosphorylation site that destabilizes the inhibitory sequence surrounding it when phosphorylated. T^{306} is a *cis* autophosphorylation site that stabilizes this region by preventing calmodulin binding.

Even more striking is the resemblance between activation by JM autophosphorylation in the insulin receptor and autophosphorylation in CaMK-IV (also known as CaMK-Gr). The kinase autophosphorylates at its N terminus (426) in an intramolecular reaction (427): this confers Ca^{++}/CaM independent activity to the enzyme. The N-terminus of this protein may function as an autoinhibitory region. Deletion of the N-terminus 21 residues had little effect on calmodulin dependent activation of the enzyme, nor did single mutations of either autophosphorylation site S^{12} or S^{13}. The mutant $S^{12,13}A$, however, was inactive despite phosphorylation of T^{196} in the activation loop (Table 1-2) *and* deletion of the C-terminal calmodulin-binding autoinhibitory domain discussed below, which otherwise render the enzyme fully active and Ca^{++} independent (428). Despite its lack of a consensus peptide binding site, this region appears to be a very powerful inhibitory region.

Another CaMK, CaMK-II, has been the subject of an incisive series of investigations in the laboratory of T.R. Soderling (118,341,424,425,430-437). This enzyme is multimeric, with 10-12 α and/or β subunits. It does not share the N-terminus autoinhibitory region of CaMK-IV and does not require phosphorylation of its activation loop for autophosphorylation. The C-terminus of CaMK-II, like CaMK-IV, CaMK-I and CaMK-V, has a calmodulin binding region (residues 296-309) that overlaps a well-defined pseudosubstrate (underlined in Table 6-2). Ca^{++}/calmodulin results in *trans* (intraholomeric *trans*, in the parlance of Figure 1-2) autophosphorylation of T^{286}, which results in Ca^{++}/calmodulin independent activity. In contrast, slow Ca^{++}-independent *cis* autophosphorylation of T^{306} blocks calmodulin binding and calmodulin-dependent

autophosphorylation of T^{286}. When T^{286} is mutated to Ala, the enzyme is still activated by Ca^{++}/calmodulin but does not autophosphorylate and does not become Ca^{++} independent, arguing that Ca^{++}/calmodulin binding alone is sufficient to release the pseudosubstrate.

The structure of the related monomeric enzyme CaMK-I has been determined (422). Like CaMK-II and CaMK-IV, CaMK-I binds Ca^{++}/calmodulin in its C-terminus to relieve an autoinhibitory domain (438). CaMK-I is monomeric and regulated by phosphorylation of its activation loop instead of its calmodulin-binding autoinhibitory domain or N-terminus. CaMK-I and CaMK-IV have substantial differences at their N-terminus, and CaMK-I does not share the mechanism described above for N-terminal regulation of CaMK-IV. In the crystal structure, the C-terminus calmodulin binding domain of CaMK-I is bound to the glycine-rich loop, resulting in the occlusion of the adenine binding pocket by F^{31}. Additionally, the unphosphorylated activation loop occupied the peptide binding site. Despite this, a peptide including the consensus peptide pseudosubstrate from the C-terminal autoinhibitory region of CaMK-I is competitive with peptide substrate rather than ATP (438). This suggests that regulation of the enzyme could be much more complex than a simple pseudosubstrate mechanism.

Protein kinase C is a well-studied protein kinase with many isozymes (reviewed in (439)). The βII isozyme contains a pseudosubstrate sequence near their N-terminus (304). This site is adjacent to the phosphorylation sites S^{16} and T^{17} (440), which autophosphorylate in an intramolecular manner (429). Both the pseudosubstrate and autophosphorylation sites are conserved in other conventional PKCs (α, βI, and γ isozymes) (439). The phosphorylation of S^{16} and T^{17} in response to Ca^{++} has been

proposed to contribute to the activation of this enzyme. However, mutation of these residues to Ala actually activates PKC (441), and their state of phosphorylation has no kinetic correlation with enzyme activation (442). This points out the need for kinetic verification of activation such as was done in Chapter 5. The mere existence of *cis* autophosphorylation sites near a potential inhibitory sequence does not constitute proof that phosphorylation of these sites relieves inhibition. In PKC, it is a ligand induced conformational change, not phosphorylation of S^{16} and T^{17}, that appears to relieve the pseudosubstrate inhibition from this region.

What lessons can we learn from these regulatory mechanisms of PKC, cGPK, CaMK-II and CaMK-IV? First, we see that regulation by *cis* autophosphorylation is found in diverse parts of the protein kinase tree. The kinases in Table 6-2 come from three of the four families of protein kinases described in Figure 1-5, suggesting that this mechanism was either present in a common ancestor or, more likely, evolved multiple times throughout the protein kinase family. Also note the diversity of domain structures in these kinases: the IR and cGPK-Iβ are dimeric with respect to kinase domains, while CaMK-IV is monomeric and CaMK-II is multimeric. *Cis* autophosphorylation is thus not associated with any particular quaternary structure but can evidently be applied to a broad range of structures. Each of the kinases in Table 6-2 is physiologically regulated by ligand binding: insulin to the α subunit of the IR, cGMP (or cAMP) to cGPK, Ca^{++}/CaM to CaMK-II and IV, and Ca^{++} and phospholipids to PKC. The IR is the only one of these to have the ligand binding and kinase domains separated by a cell membrane and additionally, occurring on separate subunits, and so is likely to have a more complex

regulatory scheme than these others. It is clear that regulation by *cis* autophosphorylation is not restricted to multistage activation processes such as we will propose below for the IR.

Regulation in CaMK-IV in particular shows very strong resemblance to regulation of the CKD. 1) Both kinases are at least as active when these regions are deleted, strongly arguing that they are not required for catalysis but rather play an inhibitory role when present. 2) Both autoinhibitory regions are at the extreme N-terminus of their kinase domains. 3) Neither region contains a readily identifiable pseudosubstrate region. 4) Neither pair of autophosphorylation sites are consensus sequences for the kinases in question. The $EY^{972}L$ is at best an incomplete motif, and there is no negative charge preceding Y^{965} or positive charge preceding $S^{12,13}$. 5) Both autoinhibitory regions are relieved by *cis* autophosphorylation. 6) Both regions have two phosphorylation sites, and either of them can functionally substitute for the other (with regards to enzyme activation). Only double mutants show an effect (365,428). 7) Like the IR, CaMK-IV is activated by phosphorylation at the activation loop (Table 1-2). CaMK-IV is dependent on phosphorylation of the activation loop (at T^{200} in the human form of CaMK-IV, T^{196} in the rat) for full activity (428,443). As in the IR, this occurs in *trans*, although here the reaction is catalyzed by a distinct CaMK-Ia kinase (443,444). Instead of insulin binding, CaMK-IV is additionally regulated by a Ca^{++}/CaM binding domain in its C-terminus, common to the members of the CaMK family. So many features in common would suggest that the structural basis for inhibition by these two regions would also be similar. Unfortunately, the mechanism of autoregulation in CaMK-IV is at present no better defined than for the JM region of the IR. The existence of this many parallels between

two distant relatives in the protein kinase family (Figure 1-5) is somewhat surprising, and suggests that a mechanism may be discovered in other protein kinases as well.

The lack of a consensus phosphorylation sequence in CaMK-IV and the IR suggests that instead of a true pseudosubstrate, the autophosphorylation sites in these enzymes may themselves be acting as competitive, albeit poor, substrates. As mentioned above, the existence of *cis* autophosphorylation requires that these phosphorylation sites be able to occupy the active site. Thus, an intrasteric mechanism of this type has already been proposed for CaMK-IV (428). The poorly conserved binding determinants around these autophosphorylation sites may actually contribute to their autoinhibitory potency by inhibiting autophosphorylation in the absence of ligand. "Substrate inhibition" has been well-characterized in at least cAPK, and is though to involve a nonproductive mode of peptide binding (see page 25). Such a binding mode could be invoked to explain autoinhibition in the special case of intramolecular binding. Not every *cis* autophosphorylation site can bind by such a mode, however, as shown by the counter-example of PKC-βII.

An alternative explanation is that neither region acts by mimicking binding of diffusible substrate, but rather distorts the catalytic domain in some other way such as has been observed in CaMK-I (422), Hck (325), or Src (324). The lack of inhibition of autophosphorylation by IRS939 makes peptide binding to the JM-inhibited form unlikely, but peptide binding can be prevented by means other than simple binding of the JM region to the peptide binding site. As the case of CaMK-I above illustrates, defining the mechanism of inhibition by inhibition studies alone can produce misleading results, so

differentiating between these two possibilities would best be done by structural studies of a complete CKD or CaMK-IV molecule. Given the already-known ability of these regions to bind to the active site, *vs.* the unknown ability of these sequences to bind to other parts of their respective kinases, the "competitive blocking substrate" mechanism seems the more plausible. We will next explore the structural consequences of such a state and the interaction between this region and the activation loop of the IR.

The Basal State of the Insulin Receptor's Kinase and Kinase Regulation.

Elevated basal activity in activation loop Tyr-> Phe mutants in the IR has been previously observed, but not explained (70,73). We also observed enhanced initial autophosphorylation in the ALY2F construct (Figure 4-2), which we ascribed to a reduced K^{MnATP} for autophosphorylation (Figure 4-3 and Table 4-1). This effect was not related to activation loop autophosphorylation, which did not occur in either the WT or ALY2F CKDs (Figure 5-8). As illustrated in Figure 4-6, binding of the activation loop tyrosine residues to the active site appears to preclude ATP binding *via* the linked DF^{1151} (21). This suggests a possible explanation for elevated basal activity in Tyr->Phe mutants of the activation loop: Removal of the hydrogen bond between Y^{1162} and catalytic base allows the activation loop to fall away from the active site and facilitates ATP access. In the crystal structure of Hubbard *et al.*, D^{1161} also makes numerous contacts stabilizing this loop (illustrated in Figure 4-6), and mutation of this residue to Ala also lowers the K^{ATP} for JM autophosphorylation (Figure 4-7). Deletion of 5 residues in the activation loop (ΔGATE2) also has a similar effect. However, mutation of Y^{1158} (which

makes no such stabilizing effects in the crystal structure) has little impact on this process (Figure 4-7). Thus, our findings support the model of *cis* inhibition by activation loop blockade of ATP binding, as proposed on structural grounds (21).

The energetic effects implied by the changes in JM autophosphorylation in Table 4-1 and Table 4-2 do not appear to correlate with the number of hydrogen bonds made by these residues (Figure 4-6). Mutation of D^{1161}, an essential residue in holding the activation loop in an autoinhibitory conformation, appears to have the same effect as mutation of $Y^{1162/3}$ or deletion of the region containing all these residues. Similarly, in crystallographic studies, Elizabeth Goldsmith and co-workers demonstrated that minor mutations in the activation loop of a MAP kinase caused disproportionately large disorder of the entire activation loop (445). A possible cause for this disparity can be illustrated by an example of activation loop mutation in another receptor tyrosine kinase, the fibroblast growth factor receptor (FGFR).

Mutation of the activation loop in FGFR-3 has been observed to produce a large increase in ligand-independent kinase activity (446), resulting in thanatophoric dysplasia type II, a fatal skeletal growth disorder (447). Using carrier-free [γ-^{32}P] ATP, Webster and co-workers demonstrated that a $K^{650}E$ mutant in the activation loop of FGFR-3 resulted in an apparent 100-fold activation of basal autophosphorylation. The autophosphorylation occurred at unidentified sites not including the two activating tyrosine phosphorylation sites in the activation loop, since additional mutants at these sites had no further effect. The crystal structure of the closely related FGFR-1 in the unphosphorylated state (352) does not show a clear role for K^{650} in stabilizing the

activation loop, leading the authors to suggest that E^{650} may play a role in stabilizing a noninhibitory conformation of the AL in this enzyme. In support of this role, Webster *et al.* found that activation in FGFR-3 was quite selective for the particular mutation $K^{650}E$.

The activation of the CKD by mutagenesis reflects an energetic difference between two states, one with the AL bound in an inhibitory conformation (illustrated in Figure 1-9 and corresponding to State I in Figure 6-3 and Figure 1-11) and the other with the AL region free but unphosphorylated (State II, illustrated below). Activation of the enzyme may be achieved by either destabilizing State I, as we apparently did in the D1161A or ΔGATE2 mutants, or stabilizing State II, as may occur in the $K^{650}E$ mutant of FGFR-3. In fact, any mutagenic change will alter the free-energy state of *both* conformations; the precise contribution of altered contacts can only be known if solution structures are known for both forms. The unknown contribution of new interactions in the altered State II conformation of D1161A, ALY2F, and ΔGATE2 may account for the poor correlation between the number of bonds disrupted by these mutants and their apparent kinetic effects.

Structural Consequences of *Cis* Autophosphorylation

The ability of the CKD to autophosphorylate by an intramolecular mechanism implies that the juxtamembrane region of a CKD molecule can occupy its own active site, with ATP bound. To explore the structural consequences of our conclusions, we developed a model structure for JM autophosphorylation. Such a conformation could not have been observed in the pioneering crystal structure of Hubbard *et al.* (21), since the catalytic core they crystallized had a truncated N-terminus lacking this region of the

CKD. In that structure, the active site was occupied by Y^{1162}, which made a hydrogen bond with the catalytic base (D^{1132}) and was seemingly poised for *cis* autophosphorylation (Figure 4-6). However, two structural features argued that the crystallized form of the kinase was catalytically incompetent. First, the large and small lobes of the kinase were rotated too far apart for correct positioning of the active site; and second, the ATP-binding site was blocked. Both of these structural features were mediated by the placement of the region near F^{1151} in the ATP binding site of the CKD. Hubbard *et al.* suggested that in an active conformation of the kinase, F^{1151} would occupy the pocket formed by H^{1130} and M^{1051}, by analogy with the ternary complex cAPK with ATP and the peptide inhibitor PKI (283). This placement of F^{1151} would allow both proper lobe orientation and ATP binding, but would remove Y^{1162} from the active site of the kinase.

We began construction of our model by relieving the CKD of the structural constraints on catalysis. We superimposed each lobe of the CKD separately onto the corresponding lobes of the cAPK crystal structure, giving a relative orientation more appropriate for catalysis. The induced steric overlap of F^{1151} with the ATP binding pocket, and the blockade of the peptide binding site by Y^{1162}, were relieved when residues of the activation loop of the cAPK were used as an initial guide for the activation loop of the CKD. This placed F^{1151} in the pocket formed by H^{1130} and M^{1051}, as proposed by Hubbard *et al.* The 5-aa insert of the activation loop of IRK (Y^{1163}-G^{1167}) was added at the apparent peptide bond between D^{1161} and L^{1168}, followed by bond angle and length normalization and energy minimization. ATP was inserted into its now-unoccupied binding site, again by homology with cAPK, although the phosphate chain was shifted

slightly because of small differences in orientation between the glycine rich loops (G^{1003}-G^{1008} in IR) of cAPK and the CKD. At this point, the model structure was seemingly poised for catalysis, except for the lack of a peptide substrate.

To complete our model for *cis* juxtamembrane autophosphorylation, we had to add these residues to our model. We began by positioning E^{972}YL of the juxtamembrane region relative to the catalytic loop as in the sequence $DY^{1162}Y$ of the CKD structure. This also oriented the hydroxyl group of Y^{972} towards the catalytic base D^{1132} and placed it near the γ-phosphoryl of ATP. Residues 974-984 were inserted as an extended surface loop connecting E^{972}YL to the first defined residue in the crystal structure, i.e. V^{985}. The connection did not require any changes in the established peptide backbone structure of the catalytic core, as generated above. However, the side chains of two residues in helix C (R^{1030} and N^{1046}) were repositioned to accommodate the new juxtamembrane loop. Finally, the repositioned activation and juxtamembrane loops and all splice sites were energy minimized. The resulting model structure is shown in Figure 6-2. To the extent that the structure presented by Hubbard *et al.* is evidence against a *cis*-reaction for Y^{1162}, the model developed here is consistent with *cis* autophosphorylation of Y^{972}. It illustrates a basal state confomer of this kinase that is derived from the evidence for intramolecular reaction mechanism within the JM subdomain, as presented in Chapter 4. This confomer corresponds to State II in Figure 6-3.

Functional Interactions Between the JM and AL Regions.

The observation of *cis* autophosphorylation at the JM sites demonstrates that the JM region can bind the active site of the enzyme in solution, and the model in Figure 6-2

appears to show this is structurally feasible Evidence that the activation loop can also make this interaction comes from the crystal structure of the CKD and the corresponding observation that mutations that would be expected to disrupt this structure modulate juxtamembrane autophosphorylation. This demonstrates a functional interaction between these two disparate parts of the enzyme in the basal state of the CKD, as illustrated in Figure 6-3. The scheme in Figure 6-3 encompasses the three major configurations of the CKD apparent from this study. In the basal state of the CKD (Region A) the kinase exists in equilibrium between State I (AL in, JM out) and State II (AL out, JM in). Disruption of State I in the ALY2F, D1161A, and ΔGATE2 mutants leads to a greater fraction of the enzyme existing in State II, which can bind ATP; hence the reduced K^{ATP} observed in Table 4-2. Upon juxtamembrane autophosphorylation, the enzyme moves to the partially activated state in Region C, between the partially active State IV and an AL-inhibited State V. This is the transition responsible for the lag phase in Chapter 5, and the inability of the JMY2F to pursue this pathway accounts for its inactivity. Alternatively, *trans* autophosphorylation can lead directly to the fully active State III. Since juxtamembrane mutants have been observed to have full insulin-stimulated kinase activity (81), we propose that State III is *not* in equilibrium with a JM-bound conformation. Further support from this model comes the observation that the D1161A, but not Y1158F, mutant shows enhanced sensitivity to chymotryptic cleavage at the activation loop relative to wild type CKD (365).

Implications for Insulin-Dependent Signaling in the Tetrameric IR.

Given the requirement for pY^{972} in phosphorylation of IRS-1 *in vivo*, any IR not phosphorylated in at least one β subunit JM region is unlikely to play a role in phosphorylating this key intermediate or subsequent signal transduction. Nevertheless, insulin-stimulated kinase activity of tetrameric IR bearing JM mutations is seemingly normal (81). It appears that upon stimulation by insulin, complete activation of the kinase occurs, even when the JM region is mutated (448). This is consistent with our apparent results in Chapter 5, that activation by JM autophosphorylation is only partial—being much less, for example, than protamine-stimulated activation (Figure 5-1), which favors the activation loop sites (Figure 4-4).

What, therefore, are the consequences of *cis* autophosphorylation in the $\alpha_2\beta_2$ IR? The complete answer will necessarily require study of the intact tetrameric form of the IR. At least one major environmental feature of the native IR (the cell membrane) is absent in the studies described in Chapters 4 and 5. For that matter, a physiological cell membrane is only poorly mimicked by the nonionic detergents often used to solubilize tetrameric receptor forms for study *in vitro*, and careful reconstitution of a native lipid environment may be required. However, we can incorporate the autophosphorylation scheme in Figure 6-1, the inhibitory role of the JM region suggested in Figure 6-2, and the reaction pathways in Figure 6-3, together with the known role of pY^{972} in substrate docking, to create a new hypothetical model for activation of the IR in response to insulin (Figure 6-4).

In this scheme, the IR is *cis* inhibited by its JM regions in the absence of insulin (1). Insulin binding causes a conformational change *within* a β subunit that allows *cis* autophosphorylation and partial activation (2). This partially activated receptor then phosphorylates its partner in *trans* (3). The second β subunit then phosphorylates the first in *trans*, and one or both β subunits phosphorylate docked IRS-1 at multiple sites (4). This model accounts for the low fraction of JM autophosphorylation in most mapping studies, since the JM sites on only one β subunit need be phosphorylated. Note that this model does *not* require a large conformational change altering the relative orientation of the β subunits, as is often proposed (so far without evidence) in models of *trans* activation of the IR. Rather, a *cis* "pre-ignition" stage can supplant this role. The mechanism of activation of *cis* autophosphorylation could then be as simple as a normal displacement of the transmembrane sequence by a few angstroms. This would alter the position of the RKR motif discussed above relative to the phosphate layer of the inner leaflet of the cell membrane, and thereby modulate the conformation of the juxtamembrane inhibitory sequence.

The scheme in Figure 6-4 is supported by several lines of evidence. First, it reconciles the need for *trans* activation of the AL with the need for *cis* autophosphorylation at the important docking site Y^{972}. Autophosphorylation of the JM region is one of the earliest responses to insulin (66), consistent with a role for a *cis* "pre-ignition" stage involving this region. Similarly, an antibody against residues 964-979 blocks insulin-dependent signal transduction and autophosphorylation—but not the kinase activity of prephosphorylated receptor (449). The principle of microscopic

reversibility would seem to require that if insulin causes a localized conformation change in the JM region, than alteration of JM conformation should increase the binding of insulin. This has been observed with anti-JM antibodies (450) and there is evidence that basal, possibly juxtamembrane, autophosphorylation increases the affinity of the IR for insulin (451).[19] Thus, multiple independent lines of *circumstantial* evidence are consistent with (but do not directly demonstrate) the model in Figure 6-4.

One possible argument against this model is the report of Lee and co-workers that equivalent sites in both β subunits are phosphorylated regardless of which α subunit binds insulin (452). However, the tryptic mapping methods used in this study were probably unable to resolve the highly hydrophobic JM phosphopeptides. Very similar techniques were once used to argue that JM autophosphorylation does not occur (32) and have since been supplanted both by these authors (66) and others (63,64,67). The observation that overall phosphorylation was 50% stronger in the β subunit whose associated α subunit did *not* bind BBA-insulin is consistent with this scheme as well, if one allows that the second-stage β subunit phosphorylation may not be as complete as the first round events it requires.

Since kinase activation and gross autophosphorylation are approximately normal in juxtamembrane point mutants, relief of JM autoinhibition by autophosphorylation cannot be absolutely required for activation of *trans* autophosphorylation. An additional

---

[19] An asymmetric role for the two β subunits in IRS-1 phosphorylation, as proposed in this model, could explain the observation that IRS-1 overexpression only partially rescues the effects of Y^{972} mutants (458). Some phosphorylation sites on IRS-1 might require the particular orientation of IRS-1 stabilized by the interaction with pY^{972}. Of course, there are several other possible explanations for these observations (458).

conformational change must be required to relieve *cis* inhibition by this sequence in JM mutants in response to insulin. Thus, although *cis* autophosphorylation of JM tyrosines may cause activation of the CKD, the causal role of JM autophosphorylation in the tetrameric IR remains to be established. It is possible that JM autophosphorylation and insulin can *both* partially activate the IR *via* relief of JM autoinhibition. This scenario would allow autophosphorylation at physiologically low insulin concentrations (where the JM sites are preferred (67,75)) to potentiate the IR to signal transduction by insulin, as has been observed (451). Relief of pseudosubstrate inhibition by either ligand binding *or* ligand-dependent autophosphorylation has been well-documented in at least one other protein kinase, CaMK-II (discussed above). The hypothetical scheme in Figure 6-4 would only be ruled out if *neither* insulin-dependent conformation change *nor* insulin-dependent juxtamembrane autophosphorylation affected the conformation of the juxtamembrane region.

In summary, we have clarified the molecular mechanism of autophosphorylation in the insulin receptor's cytoplasmic kinase domain. We have also found that *cis* autophosphorylation can activate the CKD, which suggests a possible inhibitory role for the juxtamembrane region in inhibition of the receptor's basal state. This activating role of juxtamembrane autophosphorylation is complementary to the proposed substrate docking role of pY^{972} and may contribute to the exquisite regulation IR autophosphorylation and IRS-1 phosphorylation in response to insulin.

Figures for Chapter 6

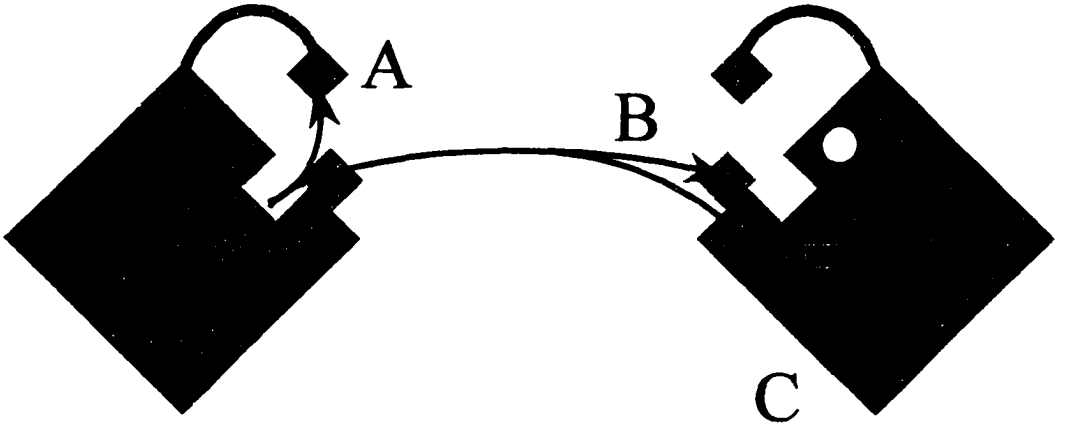

Figure 6-1 Unified Scheme of Autophosphorylation in the CKD.

The CKD is shown as in Figure 1-11, with the addition of a green stalk representing the juxtamembrane region of the kinase. The two pathways of autophosphorylation suggested by this and previous work are illustrated as red arrows, denoting *cis* autophosphorylation of the JM sites (A) and *trans* autophosphorylation of the AL (B) and CT sites (C).

Figure 6-2 Molecular Model for Juxtamembrane *cis* Autophosphorylation.

A possible basal state conformer allowing JM *cis*-autophosphorylation was built on the crystal structures of the CKD (21) and the ternary complex of cAPK with peptide inhibitor and nucleotide (359), as described in the text. The space-filling model shows the small lobe in yellow, the large lobe in white, the activation loop in cyan (with Y^{1162} in red) and F^{1151} in khaki, the putative catalytic base D^{1132} in dark blue, the bound ATP in magenta, G^{1003}-G^{1008} of the glycine rich nucleotide binding loop in green, and the amino acid sequence E^{971}-Y^{984} (from the JM domain) as a stick drawing in red. Y^{972} is shown poised for *cis* autophosphorylation. Further details of model construction are in the text.

Figure 6-3 Reciprocal Regulation by JM and AL Regions.

This scheme extends the model shown in Figure 1-11 by incorporating our findings about the JM region of the CKD. The unphosphorylated state of the enzyme (area *A*) exists in an equilibrium between States I (AL bound) and II (JM region bound). State II can bind ATP, which can lead to *cis* autophosphorylation, generating State IV, which again is in equilibrium with a gate-out state (V). This latter form was the state crystallized by the Hendrickson laboratory. Because of this, and because of the lack of new contacts formed by the phosphorylated activation loop, a kinase population in area *C* is only partially activated. Under conditions favoring *trans* autophosphorylation, State II can have an alternate path towards activation, *via trans* autophosphorylation of the AL (area *B*). This leads to full activation (State III) regardless of the phosphorylation state of the JM region. ATP binding is explicitly shown only for State II, although it can occur to any of the kinase forms with an unoccupied ATP binding site (II, III, IV).

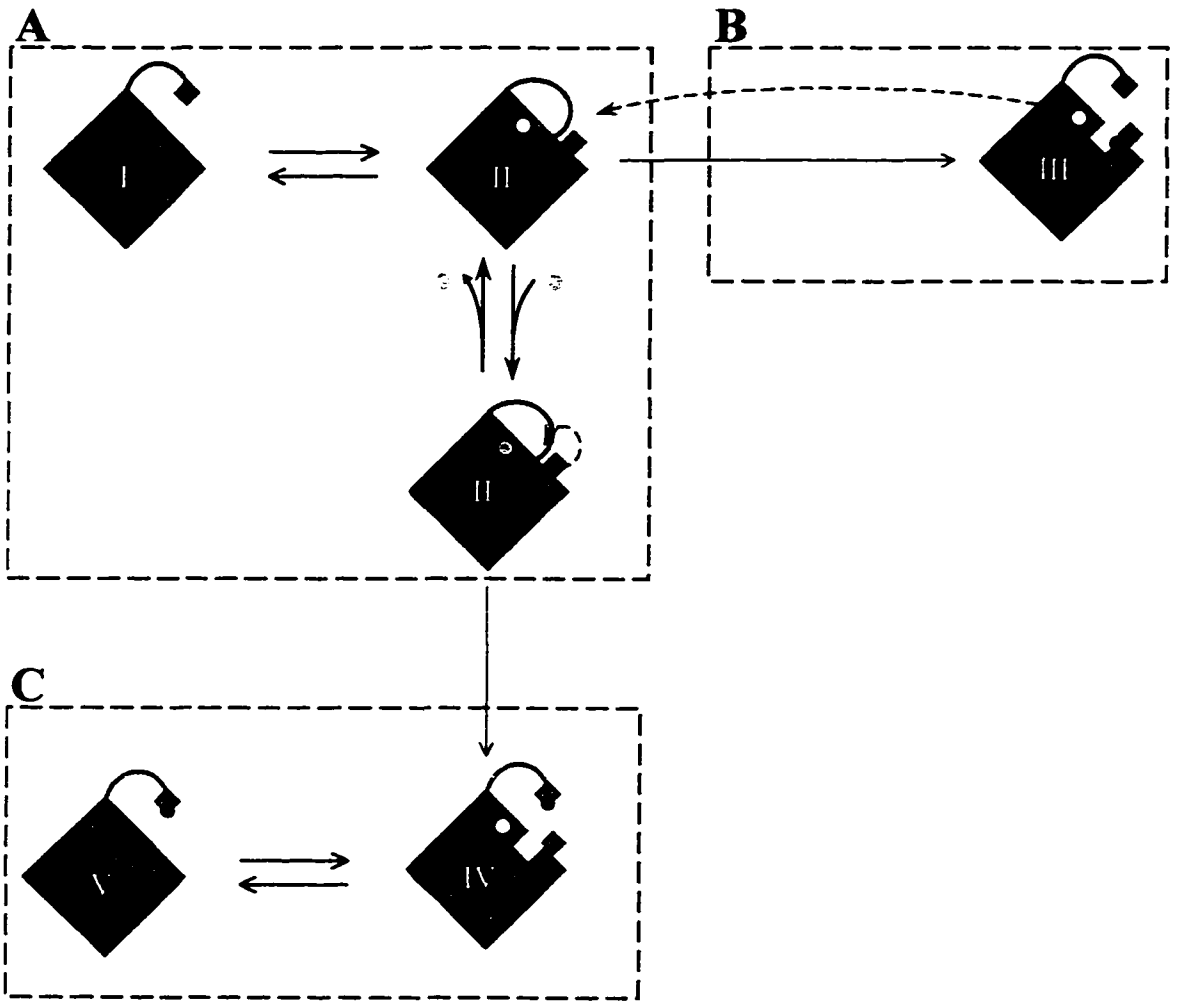

Figure 6-3 Reciprocal Regulation by JM and AL Regions.

Figure 6-4 Hypothetical model of Insulin's Activation of the Tetrameric IR.

The tetrameric IR is shown in a modification of the style of Figure 1-1. The JM and AL regions are shown as green (upper) and gray (lower) flags, respectively, over a notch representing the active site; the ATP binding site is no longer shown separately. Phosphorylated regions are striped red and are targeted by dashed arrows. In the basal state of the IR (*1*, corresponding to area A in Figure 6-3) the enzyme is unphosphorylated and has low activity. Insulin binding (pink sphere) stimulates *cis* autophosphorylation and partial activation of one β subunit *via* relief of JM autoinhibition (*2*). This partially activated subunit can then phosphorylate and fully activate its partner in *trans*, as well as dock IRS-1 (*3*) and can then be activated by its partner (*4*). Note that in this asymmetric model of β subunit autophosphorylation, only one β subunit docks IRS-1 and the interactions of the two β subunits with this molecule could thus be distinct.

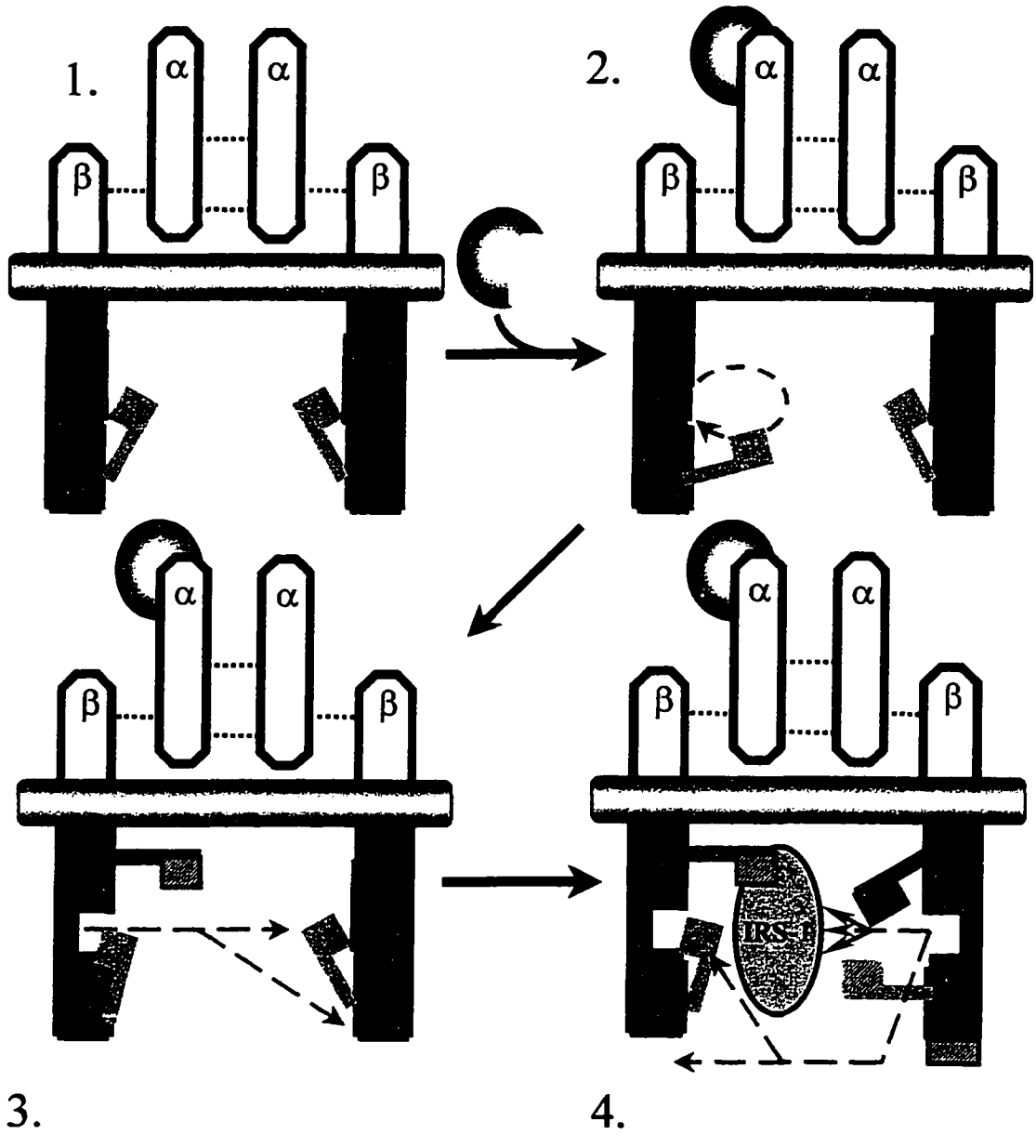

Figure 6-4 Hypothetical model of Insulin's Activation of the Tetrameric IR.

7. References

1. Ebina, Y., Ellis, L., Jarnagin, K., Edery, M., Graf, L., Clauser, E. *et al.* (1985) The human insulin receptor cDNA: the structural basis for hormone-activated transmembrane signalling. *Cell* **40**(4), 747-758.

2. Banting, F. G., Best, C. H., and Collips, J. B. (1923) Insulin patent. *Chemical Abstracts* **7**, 3571.

3. Cuatrecasas, P. (1972) Affinity chromatography and purification of the insulin receptor of liver cell membranes. *Proc.Natl.Acad.Sci.U.S.A.* **69**(5), 1277-1281.

4. Hunter, T. and Sefton, B. M. (1980) Transforming gene product of Rous sarcoma virus phosphorylates tyrosine. *Proc.Natl.Acad.Sci.U.S.A.* **77**(3), 1311-1315.

5. Ushiro, H. and Cohen, S. (1980) Identification of phosphotyrosine as a product of epidermal growth factor-activated protein kinase in A-431 cell membranes. *J.Biol.Chem.* **255**(18), 8363-8365.

6. Kasuga, M., Karlsson, F. A., and Kahn, C. R. (1982) Insulin stimulates the phosphorylation of the 95,000-dalton subunit of its own receptor. *Science* **215**(4529), 185-187.

7. Häring, H. U., Kasuga, M., and Kahn, C. R. (1982) Insulin receptor phosphorylation in intact adipocytes and in a cell-free system. *Biochem.Biophys.Res.Commun.* **108**(4), 1538-1545.

8. Kasuga, M., Zick, Y., Blithe, D. L., Crettaz, M., and Kahn, C. R. (1982) Insulin stimulates tyrosine phosphorylation of the insulin receptor in a cell-free system. *Nature* **298**(5875), 667-669.

9. Kasuga, M., Zick, Y., Blith, D. L., Karlsson, F. A., Häring, H. U., and Kahn, C. R. (1982) Insulin stimulation of phosphorylation of the β subunit of the insulin receptor. Formation of both phosphoserine and phosphotyrosine. *J.Biol.Chem.* **257**(17), 9891-9894.

10. Roth, R. A. and Cassell, D. J. (1983) Insulin receptor: evidence that it is a protein kinase. *Science* **219**(4582), 299-301.

11. Shia, M. A. and Pilch, P. F. (1983) The β subunit of the insulin receptor is an insulin-activated protein kinase. *Biochemistry* **22**(4), 717-721.

12. Van Obberghen, E., Rossi, B., Kowalski, A., Gazzano, H., and Ponzio, G. (1983) Receptor-mediated phosphorylation of the hepatic insulin receptor: evidence that the M_r 95,000 receptor subunit is its own kinase. *Proc.Natl.Acad.Sci.U.S.A.* **80**(4), 945-949.

13. Petruzzelli, L., Herrera, R., and Rosen, O. M. (1984) Insulin receptor is an insulin-dependent tyrosine protein kinase: copurification of insulin-binding activity and protein kinase activity to homogeneity from human placenta. *Proc.Natl.Acad.Sci.U.S.A.* **81**(11), 3327-3331.

14. Rosen, O. M., Herrera, R., Olowe, Y., Petruzzelli, L. M., and Cobb, M. H. (1983) Phosphorylation activates the insulin receptor tyrosine protein kinase. *Proc.Natl.Acad.Sci.U.S.A.* **80**(11), 3237-3240.

15. Massague, J., Pilch, P. F., and Czech, M. P. (1980) Electrophoretic resolution of three major insulin receptor structures with unique subunit stoichiometries. *Proc.Natl.Acad.Sci.U.S.A.* **77**(12), 7137-7141.

16. Hedo, J. A., Kasuga, M., Van Obberghen, E., Roth, J., and Kahn, C. R. (1981) Direct demonstration of glycosylation of insulin receptor subunits by biosynthetic and external labeling: evidence for heterogeneity. *Proc.Natl.Acad.Sci.U.S.A.* **78**(8), 4791-4795.

17. Ullrich, A., Bell, J. R., Chen, E Y., Herrera, R., Petruzzelli, L. M., Dull, T. J. *et al.* (1985) Human insulin receptor and its relationship to the tyrosine kinase family of oncogenes. *Nature* **313**(6005), 756-761.

18. Hanks, S. K. and Hunter, T. (1995) Protein kinases 6. The eukaryotic protein kinase superfamily: kinase (catalytic) domain structure and classification. *FASEB J.* **9** (8), 576-596.

19. Hanks, S. K., Quinn, A. M., and Hunter, T. (1988) The protein kinase family: conserved features and deduced phylogeny of the catalytic domains. *Science* **241**(4861), 42-52.

20. Hanks, S. K. and Quinn, A. M. (1991) Protein kinase catalytic domain sequence database: identification of conserved features of primary structure and classification of family members. *Methods Enzymol.* **200**, 38-62.

21. Hubbard, S. R., Wei, L., Ellis, L., and Hendrickson, W. A. (1994) Crystal structure of the tyrosine kinase domain of the human insulin receptor. *Nature* **372**(6508), 746-754.

22. Kobayashi, M., Olefsky, J. M., Elders, J., Mako, M. E., Given, B. D., Schedwie, H. K. *et al.* (1978) Insulin resistance due to a defect distal to the insulin receptor:

demonstration in a patient with leprechaunism. *Proc.Natl.Acad.Sci.U.S.A.* **75**(7), 3469-3473.

23. Taira, M., Hashimoto, N., Shimada, F., Suzuki, Y., Kanatsuka, A., Nakamura, F. *et al.* (1989) Human diabetes associated with a deletion of the tyrosine kinase domain of the insulin receptor. *Science* **245**(4913), 63-66.

24. Odawara, M., Kadowaki, T., Yamamoto, R., Shibasaki, Y., Tobe, K., Accili, D. *et al.* (1989) Human diabetes associated with a mutation in the tyrosine kinase domain of the insulin receptor. *Science* **245**(4913), 66-68.

25. Moller, D. E., Yokota, A., Ginsberg Fellner, F., and Flier, J. S. (1990) Functional properties of a naturally occurring Trp1200---- Ser1200 mutation of the insulin receptor. *Mol.Endocrinol.* **4**(8), 1183-1191.

26. Moller, D. E., Yokota, A., White, M. F., Pazianos, A. G., and Flier, J. S. (1990) A naturally occurring mutation of insulin receptor alanine 1134 impairs tyrosine kinase function and is associated with dominantly inherited insulin resistance. *J.Biol.Chem.* **265**(25), 14979-14985.

27. Cama, A., de la Luz Sierra, M., Quon, M. J., Ottini, L., Gorden, P., and Taylor, S. I. (1993) Substitution of glutamic acid for alanine 1135 in the putative "catalytic loop" of the tyrosine kinase domain of the human insulin receptor. A mutation that impairs proteolytic processing into subunits and inhibits receptor tyrosine kinase activity. *J.Biol.Chem.* **268**(11), 8060-8069.

28. Cama, A., de la Luz Sierra, M., Ottini, L., Kadowaki, T., Gorden, P., Imperato McGinley, J. *et al.* (1991) A mutation in the tyrosine kinase domain of the insulin receptor associated with insulin resistance in an obese woman. *J.Clin.Endocrinol.Metab.* **73**(4), 894-901.

29. McClain, D. A., Maegawa, H., Lee, J., Dull, T. J., Ulrich, A., and Olefsky, J. M. (1987) A mutant insulin receptor with defective tyrosine kinase displays no biologic activity and does not undergo endocytosis. *J.Biol.Chem.* **262**(30), 14663-14671.

30. Chou, C. K., Dull, T. J., Russell, D. S., Gherzi, R., Lebwohl, D., Ullrich, A. *et al.* (1987) Human insulin receptors mutated at the ATP-binding site lack protein tyrosine kinase activity and fail to mediate postreceptor effects of insulin. *J.Biol.Chem.* **262**(4), 1842-1847.

31. Wilden, P. A., Siddle, K., Haring, E., Backer, J. M., White, M. F., and Kahn, C. R. (1992) The role of insulin receptor kinase domain autophosphorylation in receptor-mediated activities. Analysis with insulin and anti- receptor antibodies. *J.Biol.Chem.* **267**(19), 13719-13727.

32. White, M. F., Livingston, J. N., Backer, J. M., Lauris, V., Dull, T. J., Ullrich, A. *et al.* (1988) Mutation of the insulin receptor at tyrosine 960 inhibits signal transmission but does not affect its tyrosine kinase activity. *Cell* **54**(5), 641-649.

33. Kasuga, M., Fujita-Yamaguchi, Y., Blithe, D. L., White, M. F., and Kahn, C. R. (1983) Characterization of the insulin receptor kinase purified from human placental membranes. *J.Biol.Chem.* **258**(18), 10973-10980.

34. Stadtmauer, L. A. and Rosen, O. M. (1983) Phosphorylation of exogenous substrates by the insulin receptor- associated protein kinase. *J.Biol.Chem.* **258**(11), 6682-6685.

35. Zhou, S. and Cantley, L. C. (1995) Recognition and specificity in protein tyrosine kinase-mediated signalling. *Trends.Biochem.Sci.* **20**(11), 470-475.

36. Cheng, H. C., Matsuura, I., and Wang, J. H. (1993) *In vitro* substrate specificity of protein tyrosine kinases. *Mol.Cell Biochem.* **127-128**, 103-112.

37. Zhou, S., Carraway, K. L., Eck, M. J., Harrison, S. C., Feldman, R. A., Mohammadi, M. *et al.* (1995) Catalytic specificity of protein-tyrosine kinases is critical for selective signalling. *Nature* **373**(6514), 536-539.

38. Shoelson, S. E., Chatterjee, S., Chaudhuri, M., and White, M. F. (1992) YMXM motifs of IRS-1 define substrate specificity of the insulin receptor kinase. *Proc.Natl.Acad.Sci.U.S.A.* **89**(6), 2027-2031.

39. Ellis, L., Morgan, D. O., Jong, S. M., Wang, L. H., Roth, R. A., and Rutter, W. J. (1987) Heterologous transmembrane signaling by a human insulin receptor- v-ros hybrid in Chinese hamster ovary cells. *Proc.Natl.Acad.Sci.U.S.A.* **84**(15), 5101-5105.

40. Seino, S., Seino, M., Nishi, S., and Bell, G. I. (1989) Structure of the human insulin receptor gene and characterization of its promoter. *Proc.Natl.Acad.Sci.U.S.A.* **86**(1), 114-118.

41. Hedo, J. A., Kahn, C. R., Hayashi, M., Yamada, K. M., and Kasuga, M. (1983) Biosynthesis and glycosylation of the insulin receptor. Evidence for a single polypeptide precursor of the two major subunits. *J.Biol.Chem.* **258**(16), 10020-10026.

42. Salzman, A., Wan, C. F., and Rubin, C. S. (1984) Biogenesis, transit, and functional properties of the insulin proreceptor and modified insulin receptors in 3T3-L1 adipocytes. Use of monensin to probe proreceptor cleavage and generate altered receptor subunits. *Biochemistry* **23**(26), 6555-6565.

43. Hedo, J. A., Collier, E., and Watkinson, A. (1987) Myristyl and palmityl acylation of the insulin receptor. *J.Biol.Chem.* **262**(3), 954-957.

44. Magee, A. I. and Siddle, K. (1988) Insulin and IGF-1 receptors contain covalently bound palmitic acid. *J.Cell Biochem.* **37**(4), 347-357.

45. Kohanski, R. A., Frost, S. C., and Lane, M. D. (1986) Insulin-dependent phosphorylation of the insulin receptor- protein kinase and activation of glucose transport in 3T3-L1 adipocytes. *J.Biol.Chem.* **261**(26), 12272-12281.

46. Schenker, E. and Kohanski, R. A. (1991) The native $\alpha_2\beta_2$ tetramer is the only subunit structure of the insulin receptor in intact cells and purified receptor preparations. *Arch.Biochem.Biophys.* **290**(1), 79-85.

47. Schaffer, L. and Ljungqvist, L. (1992) Identification of a disulfide bridge connecting the α- subunits of the extracellular domain of the insulin receptor. *Biochem.Biophys.Res.Commun.* **189**(2), 650-653.

48. Lu, K. and Guidotti, G. (1996) Identification of the cysteine residues involved in the class I disulfide bonds of the human insulin receptor: properties of insulin receptor monomers. *Mol.Biol.Cell* **7**(5), 679-691.

49. Bilan, P. J. and Yip, C. C. (1994) Unusual insulin binding to cells expressing an insulin receptor mutated at cysteine 524. *Biochem.Biophys.Res.Commun.* **205**(3), 1891-1898.

50. Macaulay, S. L., Polites, M., Hewish, D. R., and Ward, C. W. (1994) Cysteine-524 is not the only residue involved in the formation of disulphide-bonded dimers of the insulin receptor. *Biochem.J.* **303**(Pt 2), 575-581.

51. Cheatham, B. and Kahn, C. R. (1992) Cysteine 647 in the insulin receptor is required for normal covalent interaction between α- and β-subunits and signal transduction. *J.Biol.Chem.* **267**(10), 7108-7115.

52. Cheatham, B., Shoelson, S. E., Yamada, K., Goncalves, E., and Kahn, C. R. (1993) Substitution of the erbB-2 oncoprotein transmembrane domain activates the insulin receptor and modulates the action of insulin and insulin-receptor substrate 1. *Proc.Natl.Acad.Sci.U.S.A.* **90**(15), 7336-7340.

53. Frattali, A. L., Treadway, J. L., and Pessin, J. E. (1991) Evidence supporting a passive role for the insulin receptor transmembrane domain in insulin-dependent signal transduction. *J.Biol.Chem.* **266**(15), 9829-9834.

54. Yamada, K., Goncalves, E., Kahn, C. R., and Shoelson, S. E. (1992) Substitution of the insulin receptor transmembrane domain with the c-neu/erbB2 transmembrane

domain constitutively activates the insulin receptor kinase *in vitro*. *J.Biol.Chem.* **267**(18), 12452-12461.

55. Yamada, K., Goncalves, E., Carpentier, J. L., Kahn, C. R., and Shoelson, S. E. (1995) Transmembrane domain inversion blocks ER release and insulin receptor signaling. *Biochemistry* **34**(3), 946-954.

56. Goncalves, E., Yamada, K., Thatte, H. S., Backer, J. M., Golan, D. E., Kahn, C. R. *et al.* (1993) Optimizing transmembrane domain helicity accelerates insulin receptor internalization and lateral mobility. *Proc.Natl.Acad.Sci.U.S.A.* **90**(12), 5762-5766.

57. Yu, K. T. and Czech, M. P. (1984) Tyrosine phosphorylation of the insulin receptor β subunit activates the receptor-associated tyrosine kinase activity. *J.Biol.Chem.* **259**(8), 5277-5286.

58. Yu, K. T. and Czech, M. P. (1986) Tyrosine phosphorylation of insulin receptor β subunit activates the receptor tyrosine kinase in intact H-35 hepatoma cells. *J.Biol.Chem.* **261**(10), 4715-4722.

59. White, M. F., Häring, H. U., Kasuga, M., and Kahn, C. R. (1984) Kinetic properties and sites of autophosphorylation of the partially purified insulin receptor from hepatoma cells. *J.Biol.Chem.* **259**(1), 255-264.

60. Tornqvist, H. E., Pierce, M. W., Frackelton, A. R., Nemenoff, R. A., and Avruch, J. (1987) Identification of insulin receptor tyrosine residues autophosphorylated *in vitro*. *J.Biol.Chem.* **262**(21), 10212-10219.

61. Tornqvist, H. E., Gunsalus, J. R., Nemenoff, R. A., Frackelton, A. R., Pierce, M. W., and Avruch, J. (1988) Identification of the insulin receptor tyrosine residues undergoing insulin-stimulated phosphorylation in intact rat hepatoma cells. *J.Biol.Chem.* **263**(1), 350-359.

62. Tornqvist, H. E. and Avruch, J. (1988) Relationship of site-specific β subunit tyrosine autophosphorylation to insulin activation of the insulin receptor (tyrosine) protein kinase activity. *J.Biol.Chem.* **263**(10), 4593-4601.

63. Tavaré, J. M. and Denton, R. M. (1988) Studies on the autophosphorylation of the insulin receptor from human placenta. Analysis of the sites phosphorylated by two-dimensional peptide mapping. *Biochem.J.* **252**(2), 607-615.

64. Tavaré, J. M., O'Brien, R. M., Siddle, K., and Denton, R. M. (1988) Analysis of insulin-receptor phosphorylation sites in intact cells by two-dimensional phosphopeptide mapping. *Biochem.J.* **253**(3), 783-788.

65. White, M. F., Shoelson, S. E., Keutmann, H., and Kahn, C. R. (1988) A cascade of tyrosine autophosphorylation in the β-subunit activates the phosphotransferase of the insulin receptor. *J.Biol.Chem.* **263**(6), 2969-2980.

66. Feener, E. P., Backer, J. M., King, G. L., Wilden, P. A., Sun, X. J., Kahn, C. R. *et al.* (1993) Insulin stimulates serine and tyrosine phosphorylation in the juxtamembrane region of the insulin receptor. *J.Biol.Chem.* **268**(15), 11256-11264.

67. Kohanski, R. A. (1993) Insulin receptor autophosphorylation. II. Determination of autophosphorylation sites by chemical sequence analysis and identification of the juxtamembrane sites. *Biochemistry* **32**(22), 5773-5780.

68. Herrera, R. and Rosen, O. M. (1986) Autophosphorylation of the insulin receptor *in vitro*. Designation of phosphorylation sites and correlation with receptor kinase activation. *J.Biol.Chem.* **261**(26), 11980-11985.

69. Ellis, L., Clauser, E., Morgan, D. O., Edery, M., Roth, R. A., and Rutter, W. J. (1986) Replacement of insulin receptor tyrosine residues 1162 and 1163 compromises insulin-stimulated kinase activity and uptake of 2- deoxyglucose. *Cell* **45**(5), 721-732.

70. Murakami, M. S. and Rosen, O. M. (1991) The role of insulin receptor autophosphorylation in signal transduction. *J.Biol.Chem.* **266**(33), 22653-22660.

71. Flores-Riveros, J. R., Sibley, E., Kastelic, T., and Lane, M. D. (1989) Substrate phosphorylation catalyzed by the insulin receptor tyrosine kinase. Kinetic correlation to autophosphorylation of specific sites in the β subunit. *J.Biol.Chem.* **264**(36), 21557-21572.

72. Cherqui, G., Reynet, C., Caron, M., Melin, B., Wicek, D., Clauser, E. *et al.* (1990) Insulin receptor tyrosine residues 1162 and 1163 control insulin stimulation of myristoyl-diacylglycerol generation and subsequent activation of glucose transport. *J.Biol.Chem.* **265**(34), 21254-21261.

73 Zhang, B., Tavaré, J. M., Ellis, L., and Roth, R. A. (1991) The regulatory role of known tyrosine autophosphorylation sites of the insulin receptor kinase domain. An assessment by replacement with neutral and negatively charged amino acids. *J.Biol.Chem.* **266**(2), 990-996.

74. Reynet, C., Caron, M., Magre, J., Cherqui, G., Clauser, E., Picard, J. *et al.* (1990) Mutation of tyrosine residues 1162 and 1163 of the insulin receptor affects hormone and receptor internalization. *Mol.Endocrinol.* **4** (2), 304-311.

75. Kohanski, R. A. (1993) Insulin receptor autophosphorylation. I. Autophosphorylation kinetics of the native receptor and its cytoplasmic kinase domain. *Biochemistry* **32**(22), 5766-5772.

76. Eck, M. J., Dhe-Paganon, S., Trub, T., Nolte, R. T., and Shoelson, S. E. (1996) Structure of the IRS-1 PTB domain bound to the juxtamembrane region of the insulin receptor. *Cell* **85**(5), 695-705.

77. Wilden, P. A., Rovira, I., and Broadway, D. E. (1996) Insulin receptor structural requirements for the formation of a ternary complex with IRS-1 and PI 3-kinase. *Mol.Cell Endocrinol.* **122**(2), 131-140.

78. Sawka-Verhelle, D., Tartare-Deckert, S., White, M. F., and Van, O. E. (1996) Insulin receptor substrate-2 binds to the insulin receptor through its phosphotyrosine-binding domain and through a newly identified domain comprising amino acids 591-786. *J.Biol.Chem.* **271**(11), 5980-5983.

79. Isakoff, S. J., Yu, Y. P., Su, Y. C., Blaikie, P., Yajnik, V., Rose, E. *et al.* (1996) Interaction between the phosphotyrosine binding domain of Shc and the insulin receptor is required for Shc phosphorylation by insulin *in vivo*. *J.Biol.Chem.* **271**(8), 3959-3962.

80. van der Geer, P., Wiley, S., Gish, G. D., Lai, V. K., Stephens, R., White, M. F. *et al.* (1996) Identification of residues that control specific binding of the Shc phosphotyrosine-binding domain to phosphotyrosine sites. *Proc.Natl.Acad.Sci.U.S.A.* **93**(3), 963-968.

81. Backer, J. M., Schroeder, G. G., Cahill, D. A., Ullrich, A., Siddle, K., and White, M. F. (1991) Cytoplasmic juxtamembrane region of the insulin receptor: a critical role in ATP binding, endogenous substrate phosphorylation, and insulin-stimulated bioeffects in CHO cells. *Biochemistry* **30**(26), 6366-6372.

82. Backer, J. M., Schroeder, G. G., Kahn, C. R., Myers, M. G., Jr., Wilden, P. A., Cahill, D. A. *et al.* (1992) Insulin stimulation of phosphatidylinositol 3-kinase activity maps to insulin receptor regions required for endogenous substrate phosphorylation. *J.Biol.Chem.* **267**(2), 1367-1374.

83. Kaburagi, Y., Momomura, K., Yamamoto-Honda, R., Tobe, K., Tamori, Y., Sakura, H. *et al.* (1993) Site-directed mutagenesis of the juxtamembrane domain of the human insulin receptor. *J.Biol.Chem.* **268**(22), 16610-16622.

84. Kaburagi, Y., Yamamoto-Honda, R., Tobe, K., Ueki, K., Yachi, M., Akanuma, Y. *et al.* (1995) The role of the NPXY motif in the insulin receptor in tyrosine phosphorylation of insulin receptor substrate-1 and Shc. *Endocrinology* **136**(8), 3437-3443.

85. Tartare-Deckert, S., Sawka-Verhelle, D., Murdaca, J., and Van Obberghen, E. (1995) Evidence for a differential interaction of SHC and the insulin receptor substrate-1 (IRS-1) with the insulin-like growth factor- I (IGF-I) receptor in the yeast two-hybrid system. *J.Biol.Chem.* **270**(40), 23456-23460.

86. Giorgetti Peraldi, S., Ottinger, E., Wolf, G., Ye, B., Burke, T. R., Jr., and Shoelson, S. E. (1997) Cellular effects of phosphotyrosine-binding domain inhibitors on insulin receptor signaling and trafficking. *Mol.Cell Biol.* **17**(3), 1180-1188.

87. Keegan, A. D., Nelms, K., White, M., Wang, L. M., Pierce, J. H., and Paul, W. E. (1994) An IL-4 receptor region containing an insulin receptor motif is important for IL-4-mediated IRS-1 phosphorylation and cell growth. *Cell* **76**(5), 811-820.

88. Backer, J. M., Wjasow, C., and Zhang, Y. (1997) *In vitro* binding and phosphorylation of insulin receptor substrate 1 by the insulin receptor. Role of interactions mediated by the phosphotyrosine-binding domain and the pleckstrin-homology domain. *Eur.J.Biochem.* **245**(1), 91-96.

89. Carpentier, J. L., Paccaud, J. P., Backer, J., Gilbert, A., Orci, L., Kahn, C. R. *et al.* (1993) Two steps of insulin receptor internalization depend on different domains of the β-subunit. *J.Cell Biol.* **122**(6), 1243-1252.

90. Backer, J. M., Shoelson, S. E., Weiss, M. A., Hua, Q. X., Cheatham, R. B., Haring, E. *et al.* (1992) The insulin receptor juxtamembrane region contains two independent tyrosine/β-turn internalization signals. *J.Cell Biol.* **118**(4), 831-839.

91. Backer, J. M., Kahn, C. R., Cahill, D. A., Ullrich, A., and White, M. F. (1990) Receptor-mediated internalization of insulin requires a 12-amino acid sequence in the juxtamembrane region of the insulin receptor β-subunit. *J.Biol.Chem.* **265**(27), 16450-16454.

92. Backer, J. M., Shoelson, S. E., Haring, E., and White, M. F. (1991) Insulin receptors internalize by a rapid, saturable pathway requiring receptor autophosphorylation and an intact juxtamembrane region. *J.Cell Biol.* **115**(6), 1535-1545.

93. Haft, C. R., Klausner, R. D., and Taylor, S. I. (1994) Involvement of dileucine motifs in the internalization and degradation of the insulin receptor. *J.Biol.Chem.* **269**(42), 26286-26294.

94. Smith, J. E., Sheng, Z. F., and Kallen, R. G. (1994) Effects of tyrosine-->phenylalanine mutations on auto- and trans- phosphorylation reactions catalyzed by the insulin receptor β- subunit cytoplasmic domain. *DNA Cell Biol.* **13**(6), 593-604.

95. Myers, M. G., Backer, J. M., Siddle, K., and White, M. F. (1991) The insulin receptor functions normally in Chinese hamster ovary cells after truncation of the C terminus. *J.Biol.Chem.* **266**(16), 10616-10623.

96. Maegawa, H., McClain, D. A., Freidenberg, G., Olefsky, J. M., Napier, M., Lipari, T. *et al.* (1988) Properties of a human insulin receptor with a COOH-terminal

truncation. II. Truncated receptors have normal kinase activity but are defective in signaling metabolic effects. *J.Biol.Chem.* **263**(18), 8912-8917.

97. McClain, D. A., Maegawa, H., Levy, J., Huecksteadt, T., Dull, T. J., Lee, J. *et al.* (1988) Properties of a human insulin receptor with a COOH-terminal truncation. I. Insulin binding, autophosphorylation, and endocytosis. *J.Biol.Chem.* **263**(18), 8904-8911.

98. Baron, V., Gautier, N., Kaliman, P., Dolais-Kitabgi, J., and Van Obberghen, E. (1991) The carboxyl-terminal domain of the insulin receptor: its potential role in growth-promoting effects. *Biochemistry* **30**(38), 9365-9370.

99. Takata, Y., Webster, N. J., and Olefsky, J. M. (1991) Mutation of the two carboxyl-terminal tyrosines results in an insulin receptor with normal metabolic signaling but enhanced mitogenic signaling properties. *J.Biol.Chem.* **266**(14), 9135-9139.

100. Faria, T. N., Blakesley, V. A., Kato, H., Stannard, B., LeRoith, D., and Roberts, C. T., Jr. (1994) Role of the carboxyl-terminal domains of the insulin and insulin- like growth factor I receptors in receptor function. *J.Biol.Chem.* **269**(19), 13922-13928.

101. Issad, T., Tavaré, J. M., and Denton, R. M. (1991) Analysis of insulin receptor phosphorylation sites in intact rat liver cells by two-dimensional phosphopeptide mapping. Predominance of the tris-phosphorylated form of the kinase domain after stimulation by insulin. *Biochem.J.* **275**(Pt 1), 15-21.

102. Baltensperger, K., Lewis, R. E., Woon, C. W., Vissavajjhala, P., Ross, A. H., and Czech, M. P. (1992) Catalysis of serine and tyrosine autophosphorylation by the human insulin receptor. *Proc.Natl.Acad.Sci.U.S.A.* **89**(17), 7885-7889.

103. Heidenreich, K., Paduschek, M., Molders, M., and Klein, H. W. (1994) The insulin receptor: a protein kinase with dual specificity? *Biol.Chem.Hoppe Seyler* **375**(2), 99-104.

104. Tauer, T. J., Volle, D. J., Rhode, S. L., and Lewis, R. E. (1996) Expression of the insulin receptor with a recombinant vaccinia virus. Biochemical evidence that the insulin receptor has intrinsic serine kinase activity. *J.Biol.Chem.* **271**(1), 331-336.

105. Al-Hasani, H., Eisermann, B., Tennagels, N., Magg, C., Paβlack, W., Koenen, M. *et al.* (1997) Identification of Ser-1275 and Ser-1309 as autophosphorylation sites of the insulin receptor. *FEBS Lett.* **400**(1), 65-70.

106. Kasuga, M., Fujita-Yamaguchi, Y., Blithe, D. L., and Kahn, C. R. (1983) Tyrosine-specific protein kinase activity is associated with the purified insulin receptor. *Proc.Natl.Acad.Sci.U.S.A.* **80**(8), 2137-2141.

107. Smith, D. M., King, M. J., and Sale, G. J. (1988) Two systems *in vitro* that show insulin-stimulated serine kinase activity towards the insulin receptor. *Biochem.J.* **250**(2), 509-519.

108. Ellis, L., Levitan, A., Cobb, M. H., and Ramos, P. (1988) Efficient expression in insect cells of a soluble, active human insulin receptor protein-tyrosine kinase domain by use of a baculovirus vector. *J.Virol.* **62**(5), 1634-1639.

109. White, M. F., Takayama, S., and Kahn, C. R. (1985) Differences in the sites of phosphorylation of the insulin receptor *in vivo* and *in vitro*. *J.Biol.Chem.* **260**(16), 9470-9478.

110. Zick, Y., Rees Jones, R. W., Grunberger, G., Taylor, S. I., Moncada, V., Gorden, P. *et al.* (1983) The insulin-stimulated receptor kinase is a tyrosine-specific casein kinase. *Eur.J.Biochem.* **137**(3), 631-637.

111. Walker, D. H., Kuppuswamy, D., Visvanathan, A., and Pike, L. J. (1987) Substrate specificity and kinetic mechanism of human placental insulin receptor/kinase. *Biochemistry* **26**(5), 1428-1433.

112. Todhunter, J. A. and Purich, D. L. (1977) Autophosphorylation of cardiac 3',5'-cyclic AMP-stimulated protein kinase. Kinetic evidence for the regulatory subunit directly acting at the active site in the R_2C_2 complex. *Biochim.Biophys.Acta* **485**(1), 87-94.

113. Yarden, Y. and Schlessinger, J. (1987) Self-phosphorylation of epidermal growth factor receptor: evidence for a model of intermolecular allosteric activation. *Biochemistry* **26**(5), 1434-1442.

114. Barker, S. C., Kassel, D. B., Weigl, D., Huang, X., Luther, M. A., and Knight, W. B. (1995) Characterization of pp60$^{c\text{-}src}$ tyrosine kinase activities using a continuous assay: autoactivation of the enzyme is an intermolecular autophosphorylation process. *Biochemistry* **34**(45), 14843-14851.

115. Smith, J. A., Francis, S. H., Walsh, K. A., Kumar, S., and Corbin, J. D. (1996) Autophosphorylation of type Iβ cGMP-dependent protein kinase increases basal catalytic activity and enhances allosteric activation by cGMP or cAMP. *J.Biol.Chem.* **271**(34), 20756-20762.

116. Iwasaki, Y., Nishiyama, H., Suzuki, K., and Koizumi, S. (1997) Sequential *cis/trans* autophosphorylation in TrkB tyrosine kinase. *Biochemistry* **36**(9), 2694-2700.

117. Sobieszek, A. (1995) Calmodulin-dependent autophosphorylation of smooth muscle myosin light chain kinase: intermolecular reaction mechanism *via* dimerization of the kinase and potentiation of the catalytic activity following activation. *Biochemistry* **34**(37), 11855-11863.

118. Mukherji, S. and Soderling, T. R. (1994) Regulation of Ca^{2+}/calmodulin-dependent protein kinase II by inter- and intrasubunit-catalyzed autophosphorylations. *J.Biol.Chem.* **269**(19), 13744-13747.

119. Shia, M. A., Rubin, J. B., and Pilch, P. F. (1983) The insulin receptor protein kinase. Physicochemical requirements for activity. *J.Biol.Chem.* **258**(23), 14450-14455.

120. Kwok, Y. C., Nemenoff, R. A., Powers, A. C., and Avruch, J. (1986) Kinetic properties of the insulin receptor tyrosine protein kinase: activation through an insulin-stimulated tyrosine- specific, intramolecular autophosphorylation. *Arch.Biochem.Biophys.* **244**(1), 102-113.

121. Ridge, K. D., Hofmann, K., and Finn, F. M. (1988) ATP sensitizes the insulin receptor to insulin. *Proc.Natl.Acad.Sci.U.S.A.* **85**(24), 9489-9493.

122. Lee, J., Shoelson, S. E., and Pilch, P. F. (1995) Intermolecular phosphorylation between insulin holoreceptors does not stimulate substrate kinase activity. *J.Biol.Chem.* **270**(52), 31136-31140.

123. Taouis, M., Levy-Toledano, R., Roach, P., Taylor, S. I., and Gorden, P. (1994) Rescue and activation of a binding-deficient insulin receptor. Evidence for intermolecular transphosphorylation. *J.Biol.Chem.* **269**(44), 27762-27766.

124. Kohanski, R. A. and Schenker, E. (1991) Control of insulin receptor autophosphorylation by polypeptide substrates: inhibition and stimulation by interaction with the catalytic subunit. *Biochemistry* **30**(9), 2406-2414.

125. Cobb, M. H., Sang, B. C., Gonzalez, R., Goldsmith, E., and Ellis, L. (1989) Autophosphorylation activates the soluble cytoplasmic domain of the insulin receptor in an intermolecular reaction. *J.Biol.Chem.* **264**(31), 18701-18706.

126. Wei, L., Hubbard, S. R., Hendrickson, W. A., and Ellis, L. (1995) Expression, characterization, and crystallization of the catalytic core of the human insulin receptor protein-tyrosine kinase domain. *J.Biol.Chem.* **270**(14), 8122-8130.

127. Herrera, R., Lebwohl, D., Garcia de Herreros, A., Kallen, R. G., and Rosen, O. M. (1988) Synthesis, purification, and characterization of the cytoplasmic domain of the human insulin receptor using a baculovirus expression system. *J.Biol.Chem.* **263**(12), 5560-5568.

128. Villalba, M., Wente, S. R., Russell, D. S., Ahn, J. C., Reichelderfer, C. F., and Rosen, O. M. (1989) Another version of the human insulin receptor kinase domain: expression, purification, and characterization. *Proc.Natl.Acad.Sci.U.S.A.* **86**(20), 7848-7852.

129. Shoelson, S. E., Böni-Schnetzler, M., Pilch, P. F., and Kahn, C. R. (1991) Autophosphorylation within insulin receptor β-subunits can occur as an intramolecular process. *Biochemistry* **30**(31), 7740-7746.

130. Frattali, A. L., Treadway, J. L., and Pessin, J. E. (1992) Transmembrane signaling by the human insulin receptor kinase. Relationship between intramolecular β subunit *trans-* and *cis-* autophosphorylation and substrate kinase activation. *J.Biol.Chem.* **267**(27), 19521-19528.

131. Zick, Y., Grunberger, G., Podskalny, J. M., Moncada, V., Taylor, S. I., Gorden, P. *et al.* (1983) Insulin stimulates phosphorylation of serine residues in soluble insulin receptors. *Biochem.Biophys.Res.Commun.* **116**(3), 1129-1135.

132. Pang, D. T., Sharma, B. R., Shafer, J. A., White, M. F., and Kahn, C. R. (1985) Predominance of tyrosine phosphorylation of insulin receptors during the initial response of intact cells to insulin. *J.Biol.Chem.* **260**(11), 7131-7136.

133. Jacobs, S. and Cuatrecasas, P. (1986) Phosphorylation of receptors for insulin and insulin-like growth factor I. Effects of hormones and phorbol esters. *J.Biol.Chem.* **261**(2), 934-939.

134. Ballotti, R., Kowalski, A., White, M. F., Le Marchand Brustel, Y., and Van Obberghen, E. (1987) Insulin stimulates tyrosine phosphorylation of its receptor β-subunit in intact rat hepatocytes. *Biochem.J.* **241**(1), 99-104.

135. Magre, J., Grigorescu, F., Reynet, C., Caron, M., Capony, J. P., White, M. F. *et al.* (1989) Tyrosine-kinase defect of the insulin receptor in cultured fibroblasts from patients with lipoatropic diabetes. *J.Clin.Endocrinol.Metab.* **69**(1), 142-150.

136. Khan, M. N., Baquiran, G., Brule, C., Burgess, J., Foster, B., Bergeron, J. J. *et al.* (1989) Internalization and activation of the rat liver insulin receptor kinase *in vivo*. *J.Biol.Chem.* **264**(22), 12931-12940.

137. Dunaif, A., Xia, J., Book, C. B., Schenker, E., and Tang, Z. (1995) Excessive insulin receptor serine phosphorylation in cultured fibroblasts and in skeletal muscle. A potential mechanism for insulin resistance in the polycystic ovary syndrome. *J.Clin.Invest.* **96**(2), 801-810.

138. Iwama, N., Watarai, T., Kajimoto, Y., Yamasaki, Y., Yokoyama, T., Kawamori, R. *et al.* (1991) Dephosphorylation of the insulin receptor partially restores the decreased autophosphorylation in streptozotocin induced diabetic rats. *Diabetes Res.* **17**(1), 25-32.

139. Karasik, A., Rothenberg, P. L., Yamada, K., White, M. F., and Kahn, C. R. (1990) Increased protein kinase C activity is linked to reduced insulin receptor autophosphorylation in liver of starved rats. *J.Biol.Chem.* **265**(18), 10226-10231.

140. Carter, W. G., Asamoah, K. A., and Sale, G. J. (1995) Studies into the identity of the sites of insulin-stimulated insulin receptor serine phosphorylation. Characterization of synthetic peptide substrates for the insulin-stimulated insulin receptor serine kinase. *Biochemistry* **34**(29), 9488-9499.

141. Bollag, G. E., Roth, R. A., Beaudoin, J., Mochly Rosen, D., and Koshland, D. E., Jr. (1986) Protein kinase C directly phosphorylates the insulin receptor *in vitro* and reduces its protein-tyrosine kinase activity. *Proc.Natl.Acad.Sci.U.S.A.* **83**(16), 5822-5824.

142. Ahn, J., Donner, D. B., and Rosen, O. M. (1993) Interaction of the human insulin receptor tyrosine kinase from the baculovirus expression system with protein kinase C in a cell- free system. *J.Biol.Chem.* **268**(10), 7571-7576.

143. Koshio, O., Akanuma, Y., and Kasuga, M. (1989) Identification of a phosphorylation site of the rat insulin receptor catalyzed by protein kinase C in an intact cell. *FEBS Lett.* **254**(1-2), 22-24.

144. Lewis, R. E., Cao, L., Perregaux, D., and Czech, M. P. (1990) Threonine 1336 of the human insulin receptor is a major target for phosphorylation by protein kinase C. *Biochemistry* **29**(7), 1807-1813.

145. Liu, F. and Roth, R. A. (1994) Identification of serines-1035/1037 in the kinase domain of the insulin receptor as protein kinase C α mediated phosphorylation sites. *FEBS Lett.* **352**(3), 389-392.

146. Lewis, R. E., Volle, D. J., and Sanderson, S. D. (1994) Phorbol ester stimulates phosphorylation on serine 1327 of the human insulin receptor. *J.Biol.Chem.* **269**(42), 26259-26266.

147. Coghlan, M. P., Pillay, T. S., Tavaré, J. M., and Siddle, K. (1994) Site-specific anti-phosphopeptide antibodies: use in assessing insulin receptor serine/threonine phosphorylation state and identification of serine-1327 as a novel site of phorbol ester- induced phosphorylation. *Biochem.J.* **303**(Pt 3), 893-899.

148. Feener, E. P., Shiba, T., Hu, K. Q., Wilden, P. A., White, M. F., and King, G. L. (1994) Characterization of phorbol ester-stimulated serine phosphorylation of the human insulin receptor. *Biochem.J.* **303**(Pt 1), 43-50.

149. Takayama, S., White, M. F., and Kahn, C. R. (1988) Phorbol ester-induced serine phosphorylation of the insulin receptor decreases its tyrosine kinase activity. *J.Biol.Chem.* **263**(7), 3440-3447.

150. Takayama, S., White, M. F., Lauris, V., and Kahn, C. R. (1984) Phorbol esters modulate insulin receptor phosphorylation and insulin action in cultured hepatoma cells. *Proc.Natl.Acad.Sci.U.S.A.* **81**(24), 7797-7801.

151. Häring, H. U., Tippmer, S., Kellerer, M., Mosthaf, L., Kroder, G., Bossenmaier, B. *et al.* (1996) Modulation of insulin receptor signaling. Potential mechanisms of a cross talk between bradykinin and the insulin receptor. *Diabetes* **45** (Suppl. 1), S115-9.

152. Chin, J. E., Dickens, M., Tavaré, J. M., and Roth, R. A. (1993) Overexpression of protein kinase C isoenzymes α, β I, γ, and ε in cells overexpressing the insulin receptor. Effects on receptor phosphorylation and signaling. *J.Biol.Chem.* **268**(9), 6338-6347.

153. Häring, H. U., Kellerer, M., and Mosthaf, L. (1994) Modulation of insulin signalling in non-insulin-dependent diabetes mellitus: significance of altered receptor isoform patterns and mechanisms of glucose-induced receptor modulation. *Horm.Res.* **41**(Suppl. 2), 87-91.

154. Tavaré, J. M., Zhang, B., Ellis, L., and Roth, R. A. (1991) Insulin-stimulated serine and threonine phosphorylation of the human insulin receptor. An assessment of the role of serines 1305/1306 and threonine 1348 by their replacement with neutral or negatively charged amino acids. *J.Biol.Chem.* **266**(32), 21804-21809.

155. Ahn, J., Rosen, O. M., and Donner, D. B. (1993) Human insulin receptor mutated at threonine 1336 functions normally in Chinese hamster ovary cells. *J.Biol.Chem.* **268**(22), 16839-16844.

156. Mosthaf, L., Berti, L., Kellerer, M., Mushack, J., Seffer, E., Bossenmaier, B. *et al.* (1995) C-terminus or juxtamembrane deletions in the insulin receptor do not affect the glucose-dependent inhibition of the tyrosine kinase activity. *Eur.J.Biochem.* **227**(3), 787-791.

157. Anderson, C. M. and Olefsky, J. M. (1991) Phorbol ester-mediated protein kinase C interaction with wild- type and COOH-terminal truncated insulin receptors. *J.Biol.Chem.* **266**(32), 21760-21764.

158. Kellerer, M., Coghlan, M., Capp, E., Muhlhofer, A., Kroder, G., Mosthaf, L. *et al.* (1995) Mechanism of insulin receptor kinase inhibition in non-insulin- dependent diabetes mellitus patients. Phosphorylation of serine 1327 or threonine 1348 is unaltered. *J.Clin.Invest.* **96**(1), 6-11.

159. Liu, F. and Roth, R. A. (1994) Identification of serines-967/968 in the juxtamembrane region of the insulin receptor as insulin-stimulated phosphorylation sites. *Biochem.J.* **298**(Pt 2), 471-477.

160. Zachayus, J. L., Cherqui, G., and Plas, C. (1994) Protein kinase C and insulin receptor beta-subunit serine phosphorylation in cultured foetal rat hepatocytes. *Mol.Cell Endocrinol.* **105**(1), 11-20.

161. Gazzano, H., Kowalski, A., Fehlmann, M., and Van Obberghen, E. (1983) Two different protein kinase activities are associated with the insulin receptor. *Biochem.J.* **216**(3), 575-582.

162. Smith, D. M. and Sale, G. J. (1988) Evidence that a novel serine kinase catalyses phosphorylation of the insulin receptor in an insulin-dependent and tyrosine kinase-dependent manner. *Biochem.J.* **256**(3), 903-909.

163. Lewis, R. E., Wu, G. P., MacDonald, R. G., and Czech, M. P. (1990) Insulin-sensitive phosphorylation of serine 1293/1294 on the human insulin receptor by a tightly associated serine kinase. *J.Biol.Chem.* **265**(2), 947-954.

164. Smith, D. M. and Sale, G. J. (1989) Characterization of sites of serine phosphorylation in human placental insulin receptor copurified with insulin-stimulated serine kinase activity by two-dimensional thin-layer peptide mapping. *FEBS Lett.* **242**(2), 301-304.

165. Asamoah, K. A., Atkinson, P. G., Carter, W. G., and Sale, G. J. (1995) Studies on an insulin-stimulated insulin receptor serine kinase activity: separation of the kinase activity from the insulin receptor and its reconstitution back to the insulin receptor. *Biochem.J.* **308**(Pt 3), 915-922.

166. Carter, W. G., Sullivan, A. C., Asamoah, K. A., and Sale, G. J. (1996) Purification and characterization of an insulin-stimulated insulin receptor serine kinase. *Biochemistry* **35**(45), 14340-14351.

167. Singh, T. J. (1993) Insulin receptor serine kinase activation by casein kinase 2 and a membrane tyrosine kinase. *Mol.Cell Biochem.* **121**(2), 167-174.

168. Yamauchi, K., Hashizume, K., Ichikawa, K., Ohtsuka, H., Ohara, N., Miyamoto, T. *et al.* (1991) Adenosine 3',5'-cyclic monophosphate-dependent protein kinase (A kinase) regulation of insulin receptor function: phosphorylation of insulin receptor with A kinase decreases the insulin binding activity. *Endocrinol.Jpn.* **38**(2), 175-182.

169. Tuazon, P. T., Pang, D. T., Shafer, J. A., and Traugh, J. A. (1985) Phosphorylation of the insulin receptor by casein kinase I. *J.Cell Biochem.* **28**(2), 159-170.

170. Rapuano, M. and Rosen, O. M. (1991) Phosphorylation of the insulin receptor by a casein kinase I- like enzyme. *J.Biol.Chem.* **266**(20), 12902-12907.

171. Grande, J., Perez, M., and Itarte, E. (1988) Phosphorylation of hepatic insulin receptor by casein kinase 2. *FEBS Lett.* **232**(1), 130-134.

172. Yu, K. T., Werth, D. K., Pastan, I. H., and Czech, M. P. (1985) src kinase catalyzes the phosphorylation and activation of the insulin receptor kinase. *J.Biol.Chem.* **260**(9), 5838-5846.

173. Häring, H. U., White, M. F., Kahn, C. R., Ahmad, Z., DePaoli-Roach, A. A., and Roach, P. J. (1985) Interaction of the insulin receptor kinase with serine/threonine kinases *in vitro*. *J.Cell Biochem.* **28**(2), 171-182.

174. Tanti, J. F., Gremeaux, T., Rochet, N., Van Obberghen, E., and Le Marchand Brustel, Y. (1987) Effect of cyclic AMP-dependent protein kinase on insulin receptor tyrosine kinase activity. *Biochem.J.* **245**(1), 19-26.

175. White, M. F., Maron, R., and Kahn, C. R. (1985) Insulin rapidly stimulates tyrosine phosphorylation of a Mr-185, 000 protein in intact cells. *Nature* **318**(6042), 183-186.

176. Sun, X. J., Rothenberg, P., Kahn, C. R., Backer, J. M., Araki, E., Wilden, P. A. *et al.* (1991) Structure of the insulin receptor substrate IRS-1 defines a unique signal transduction protein. *Nature* **352**(6330), 73-77.

177. Myers, M. G., Jr., Grammer, T. C., Brooks, J., Glasheen, E. M., Wang, L. M., Sun, X. J. *et al.* (1995) The pleckstrin homology domain in insulin receptor substrate-1 sensitizes insulin signaling. *J.Biol.Chem.* **270**(20), 11715-11718.

178. Yenush, L., Makati, K. J., Smith Hall, J., Ishibashi, O., Myers, M. G., Jr., and White, M. F. (1996) The pleckstrin homology domain is the principal link between the insulin receptor and IRS-1. *J.Biol.Chem.* **271**(39), 24300-24306.

179. Voliovitch, H., Schindler, D. G., Hadari, Y. R., Taylor, S. I., Accili, D., and Zick, Y. (1995) Tyrosine phosphorylation of insulin receptor substrate-1 *in vivo* depends upon the presence of its pleckstrin homology region. *J.Biol.Chem.* **270**(30), 18083-18087.

180. Skolnik, E. Y., Lee, C. H., Batzer, A., Vicentini, L. M., Zhou, M., Daly, R. *et al.* (1993) The SH2/SH3 domain-containing protein GRB2 interacts with tyrosine-phosphorylated IRS1 and Shc: implications for insulin control of ras signalling. *EMBO J.* **12**(5), 1929-1936.

181. Skolnik, E. Y., Batzer, A., Li, N., Lee, C. H., Lowenstein, E., Mohammadi, M. *et al.* (1993) The function of GRB2 in linking the insulin receptor to Ras signaling pathways. *Science* **260**(5116), 1953-1955.

182. Folli, F., Saad, M. J., Backer, J. M., and Kahn, C. R. (1992) Insulin stimulation of phosphatidylinositol 3-kinase activity and association with insulin receptor substrate 1 in liver and muscle of the intact rat. *J.Biol.Chem.* **267**(31), 22171-22177.

183. Myers, M. G. J., Backer, J. M., Sun, X. J., Shoelson, S., Hu, P., Schlessinger, J. *et al.* (1992) IRS-1 activates phosphatidylinositol 3'-kinase by associating with src homology 2 domains of p85. *Proc.Natl.Acad.Sci.U.S.A.* **89**(21), 10350-10354.

184. Kuhne, M. R., Pawson, T., Lienhard, G. E., and Feng, G. S. (1993) The insulin receptor substrate 1 associates with the SH2- containing phosphotyrosine phosphatase Syp. *J.Biol.Chem.* **268**(16), 11479-11481.

185. Myers, M. G., Jr., Sun, X. J., and White, M. F. (1994) The IRS-1 signaling system. *Trends.Biochem.Sci.* **19**(7), 289-293.

186. White, M. F. and Kahn, C. R. (1994) The insulin signaling system. *J.Biol.Chem.* **269** (1), 1-4.

187. Graves, J. D., Campbell, J. S., and Krebs, E. G. (1995) Protein serine/threonine kinases of the MAPK cascade. *Ann.N.Y.Acad.Sci.* **766**, 320-343.

188. Liu, F. and Roth, R. A. (1995) Grb-IR: a SH2-domain-containing protein that binds to the insulin receptor and inhibits its function. *Proc.Natl.Acad.Sci.U.S.A.* **92**(22), 10287-10291.

189. Frantz, J. D., Giorgetti-Peraldi, S., Ottinger, E. A., and Shoelson, S. E. (1997) Human GRB-IRβ/GRB10. Splice variants of an insulin and growth factor receptor-binding protein with PH and SH2 domains. *J.Biol.Chem.* **272**(5), 2659-2667.

190. Holgado Madruga, M., Emlet, D. R., Moscatello, D. K., Godwin, A. K., and Wong, A. J. (1996) A Grb2-associated docking protein in EGF- and insulin-receptor signalling. *Nature* **379**(6565), 560-564.

191. Tamemoto, H., Kadowaki, T., Tobe, K., Yagi, T., Sakura, H., Hayakawa, T. *et al.* (1994) Insulin resistance and growth retardation in mice lacking insulin receptor substrate-1. *Nature* **372**(6502), 182-186.

192. Kadowaki, T., Tamemoto, H., Tobe, K., Terauchi, Y., Ueki, K., Kaburagi, Y. *et al.* (1996) Insulin resistance and growth retardation in mice lacking insulin receptor substrate-1 and identification of insulin receptor substrate-2. *Diabet.Med.* **13**(9 Suppl 6), S103-8.

193. Patti, M. E., Sun, X. J., Bruening, J. C., Araki, E., Lipes, M. A., White, M. F. *et al.* (1995) 4PS/insulin receptor substrate (IRS)-2 is the alternative substrate of the insulin receptor in IRS-1-deficient mice. *J.Biol.Chem.* **270**(42), 24670-24673.

194. Welham, M. J., Bone, H., Levings, M., Learmonth, L., Wang, L. M., Leslie, K. B. *et al.* (1997) Insulin receptor substrate-2 is the major 170-kDa protein phosphorylated on tyrosine in response to cytokines in murine lymphohemopoietic cells. *J.Biol.Chem.* **272**(2), 1377-1381.

195. Wang, H. Y., Zamorano, J., Yoerkie, J. L., Paul, W. E., and Keegan, A. D. (1997) The IL-4-induced tyrosine phosphorylation of the insulin receptor substrate is dependent on JAK1 expression in human fibrosarcoma cells. *J.Immunol.* **158**(3), 1037-1040.

196. Platanias, L. C., Uddin, S., Yetter, A., Sun, X. J., and White, M. F. (1996) The type I interferon receptor mediates tyrosine phosphorylation of insulin receptor substrate 2. *J.Biol.Chem.* **271**(1), 278-282.

197. Johnston, J. A., Wang, L. M., Hanson, E. P., Sun, X. J., White, M. F., Oakes, S. A. *et al.* (1995) Interleukins 2, 4, 7, and 15 stimulate tyrosine phosphorylation of insulin receptor substrates 1 and 2 in T cells. Potential role of JAK kinases. *J.Biol.Chem.* **270**(48), 28527-28530.

198. Rondinone, C. M., Wang, L. M., Lonnroth, P., Wesslau, C., Pierce, J. H., and Smith, U. (1997) Insulin receptor substrate (IRS) 1 is reduced and IRS-2 is the main docking protein for phosphatidylinositol 3-kinase in adipocytes from subjects with non-insulin-dependent diabetes mellitus. *Proc.Natl.Acad.Sci.U.S.A.* **94**(8), 4171-4175.

199. Myers, M. G. J., Sun, X. J., Cheatham, B., Jachna, B. R., Glasheen, E. M., Backer, J. M. *et al.* (1993) IRS-1 is a common element in insulin and insulin-like growth factor-I signaling to the phosphatidylinositol 3'-kinase. *Endocrinology* **132**(4), 1421-1430.

200. Myers, M. G., Jr. and White, M. F. (1996) Insulin signal transduction and the IRS proteins. *Annu.Rev.Pharmacol.Toxicol.* **36**, 615-658.

201. Lavan, B. E., Lane, W. S., and Lienhard, G. E. (1997) The 60-kDa phosphotyrosine protein in insulin-treated adipocytes is a new member of the insulin receptor substrate family. *J.Biol.Chem.* **272**(17), 11439-11443.

202. Lavan, B. E., Fantin, V. R., Chang, E. T., Lane, W. S., Keller, S. R., and Lienhard, G. E. (1997) A novel 160-kDa phosphotyrosine protein in insulin-treated embryonic kidney cells is a new member of the insulin receptor substrate family. *J.Biol.Chem.* **272**(34), 21403-21407.

203. Knutson, V. P., Ronnett, G. V., and Lane, M. D. (1983) Rapid, reversible internalization of cell surface insulin receptors. Correlation with insulin-induced down-regulation. *J.Biol.Chem.* **258**(20), 12139-12142.

204. Reed, B. C., Ronnett, G. V., and Lane, M. D. (1981) Role of glycosylation and protein synthesis in insulin receptor metabolism by 3T3-L1 mouse adipocytes. *Proc.Natl.Acad.Sci.U.S.A.* **78**(5), 2908-2912.

205. Ronnett, G. V., Knutson, V. P., and Lane, M. D. (1982) Insulin-induced down-regulation of insulin receptors in 3T3-L1 adipocytes. Altered rate of receptor inactivation. *J.Biol.Chem.* **257**(8), 4285-4291.

206. Knutson, V. P., Ronnett, G. V., and Lane, M. D. (1982) Control of insulin receptor level in 3T3 cells: effect of insulin-induced down-regulation and dexamethasone-induced up- regulation on rate of receptor inactivation. *Proc.Natl.Acad.Sci.U.S.A.* **79**(9), 2822-2826.

207. Ueda, M., Robinson, F. W., Smith, M. M., and Kono, T. (1985) Effects of monensin on insulin processing in adipocytes. Evidence that the internalized insulin-receptor complex has some physiological activities. *J.Biol.Chem.* **260**(7), 3941-3946.

208. Kahn, C. R., Flier, J. S., Bar, R. S., Archer, J. A., Gorden, P., Martin, M. M. *et al.* (1976) The syndromes of insulin resistance and acanthosis nigricans. Insulin-receptor disorders in man. *N.Engl.J.Med.* **294**(14), 739-745.

209. Kahn, C. R. and Podskalny, J. M. (1980) Demonstration of a primary (? genetic) defect in insulin receptors in fibroblasts from a patient with the syndrome of insulin resistance and acanthosis nigricans type A. *J.Clin.Endocrinol.Metab.* **50**(6), 1139-1141.

210. Taylor, S. I., Samuels, B., Roth, J., Kasuga, M., Hedo, J. A., Gorden, P. *et al.* (1982) Decreased insulin binding in cultured lymphocytes from two patients with extreme insulin resistance. *J.Clin.Endocrinol.Metab.* **54**(5), 919-930.

211. Elsas, L. J., Endo, F., Strumlauf, E., Elders, J., and Priest, J. H. (1985) Leprechaunism: an inherited defect in a high-affinity insulin receptor. *Am.J.Hum.Genet.* **37**(1), 73-88.

212. Taylor, S. I., Cama, A., Accili, D., Barbetti, F., Quon, M. J., de la Luz Sierra, M. *et al.* (1992) Mutations in the insulin receptor gene. *Endocr.Rev.* **13**(3), 566-595.

213. Rabson, S. M. and Mendenhall, E. N. (1956) Familial hypertrophy of pineal body, hyperplasia of adrenal cortex and diabetes mellitus. *Am.J.Clin.Pathol.* **26**, 283-290.

214. Donohue, W. L. and Uchida, I. (1954) Leprechaunism: a euphuism for a rare familial disorder. *J.Pediatr.* **45**(5), 505-519.

215. Schilling, E. E., Rechler, M. M., Grunfeld, C., and Rosenberg, A. M. (1979) Primary defect of insulin receptors in skin fibroblasts cultured from an infant with leprechaunism and insulin resistance. *Proc.Natl.Acad.Sci.U.S.A.* **76**(11), 5877-5881.

216. Kadowaki, T., Bevins, C. L., Cama, A., Ojamaa, K., Marcus Samuels, B., Kadowaki, H. *et al.* (1988) Two mutant alleles of the insulin receptor gene in a patient with extreme insulin resistance. *Science* **240**(4853), 787-790.

217. Krook, A. and O'Rahilly, S. (1996) Mutant insulin receptors in syndromes of insulin resistance. *Baillieres.Clin.Endocrinol.Metab.* **10**(1), 97-122.

218. Jospe, N., Kaplowitz, P. B., and Furlanetto, R. W. (1996) Homozygous nonsense mutation in the insulin receptor gene of a patient with severe congenital insulin resistance: leprechaunism and the role of the insulin-like growth factor receptor. *Clin.Endocrinol.Oxf.* **45**(2), 229-235.

219. Wertheimer, E., Lu, S. P., Backeljauw, P. F., Davenport, M. L., and Taylor, S. I. (1993) Homozygous deletion of the human insulin receptor gene results in leprechaunism. *Nat.Genet.* **5**(1), 71-73.

220. Krook, A., Brueton, L., and O'Rahilly, S. (1993) Homozygous nonsense mutation in the insulin receptor gene in infant with leprechaunism. *Lancet* **342**(8866), 277-278.

221. Joshi, R. L., Lamothe, B., Cordonnier, N., Mesbah, K., Monthioux, E., Jami, J. *et al.* (1996) Targeted disruption of the insulin receptor gene in the mouse results in neonatal lethality. *EMBO J.* **15**(7), 1542-1547.

222. Accili, D., Drago, J., Lee, E. J., Johnson, M. D., Cool, M. H., Salvatore, P. *et al.* (1996) Early neonatal death in mice homozygous for a null allele of the insulin receptor gene. *Nat.Genet.* **12**(1), 106-109.

223. Chen, C., Jack, J., and Garofalo, R. S. (1996) The Drosophila insulin receptor is required for normal growth. *Endocrinology* **137**(3), 846-856.

224. Fernandez, R., Tabarini, D., Azpiazu, N., Frasch, M., and Schlessinger, J. (1995) The Drosophila insulin receptor homolog: a gene essential for embryonic development encodes two receptor isoforms with different signaling potential. *EMBO J.* **14** (14), 3373-3384.

225. Kimura, K. D., Tissenbaum, H. A., Liu, Y., and Ruvkun, G. (1997) *daf*-2, an insulin receptor-like gene that regulates longevity and diapause in *caenorhabditis elegans*. *Science* **277**(5328), 942-946.

226. Flier, J. S., Kahn, C. R., Roth, J., and Bar, R. S. (1975) Antibodies that impair insulin receptor binding in an unusual diabetic syndrome with severe insulin resistance. *Science* **190**(4209), 63-65.

227. Flier, J. S., Kahn, C. R., Jarrett, D. B., and Roth, J. (1976) Characterization of antibodies to the insulin receptor: a cause of insulin-resistant diabetes in man. *J.Clin.Invest.* **58**(6), 1442-1449.

228. Pulini, M., Raff, S. B., Chase, R., and Gordon, E. E. (1976) Insulin resistance and acanthosis nigricans. Report of a case with antibodies to insulin receptors. *Ann.Intern.Med.* **85**(6), 749-751.

229. Muggeo, M., Kahn, C. R., Bar, R. S., Rechler, M., Flier, J. S., and Roth, J. (1979) The underlying insulin receptor in patients with antireceptor autoantibodies: demonstration of normal binding and immunological properties. *J.Clin.Endocrinol.Metab.* **49**(1), 110-119.

230. Kan, M., Kanai, F., Iida, M., Jinnouchi, H., Todaka, M., Imanaka, T. *et al.* (1995) Frequency of mutations of insulin receptor gene in Japanese patients with NIDDM. *Diabetes* **44**(9), 1081-1086.

231. Accili, D. (1995) Molecular defects of the insulin receptor gene. *Diabetes Metab.Rev.* **11**(1), 47-62.

232. Bjornholm, M., Kawano, Y., Lehtihet, M., and Zierath, J. R. (1997) Insulin receptor substrate-1 phosphorylation and phosphatidylinositol 3-kinase activity in skeletal muscle from NIDDM subjects after *in vivo* insulin stimulation. *Diabetes* **46**(3), 524-527.

233. Obermaier Kusser, B., White, M. F., Pongratz, D. E., Su, Z., Ermel, B., Muhlbacher, C. *et al.* (1989) A defective intramolecular autoactivation cascade may cause the reduced kinase activity of the skeletal muscle insulin receptor from patients with non-insulin-dependent diabetes mellitus. *J.Biol.Chem.* **264**(16), 9497-9504.

234. Haring, H. and Obermaier Kusser, B. (1989) Insulin receptor kinase defects in insulin-resistant tissues and their role in the pathogenesis of NIDDM. *Diabetes Metab.Rev.* **5**(5), 431-441.

235. Okamoto, M., White, M. F., Maron, R., and Kahn, C. R. (1986) Autophosphorylation and kinase activity of insulin receptor in diabetic rats. *Am.J.Physiol.* **251**(5 Pt 1), E542-50.

236. Skolnik, E. Y. and Marcusohn, J. (1996) Inhibition of insulin receptor signaling by TNF: potential role in obesity and non-insulin-dependent diabetes mellitus. *Cytokine.Growth Factor.Rev.* **7**(2), 161-173.

237. Kanety, H., Feinstein, R., Papa, M. Z., Hemi, R., and Karasik, A. (1995) Tumor necrosis factor α-induced phosphorylation of insulin receptor substrate-1 (IRS-1). Possible mechanism for suppression of insulin-stimulated tyrosine phosphorylation of IRS-1. *J.Biol.Chem.* **270**(40), 23780-23784.

238. Hotamisligil, G. S., Peraldi, P., Budavari, A., Ellis, R., White, M. F., and Spiegelman, B. M. (1996) IRS-1-mediated inhibition of insulin receptor tyrosine

kinase activity in TNF-α- and obesity-induced insulin resistance. *Science* **271**(5249), 665-668.

239. Peraldi, P., Hotamisligil, G. S., Buurman, W. A., White, M. F., and Spiegelman, B. M. (1996) Tumor necrosis factor (TNF)–α inhibits insulin signaling through stimulation of the p55 TNF receptor and activation of sphingomyelinase. *J.Biol.Chem.* **271**(22), 13018-13022.

240. Belfiore, A., Frittitta, L., Costantino, A., Frasca, F., Pandini, G., Sciacca, L. *et al.* (1996) Insulin receptors in breast cancer. *Ann.N.Y.Acad.Sci.* **784**, 173-188.

241. Milazzo, G., Giorgino, F., Damante, G., Sung, C., Stampfer, M. R., Vigneri, R. *et al.* (1992) Insulin receptor expression and function in human breast cancer cell lines. *Cancer Res.* **52**(14), 3924-3930.

242. Giorgino, F., Belfiore, A., Milazzo, G., Costantino, A., Maddux, B., Whittaker, J. *et al.* (1991) Overexpression of insulin receptors in fibroblast and ovary cells induces a ligand-mediated transformed phenotype. *Mol.Endocrinol.* **5**(3), 452-459.

243. Giovannucci, E. (1995) Insulin and colon cancer. *Cancer Causes Control* **6**(1), 164-179.

244. LeRoith, D., Werner, H., Neuenschwander, S., Kalebic, T., and Helman, L. J. (1995) The role of the insulin-like growth factor-I receptor in cancer. *Ann.N.Y.Acad.Sci.* **766**, 402-408.

245. Neckameyer, W. S. and Wang, L. H. (1985) Nucleotide sequence of avian sarcoma virus UR2 and comparison of its transforming gene with other members of the tyrosine protein kinase oncogene family. *J.Virol.* **53**(3), 879-884.

246. Matsushime, H., Wang, L. H., and Shibuya, M. (1986) Human c-ros-1 gene homologous to the v-ros sequence of UR2 sarcoma virus encodes for a transmembrane receptorlike molecule. *Mol.Cell Biol.* **6**(8), 3000-3004.

247. Neckameyer, W. S., Shibuya, M., Hsu, M. T., and Wang, L. H. (1986) Proto-oncogene c-ros codes for a molecule with structural features common to those of growth factor receptors and displays tissue specific and developmentally regulated expression. *Mol.Cell Biol.* **6**(5), 1478-1486.

248. Zong, C. S., Poon, B., Chen, J., and Wang, L. H. (1993) Molecular and biochemical bases for activation of the transforming potential of the proto-oncogene c-ros. *J.Virol.* **67**(11), 6453-6462.

249. Jong, S. M. and Wang, L. H. (1990) Role of gag sequence in the biochemical properties and transforming activity of the avian sarcoma virus UR2-encoded gag-ros fusion protein. *J.Virol.* **64**(12), 5997-6009.

250. Zong, C. S. and Wang, L. H. (1994) Modulatory effect of the transmembrane domain of the protein- tyrosine kinase encoded by oncogene ros: biological function and substrate interaction. *Proc.Natl.Acad.Sci.U.S.A.* **91**(23), 10982-10986.

251. Poon, B., Dixon, D., Ellis, L., Roth, R. A., Rutter, W. J., and Wang, L. H. (1991) Molecular basis of the activation of the tumorigenic potential of Gag-insulin receptor chimeras. *Proc.Natl.Acad.Sci.U.S.A.* **88**(3), 877-881.

252. Wang, L. H., Lin, B., Jong, S. M., Dixon, D., Ellis, L., Roth, R. A. *et al.* (1987) Activation of transforming potential of the human insulin receptor gene. *Proc.Natl.Acad.Sci.U.S.A.* **84**(16), 5725-5729.

253. Tamura, S., Fujita-Yamaguchi, Y., and Larner, J. (1983) Insulin-like effect of trypsin on the phosphorylation of rat adipocyte insulin receptor. *J.Biol.Chem.* **258**(24), 14749-14752.

254. Chan, J. L., Lai, M., and Wang, L. H. (1997) Effect of dimerization on signal transduction and biological function of oncogenic Ros, insulin, and insulin-like growth factor I receptors. *J.Biol.Chem.* **272**(1), 146-153.

255. Krebs, E. G. and Fischer, E. H. (1956) The phosphorylase b to a converting enzyme of rabbit skeletal muscle. *Biochim.Biophys.Acta* **20**, 150-157.

256. DeLange, R. J., Kemp, R. G., Riley, W. D., Cooper, R. A., and Krebs, E. G. (1968) Activation of skeletal muscle phosphorylase kinase by adenosine triphosphate and adenosine 3',5'-monophosphate. *J.Biol.Chem.* **243**(9), 2200-2208.

257. Walsh, D. A., Perkins, J. P., and Krebs, E. G. (1968) An adenosine 3',5'-monophosphate-dependant protein kinase from rabbit skeletal muscle. *J.Biol.Chem.* **243**(13), 3763-3765.

258. Reimann, E. M., Walsh, D. A., and Krebs, E. G. (1971) Purification and properties of rabbit skeletal muscle adenosine 3',5'- monophosphate-dependent protein kinases. *J.Biol.Chem.* **246**(7), 1986-1995.

259. Ullrich, A. and Schlessinger, J. (1990) Signal transduction by receptors with tyrosine kinase activity. *Cell* **61**(2), 203-212.

260. Pulido, D. Growth factor receptors with tyrosine protein kinase activity. Chapter 6, pp. 225-272. In: The molecular basis of human cancer., Neel, G. N. and Kumar, S., eds. Futura Publishing Company., Mount Kisco, N.Y., 1993.

261. Gammeltoft, S. and Gliemann, J. (1977) Degradation, receptor binding affinity, and potency of insulin from the Atlantic hagfish (Myxine glutinosa) determined in isolated rat fat cells. *J.Biol.Chem.* **252**(2), 602-608.

262. Muggeo, M., Van Obberghen, E., Kahn, C. R., Roth, J., Ginsberg, B. H., De Meyts, B. H. *et al.* (1979) The insulin receptor and insulin of the Atlantic hagfish. Extraordinary conservation of binding specificity and negative cooperativity in the most primitive vertebrate. *Diabetes* **28**(3), 175-181.

263. Thompson, K. L., Decker, S. J., and Rosner, M. R. (1985) Identification of a novel receptor in Drosophila for both epidermal growth factor and insulin. *Proc.Natl.Acad.Sci.U.S.A.* **82**(24), 8443-8447.

264. Petruzzelli, L., Herrera, R., Arenas Garcia, R., Fernandez, R., Birnbaum, M. J., and Rosen, O. M. (1986) Isolation of a Drosophila genomic sequence homologous to the kinase domain of the human insulin receptor and detection of the phosphorylated Drosophila receptor with an anti-peptide antibody. *Proc.Natl.Acad.Sci.U.S.A.* **83**(13), 4710-4714.

265. Nishida, Y., Hata, M., Nishizuka, Y., Rutter, W. J., and Ebina, Y. (1986) Cloning of a Drosophila cDNA encoding a polypeptide similar to the human insulin receptor precursor. *Biochem.Biophys.Res.Commun.* **141**(2), 474-481.

266. Ginsberg, B. H., Kahn, C. R., and Roth, J. (1977) The insulin receptor of the turkey erythrocyte: similarity to mammalian insulin receptors. *Endocrinology* **100**(1), 82-90.

267. LeBon, T. R., Jacobs, S., Cuatrecasas, P., Kathuria, S., and Fujita-Yamaguchi, Y. (1986) Purification of insulin-like growth factor I receptor from human placental membranes. *J.Biol.Chem.* **261**(17), 7685-7689.

268. Morgan, D. O., Jarnagin, K., and Roth, R. A. (1986) Purification and characterization of the receptor for insulin- like growth factor I. *Biochemistry* **25**(19), 5560-5564.

269. Yu, K. T., Peters, M. A., and Czech, M. P. (1986) Similar control mechanisms regulate the insulin and type I insulin-like growth factor receptor kinases. Affinity-purified insulin-like growth factor I receptor kinase is activated by tyrosine phosphorylation of its β subunit. *J.Biol.Chem.* **261**(24), 11341-11349.

270. Shier, P. and Watt, V. M. (1989) Primary structure of a putative receptor for a ligand of the insulin family. *J.Biol.Chem.* **264**(25), 14605-14608.

271. Zhang, B. and Roth, R. A. (1992) The insulin receptor-related receptor. Tissue expression, ligand binding specificity, and signaling capabilities. *J.Biol.Chem.* **267**(26), 18320-18328.

272. Goldstein, B. J. and Dudley, A. L. (1990) The rat insulin receptor: primary structure and conservation of tissue-specific alternative messenger RNA splicing. *Mol.Endocrinol.* **4**(2), 235-244.

273. Ullrich, A., Gray, A., Tam, A. W., Yang Feng, T., Tsubokawa, M., Collins, C. *et al.* (1986) Insulin-like growth factor I receptor primary structure: comparison with insulin receptor suggests structural determinants that define functional specificity. *EMBO J.* **5**(10), 2503-2512.

274. Sneyers, M., Kettmann, R., Massart, S., Renaville, R., Burny, A., and Portetelle, D. (1991) Cloning and characterization of a cDNA encoding the β-subunit of the bovine insulin-like growth factor-1 receptor. *DNA Seq.* **1**(6), 405-406.

275. Groigno, L., Bonnec, G., Woiff, J., Joly, J., and Boujard, D. (1996) Insulin-like growth factor I receptor messenger expression during oogenesis in Xenopus laevis. *Endocrinology* **137**(9), 3856-3863.

276. Du, J. and Delafontaine, P. (1994) Cloning of a full length rat insulin-like growth factor I receptor cDNA : Evidence that antisense transcription inhibits vascular smooth muscle cell growth. *(unpublished)* .

277. Pashmforoush, M., Chan, S. J., and Steiner, D. F. (1996) Structure and expression of the insulin-like peptide receptor from amphioxus. *Mol.Endocrinol.* **10**(7), 857-866.

278. Roovers, E., Vincent, M. E., van Kesteren, E., Geraerts, W. P., Planta, R. J., Vreugdenhil, E. *et al.* (1995) Characterization of a putative molluscan insulin-related peptide receptor. *Gene* **162**(2), 181-188.

279. Mano, H., Yamashita, Y., Miyazato, A., Miura, Y., and Ozawa, K. (1996) Tec protein-tyrosine kinase is an effector molecule of Lyn protein-tyrosine kinase. *FASEB J.* **10**(5), 637-642.

280. The Wisconsin Package, version 8.1 (1994).

281. Shoji, S., Titani, K., Demaille, J. G., and Fischer, E. H. (1979) Sequence of two phosphorylated sites in the catalytic subunit of bovine cardiac muscle adenosine 3':5'-monophosphate-dependent protein kinase. *J.Biol.Chem.* **254**(14), 6211-6214.

282. Knighton, D. R., Zheng, J. H., Ten Eyck, L. F., Xuong, N. H., Taylor, S. S., and Sowadski, J. M. (1991) Structure of a peptide inhibitor bound to the catalytic subunit of cyclic adenosine monophosphate-dependent protein kinase. *Science* **253**(5018), 414-420.

283. Knighton, D. R., Zheng, J. H., Ten Eyck, L. F., Ashford, V. A., Xuong, N. H., Taylor, S. S. *et al.* (1991) Crystal structure of the catalytic subunit of cyclic adenosine monophosphate-dependent protein kinase. *Science* **253**(5018), 407-414.

284. Kong, C. T. and Cook, P. F. (1988) Isotope partitioning in the adenosine 3',5'-monophosphate dependent protein kinase reaction indicates a steady-state random kinetic mechanism. *Biochemistry* **27**(13), 4795-4799.

285. Whitehouse, S., Feramisco, J. R., Casnellie, J. E., Krebs, E. G., and Walsh, D. A. (1983) Studies on the kinetic mechanism of the catalytic subunit of the cAMP-dependent protein kinase. *J.Biol.Chem.* **258**(6), 3693-3701.

286. Cook, P. F., Neville, M. E., Jr., Vrana, K. E., Hartl, F. T., and Roskoski, R., Jr. (1982) Adenosine cyclic 3',5'-monophosphate dependent protein kinase: kinetic mechanism for the bovine skeletal muscle catalytic subunit. *Biochemistry* **21**(23), 5794-5799.

287. Adams, J. A. and Taylor, S. S. (1992) Energetic limits of phosphotransfer in the catalytic subunit of cAMP-dependent protein kinase as measured by viscosity experiments. *Biochemistry* **31**(36), 8516-8522.

288. Adams, J. A. (1996) Insight into tyrosine phosphorylation in v-Fps using proton inventory techniques. *Biochemistry* **35**(33), 10949-10956.

289. Wang, C., Lee, T. R., Lawrence, D. S., and Adams, J. A. (1996) Rate-determining steps for tyrosine phosphorylation by the kinase domain of v-fps. *Biochemistry* **35**(5), 1533-1539.

290. Ebina, Y., Araki, E., Taira, M., Shimada, F., Mori, M., Craik, C. S. *et al.* (1987) Replacement of lysine residue 1030 in the putative ATP-binding region of the insulin receptor abolishes insulin- and antibody- stimulated glucose uptake and receptor kinase activity. *Proc.Natl.Acad.Sci.U.S.A.* **84**(3), 704-708.

291. Carrera, A. C., Alexandrov, K., and Roberts, T. M. (1993) The conserved lysine of the catalytic domain of protein kinases is actively involved in the phosphotransfer reaction and not required for anchoring ATP. *Proc.Natl.Acad.Sci.U.S.A.* **90**(2), 442-446.

292. Robinson, M. J., Harkins, P. C., Zhang, J., Baer, R., Haycock, J. W., Cobb, M. H. *et al.* (1996) Mutation of position 52 in ERK2 creates a nonproductive binding mode for adenosine 5'-triphosphate. *Biochemistry* **35**(18), 5641-5646.

293. Yamaguchi, H. and Hendrickson, W. A. (1996) Structural basis for activation of human lymphocyte kinase Lck upon tyrosine phosphorylation. *Nature* **384**(6608), 484-489.

294. Russo, A. A., Jeffrey, P. D., and Pavletich, N. P. (1996) Structural basis of cyclin-dependent kinase activation by phosphorylation. *Nat.Struct.Biol.* **3**(8), 696-700.

295. Canagarajah, B. J., Khokhlatchev, A., Cobb, M. H., and Goldsmith, E. J. (1997) Activation mechanism of the MAP kinase ERK2 by dual phosphorylation. *Cell* **90**, 859-869.

296. Gibbs, C. S. and Zoller, M. J. (1991) Rational scanning mutagenesis of a protein kinase identifies functional regions involved in catalysis and substrate interactions. *J.Biol.Chem.* **266**(14), 8923-8931.

297. Zhou, J. and Adams, J. A. (1997) Is there a catalytic base in the active site of cAMP-dependent protein kinase? *Biochemistry* **36**(10), 2977-2984.

298. Cole, P. A., Grace, M. R., Phillips, R. S., Burn, P., and Walsh, C. T. (1995) The role of the catalytic base in the protein tyrosine kinase Csk. *J.Biol.Chem.* **270**(38), 22105-22108.

299. Martin, B. L., Wu, D., Jakes, S., and Graves, D. J. (1990) Chemical influences on the specificity of tyrosine phosphorylation. *J.Biol.Chem.* **265**(13), 7108-7111.

300. Adams, J. A., McGlone, M. L., Gibson, R., and Taylor, S. S. (1995) Phosphorylation modulates catalytic function and regulation in the cAMP-dependent protein kinase. *Biochemistry* **34**(8), 2447-2454.

301. Steinberg, R. A., Cauthron, R. D., Symcox, M. M., and Shuntoh, H. (1993) Autoactivation of catalytic (Cα) subunit of cyclic AMP-dependent protein kinase by phosphorylation of threonine 197. *Mol.Cell Biol.* **13**(4), 2332-2341.

302. Toner-Webb, J., Van Patten, S. M., Walsh, D. A., and Taylor, S. S. (1992) Autophosphorylation of the catalytic subunit of cAMP-dependent protein kinase. *J.Biol.Chem.* **267**(35), 25174-25180.

303. Huang, W. and Erikson, R. L. (1994) Constitutive activation of Mek1 by mutation of serine phosphorylation sites. *Proc.Natl.Acad.Sci.U.S.A.* **91**(19), 8960-8963.

304. Orr, J. W. and Newton, A. C. (1994) Requirement for negative charge on "activation loop" of protein kinase C. *J.Biol.Chem.* **269**(44), 27715-27718.

305. Abraham, N. and Veillette, A. (1990) Activation of $p56^{lck}$ through mutation of a regulatory carboxy-terminal tyrosine residue requires intact sites of autophosphorylation and myristylation. *Mol.Cell Biol.* **10**(10), 5197-5206.

306. Kmiecik, T. E., Johnson, P. J., and Shalloway, D. (1988) Regulation by the autophosphorylation site in overexpressed pp60c-src. *Mol.Cell Biol.* **8**(10), 4541-4546.

307. Mitra, G. (1991) Mutational analysis of conserved residues in the tyrosine kinase domain of the human trk oncogene. *Oncogene* **6**(12), 2237-2241.

308. Kazlauskas, A., Durden, D. L., and Cooper, J. A. (1991) Functions of the major tyrosine phosphorylation site of the PDGF receptor β subunit. *Cell Regul.* **2**(6), 413-425.

309. Boyle, W.J., van der Geer, P., Hunter, T. (1991) Phosphopeptide mapping and phosphoamino acid analysis by two-dimensional separation on thin-layer cellulose plates. *Methods Enzymol.* (**201**), 110-149.

310. Kato, H., Faria, T. N., Stannard, B., Roberts, C. T., Jr., and LeRoith, D. (1994) Essential role of tyrosine residues 1131, 1135, and 1136 of the insulin-like growth factor-I (IGF-I) receptor in IGF-I action. *Mol.Endocrinol.* **8**(1), 40-50.

311. Selbert, M. A., Anderson, K. A., Huang, Q. H., Goldstein, E. G., Means, A. R., and Edelman, A. M. (1995) Phosphorylation and activation of Ca^{2+}-calmodulin-dependent protein kinase IV by Ca^{2+}-calmodulin-dependent protein kinase Ia kinase. Phosphorylation of threonine 196 is essential for activation. *J.Biol.Chem.* **270**(29), 17616-17621.

312. Desai, D., Gu, Y., and Morgan, D. O. (1992) Activation of human cyclin-dependent kinases *in vitro*. *Mol.Biol.Cell* **3**(5), 571-582.

313. Robbins, D.J., Zhen, E., Owaki, H., Vanderbilt, C.A., Ebert, D., Geppert, T.D., and Cobb, M.H. (1993) Regulation and properties of extracellular signal-regulated protein kinases 1 and 2 *in vitro*. *J.Biol.Chem.* **268**(7), 5097-5106.

314. Cazaubon, S., Bornancin, F., and Parker, P. J. (1994) Threonine-497 is a critical site for permissive activation of protein kinase C α. *Biochem.J.* **301**(Pt 2), 443-448.

315. Mohammadi, M., Dikic, I., Sorokin, A., Burgess, W. H., Jaye, M., and Schlessinger, J. (1996) Identification of six novel autophosphorylation sites on fibroblast growth factor receptor 1 and elucidation of their importance in receptor activation and signal transduction. *Mol.Cell Biol.* **16**(3), 977-989.

316. Hon, W.-C., McKay, G. A., Thompson, P. R., Sweet, R. M., Yang, D. S. C., Wright, G. D. *et al.* (1997) Structure of an enzyme required for aminoglycoside antibiotic resistance reveals homology to eukaryotic protein kinases. *Cell* **86**, 887-895.

317. Banerjee, U., Renfranz, P. J., Hinton, D. R., Rabin, B. A., and Benzer, S. (1987) The sevenless+ protein is expressed apically in cell membranes of developing Drosophila retina; it is not restricted to cell R7. *Cell* **51**(1), 151-158.

318. Tomlinson, A., Bowtell, D. D., Hafen, E., and Rubin, G. M. (1987) Localization of the sevenless protein, a putative receptor for positional information, in the eye imaginal disc of Drosophila. *Cell* **51**(1), 143-150.

319. Rittinger, K., Walker, P. A., Eccleston, J. F., Nurmahomed, K., Owen, D., Laue, E. *et al.* (1997) Crystal structure of a small G protein in complex with the GTPase-activating protein rhoGAP. *Nature* **388**(6643), 693-697.

320. Taylor, S. S., Buechler, J. A., and Yonemoto, W. (1990) cAMP-dependent protein kinase: framework for a diverse family of regulatory enzymes. *Annu.Rev.Biochem.* **59**, 971-1005.

321. Maddux, B. A., Sbraccia, P., Kumakura, S., Sasson, S., Youngren, J., Fisher, A. *et al.* (1993) Membrane glycoprotein PC-1 and insulin resistance in non-insulin-dependent diabetes mellitus. *Nature* **373**(6513), 448-451.

322. Kemp, B. E. and Pearson, R. B. (1991) Intrasteric regulation of protein kinases and phosphatases. *Biochim.Biophys.Acta* **1094**, 67-76.

323. Kemp, B. E., Pearson, R. B., and House, C. M. (1991) Pseudosubstrate-based peptide inhibitors. *Methods Enzymol.* **201**, 287-304.

324. Sicheri, F., Moarefi, I., and Kuriyan, J. (1997) Crystal structure of the Src family tyrosine kinase Hck. *Nature* **385**(6617), 602-609.

325. Xu, W., Harrison, S. C., and Eck, M. J. (1997) Three-dimensional structure of the tyrosine kinase c-Src. *Nature* **385**(6617), 595-602.

326. Schenker, E. and Kohanski, R. A. (1988) Conformational states of the insulin receptor. *Biochem.Biophys.Res.Commun.* **157**(1), 140-145.

327. Pilch, P. F. and Czech, M. P. (1980) Hormone binding alters the conformation of the insulin receptor. *Science* **210**(4474), 1152-1153.

328. Donner, D. B. and Yonkers, K. (1983) Hormone-induced conformational changes in the hepatic insulin receptor. *J.Biol.Chem.* **258**(15), 9413-9418.

329. Lee, J., Pilch, P. F., Shoelson, S. E., and Scarlata, S. F. (1997) Conformational changes of the insulin receptor upon insulin binding and activation as monitored by fluorescence spectroscopy. *Biochemistry* **36**(9), 2701-2708.

330. Baron, V., Gautier, N., Komoriya, A., Hainaut, P., Scimeca, J. C., Mervic, M. *et al.* (1990) Insulin binding to its receptor induces a conformational change in the receptor C-terminus. *Biochemistry* **29**(19), 4634-4641.

331. Baron, V., Kaliman, P., Gautier, N., and Van Obberghen, E. (1992) The insulin receptor activation process involves localized conformational changes. *J.Biol.Chem.* **267**(32), 23290-23294.

332. Maddux, B. A. and Goldfine, I. D. (1991) Evidence that insulin plus ATP may induce a conformational change in the β subunit of the insulin receptor without inducing receptor autophosphorylation. *J.Biol.Chem.* **266**(11), 6731-6736.

333. Malencik, D. A., Zhao, Z., and Anderson, S. R. (1993) Preparation and functional characterization of a catalytically active fragment of phosphorylase kinase. *Mol.Cell Biochem.* **127-128**, 31-43.

334. Gu, Y., Rosenblatt, J., and Morgan, D. O. (1992) Cell cycle regulation of CDK2 activity by phosphorylation of Thr160 and Tyr15. *EMBO J.* **11**(11), 3995-4005.

335. Owen, D. J., Noble, M. E., Garman, E. F., Papageorgiou, A. C., and Johnson, L. N. (1995) Two structures of the catalytic domain of phosphorylase kinase: an active protein kinase complexed with substrate analogue and product. *Structure.* **3**(5), 467-482.

336. De Bondt, H. L., Rosenblatt, J., Jancarik, J., Jones, H. D., Morgan, D. O., and Kim, S. H. (1993) Crystal structure of cyclin-dependent kinase 2. *Nature* **363**(6430), 595-602.

337. Colbran, R. J. (1993) Inactivation of Ca^{2+}/calmodulin-dependent protein kinase II by basal autophosphorylation. *J.Biol.Chem.* **268**(10), 7163-7170.

338. Piwnica-Worms, H., Saunders, K. B., Roberts, T. M., Smith, A. E., and Cheng, S. H. (1987) Tyrosine phosphorylation regulates the biochemical and biological properties of $pp60^{c\text{-}src}$. *Cell* **49**(1), 75-82.

339. Cartwright, C. A., Eckhart, W., Simon, S., and Kaplan, P. L. (1987) Cell transformation by $pp60^{c\text{-}src}$ mutated in the carboxy-terminal regulatory domain. *Cell* **49**(1), 83-91.

340. Kmiecik, T. E. and Shalloway, D. (1987) Activation and suppression of pp60c-src transforming ability by mutation of its primary sites of tyrosine phosphorylation. *Cell* **49**(1), 65-73.

341. Colbran, R. J., Smith, M. K., Schworer, C. M., Fong, Y. L., and Soderling, T. R. (1989) Regulatory domain of calcium/calmodulin-dependent protein kinase II. Mechanism of inhibition and regulation by phosphorylation. *J.Biol.Chem.* **264**(9), 4800-4804.

342. Lisman, J. (1994) The CaM kinase II hypothesis for the storage of synaptic memory. *Trends.Neurosci.* **17**(10), 406-412.

343. Morgan, D. O. (1995) Principles of CDK regulation. *Nature* **374**(6518), 131-134.

344. Veron, M., Radzio-Andzelm, E., Tsigelny, I., and Taylor, S. (1994) Protein kinases share a common structural motif outside the conserved catalytic domain. *Cell Mol.Biol.(Noisy.-le.-grand.)* **40**(5), 587-596.

345. Johnson, L. N., Noble, M. E., and Owen, D. J. (1996) Active and inactive protein kinases: structural basis for regulation. *Cell* **85**(2), 149-158.

346. Kishimoto, M., Hashiramoto, M., Yonezawa, K., Shii, K., Kazumi, T., and Kasuga, M. (1994) Substitution of glutamine for arginine 1131. A newly identified mutation in the catalytic loop of the tyrosine kinase domain of the human insulin receptor. *J.Biol.Chem.* **269**(15), 11349-11355.

347. Cox, S. and Taylor, S. S. (1995) Kinetic analysis of cAMP-dependent protein kinase: mutations at histidine 87 affect peptide binding and pH dependence. *Biochemistry* **34**(49), 16203-16209.

348. Cox, S. and Taylor, S. S. (1994) Holoenzyme interaction sites in the cAMP-dependent protein kinase. Histidine 87 in the catalytic subunit complements serine 99 in the type I regulatory subunit. *J.Biol.Chem.* **269**(36), 22614-22622.

349. Jeffrey, P. D., Russo, A. A., Polyak, K., Gibbs, E., Hurwitz, J., Massague, J. *et al.* (1995) Mechanism of CDK activation revealed by the structure of a cyclinA-CDK2 complex. *Nature* **376**(6538), 313-320.

350. Tokmakov, A. A., Sahara, S., Sato, K., Nishida, E., and Fukami, Y. (1996) Phosphoregulatory tyrosine of Xenopus mitogen-activated protein kinase is out of the reach of the enzyme catalytic center after autophosphorylation. Biochemical evidence for conformational changes upon phosphorylation. *Eur.J.Biochem.* **241**(2), 322-329.

351. Filipek, A. and Soderling, T. R. (1993) Identification of an autoinhibitory domain in the insulin receptor tyrosine kinase. *Mol.Cell Biochem.* **120**(2), 103-110.

352. Mohammadi, M., Schlessinger, J., and Hubbard, S. R. (1996) Structure of the FGF receptor tyrosine kinase domain reveals a novel autoinhibitory mechanism. *Cell* **86**(4), 577-587.

353. Wilson, K. P., Fitzgibbon, M. J., Caron, P. R., Griffith, J. P., Chen, W., McCaffrey, P. G. *et al.* (1996) Crystal structure of p38 mitogen-activated protein kinase. *J.Biol.Chem.* **271**(44), 27696-27700.

354. Zhang, F., Strand, A., Robbins, D., Cobb, M. H., and Goldsmith, E. J. (1994) Atomic structure of the MAP kinase ERK2 at 2.3 A resolution. *Nature* **367**(6465), 704-711.

355. Blackshear, P.J. Carbohydrate metabolism. Chapter 410. pp. 1948-1952. In: Textbook of Principles of Internal Medicine, 2nd edition. Kelley, eds. J.B. Lippincott Company. Philadelphia. 1992.

356. Sudol, M. Nonreceptor protein tyrosine kinases. Chapter 5. pp. 203-224. In: The molecular basis of human cancer., Neel, G. N. and Kumar, S., eds. Futura Publishing Company., Mount Kisco, N.Y., 1993.

357. Blechman, J. M. and Yarden, Y. (1995) Structural aspects of receptor dimerization. c-kit as an example. *Ann.N.Y.Acad.Sci.* **766**, 344-362.

358. Uhler, M. D., Carmichael, D. F., Lee, D. C., Chrivia, J. C., Krebs, E. G., and McKnight, G. S. (1986) Isolation of cDNA clones coding for the catalytic subunit of mouse cAMP- dependent protein kinase. *Proc.Natl.Acad.Sci.U.S.A.* **83**(5), 1300-1304.

359. Zheng, J., Knighton, D. R., Ten Eyck, L. F., Karlsson, R., Xuong, N., Taylor, S. S. *et al.* (1993) Crystal structure of the catalytic subunit of cAMP-dependent protein kinase complexed with MgATP and peptide inhibitor. *Biochemistry* **32**(9), 2154-2161.

360. Walseth, T. F. and Johnson, R. A. (1979) The enzymatic preparation of [α-^{32}P]nucleoside triphosphates, cyclic [^{32}P] AMP, and cyclic [^{32}P] GMP. *Biochim.Biophys.Acta* **562**(1), 11-31.

361. Palmer, J. L. and Avruch, J. (1981) A rapid and convenient method for preparing salt-free [γ- ^{32}P]ATP. *Anal.Biochem.* **116**(2), 372-373.

362. Maniatis, T., Fritsch, E.F., and Sambrook, J. Molecular Cloning: A Laboratory Manual. Cold Spring Harbory Laboratory., 1982.

363. Sanger, F., Nicklen, S., and Coulson, A. R. (1977) DNA sequencing with chain-terminating inhibitors. *Proc.Natl.Acad.Sci.U.S.A.* **74**(12), 5463-5467.

364. Ho, S. N., Hunt, H. D., Horton, R. M., Pullen, J. K., and Pease, L. R. (1989) *Gene* **77**, 51-59.

365. Bishop, S.M. and Kohanski, R.A., personal communcation.

366. Braun, S., Raymond, W. E., and Racker, E. (1984) Synthetic tyrosine polymers as substrates and inhibitors of tyrosine- specific protein kinases. *J.Biol.Chem.* **259**(4), 2051-2054.

367. Racker, E. (1991) Use of synthetic amino acid polymers for assay of protein-tyrosine and protein-serine kinases. *Methods Enzymol.* **200:107-11**, 107-111.

368. Kohanski, R. A. and Lane, M. D. (1986) Kinetic evidence for activating and non-activating components of autophosphorylation of the insulin receptor protein kinase. *Biochem.Biophys.Res.Commun.* **134**(3), 1312-1318.

369. Hunter, T. (1982) Synthetic peptide substrates for a tyrosine protein kinase. *J.Biol.Chem.* **257**(9), 4843-4848.

370. Witt, J. J. and Roskoski, R., Jr. (1975) Rapid protein kinase assay using phosphocellulose-paper absorption. *Anal.Biochem.* **66**(1), 253-258.

371. Glass, D. B., Masaracchia, R. A., Feramisco, J. R., and Kemp, B. E. (1978) Isolation of phosphorylated peptides and proteins on ion exchange papers. *Anal.Biochem.* **87**(2), 566-575.

372. Moll, G. W., Jr. and Kaiser, E. T. (1976) Phosphorylation of histone catalyzed by a bovine brain protein kinase. *J.Biol.Chem.* **251**(13), 3993-4000.

373. Budde, R. J., McMurray, J. S., and Tinker, D. A. (1992) An assay for acidic peptide substrates of protein kinases. *Anal.Biochem.* **200**(2), 347-351.

374. Boutin, J. A., Ernould, A. P., Ferry, G., Genton, A., and Alpert, A. J. (1992) Use of hydrophilic interaction chromatography for the study of tyrosine protein kinase specificity. *J.Chromatogr.* **583**(2), 137-143.

375. Ferry, G., Ernould, A. P., Genton, A., and Boutin, J. A. (1990) Assay of tyrosine protein kinase activity from HL-60 by high- performance liquid chromatography for specificity studies. *Anal.Biochem.* **190**(1), 32-38.

376. Toomik, R., Ekman, P., Eller, M., Jarv, J., Zaitsev, D., Myasoedov, N. *et al.* (1993) Protein kinase assay using tritiated peptide substrates and ferric adsorbent paper for phosphopeptide binding. *Anal.Biochem.* **209**(2), 348-353.

377. Casnellie, J. E. (1991) Assay of protein kinases using peptides with basic residues for phosphocellulose binding. *Methods Enzymol.* **200:115-20**, 115-120.

378. Kemp, B. E., Graves, D. J., Benjamini, E., and Krebs, E. G. (1977) Role of multiple basic residues in determining the substrate specificity of cyclic AMP-dependent protein kinase. *J.Biol.Chem.* **252**(14), 4888-4894.

379. Xu, B., Bird, V. G., and Miller, W. T. (1995) Substrate specificities of the insulin and insulin-like growth factor 1 receptor tyrosine kinase catalytic domains. *J.Biol.Chem.* **270**(50), 29825-29830.

380. Stadtmauer, L. and Rosen, O. M. (1986) Phosphorylation of synthetic insulin receptor peptides by the insulin receptor kinase and evidence that the preferred sequence containing Tyr-1150 is phosphorylated *in vivo*. *J.Biol.Chem.* **261**(21), 10000-10005.

381. Kohanski, R. A. (1989) Insulin receptor aggregation and autophosphorylation in the presence of cationic polyamino acids. *J.Biol.Chem.* **264**(35), 20984-20991.

382. Keane, N. E., Chavanieu, A., Quirk, P. G., Evans, J. S., Levine, B. A., Calas, B. *et al.* (1994) Structural determinants of substrate selection by the human insulin-receptor protein-tyrosine kinase. *Eur.J.Biochem.* **226**(2), 525-536.

383. Newton, R. P., Evans, A. M., Langridge, J. I., Walton, T. J., Harris, F. M., and Brenton, A. G. (1995) Assay of adenosine 3',5'-cyclic monophosphate-dependent protein kinase activity by quantitative fast atom bombardment mass spectrometry. *Anal.Biochem.* **224**(1), 32-38.

384. Dawson, J. F., Boland, M. P., and Holmes, C. F. (1994) A capillary electrophoresis-based assay for protein kinases and protein phosphatases using peptide substrates. *Anal.Biochem.* **220**(2), 340-345.

385. Wang, Z. X., Cheng, Q., and Killilea, S. D. (1995) A continuous spectrophotometric assay for phosphorylase kinase. *Anal.Biochem.* **230**(1), 55-61.

386. Lambeth, D. O. and Muhonen, W. W. (1993) The direct assay of kinases and acyl-CoA synthetases by HPLC: application to nucleoside diphosphate kinase and succinyl-CoA synthetase. *Anal.Biochem.* **209**(1), 192-198.

387. Paudel, H. K. and Carlson, G. M. (1991) The ATPase activity of phosphorylase kinase is regulated in parallel with its protein kinase activity. *J.Biol.Chem.* **266**(25), 16524-16529.

388. O'Brian, C. A. and Ward, N. E. (1990) Characterization of a Ca^{2+}- and phospholipid-dependent ATPase reaction catalyzed by rat brain protein kinase C. *Biochemistry* **29**(18), 4278-4282.

389. Al-Hasani, H., Paβlack, W., and Klein, H. W. (1994) Phosphoryl exchange is involved in the mechanism of the insulin receptor kinase. *FEBS Lett.* **349**(1), 17-22.

390. Goueli, B. S., Hsiao, K., Tereba, A., and Goueli, S. A. (1995) A novel and simple method to assay the activity of individual protein kinases in a crude tissue extract. *Anal.Biochem.* **225**(1), 10-17.

391. Boge, A. and Roth, R. A. (1995) A nonradioactive assay for the insulin receptor tyrosine kinase: use in monitoring receptor kinase activity after activation of overexpressed protein kinase C α and high glucose treatment. *Anal.Biochem.* **231**(2), 323-332.

392. Isbell, J. C., Christian, S. T., Mashburn, N. A., and Bell, P. D. (1995) A non-radioactive fluorescent method for measuring protein kinase C activity. *Life Sci.* **57**(18), 1701-1707.

393. Lutz, M. P., Pinon, D. I., and Miller, L. J. (1994) A nonradioactive fluorescent gel-shift assay for the analysis of protein phosphatase and kinase activities toward protein-specific peptide substrates *Anal.Biochem.* **220**(2), 268-274.

394. Apostol, I., Kuciel, R., Wasylewska, E., and Ostrowski, W. S. (1985) Phosphotyrosine as a substrate of acid and alkaline phosphatases. *Acta Biochim.Pol.* **32**(3), 187-197.

395. Vicario, P. P., Saperstein, R., and Bennun, A. (1988) Role of divalent metals in the activation and regulation of insulin receptor tyrosine kinase. *Biosystems* **22**(1), 55-66.

396. Ohguro, H. and Palczewski, K. (1995) Separation of phospho- and non-phosphopeptides using reverse phase column chromatography. *FEBS Lett.* **368**(3), 452-454.

397. Nakanishi, S., Kase, H., and Matsuda, Y. (1991) Assay of myosin light chain kinase activity by high-performance liquid chromatography using a synthetic peptide as substrate. *Anal.Biochem.* **195**(2), 313-318.

398. Segel, I. H. Enzyme Kinetics . Wiley, New York, 1975.

399. Toomik, R., Ekman, P., and Engstrom, L. (1992) A potential pitfall in protein kinase assay: phosphocellulose paper as an unreliable adsorbent of produced phosphopeptides. *Anal.Biochem.* **204**(2), 311-314.

400. Engl, J., Moule, M., and Yip, C. C. (1994) Dithiothreitol stimulates insulin receptor autophosphorylation at the juxtamembrane domain. *Biochem.Biophys.Res.Commun.* **201**(3), 1439-1444.

401. Tavaré, J. M., Clack, B., and Ellis, L. (1991) Two-dimensional phosphopeptide analysis of the autophosphorylation cascade of a soluble insulin receptor tyrosine kinase. The tyrosines phosphorylated are typical of those observed following phosphorylation of the heterotetrameric insulin receptor in intact cells. *J.Biol.Chem.* **266**(3), 1390-1395.

402. Guex, N. and Peitsch, M. C. (1996) Swiss-PdbViewer: A Fast and Easy-to-use Viewer for Macintosh and PC. *Protein Data Bank Quarterly Newsletter* **77**, 7.

403. Anger, S.,*et al.* (1997) POV-Ray 3.02. http://www.povray.org

404. Neet, K. E. and Ainslie, G. R. (1980) Hysteretic enzymes. *Methods Enzymol.* **64**, 192-226.

405. Rosen, O. M. and Lebwohl, D. E. (1988) Polylysine activates and alters the divalent cation requirements of the insulin receptor protein tyrosine kinase. *FEBS Lett.* **231**(2), 397-401.

406. Zick, Y., Kasuga, M., Kahn, C. R., and Roth, J. (1983) Characterization of insulin-mediated phosphorylation of the insulin receptor in a cell-free system. *J.Biol.Chem.* **258**(1), 75-80.

407. Wente, S. R., Villalba, M., Schramm, V. L., and Rosen, O. M. (1990) Mn^{2+}-binding properties of a recombinant protein-tyrosine kinase derived from the human insulin receptor. *Proc.Natl.Acad.Sci.U.S.A.* **87**(7), 2805-2809.

408. Nemenoff, R. A., Kwok, Y. C., Shulman, G. I., Blackshear, P. J., Osathanondh, R., and Avruch, J. (1984) Insulin-stimulated tyrosine protein kinase. Characterization and relation to the insulin receptor. *J.Biol.Chem.* **259**(8), 5058-5065.

409. Vicario, P. P., Saperstein, R., and Bennun, A. (1988) Role of divalent metals in the kinetic mechanism of insulin receptor tyrosine kinase. *Arch.Biochem.Biophys.* **261**(2), 336-345.

410. Vicario, P. P. and Bennun, A. (1990) Separate effects of Mg^{2+}, MgATP, and ATP^{4-} on the kinetic mechanism for insulin receptor tyrosine kinase. *Arch.Biochem.Biophys.* **278**(1), 99-105.

411. Laurino, J. P., Colca, J. R., Pearson, J. D., DeWald, D. B., and McDonald, J. M. (1988) The *in vitro* phosphorylation of calmodulin by the insulin receptor tyrosine kinase. *Arch.Biochem.Biophys.* **265**(1), 8-21.

412. Yuan, C. J., Huang, C. Y., and Graves, D. J. (1993) Phosphorylase kinase, a metal ion-dependent dual specificity kinase. *J.Biol.Chem.* **268**(24), 17683-17686.

413. Hallenbeck, P. C. and Walsh, D. A. (1983) Autophosphorylation of phosphorylase kinase. Divalent metal cation and nucleotide dependency. *J.Biol.Chem.* **258**(22), 13493-13501.

414. Böni-Schnetzler, M., Rubin, J. B., and Pilch, P. F. (1986) Structural requirements for the transmembrane activation of the insulin receptor kinase. *J.Biol.Chem.* **261**(32), 15281-15287.

415. Sweet, L. J., Morrison, B. D., and Pessin, J. E. (1987) Isolation of functional αβ heterodimers from the purified human placental $\alpha_2\beta_2$ heterotetrameric insulin receptor complex. A structural basis for insulin binding heterogeneity. *J.Biol.Chem.* **262**(15), 6939-6942.

416. Morrison, B. D., Swanson, M. L., Sweet, L. J., and Pessin, J. E. (1988) Insulin-dependent covalent reassociation of isolated αβ heterodimeric insulin receptors into

an $\alpha_2\beta_2$ heterotetrameric disulfide-linked complex. *J.Biol.Chem.* **263**(16), 7806-7813.

417. Sweet, L. J., Morrison, B. D., Wilden, P. A., and Pessin, J. E. (1987) Insulin-dependent intermolecular subunit communication between isolated αβ heterodimeric insulin receptor complexes. *J.Biol.Chem.* **262**(34), 16730-16738.

418. Wilden, P. A., Morrison, B. D., and Pessin, J. E. (1989) Relationship between insulin receptor subunit association and protein kinase activation: insulin-dependent covalent and Mn/MgATP-dependent noncovalent association of αβ heterodimeric insulin receptors into an $\alpha_2\beta_2$ heterotetrameric state. *Biochemistry* **28**(2), 785-792.

419. Sweet, L. J., Wilden, P. A., and Pessin, J. E. (1986) Dithiothreitol activation of the insulin receptor/kinase does not involve subunit dissociation of the native $\alpha_2\beta_2$ insulin receptor subunit complex. *Biochemistry* **25**(22), 7068-7074.

420. Feltz, S. M., Swanson, M. L., Wemmie, J. A., and Pessin, J. E. (1988) Functional properties of an isolated αβ heterodimeric human placenta insulin-like growth factor 1 receptor complex. *Biochemistry* **27**(9), 3234-3242.

421. Treadway, J. L., Morrison, B. D., Soos, M. A., Siddle, K., Olefsky, J., Ullrich, A. *et al.* (1991) Transdominant inhibition of tyrosine kinase activity in mutant insulin/insulin-like growth factor I hybrid receptors. *Proc.Natl.Acad.Sci.U.S.A.* **88**(1), 214-218.

422. Goldberg, J., Nairn, A. C., and Kuriyan, J. (1996) Structural basis for the autoinhibition of calcium/calmodulin- dependent protein kinase I. *Cell* **84**(6), 875-887.

423. Francis, S. H., Smith, J. A., Colbran, J. L., Grimes, K., Walsh, K. A., Kumar, S. *et al.* (1996) Arginine 75 in the pseudosubstrate sequence of type Iβ cGMP-dependent protein kinase is critical for autoinhibition, although autophosphorylated serine 63 is outside this sequence. *J.Biol.Chem.* **271**(34), 20748-20755.

424. Mukherji, S., Brickey, D. A., and Soderling, T. R. (1994) Mutational analysis of secondary structure in the autoinhibitory and autophosphorylation domains of calmodulin kinase II. *J.Biol.Chem.* **269**(32), 20733-20738.

425. Mukherji, S. and Soderling, T. R. (1995) Mutational analysis of Ca^{2+}-independent autophosphorylation of calcium/calmodulin-dependent protein kinase II. *J.Biol.Chem.* **270**(23), 14062-14067.

426. McDonald, O. B., Merrill, B. M., Bland, M. M., Taylor, L. C., and Sahyoun, N. (1993) Site and consequences of the autophosphorylation of Ca^{2+}/calmodulin-dependent protein kinase type "Gr". *J.Biol.Chem.* **268**(14), 10054-10059.

427. Kameshita, I. and Fujisawa, H. (1995) Preparation and characterization of calmodulin-dependent protein kinase IV (CaM-kinase IV) free of CaM-kinase IV kinase from rat cerebral cortex. *J.Biochem.Tokyo.* **117**(1), 85-90.

428. Chatila, T., Anderson, K. A., Ho, N., and Means, A. R. (1996) A unique phosphorylation-dependent mechanism for the activation of Ca^{2+}/calmodulin-dependent protein kinase type IV/GR. *J.Biol.Chem.* **271**(35), 21542-21548.

429. Newton, A. C. and Koshland, D. E. J. (1987) Protein kinase C autophosphorylates by an intrapeptide reaction. *J.Biol.Chem.* **262**(21), 10185-10188.

430. Brickey, D. A., Bann, J. G., Fong, Y. L., Perrino, L., Brennan, R. G., and Soderling, T. R. (1994) Mutational analysis of the autoinhibitory domain of calmodulin kinase II. *J.Biol.Chem.* **269**(46), 29047-29054.

431. Colbran, R. J., Fong, Y. L., Schworer, C. M., and Soderling, T. R. (1988) Regulatory interactions of the calmodulin-binding, inhibitory, and autophosphorylation domains of Ca^{2+}/calmodulin-dependent protein kinase II. *J.Biol.Chem.* **263**(34), 18145-18151.

432. Colbran, R. J. and Soderling, T. R. (1990) Calcium/calmodulin-independent autophosphorylation sites of calcium/calmodulin-dependent protein kinase II. Studies on the effect of phosphorylation of threonine 305/306 and serine 314 on calmodulin binding using synthetic peptides. *J.Biol.Chem.* **265**(19), 11213-11219.

433. Fong, Y. L., Taylor, W. L., Means, A. R., and Soderling, T. R. (1989) Studies of the regulatory mechanism of Ca^{2+}/calmodulin-dependent protein kinase II. Mutation of threonine 286 to alanine and aspartate. *J.Biol.Chem.* **264**(28), 16759-16763.

434. Fong, Y. L. and Soderling, T. R. (1990) Studies on the regulatory domain of Ca^{2+}/calmodulin-dependent protein kinase II. Functional analyses of arginine 283 using synthetic inhibitory peptides and site-directed mutagenesis of the α subunit. *J.Biol.Chem.* **265**(19), 11091-11097.

435. Hashimoto, Y., Schworer, C. M., Colbran, R. J., and Soderling, T. R. (1987) Autophosphorylation of Ca^{2+}/calmodulin-dependent protein kinase II. Effects on total and Ca2+-independent activities and kinetic parameters. *J.Biol.Chem.* **262**(17), 8051-8055.

436. Schworer, C. M., Colbran, R. J., and Soderling, T. R. (1986) Reversible generation of a Ca^{2+}-independent form of Ca^{2+}(calmodulin)- dependent protein kinase II by an autophosphorylation mechanism. *J.Biol.Chem.* **261**(19), 8581-8584.

437. Schworer, C. M., Colbran, R. J., Keefer, J. R., and Soderling, T. R. (1988) Ca^{2+}/calmodulin-dependent protein kinase II. Identification of a regulatory

autophosphorylation site adjacent to the inhibitory and calmodulin-binding domains. *J.Biol.Chem.* **263**(27), 13486-13489.

438. Yokokura, H., Picciotto, M. R., Nairn, A. C., and Hidaka, H. (1995) The regulatory region of calcium/calmodulin-dependent protein kinase I contains closely associated autoinhibitory and calmodulin-binding domains. *J.Biol.Chem.* **270**(40), 23851-23859.

439. Newton, A. C. (1995) Protein kinase C: structure, function, and regulation. *J.Biol.Chem.* **270**(48), 28495-28498.

440. Flint, A. J., Paladini, R. D., and Koshland, D. E. J. (1990) Autophosphorylation of protein kinase C at three separated regions of its primary sequence. *Science* **249**(4967), 408-411.

441. Zhang, J., Wang, L., Petrin, J., Bishop, W. R., and Bond, R. W. (1993) Characterization of site-specific mutants altered at protein kinase C β1 isozyme autophosphorylation sites. *Proc.Natl.Acad.Sci.U.S.A.* **90**(13), 6130-6134.

442. Newton, A.C., personal communcation.

443. Selbert, M. A., Anderson, K. A., Huang, Q. H., Goldstein, E. G., Means, A. R., and Edelman, A. M. (1995) Phosphorylation and activation of Ca^{2+}-calmodulin dependent protein kinase IV by Ca^{2+}-calmodulin dependent protein kinase Ia kinase. *J.Biol.Chem.* **270**(29), 17616-17621.

444. Edelman, A. M., Mitchelhill, K. I., Selbert, M. A., Anderson, K. A., Hook, S. S., Stapleton, D. *et al.* (1996) Multiple Ca^{2+}-calmodulin-dependent protein kinase kinases from rat brain. Purification, regulation by Ca^{2+}-calmodulin, and partial amino acid sequence. *J.Biol.Chem.* **271**(18), 10806-10810.

445. Zhang, J., Zhang, F., Ebert, D., Cobb, M. H., and Goldsmith, E. J. (1995) Activity of the MAP kinase ERK2 is controlled by a flexible surface loop. *Structure.* **3**(3), 299-307.

446. Webster, M. K., D'Avis, P. Y., Robertson, S. C., and Donoghue, D. J. (1996) Profound ligand-independent kinase activation of fibroblast growth factor receptor 3 by the activation loop mutation responsible for a lethal skeletal dysplasia, thanatophoric dysplasia type II. *Mol.Cell Biol.* **16**(8), 4081-4087.

447. Tavormina, P. L., Shiang, R., Thompson, L. M., Zhu, Y. Z., Wilkin, D. J., Lachman, R. S. *et al.* (1995) Thanotropic dysplasia (types I and II) caused by distinct mutations in fibroblast growth factor receptor 3. *Nat.Genet.* **9**, 321-328.

448. White, M. F. and Kahn, C. R. (1989) Cascade of autophosphorylation in the β-subunit of the insulin receptor. *J.Cell Biochem.* **39**(4), 429-441.

449. Herrera, R., Petruzzelli, L., Thomas, N., Bramson, H. N., Kaiser, E. T., and Rosen, O. M. (1985) An antipeptide antibody that specifically inhibits insulin receptor autophosphorylation and protein kinase activity. *Proc.Natl.Acad.Sci.U.S.A.* **82** (23), 7899-7903.

450. Goodman, D. W., Romero, G., and Isakson, P. (1994) Antibody binding to the juxtamembrane region of the insulin receptor alters receptor affinity. *J.Recept.Res.* **14** (6-8), 381-398.

451. Kubar, J. and Rochet, N. (1990) Basal autophosphorylation of insulin receptor occurs preferentially on the receptor conformation exhibiting high affinity for insulin and stabilizes this conformation. *Cell Signal.* **2**(6), 587-594.

452. Lee, J., O'Hare, T., Pilch, P. F., and Shoelson, S. E. (1993) Insulin receptor autophosphorylation occurs asymmetrically. *J.Biol.Chem.* **268**(6), 4092-4098.

453. Lemmon, M. A., Ferguson, K. M., and Schlessinger, J. (1996) PH Domains: Diverse sequences with a common fold recruit signaling molecules to the cell surface. *Cell* **85**, 621-624.

454. Whittaker, J., Okamoto, A. K., Thys, R., Bell, G. I., Steiner, D. F., and Hofmann, C. A. (1987) High-level expression of human insulin receptor cDNA in mouse NIH 3T3 cells. *Proc.Natl.Acad.Sci.U.S.A.* **84**(15), 5237-5241.

455. Cann, A. D., Wolf, I., and Kohanski, R. A. (1997) A tyrosine kinase assay using reverse-phase high-performance liquid chromatography. *Anal.Biochem.* **247**(2), 327-332.

456. Cann, A. D. and Kohanski, R. A. (1997) *Cis*-autophosphorylation of juxtamembrane tyrosines in the insulin receptor kinase domain. *Biochemistry* **36**(25), 7681-7689.

457. Cann, A. D. and Kohanski, R. A. (1996) Partial activation of the insulin receptor's kinase domain without activation loop autophosphorylation. *Protein Sci.* **5**(Supplement 1), 156 (abstract).

458. Chen, D., Van Horn, D. J., White, M. F., and Backer, J. M. (1995) Insulin receptor substrate 1 rescues insulin action in CHO cells expressing mutant insulin receptors that lack a juxtamembrane NPXY motif. *Mol.Cell Biol.* **15**(9), 4711-4717.

IMAGE EVALUATION TEST TARGET (QA-3)

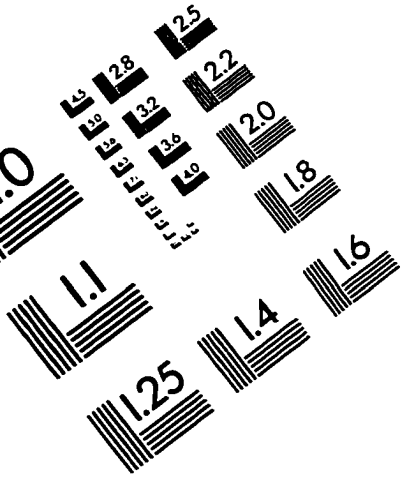

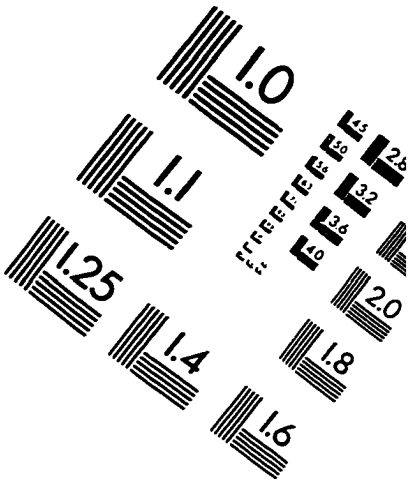

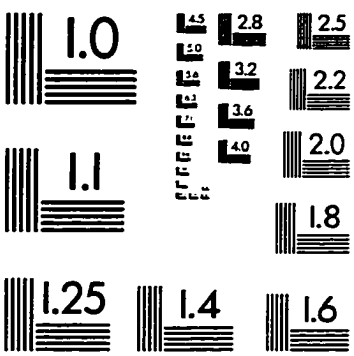

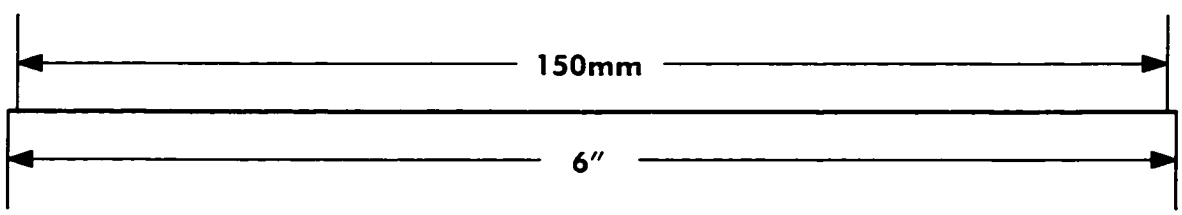

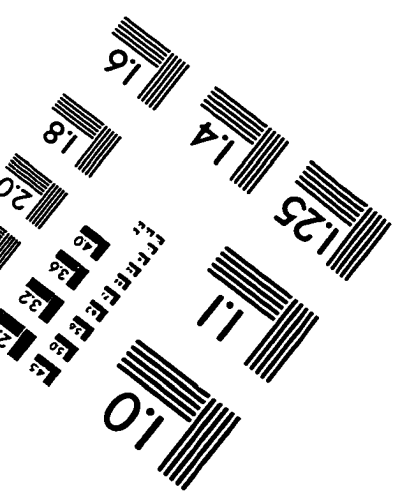

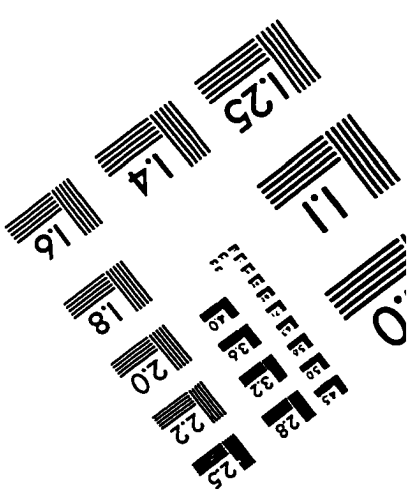

APPLIED IMAGE, Inc
1653 East Main Street
Rochester, NY 14609 USA
Phone: 716/482-0300
Fax: 716/288-5989